UNIVERSITY *of* TASMANIA

Imaging for Cardiac Dysfunction Secondary to Cancer Treatment

By

Mark Travers Nolan

MBBS, B.Sc. (Hons)

A thesis submitted in fulfilment of the requirements for

the degree of Doctor of Philosophy (Medical Research)

Menzies Institute for Medical Research

University of Tasmania

Hobart, Australia

February 2019

This thesis was supervised by

Primary Supervisor

Professor Thomas H. Marwick, MBBS, PhD, MPH

Menzies Institute for Medical Research

University of Tasmania

Hobart, Australia

And

Co-supervisor

Dr Kazuaki Negishi, MD, PhD

Menzies Institute for Medical Research

University of Tasmania

Hobart, Australia

Declaration of originality

This thesis contains no material which has been accepted for a degree or diploma by the University or any other institution, except by way of background information and duly acknowledged in the thesis, and**,** to the best of my knowledge and belief**,** no material previously published or written by another person**,** except where due acknowledgement is made in the text of the thesis, nor does the thesis contain any material that infringes copyright.

Name: Mark Travers Nolan

Signed: _____

25th February, 2019

Date: _____

Statement of Authority of Access

Name: Mark Travers Nolan

Signed: _____

25th February, 2019

Date: _____

Statement of Ethical Conduct

All research associated with this thesis abides by the International and Australian codes on human and animal experimentation, and full ethical approval from the relevant institutions was obtained for all studies outlined in this thesis. All individual participants provided written informed consent for involvement in the respective research studies.

Name: Mark Travers Nolan

Signed: _____

25th February, 2019

Date: _____

Statement of Sponsorship

The research reported in this thesis was supported by a Health Professional Scholarship from the National Heart Foundation of Australia (Reference Number 100687) and by a Hosinec Family Scholarship from the University of Toronto.

Name: Mark Travers Nolan

Signed:

_____

25th February, 2019

Date: _____

Statement of Co-Authorship

The following people and institutions contributed to the publication of work undertaken as part of this thesis:

Candidate – Mark Travers Nolan, Menzies Institute for Medical Research

Author 1 – Professor Thomas Marwick, Menzies Institute for Medical Research.

Author 2 -- Associate Professor Paaladinesh Thavendiranathan, University of Toronto.

Author 3 -- Professor Alison Venn, Menzies Institute for Medical Research.

Author 4 – Professor Lowenthal, University of Tasmania.

Author 5 -- Dr Husam Abdel-Qadir, University of Toronto.

Author 6 -- Dr. David J Russell, Royal Hobart Hospital.

Author 7 - Professor Kazuaki Negishi, Menzies Institute for Medical Research.

Author 8 -- Professor Juan-Carlos Plana, Baylor College of Medicine.

Author 9 -- Dr Zhenghong Li, St Jude Children's Research Hospital.

Author 10 – Dr Kirsten K. Ness, St Jude Children's Research Hospital.

Author 11 -- Dr Vijaya M. Joshi, University of Tennessee Health Science Centre.

Author 12 – Dr Daniel M. Green, St Jude Children's Research Hospital.

Author 13 – Dr Leslie L. Robison, St Jude Children's Research Hospital.

Author 14 -- Dr Melissa M. Hudson, St Jude Children's Research Hospital.

Author 15 – Professor Gregory T. Armstrong, St Jude Children's Research Hospital.

Author 16 – Dr. Mustafa Altaha, University of Toronto.

Author 17 -- Professor Eitan Amir, Princess Margaret Cancer Centre.

Author 18 -- Dr Anne Koch, University of Toronto.

Author 19 – Dr Paul Yip, University of Toronto.

Author 20 – Ms. Maria Michalowska, Peter Munk Cardiac Centre.

Author 21 – Professor Bernd Wintersperger, University of Toronto.

Author 22 – Dr Leslie Shaw, Emory University.

Author 23 – Dr Lei Si, Menzies Institute for Medical Research.

Author 24 – Dr. Reis Hanson, University of Calgary

Author 25 – Ms. Babitha Thampinathan, University of Toronto.

Author 26 – Dr. Christine Brezden-Masley, Princess Margaret Cancer Centre.

Author 27 – Dr. Alessandro Satriano, University of Calgary.
Author 28 – Dr Kim Connelly, University of Toronto.

Author details and their roles:

Paper 1: Located in Chapter 1

Nolan MT, Lowenthal RM, Venn A, Marwick TH. Chemotherapy-related cardiomyopathy: a neglected aspect of cancer survivorship. Intern Med J. 2014; 44(10):939-50/

Author 4 contributed to the themes of the paper. The candidate (Author 1) was first author and worked in conjunction with author 2 to design the manuscript. Author 1 was responsible for literature review, creating tables and figures and writing the majority of the manuscript. Author 3 assisted with editing. Author 4 edited the manuscript, provided guidance for communication and technical aspects of cardiac imaging and approved the final manuscript. All the authors had access to all data, including statistical reports and tables, and reviewed and approved the manuscript prior to submission.

Paper 2: Located in Chapter 1

Thavendiranathan P, **Nolan MT**. An emerging epidemic: cancer and heart failure. Clin Sci. 2017; 131(2): 113-21.

Author 1 contributed by developing the original idea and contributed to the themes of the paper. The candidate (Author 2) performed a literature review and wrote the majority of the manuscript. The candidate and Author 1 contributed equal shares of figures and tables. Author 1 edited and approved the final manuscript.

Paper 3: Located in Chapter 1

Abdel-Qadir H, **Nolan MT,** Thavendiranathan P. Routine Prophylactic Cardioprotective Therapy Should be Given to All Recipients at Risk of Cardiotoxicity from Cancer Chemotherapy. Can J Cardiol. 2016; 32(7): 921-5.

Authors 2 and 3 contributed by developing the original idea. All three authors agreed on the themes and structure of the paper. Author 1 and author 2 wrote approximately 50% of the manuscript each. Author 3 edited and approved the final manuscript.

Paper 4: Located in Chapter 2

Nolan MT, Russell DJ, Marwick TH. Long-term Risk of Heart Failure and Myocardial dysfunction after Thoracic Radiotherapy: A Systematic Review. Can J Cardiol. 2016; 32(7): 908-20.

Author 3 and Author 1 contributed by developing the original idea. The candidate (Author 1) performed a systematic literature review, created the tables and figure and wrote the majority of the manuscript. Author 2 also performed a systematic literature review, and results of literature reviews conducted by author 1 and author 2 were combined. Author 3 arbitrated any disagreements regarding study inclusion, edited and approved the final manuscript. All of the authors had full access to all data.

Paper 5: Located in Chapter 3

Nolan MT, Russell DJ, Negishi K, Marwick TH. Meta-Analysis of association between Mediastinal Radiotherapy and Long-Term Heart Failure. Am J Cardiol. 2016; 118(11): 1685-91.

Author 1 and Author 4 contributed by developing the original idea. The candidate (Author 1) performed a systematic literature review, used statistical software to perform the meta-analysis, created the tables and figure and wrote the majority of the manuscript. Author 2 also performed a systematic literature review, and results of literature reviews conducted by author 1 and author 2 were combined. Author 2 also assisted by

assessing for publication bias. Author 3 assisted with editing. Author 4 arbitrated any disagreements regarding study inclusion, edited and approved the final manuscript. All of the authors had full access to all data.

Paper 6: Located in Chapter 4

Nolan MT, Marwick TH, Plana JC, Li Z, Ness KK, Joshi VM, Green DM, Robison LL, Hudson MM, Armstrong GT. Effect of Traditional Heart Failure Risk Factors on Myocardial Dysfunction in Adult Survivors of Childhood Cancer. JACC Cardiovasc Imaging. 2018; 11(8): 1202-3.

Author 1 and Author 2 contributed by developing the original idea. Author 10 contributed the deidentified longitudinal data. Author 4 performed majority of the statistical analysis. The candidate (Author 1) wrote the study proposal, assisted with statistical analysis, analyzed the results, created the tables and figures and wrote the majority of the manuscript. Author 10 edited and approved the final manuscript. All of the authors had access to all data and reviewed and approved the manuscript prior to submission.

Paper 7: Located in Chapter 6

Nolan MT, Thavendiranathan P. Automation in Echocardiography. JACC Cardiovasc Imaging. 2019; 12(6): 1073-1092.

Author 1 and Author 2 contributed by developing the original idea. The candidate (Author 1) was the first author, and with author 2 designed the manuscript. Author 1 was responsible for literature review, writing the majority of the manuscript, creating figures and tables under the supervision of Author 2. Author 2 edited and approved the final manuscript. Both authors had access to all data

Paper 8: Located in Chapter 7

Nolan MT, Altaha MA, Hanson R, Thampinathan B, Amir E, Brezden-Masley C, Satriano A, Connelly K, Mikami Y, Michalowska M, White JA, Wintersperger BJ, Thavendiranathan P. Myocardial Remodeling Early during Cancer Therapy in women With Breast Cancer – A Cardiac MRI and Echocardiography Strain Study. *In process of submission.*

Author 1 and Author 13 contributed by developing the original idea. The candidate (Author 1) and author 2 were responsible for performing data extraction for 72% of cardiac MRIs performed, with remaining cardiac MRI study data extracted by Author 7, author 9 and author 11 at a second study site. Author 4 extracted the echocardiographic data. Data collection, statistical analysis, figure and table collection were performed by both the candidate and author 2 in an approximately 50:50 ratio. The candidate wrote approximately 60% of the original manuscript, with author 2 writing approximately 40%. Author 13 edited and approved the final manuscript. All of the authors had access to all data and approved the manuscript prior to submission.

Paper 9: Located in Chapter 8

Nolan MT, Altaha MA, Amir E, Koch A, Yip P, Michalowska M, Wintersperger B, Thavendiranathan P. Cardiotoxicity Phenotypes in Women with Early Stage Breast Cancer Receiving Cancer Therapy. *In process of submission*

Author 8 contributed by developing the original idea. The candidate (Author 1) extracted all diastolic data from all cardiac MRI studies. Both Author 1 and Author 2 extracted systolic data from all cardiac MRI studies. Author 1 performed the statistical analyses, created all figures and tables and wrote majority of manuscript. Authors 2, 3, 4, 5, 6 edited the manuscript. Author 7 edited and approved the final manuscript. All authors had full access to all data and approved the final manuscript prior to submission.

Paper 10: Located in Chapter 9

Nolan MT, Plana JC, Thavendiranathan P, Shaw L, Si L, Marwick TH. Cost-Effectiveness of Strain-Targeted Cardioprotection for prevention of chemotherapy-induced cardiotoxicity. Int J Cardiol. 2016; 212:336-45.

Author 1 and Author 4 contributed by developing the original idea. The candidate (Author 1) performed the systematic literature review, performed economic statistical analysis, created all tables and figures and wrote the majority of the manuscript. Author 4 provided guidance and education regarding how to conduct an economic analysis. Author 6 edited and approved the final manuscript. All authors had access to all data and approved the manuscript prior to submission.

We, the undersigned, endorse the above stated contribution of work undertaken for each of the published (or submitted) peer-reviewed manuscripts contributing to this thesis:

Signed:	Signed:	Signed:
Mark Travers Nolan Candidate Menzies Institute for Medical Research University of Tasmania	Professor Thomas Marwick Supervisor Adjunct Professor Menzies Institute for Medical Research University of Tasmania	Professor Alison Venn Head of School Menzies Institute for Medical Research University of Tasmania
Date: 8th November, 2019	Date: 25th February, 2019	Date: 06 March, 2019

Table of contents

List of Abbreviations

2D	Two-Dimensional
ACE	Angiotensin Converting Enzyme
CMR	Cardiovascular Magnetic Resonance
CTRCD	Cancer-Therapy-Related Cardiac Dysfunction
DecT	Deceleration Time
DNA	Deoxyribonucleic Acid
EBC	Early Breast Cancer
HD	Hodgkin's Disease
HF	Heart Failure
HFRF	Heart Failure Risk Factors
HR	Hazard Ratio
ICER	Incremental Cost-Effectiveness Ratio
IVRT	Isovolumetric Relaxation Time
GLS	Global Longitudinal Strain
LAVi	Indexed Left Atrial Volume
LGE	Late Gadolinium Enhancement
MUGA	Multi-planar Gated Acquisition scan
LV	Left Ventricle
LVEF	Left Ventricular Systolic Function
NS	Non-Significant
OR	Odds Ratio
QALY	Quality-Adjusted Life Year
RNA	Ribonucleic Acid
RNV	Radionuclide Ventriculography
RT	Radiotherapy
RV	Right Ventricle
RVEF	Right Ventricular Systolic Function
SD	Standard Deviation
SIR	Standardized Incidence Ratio
TTE	Trans-Thoracic Echocardiography

List of Tables

List of Figures

Abstract

Background: Cancer treatment-related cardiac dysfunction (CTRCD) and heart failure were first described in the published literature over 50 years ago. Once it was determined that CTRCD was frequently irreversible with a high mortality burden, cardiologists and oncologists worked together to utilize cardiac imaging to tailor anti-cancer treatments to reduce cardiac dysfunction risk. However, the guidelines established at that time predated several modern techniques for imaging the heart, and many cardiovascular treatments with demonstrated efficacy in reducing heart failure mortality were not available when traditional strategies for managing cardiac risk in cancer patients were established. Currently the morbidity and mortality of cancer-treatment-related cardiac dysfunction remains high, and there is now a strong evidence base supporting the concept of increased long-term risk of cardiac complications in the cancer survivor community.

Cardio-oncologists today now have a number of cardiac imaging techniques to choose from for the detection of CTRCD, including nuclear multi-plane acquisition scans (MUGAs), echocardiography and cardiac MRI (CMR). Several techniques themselves have recently introduced additional imaging features that allow for more thorough and accurate interrogation of cardiac function. There is currently a limited amount of high quality published scientific evidence evaluating the utility of these imaging techniques in the cancer population, which is reflected by the lack of a consensus among practitioners about which of these imaging modalities may be optimal. Given the significant differences in clinical information provided and risks of each technique, it is possible that one technique could more appropriate than the alternatives. While novel cardiac imaging techniques such as assessment of diastolic function and myocardial mechanics by CMR offer new insights into mechanisms of cardiac dysfunction, their utility in the cancer population is yet untested.

Aims: The work in this thesis is divided into four distinct sections. The **first section** is concerned with **recognizing CTRCD secondary to either chemotherapy or radiotherapy**. The first section aims to answer the following: 1) What is the frequency and optimal imaging timing of cardiac dysfunction secondary to chemotherapy? 2) What are the most frequent cardiac imaging abnormalities in patients treated with chest-directed radiotherapy? 3) What is the quantifiable increased risk of heart failure secondary to radiotherapy? 4)

Who should be tested – in particular, what is the impact of traditional heart failure risk factors on echocardiographic measurements of cardiac function?

The **second section** is concerned with identifying the **strengths and limitations of the two most frequently utilized cardiac imaging techniques** in Australia (MUGA and echocardiography) with the intention of determining whether one technique is likely to be superior to the other. The second section aims to answer the following: 5) how do MUGA and echocardiography compare in frequency of utilization, agreement in measurements and prediction of cardiac dysfunction in the cancer population? 6) Given the importance of accurate and reproducible LVEF measurements in the cardio-oncology population, can automation in echocardiography be utilized to improve patient outcomes?

Section 3 investigates the **use of novel imaging techniques** to provide additional information regarding pathophysiology in addition to traditional cardiac imaging techniques. Cardiac MRI (CMR) is not practical for routine cardiac imaging due to issues of cost and access but may be a reasonable adjunct to either echocardiography or MUGA to further guide treatment by identifying mechanism and phenotypes of cardiac dysfunction. The third section aims to answer the following: 7) Does the observed decline in LVEF as measured by CMR in breast cancer patients reflect preload reduction or reduced myocardial contractility? 8) What does CMR tell us about the phenotypic diversity of cardiac dysfunction secondary to breast cancer therapy?

The **final section** recognizes that cardiac imaging decisions do not occur based solely on clinical characteristics, and **issues of financial burden and quality of life** must be clarified before society can invest in widespread uptake. The fourth section asks the question: 9) What is the most cost-effective approach for preventing CTRCD?

Methods: These questions were addressed using a number of study designs. First, a **narrative review** of peer-reviewed published research describes the current state of cardiac dysfunction secondary to chemotherapy. Second, a **systematic review** was performed to quantify cardiac structural and functional changes secondary to chest-directed radiotherapy. Third, **a meta-analysis** was conducted to describe and quantify the increased

risk of heart failure secondary to chest-directed-radiotherapy as treatment for cancer. Fourth, the role of traditional heart failure risk factors was tested in a **cohort study** of adult survivors of childhood cancer, in which the effect sizes of clinical and echocardiographic changes were sought. Fifth, a **prospective cohort study** of 35 consecutive cancer patients judged by their treating oncologist to be at risk of CTRCD were recruited from a single regional Australian hospital. They underwent simultaneous oncologist-guided serial cardiac imaging with nuclear multi-plane acquisition (MUGA) scans and echocardiography performed by researchers at 3-month intervals over 12 months. Sixth, a **systematic review of published literature** regarding automation in echocardiography, limited to seven common echocardiographic measurement techniques, was performed and reported. In addition, strength of scientific evidence for each automated technique was assessed, and recommendations for implementation in echo labs is provided. Seventh, the effects of preload reduction (reduction in end-diastolic volume) or reduced myocardial contractility (increase in end-systolic volume) were evaluated in a **short-term cohort** of HER2+ve early breast (EBC) cancer patients satisfying criteria for CTRCD in serial cardiac MRI examinations and global longitudinal strain measurements by echocardiography. Eighth, a **longitudinal cohort design** was used to identify different phenotypes of cardiac response to potentially cardiotoxic chemotherapy in HER2+ve EBC patients. Ninth, a **Markov model** was used to assess the cost-effectiveness of different cardioprotective strategies.

Results: First, CTRCD is a relatively frequent complication of contemporary anti-cancer treatments and sequential cardiac imaging is advised for high-risk patients. **Second**, mediastinal radiotherapy is associated with long-term heart failure due to left ventricular systolic dysfunction, with limited information suggesting significant contribution from right ventricular systolic dysfunction. Despite previous reports in the literature, long-term diastolic left ventricular dysfunction was infrequent. **Third**, meta-analysis of available quality publications revealed that mediastinal radiotherapy approximately doubled the risk of heart failure (HR 1.83 [95%CI 1.09 to 3.08], p=0.022), but with significant heterogeneity between studies (I^2 88.5%). Meta-regression demonstrated that 80% of heterogeneity could be explained by differing age at time of radiotherapy and length of follow-up. **Fourth**, traditional heart failure risk factors were demonstrated to increase risk of long-term cardiac dysfunction on echocardiographic imaging after median of 22.6 years of follow-up.

Reduced 3D-LVEF was significantly associated with hypertension (OR 1.81 [95% 1.25 to 2.62]), reduced global longitudinal strain was associated with insulin resistance (OR 1.72 [95%CI 1.30 to 2.28]) and obesity (OR 1.58 [95%CI 1.19 to 2.11]) and diastolic dysfunction was associated with hypertension (OR 1.41 [95% 1.03 – 1.94]), insulin resistance (OR 1.44 [95%CI 1.08 to 1.92]) and obesity (OR 1.92 [95%CI 1.42 to 2.58]). These findings suggest that childhood cancer survivors with traditional heart failure risk factors may benefit from long-term monitoring of cardiac function. **Fifth**, it was determined; i) there was poor correlation between LVEF measurements by MUGA and echocardiographic techniques; ii) echocardiography found that 28% of patients had a significant decline in LVEF, whereas only 3% of patients were found to have LVEF decline by MUGA, and iii) relative change in GLS at 2 months was predictive of significant later LVEF decline, with receiver-operating curve demonstrating AUC 0.74 (95%CI 0.55 – 0.94). These results suggest that MUGA and echocardiography have large limits of agreement for LVEF measurements and that echocardiography may detect cardiac dysfunction earlier than MUGA. **Sixth,** current echocardiographic LVEF measurements suffer from low reproducibility, which reduces confidence in echocardiography-guided CTRCD diagnoses. One potential strategy for improving echocardiographic LVEF reproducibility is by increased utilization of automated measurement techniques. **Seventh,** a cohort of 83 patients with early HER2 +vet breast cancer was recruited, of which 15 patients (13.4%)developed CTRCD as defined by LVEF drop measured by CMR. Of these 12 cases (80%) were due to isolated increase in LVESV, 2 cases (13.3%) were due to concurrent increase in LVESV and decrement in LVEDV and 1 case (7.7%) was due to non-significant volume changes in both LVEDV and LVESV. No patients developed CTRCD due to isolated LVEDV reduction. These results suggest that preload reduction does not significantly contribute towards observed reduction in LVEF in breast cancer patients diagnosed with CTRCD. **Eighth,** of a cohort of 66 EBC patients, 13 (19.7%) developed systolic dysfunction, 13 (19.7%) developed diastolic dysfunction with 4 patients overlapping, and 44 (66.7%) had a phenotype characterized by absence of overt systolic and diastolic dysfunction with subclinical cardiac dysfunction diagnosed by examining myocardial mechanics. Patients with diastolic dysfunction were older, more likely to have hypertension, diabetes and be treated with higher chest-directed radiotherapy doses than patients with systolic dysfunction. **Ninth,** strain-guided cardioprotective therapy dominated the alternative strategies of universal cardioprotective therapy (gain of 0.15 Quality of Life Years (QALYs) and savings of

$1808 over 5 years) and LVEF-guided cardioprotective therapy (gain of 0.26 QALYs and savings of $2874 over 5 years) in a cost-effectiveness analysis, demonstrating that strain-guided cardioprotection is the most cost-effective approach for preventing CTRCD.

Conclusions: Contemporary cancer treatments may increase the risk of cardiac dysfunction. Traditional methods of screening for CTRCD are limited by suboptimal reproducibility and sensitivity. Novel cardiac imaging techniques, specifically echocardiographic myocardial deformation imaging, can offer additional information regarding subclinical cardiac dysfunction and may provide earlier diagnosis, information regarding aetiology and assist with guiding treatment with additional cost and QALY savings.

Acknowledgements

Being accepted into the PhD path at the Menzies Institute for Medical Research and the University of Tasmania has been simultaneously the greatest challenge of my life and the greatest honour I have received. I have been deeply touched by the faith in my potential that academic supervisors and staff have demonstrated and am grateful for the resources that have been made available to me, both material and time and energy of my colleagues. Without their assistance, this thesis would not have been possible.

I would like to single out several of my colleagues and friends to express my gratitude. I would especially like to thank my two supervisors, Professor Thomas Marwick and Dr Kazuaki Negishi, for the exceptional guidance and support that they offered me. Their tireless and caring mentorship was deeply appreciated.

Tom, thank you so much for all the assistance and time you have generously shared with me over the years. You have been an inspiration and a role model and have helped me understand what is means to be a caring and benevolent physician.

Kaz, I am grateful to you for the many times you went out of your way to help me with my projects. Your advice was valuable and many times it helped me find a path forward or see a new solution that I hadn't considered before. I am even more grateful for the selfless and generous way that you made yourself available, and for the patience that you demonstrated when assisting me. I will always remember how you helped me learn how to measure global longitudinal strain and how you made it exciting and enjoyable. Your patience in explaining to me how to perform statistical analysis was truly impressive, as I am sure many others would have given up in exasperation many hours earlier. I have only the fondest memories of studying alongside you and am sure you will succeed wherever you are.

I owe my deepest gratitude to Professor Paaladinesh Thavendiranathan for his clinical and scientific mentorship and guidance. I am thankful that he chose to take a chance on me by offering me training and research opportunities in Canada. Dinesh, thank you for the hundreds of hours that you spent teaching me how to report cardiac magnetic resonance studies and perform advanced statistical analysis. I am firmly committed to using the training you have selflessly provided to improving cardiovascular health and practice worldwide.

To Professor Gregory Armstrong and the SJLIFE team in Tennessee, thank you very much for partnering with me and generously providing insight and access to the St Jude Life cohort. Your kindness, professionalism and collegiality has provided me with a role model that I intend to use throughout my career as a clinician and researcher.

To my fellow PhD student co-travelers, Hilda, Ricardo, Leah, Quan, Ying, Mokoto and Tomoko, I will always remember fondly our time together. I enjoyed working on our combined projects, helping each other with advice. Travelling to Northern Tasmania with many of you for our population study was an adventure! I hope to work alongside some of you in the future but will regardless always be happy to see you.

I wish to extend my deep thanks to the Tasmanian TasELF team, including Di, Hannah, Jasmine and Jane for their hard work. Each of you went above the call of duty, and I for one am grateful. The high-quality research produced by the cardiometabolic unit at the Menzies Institute for Medical Research would not have been possible without each of you.

I would like to extend my thanks Professor Alison Venn, Associate Professor James Sharman, Professor Leigh Blizzard and Petr Otahal for your support generous assistance.

Thank you to my graduate research officers, Professor Wendy Oddy, Associate Professor Kristy Sanderson and Dr Costan Magnussen for your kind support, patience and understanding.

I would like to thank Lisa Riddell for her support over the past years. Her kind words, dedication and the level of care that she displayed for Professor Marwick's PhD students was touching. Lisa, all that you have done for us is truly appreciated.

Lastly, I would like to thank my family for their support and love over this shared journey together. Kate, I will always be grateful for your loving support and your inexplicable knack for making me laugh when I felt overwhelmed. Elliot, you have been my true joy over this period, and I hope that my journey might one day help inspire your own.

Financial Acknowledgements

I would like to thank the National Heart Foundation of Australia for providing me the Health Professional Scholarship (107850), which assisted my family and myself during this period.

I would like to thank the Hosinec family for providing me with the Hosinec Family Scholarship, which assisted in supporting me during my studies in Canada.

Preface

Successful advances in oncology have led to cancer patients living longer than ever before, but these cancer survivors are at risk of non-cancer related morbidity and mortality. Cancer survivors are at increased risk of many chronic health conditions, including secondary cancers, renal dysfunction, severe musculoskeletal problems, endocrinopathies, cardiovascular disease and anxiety or depression. Cardiomyopathy accounts for a significant proportion of cancer survivor morbidity.

Aims of this thesis.

This thesis was compiled as response to several contemporary aspects of cardio-oncology care; 1) cancer survivors are accounting for increasingly large percentage of Australian public; 2) contemporary treatments for common cancers confer increased risk of cardiac dysfunction and heart failure; 3) early treatment with cardioprotective medications has demonstrated benefit in preventing and reversing cancer-therapeutic-related cardiac dysfunction; 4) cardioprotective medications are less efficacious if administered at later stages of CTRCD and 5) currently there is substantial disagreement regarding which cardiac imaging technique to guide starting cardioprotective medication is superior.

Therefore, the main aims of this thesis are to determine the utility of different cardiac imaging strategies for CTRCD and identify the optimal approach for targeting cardioprotective therapies. We also sought to elucidate the competing manifestations of cardiac dysfunction in response to cancer treatments, identify different phenotypes of cardiac dysfunction and identify the most cost-effective approach to cardioprotection. In order to achieve that, the studies presented in this thesis aim to address the list of issues below. This list is in similar order to the thesis chapters.

- Which patient groups are at risk of CTRCD?

- How does the risk and presentation of CTRCD differ between different anti-cancer therapies?
- Is automation a reasonable strategy for earlier diagnosis of CTRCD?
- Does chest-directed radiotherapy also contribute towards CTRCD risk?
- What is the pathophysiological mechanisms underlying CTRCD?
- What are the different phenotypic manifestations of CTRCD?
- What is the most cost-effective strategy for targeting cardioprotection?

Structure of this thesis

Chapter 1: Background – review of current literature and summarising clinical evidence and knowledge gaps

Chapter 2: Systematic Review of effects of chest-directed radiotherapy towards CTRCD

Chapter 3: Meta-analysis of risk of heart failure with chest-directed radiotherapy as treatment for cancer

Chapter 4: Impact of traditional risk factors towards heart failure in the cancer survivor cohort.

Chapter 5: Prospective cohort of cancer patients evaluated with echocardiography and nuclear imaging.

Chapter 6: Strategies for improved cardiac imaging for diagnosis of CTRCD, including automation.

Chapter 7: Using cardiac MRI to determine the aetiology of CTRCD in a breast cancer cohort.

Chapter 8: Determining different phenotypes of cardiac dysfunction in a prospective cohort of early breast cancer patients.

Chapter 9: Use of Markov model to evaluate cost-effectiveness of competing strategies for cardio-protection.

Chapter 10: Summary and Conclusions

1.11 Sources of data used in this thesis

Data used for analysis for chapter 4 was derived from the SJLIFE study (Establishment of a Lifetime of Cohort of Adults Surviving Childhood Cancer) with the ClinicalTrials.gov identifier number NCT00760656. The SJLIFE trial had 4575 patients recruited at the time that data was analysed for this thesis.

Data used in chapter 5 was derived from a prospective cohort of 31 patients from the Royal Hobart Hospital presenting with cancer that would likely require treatment with potentially cardiotoxic anticancer therapies (Tasmanian Health and Medical Human Research Ethics Committee approval reference number H13115).

Data used for analysis in chapter 8 used 112 patients with early breast cancer recruited from 2 centres in Canada. 83 patients were recruited from the Princess Margaret Cancer Centre and Toronto General Hospital, after being recruited into the EMBRACE-MRI (evaluation of Myocardial Changes during BReast Adenocarcinoma Therapy to Detect Cardiotoxicity Earlier with Cardiac MRI) prospective cohort study with the ClinicalTrials.gov identifier number NCT02306538. 29 patients were recruited from the Stephenson Cardiovascular CMR Centre at the Libin Cardiovascular Institute of Alberta.

Data used in chapter 9 used 66 patients recruited from the Princess Margaret Cancer Centre and Toronto General Hospital, after being recruited into the EMBRACE-MRI (evaluation of Myocardial Changes during BReast Adenocarcinoma Therapy to Detect Cardiotoxicity Earlier with Cardiac MRI) prospective cohort study with the ClinicalTrials.gov identifier number NCT02306538.

Chapter 1

Background – The Clinical Problem

Part of the research contained in this chapter has been published as(1,2):

- Nolan MT, Lowenthal RM, Venn A and Marwick TH. Chemotherapy-related cardiomyopathy: a neglected aspect of cancer survivorship. *Intern Med J* 2014; 44(10) 939-50

- Thavendiranathan P, Nolan MT. An emerging epidemic: cancer and heart failure. *Clin Sci*. 2017; 131(2): 113-21

- Abdel-Qadir H, Nolan MT, Thavendiranathan P. Routine prophylactic cardioprotective therapy should be given to all recipients at risk of cardiotoxicity from cancer chemotherapy. *Can J Cardiol.* 2016; 32(7): 921-5.

Epidemiology of CTRCD

Successful advances in oncology over the past decades have led to cancer patients living longer than previously. The five-year survival rate for all cancers in the US has increased from 50% in 1975-1977 to 68% in 1999-2005(3). This success has also led to a large pool of cancer survivors who are at increased risk of non-cancer related morbidity and mortality. Chronic long-term health issues arising from cancer survivorship are becoming increasingly recognized as an important issue. In Australia it is estimated that 3.2% of the population are cancer survivors, which is equivalent to 654,977 patients(4). Cancer survivors are at increased risk of many chronic health conditions, including secondary cancers, renal dysfunction, severe musculoskeletal problems, endocrinopathies, cardiovascular disease and anxiety or depression. To date, the best long-term information on cancer survivorship comes from paediatric patients, who would be expected to have lower incidence of cardiovascular disease (CVD) than adult patients followed for the same period. One retrospective cohort study of paediatric cancer survivors over a mean of 17.5 years found a 73% prevalence of any chronic health condition, and 42% prevalence of any severe or disabling health condition(5). Compared with their siblings, cancer survivors had a three-fold increased risk for any chronic health condition, and an eight-fold increased risk of a severe or life-threatening health condition. They also had an increased risk of CVD, with a fifteen-fold increase seen in relative risk for congestive heart failure (RR 15.1, 95%CI 4.8-47.9). This increase in relative risk for a chronic condition was the second highest identified, suggesting that cardiomyopathy accounts for a significant proportion of cancer survivor morbidity.

These findings have been supported by observational studies of adult cancer survivors in whom cardiovascular disease is a leading cause of mortality, even when death due to cancer recurrence is taken into account(6). In addition to increased frequency, patients with heart failure due to cytotoxic therapy also have a three-fold higher mortality rate than those with idiopathic dilated cardiomyopathy(7). The link between cancer survivorship and CVD is likely multifactorial - being partly due to the overlap in risk factors for cancer and CVD (e.g. smoking, age), but is also attributable to well-documented cardiotoxic effects of contemporary chemotherapy(8,9).

It can therefore be appreciated that cancer-therapy-related cardiac dysfunction (CTRCD) is an under-appreciated and relatively frequent cause of heart disease in the Australian community. Sequential cardiac

imaging places substantial burdens on the patient and increases healthcare costs; however, the frequency of cardiac dysfunction after cancer therapies and the high rates of associated morbidity support the use of cardiac imaging.

Table 1-1: Potential cardiovascular complications of cancer treatment.

Cardiovascular complications.	**Examples of potential aetiological agents**
Vascular	
Hypertension	Chemotherapy (cis-platinum, anti-angiogenic agents)
Premature coronary artery disease	Radiation therapy
Arterial thrombosis	Chemotherapy, malignancy
Venous thrombosis	Tamoxifen, bevacizumab
Structural	
Conduction abnormalities	Anthracyclines, thalidomide
Valvular dysfunction	Radiation therapy
Pericardial effusion	Radiation therapy, anthracyclines
Constrictive pericarditis	Radiation therapy, surgery.
Myocardial	
Myocarditis	Cyclophosphamide, anthracyclines
Cardiomyopathy	Anthracyclines, trastuzumab, mitoxantrone.

Subtypes of CTRCD

Overview: Two broadly different patterns of cytotoxicity have been recognized, and it has been prognostically useful to categorize cardiotoxic cancer drugs into groups based on these patterns. Type I cardiotoxicity refers to the effects of drugs that cause acute myocyte injury (as measured either by biomarkers or endomyocardial biopsy) causing irreversible damage and depressed cardiac function on a dose-dependent basis(10). Re-initiation of the offending drug is usually contraindicated, and even in the absence of re-exposure, a gradual and progressive deterioration of function has been reported, perhaps explained by concurrent sources of myocyte damage (see below). Anthracyclines are the prototype for this category of drug reaction. In contrast, type II cardiotoxicity refers to a pattern of often reversible cardiomyopathy with no evidence of acute myocyte injury, is not dose-dependent and re-initiation of the offending drug is usually not contraindicated. Trastuzumab is an example of an agent that could potentially cause type II cardiotoxicity. Another example of

a group of agents implicated in type II cardiotoxicity are the growth factor inhibitors, for example sunitinib, where left ventricular dysfunction appears to be mediated by hypertension(11).

This distinction between type I and type II cardiotoxicity remains clinically relevant, as they have different LVEF thresholds beyond which cancer treatment should be ceased(12). It is worth noting that the boundaries of these groupings remain unclear, and the cardiotoxic reversibility of several of these agents remains debated(13). Additionally, further studies have found that mean LVEF of traztuzumab-treated patients may remain depressed by absolute value of -3.8% at 3 years, suggesting that an element of irreversible dysfunction persists. This raises the possibility that this Type I and Type II classification of 2 arbitrary categories may be simplistic(14). It is anticipated that future research may lead to the ability to phenotype CTRCD due to intracellular pathways and histopathological findings, but until then the Type I and II categorisation based on cardiac imaging findings remains the most practical and easily communicated approach, and we will utilize it for the purposes of this chapter. Table 2 summarizes the forms and frequencies of cardiotoxicity profiles observed with different chemotherapeutic agents. For purposes of clarity, we will discuss anthracyclines and trastuzumab as representatives of class I and class II cardiotoxicity respectively.

Type I cardiotoxicity (anthracyclines): The widespread use of anthracyclines began in the 1970's, and this family of drugs remain commonly used for breast cancer, leukemias, lymphomas and sarcomas. Initial high-dose use was limited by myelosuppression, but this was largely reversible after drug discontinuation. Cardiomyopathy has since been found to be a more insidious and potentially fatal complication. Recent prescribing patterns show a fall in anthracycline use(15). This fall has a number of probable explanations, including concern regarding late cardiomyopathy and improvements in availability of alternative effective cytotoxic agents, particularly for breast cancer(16,17).

Anthracyclines exert their antineoplastic effect by intercalating with DNA and then inhibiting the topoisomerase II enzyme, thereby preventing synthesis of RNA and DNA(18). They exert their cardiotoxic effect through oxidative damage, generated by the anthracycline forming a complex with iron, which in turn catalyzes free radical production. The free radicals then act within the cell to cause membrane disruption and

cellular dysfunction. Myocytes are especially vulnerable to oxidative damage, as they lack the catalase or glutathione reductase enzymes, which could act as reserves for managing oxidative stress. Agents that protect against free radical damage, such as dexrazoxane, have been trialed with some success in preventing chemotherapeutic cardiotoxicity. However, due to concerns that dexrazoxane may reduce the anti-cancer efficacy of anthracyclines, this approach has not been widely adopted(19). An alternative, or possibly complementary, mechanism of cardiac damage is by disabling topoisomerase-IIβ, an isoform relatively specific to myocytes(20).

The risk of anthracycline cardiotoxicity is proportional to the cumulative anthracycline dose. One pivotal study showed that for total doxorubicin-equivalent dose of <400 mg/m^2 the risk of cardiotoxicity was 0.14%, for 400-700 mg/m^2 the risk was 7% and of doses >700 mg/m^2 the risk was 18%(21). It is likely that the real-life incidences of cardiotoxicity are higher, as this trial did not have a long follow-up period nor access to modern echocardiography, and changes in patient populations in the past 30 years mean that older patients with more cardiovascular comorbidities are now being treated with chemotherapy. There is strong evidence of acute cardiac injury at the time of anthracycline administration(22). Myocardial biopsies taken in the peri-chemotherapy period show characteristic cardiotoxic changes, including sarcoplasmic reticulum ballooning, depletion of myofibrillar apparatus and vacuole formation(23). Additionally, biomarker assays reveal troponin elevations in the same time frame(22). However the timeline of development of cardiotoxicity shows steady incremental gain, with prevalence increasing from 11% at 1 year, to 14% at 2 years and 20% at 5 years(24). One case report describes a patient who developed severe anthracycline cardiotoxicity (on the basis of exclusion of alternative diagnoses) 17 years after treatment with a low-to-moderate cumulative dose(25). The discrepancy between acute myocyte injury and risk of long-term cardiomyopathy suggests the possibility that anthracyclines may “prime” the heart for dysfunction, a process described in the “multiple-hit” hypothesis of heart failure development(26).

In comparison with other cardiomyopathies, anthracycline-cardiotoxicity appears to have a substantially worse prognosis, with mortality rates up to 60% at 2 years(7). The hazard ratio for mortality for anthracycline-cardiotoxicity has been reported as being over three-fold that of idiopathic dilated cardiomyopathy. The number of Australians alive in 2007 who had been diagnosed in the past 26 years with a cancer that was likely to be

treated with anthracyclines (e.g. breast cancer, hematological malignancies, sarcomas) was over 197,000, i.e. 0.9% of total Australian population(4). Hence, the combination of a large at-risk pool, delayed yet steadily increasing risk of cardiotoxicity years after treatment and resultant high mortality means that CTRCD may be an under-recognized problem that could account for a meaningful proportion of the national morbidity and mortality of heart failure.

Type II cardiotoxicity (trastuzumab): Trastuzumab is a monoclonal antibody against the human epidermal growth factor receptor tyrosine kinase (HER2-erbB2), which is a member of a cell-receptor family that aids in regulating cell growth and intracellular repair(27). Overexpression of HER2 receptor occurs in approximately 25% of breast cancers and confers increased proliferative and metastatic potential. Trastuzumab has been used in HER2+ve breast cancers, with significant reductions in recurrence rates and overall mortality, with a pivotal study in the metastatic setting demonstrating a 33% reduction in mortality at 1 year and a 5-month increase in median survival(9).

Trastuzumab's mechanism of cardiotoxicity remains unclear, but the established importance of HER2-ErbB2 complex in normal cardiac function and development suggests possible explanations(28). Erb-B2 is a co-receptor for other ErbB tyrosine kinase receptors, which activate specific pathways on dimerization. Cardiac endothelial cells release a glycoprotein called neuregulin-1, which binds to ErbB4 receptor, which heterodimerizes with the trastuzumab target, ErbB2, to activate downstream intracellular signaling pathways, namely the ERK-MAPK (extracellular signal-regulated kinase - mitogen-activated protein kinase) and PI3K (phosphatidylinositol 3-kinase) pathways. These pathways promote cardiomyocyte proliferation, contractile function and myocyte survival(29). In mice, germline deletion of ErbB2, ErbB4 or neuregulin-1 genes causes failure of embryonic ventricle formation. It is possible that trastuzumab-mediated disruption of these pathways generates a pro-apoptotic state that could lead to cardiac dysfunction after additional insult. This is supported by the absence of microscopic myocyte changes after trastuzumab administration(28). Other possible cardiotoxic mechanisms include antibody-dependent cell-mediated cytotoxicity, interactions with other chemotherapeutic agents, disordered cellular homeostasis (e.g. calcium regulation) that causes increased sensitivity to increased afterload, or by causing structural change and gain of signaling function of ErbB2.

Trastuzumab has been associated with cardiotoxicity, but its true intrinsic cardiotoxicity remains debated(13). The original trials showed significant reductions in left ventricular ejection fraction (LVEF) in up to 27% of patients, with symptomatic heart failure seen in 5%, but this trial involved trastuzumab being administered concurrently with anthracyclines(9), and it has been historically difficult to disentangle trastuzumab cardiotoxicity from anthracycline cardiotoxicity as many patients receive both. However, the trials that have imposed the longest intervals between anthracycline and trastuzumab therapy have reported the lowest rates of cardiotoxicity. One trial that compared an anthracycline-and-trastuzumab arm with a trastuzumab-alone arm found that the incidence of congestive heart failure was five fold higher in the anthracycline arm than in the trastuzumab alone arm (2.0% vs. 0.4%)(30). Interestingly amongst 10,000 patients who received trastuzumab as adjuvant therapy, only a single cardiac death was recorded(31). In the same trial, asymptomatic LVEF decrease occurred in 8%-10%, and approximately half demonstrated LVEF recovery and had trastuzumab reinitiated.

Overall, trastuzumab monotherapy appears to have a lower than expected incidence of cardiotoxicity, with no characteristic histopathological findings on endomyocardial biopsy(28). Regardless of the intrinsic cardiomyopathic potential of trastuzumab, there is clearly a synergistic effect with anthracyclines. The mechanism underlying this may be that trastuzumab turns off previously described cellular pathways required for repair of subclinical anthracyclines damage, thereby unmasking a pre-existing cardiomyopathy. Evidence that anthracycline administration upregulates HER2- receptor concentration supports this possibility(32).

Screening for cardiotoxicity: Current professional society guidelines support the use of cardiac imaging to screen for cardiotoxicity. The European Society of Cardiology guidelines for the diagnosis and treatment of acute and chronic heart failure (2012) advise both pre-and post-chemotherapy screening of LVEF(33). Responses to the development of LV dysfunction include treatment for systolic heart failure and cessation of chemotherapy. A position statement from the Heart Failure Association of the ESC (2011), further elaborates: "Regular cardiovascular evaluation should be part of routine care in patients receiving treatment regimens known to be associated with significant cardiotoxicity, and follow-up beyond the completion of chemotherapy should be considered, especially in those receiving high-doses of anthracyclines". In neither of these documents

is there a suggested modality for screening, a suggested timeframe or cut-offs for treatment. In USA, the ACC/AHA 2005 guideline update for diagnosis and management of congestive cardiac failure in the adult specifically recommends echocardiography as an imaging modality, but is similarly vague in terms of screening timeframes and cut-off points(34).

Sequential LVEF measurement is a common theme in professional society recommendations. However, a reduction in LVEF is likely a final step in a long-standing cardiomyopathic process, and the use of LVEF may therefore result in missing a window for earlier treatment. It has been reported that up to 58% of patients with CTRCD fail to recover LV systolic function despite appropriate treatment(22). The existence of a latent stage appears supported by the biomarker evidence of myocyte injury and late cardiac decompensation. The model proposed by 2005 ACC/AHA guidelines suggests that cardiomyopathy follows a predictable sequence of stages(34). The majority of chemotherapy-treated patients would be considered equivalent to stage A, i.e. at high risk of future development of cardiomyopathy. In the absence of screening, patients likely would not come to medical attention until they became symptomatic (stage C). Evidence of LV dysfunction characterizes stage B. Screening for stage B HF would detect patients at an earlier stage and enable earlier treatment. To extrapolate from the Framingham study, 26% of patients in stage B heart failure progressed to symptomatic heart failure over 5 years(35), so a strong case can be made for treating asymptomatic cardiotoxicity if it can be diagnosed early.

Table 1-2: Categories of chemotherapeutic agents associated with cardiomyopathy and description of observed pathology

Drug	Class	Cancer	Cardiotoxicity		Frequency	Histology	Cardio-vascular mortality	Ref
			Acute	Chronic				
Type I Cardiotoxicity								
Adriamycin	Anthracyclines (interfere with DNA and RNA synthesis)	Breast Leukemias Lymphomas Sarcomas	Uncommon and not usually life-threatening (approx. 3%)[1] Includes atrial fibrillation, acute heart failure, myocarditis and acute coronary syndromes.	Cardiomyopathy	Dose-dependent, approximately 5% at adriamycin dose 400-450 gm/m^2	Sarcoplasmic reticulum dilatation, Vacuole formation Myofibrillar dropout	Heart failure mortality 60% at 2 - 3years	Wojnowski et al(36) Felker et al(7)
Mitoxantrone	Anthracenedione (disrupts DNA and RNA replication)	Advanced, hormone-refractory prostate cancer	Rarely acute heart failure.	Cardiomyopathy	2-3%	Sarcoplasmic reticulum dilatation Vacuole formation Myofibrillar dropout[2]	Not reported	Murray et al[75] Benjamin et al[76]
Cyclophosphamide	Alkylating agent (promotes DNA cross-linking)	Leukemias Lymphomas Breast cancer Ovarian cancer Non-small cell lung cancer	Hemorrhagic myocarditis Coronary spasm	Nil	5-19% for high-dose regimens[1]	Interstitial edema, Extravasation of lymphocytes No inflammatory infiltrate	Up to 40%	Katayama et al(37)
Type II Cardiotoxicity								
Trastuzumab	Monoclonal antibody (targets HER2 receptor)	HER2 +ve breast cancer	Nil	Cardiomyopathy			Low (likely <1%)	
Sunitinib	Tyrosine-kinase inhibitor (predominantly anti-angiogenic)	Renal-cell carcinoma GI stromal tumors	Hypertension	Hypertension Cardiomyopathy	47% hypertension 15% cardiotoxicity 8% clinical heart failure	Myocyte hypertrophy Swollen mitochondria No inflammation, fibrosis or nexrosis[2]	1%	Chu et al(11)
Lapatinib	Small molecule	Breast cancer	Nil	Cardiomyopathy	1.6% clinical heart failure or LVEF drop >20%[1] 0.2% clinical heart failure	Not available	Low	Perez et al (38)

	inhibitor of HER2-ErbB2 receptor							
Imatinib	Tyrosine kinase inhibitor	CML GI stromal tumors	Nil	Cardiomyopathy	0.6% clinical heart failure	Not available	Low	Atallah et al(39)
Ponatinib (investigational agent)	Tyrosine kinase inhibitor	CML Philadelphia-positive acute lymphoblastic leukemia	Arterial thrombosis	Unknown	3% acute serious arterial thrombotic events	Not available	Low	Cotres et al(40)

Proposed Screening Modalities.

ECG: Due to their low cost, ready availability and provision of additional diagnostic information (e.g. heart rate, rhythm), ECGs have been studied for signs of cardiotoxicity. They are effective in detecting acute cardiotoxicity, which is often associated with rhythm disturbance, heart block, ischaemic changes or pericarditis (Table 1-3). However acute anthracycline cardiotoxicity is infrequent (approx. 1%), usually reversible, not life-threatening and probably not predictive of later cardiac events(36). Reductions in QRS voltage have been reported in the peri-anthracycline period, but this is not predictive of future events(41). There is currently no evidence suggesting that ECG monitoring has a role in identifying patients at risk of future chemotherapy-related cardiomyopathy.

Biomarkers: Histopathological evidence of acute myocyte injury at time of chemotherapy has led researchers to examine troponin as a biomarker for identifying patients at high risk of developing cardiomyopathy. Approximately a third of chemotherapy patients will have a detectable troponin rise in the peri-chemotherapy period(42). Several studies have found an association between perioperative troponin rise and LVEF decline, future cardiac events and response to HF treatment(22). A frequently cited study recruited 703 cancer patients and collected troponin levels at two timepoints, one shortly after chemotherapy and one 1 month later(43). Over a follow-up of 20 months, patients in whom both troponin levels were <0.08 ng/mL had a 1% cumulative rate of cardiac events, compared with 84% rate in patients with two troponin levels ≥0.08 ng/mL. In contrast, another study examined 81 HER2-+ve breast cancer patients, and found that troponin level > 30 ng/L was only modestly predictive of future cardiomyopathy, with PPV of 44% and NPV of 77%(44). Although the information to date suggests that troponin testing holds promise, larger trials incorporating control groups and blinding in regard to assignment to treatment groups are needed.

MUGA: Multi-acquisition gated scintigraphy (MUGA) scans are frequently used for the assessment of LVEF in patients receiving chemotherapy. They have the advantages of being accessible, accurate and reproducible with low inter-observer variability(45). Their disadvantages include being more costly, radiation exposure (approx. 8-12 mSv), the lack of additional diagnostic information obtainable from other modalities (e.g. diastolic function, valvular function) and being insensitive for cardiac dysfunction

before LVEF decline. Recent studies have also raised concern regarding the precision of MUGA-derived LVEF measurements, with limits of agreement with the gold standard of cardiac MRI being reported as wide as -19.4% to +16.0%(46).

Echocardiography: Echocardiography is the most frequently used imaging modality for screening for chemotherapy-cardiotoxicity and is specifically referred to in several guidelines as the imaging modality for this context(34). It is inexpensive, accessible, does not involve radiation exposure and provides other useful diagnostic information. Its main disadvantage is that it is operator-dependent. Two-dimensional imaging has significant test-retest variation, such that the minimum LVEF decrement for which observers can state with 95% confidence is a true LVEF decline is at least 10%(47).

Three-dimensional echocardiography is more accurate than two-dimensional echocardiography for measuring LV volumes, with significantly less test-retest variation. One study of 50 HER2-+ve breast cancer patients compared correlation between two-dimensional echocardiography and CMR with three-dimensional echocardiography with CMR, and found that the correlation coefficient improved from r=0.69 with 2D-TTE/CMR to r=0.95 with 3D-TTE/CMR, confirming the incremental higher accuracy and reproducibility of 3D-TTE(48). Further studies are required to determine the strength of correlation between LVEF measured by 3D-TTE and clinical outcomes. Again, both standard 2D and 3D imaging are dependent on accurate contouring of LV.

Speckle-tracking strain imaging: Strain is a unitless measure of the deformation of the myocardium. The reduction of longitudinal strain appears to be an initial step in the development of many early cardiomyopathic processes, with the LVEF preserved by compensatory increases in other strain parameters. Hence detection of reductions in global longitudinal strain can potentially detect derangements in systolic myocardial mechanics before LVEF decline and could lead to earlier detection of patients at risk of developing chemotherapy-related cardiotoxicity. Several studies support this hypothesis. A significant reduction of global longitudinal strain (>10% from baseline) after 3 months has been reported to predict future cardiotoxicity diagnosis with sensitivity of 78-79% and specificity of 79-82%(44). This appears to be a promising technique with the potential for earlier accurate diagnosis

of cardiotoxicity. A randomised trial comparing the strategy of using strain imaging to guide treatment compared with standard sequential LVEF measurements is currently underway(49).

Cardiac Magnetic Resonance (CMR): CMR is currently the gold standard for measuring myocardial volumes and masses, due to its excellent endocardial definition, ability to image in any plane and excellent spatial resolution. It also has the ability to image myocardial scarring by using gadolinium contrast, and new experimental techniques hold the promise of quantifying diffuse myocardial fibrosis. The use of CMR in screening for chemotherapy-related cardiomyopathy is limited by cost, access and contraindication for patients with metallic implants. Additionally gadolinium administration is contraindicated for patients with significant renal dysfunction. Although used primarily in detecting LVEF reduction (with the same considerations about the limitations of LVEF), strain measurement is possible with CMR and methods have been described to identify cardiac oedema. The value of late-gadolinium enhancement (LGE) in chemotherapy-related cardiotoxicity also remains unclear, with some studies suggesting a typical pattern of lateral subepicardial enhancement, and other studies suggesting that LGE is rarely seen in this condition (50). Presently, the role of CMR in routine screening for chemotherapy-related cardiomyopathy is not supported outside of a clinical trial.

Prevention of cardiotoxicity.

Cardioprotective medications (i.e. ACE inhibitors, β-blockers) appear to prevent or delay the progression of this problem, and early stages of this condition appear to respond well to these agents(22). Alterations to the chemotherapy regimen can substantially reduce the risk of cardiotoxicity, although there is the possibility of a trade-off of reduced anti-neoplastic efficacy. Reducing the total cumulative dose of cardiotoxic anti-cancer treatments certainly reduces the risk of cardiotoxicity(51). Using longer infusions (at least 6 hours) reduces cardiotoxic risk, but places extra demands on the patient and hospital resources. Epirubicin, a semi-synthetic anthracycline analogue, is recorded to have a lower incidence of cardiotoxicity than doxorubicin, with up to an extra 33% chemotherapy cycles allowed before epirubicin cardiotoxicity rates equal those of doxirubicin(51). Liposomal preparations of anthracyclines are also

less cardiotoxic, putatively due to an increased molecular size making the agent less diffusible over well-formed vasculature (e.g. myocardium) but retains the ability to diffuse across poorly differentiated vasculature (e.g. cancer tissue). Lastly, dexrazoxane is an anti-oxidant agent that lowers the risk of cardiotoxicity when given concurrently with anthracyclines(51). Although its efficacy in reducing cardiotoxic risk is robust(19), one trial that showed a reduced anti-neoplastic effect when given with anthracyclines(51) has led to current recommendations that it only be used in the treatment of metastatic cancers.

Cardio-protection against CTRCD

There is substantial heterogeneity in approaches to screening for CTRCD throughout the world, which has led to diagnostic confusion and possible waste of resources. This thesis aims to identify a high-yield cardiac imaging strategy that will allow earlier and more effective treatment of CTRCD. For screening with cardiac imaging to be effective, however, there is a requirement for effective treatment that alters the natural history of the disease.

Several agents have been shown to improve outcomes with CTRCD. The OVERCOME trial randomized 90 patients with malignant hemopathies, majority of whom were treated with anthracyclines, to prophylactic enalapril and carvedilol versus observation(52). A reduced composite outcome of death, heart failure or final LVEF<45% was found in the treatment group (6.7% vs. 24.4%, p=0.02). Statins may also offer protection against LV dysfunction(53). A recent meta-analysis suggested that ACE inhibitors, β-blockers, statins and dexrazoxane have similar efficacy in preventing CTRCD(19), and may be considered for preventing progression of CTRCD. Provided that LV function recovers, it would be prudent for these patients to have long-term regular cardiac monitoring and follow-up to monitor for cases of late onset.

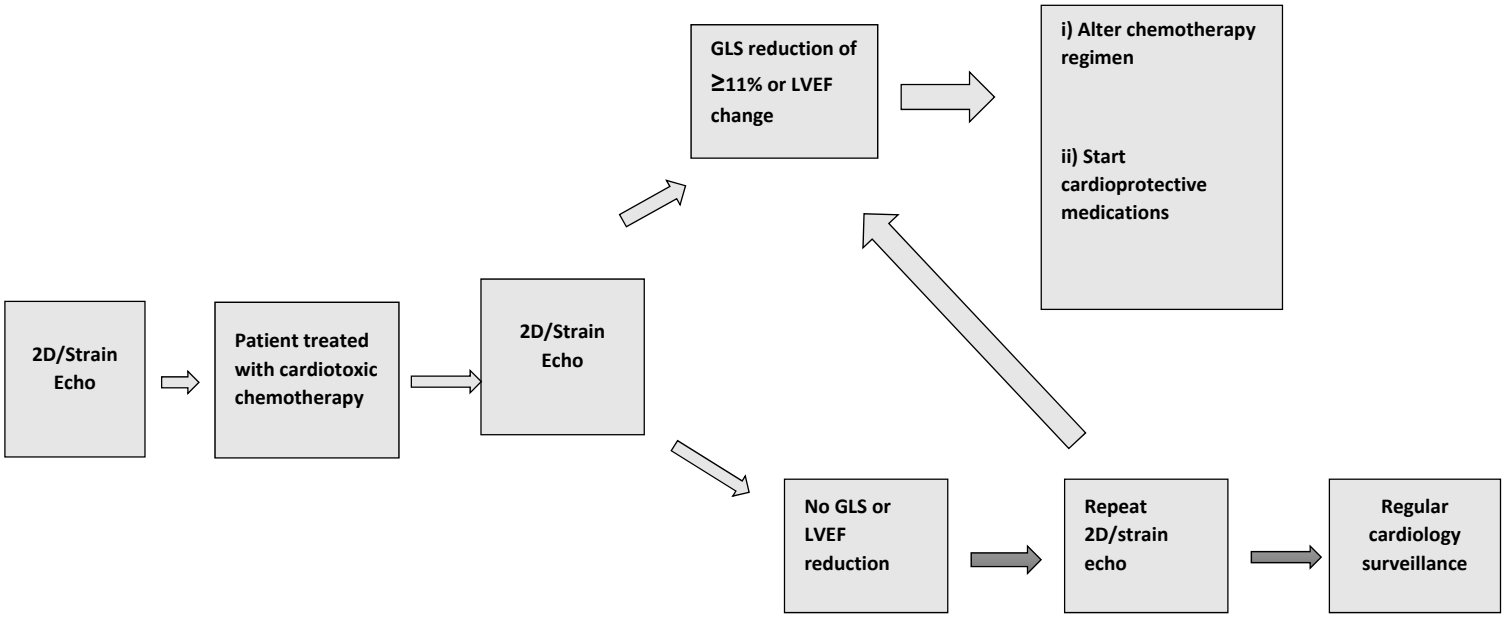

Figure 1-1: Suggested screening and treatment algorithm for patients treated with chemotherapy regimens associated with chemotherapy-related cardiomyopathy. 2D- two-dimensional; GLS- global longitudinal strain; LVEF – left ventricular ejection fraction

Concluding Remarks

This chapter provides an overview of the burden of CTRCD and utility of standard cardiac imaging techniques used for diagnosis. The following points summarise the main findings of scientific literature to date; 1) there is a substantial population of cancer survivors alive in Australia who are at risk of CTRCD; 2) CTRCD is a source of significant morbidity and mortality amongst the cancer survivor population; 3) earlier treatment of CTRCD with cardio-protective medications prevents adverse cardiac events, and this effect is attenuated with later administration of cardio-protective medications; 4) contemporary definitions of CTRCD are dependent on accurate LVEF measurements, which represent a late stage of the disease and 5) novel cardiac imaging techniques, such as global longitudinal strain, may permit earlier and more effective treatment of CTRCD, leading to better outcomes for cancer survivors (‘figure 1).

Postscript

The next chapter aims to assess the effect of chest-directed radiotherapy on cardiac function and attempt to determine whether patients who receive significant cardiac irradiation represent an at-risk group for long-term heart failure who may merit an early interventional strategy with cardioprotective medications.

Chapter 2

Risk of Cardiac Dysfunction from Chest-Directed Radiotherapy

Part of the research contained in this chapter has been published as(1,2):

- **Nolan MT**, Russell DJ and Marwick TH. Long-term risk of heart failure and myocardial dysfunction after thoracic radiotherapy: a systematic review. Can J Card 2016; 32(7): 908-20.

Preface

Chemotherapy and radiotherapy represent the two primary non-surgical approaches to treating cancer. The role of chemotherapy in causing CTRCD has previously been discussed, but the association between radiotherapy and CTRCD is less well understood. Many small breast cancers without lymph node involvement (i.e. stage 1) may be treated by surgery and radiotherapy without chemotherapy. Assessment of cardiac complications in context of radiotherapy alone can determine whether screening with cardiac imaging should be extended to this population, and which modalities would be most appropriate.

Abstract

Background: Chest irradiation is a commonly used treatment for malignancy, with demonstrated symptomatic and survival benefit. The frequency and presentation of cardiovascular complications of radiotherapy remains unclear.

Methods: We performed a systematic review to evaluate the prevalence and manifestations of myocardial dysfunction (asymptomatic and symptomatic) in long-term cancer survivors treated with radiotherapy.

Results: Thoracic radiotherapy is associated with increased risk of heart failure in long-term follow-up, with hazard ratios ranging from 2.7 to 7.4 for Hodgkin lymphoma, and 1.5-2.4 for breast cancer. Although ejection fraction is often normal, systolic dysfunction has been more widely reported with modern techniques including 2-dimensional speckle strain and cardiac magnetic resonance. This might have implications for the selection of patients for cardioprotection. Despite common emphasis, diastolic functional abnormalities were infrequent in the long term. A limited amount of data suggest that right ventricular dysfunction is important in this population.

Conclusions: The reports were heterogeneous, used different treatments, end points, and definitions of myocardial dysfunction, and most studies on the cardiac consequences of radiotherapy involved small numbers of patients and were published decades ago, making it difficult to formulate definitive conclusions for the current era.

Introduction

Radiation therapy (RT) is currently used in management of up to 50% of cancer patients, with over 100,000 courses of RT administered in Canada in 2010 (54). Significant RT-induced reductions in cancer recurrence and mortality have been demonstrated (55), but this success is partially offset by long-term complications. RT has been associated with damage to all components of the cardiovascular system, including myocardial, valvular, conduction and pericardial diseases (56). The relationship between RT and certain cardiovascular diseases has been well-characterized. For example, a large case-control study has demonstrated a relative 7.4% increase in major coronary events per Gy over 5 decades (57), and a large nested case-control study demonstrated an incidence of 12.4% for at-least moderate valvular heart disease in patients who received >35 Gy over 30 years (58). However, the relationship between radiotherapy and myocardial disease is less clear, with diastolic dysfunction and restrictive cardiomyopathy (56,59) commonly cited as common manifestations, often on the basis of single studies.

Heart failure (HF) represents a serious healthcare burden, with 54,333 HF hospitalizations in Canada in 2005/2006 alone (60). Due to a clearly identifiable population of patients and onset of risk, RT-induced myocardial disease might represent an opportunity for effective preventative screening, but consensus statements by professional guidelines have been inconsistent. According to recent HF guidelines (61), previous chemotherapy represents a HF risk factor and confers a Stage A Heart Failure status, but no specific guidance is given for patients treated with RT. The European Society of Medical Oncology 2010 guidelines (62) state that "RT-induced risk is lifelong and requires long term follow-up", but also note that "follow-up protocols are based on departmental or personal experience". Expert consensus from the American College of Cardiology and European Association of Cardiovascular Imaging suggest echocardiography at ten years post-RT, with subsequent echocardiograms every 5 years (63), but further guidance regarding high-risk populations, disease manifestations and prevalence are needed to guide screening. The purpose of this systematic review is to summarize the existing scientific literature regarding the type and prevalence of long-term myocardial dysfunction and heart failure after RT for malignancy, so to assist in guiding future screening and management.

Methods

We followed the Preferred Reporting Items for Systematic Reviews and Meta-Analyses (PRISMA) guidelines for reporting the systematic review(64). The search strategy was designed prospectively. PubMED and EMBASE were searched from inception to July 2015. Citations and details were stored in a database (EndNote X7.4, Thomson Reuters, New York, NY).

Search criteria. Due to the potentially large number of variables, including different malignancies, different cardiac imaging techniques or outcomes and different treatment descriptions (e.g. radiotherapy, chemoradiotherapy), a liberal search strategy was employed to increase sensitivity. Two reviewers conducted a literature search of Medline/PubMed and EMBASE for published reports that investigated cohorts of cancer patients treated with mediastinal radiotherapy for subclinical for clinical myocardial dysfunction, including heart failure for all years from inception to 2015. Papers were limited to those published in English. References of publications and relevant papers were also searched for further reports.

Inclusion criteria: Publications in peer-reviewed, English-language journals evaluating long-term myocardial function after radiotherapy were included in this systematic review if they met the following criteria: 1) average patient age (either median or mean) of ≥18 years at time of RT administration, 2) administration of RT therapy for cancer, 3) quantification of myocardial function, either by using noninvasive cardiac imaging to report ventricular function, or reporting outcome of symptomatic heart failure as a specific outcome of study design, 4) presence of a time interval of at least 5 years between RT and measurement of myocardial function. Exclusion criteria included 1) studies not meeting all of the inclusion criteria, 2) non-human studies and 3) abstracts or conference proceedings. No restrictions were applied to the types of patients, study's country of origin or type of institution where outcomes were evaluated.

Outcomes: For selected studies reporting subclinical myocardial dysfunction, primary outcomes were cardiac imaging parameters that quantified the degree of myocardial dysfunction, including but not limited to, left ventricular ejection fraction and volumes, measures of diastolic dysfunction and

myocardial deformation measurements. For selected studies reporting the outcome of clinical myocardial outcome, primary outcome was cumulative incidence of heart failure and measure of effect size associated with mediastinal radiotherapy (reported as odds ratio, relative risk or hazard ratio).

Data extraction: Data were extracted by one review author (M.N.) and checked by a second review author (D.R.) Discrepancies between review authors were resolved by consensus or, if necessary, by a third author (T.H.M). Information on publication year, sample size, type of malignancy, average age (either median or mean), gender ratio, total radiation dose (mean or median), follow-up and outcome findings were extracted independently from every study.

Results

Study selection. From the original screening set of 7,329 papers, 766 were deemed suitable for abstract review, to which a further three papers were added from bibliographic review of review articles (Figure 1). From the 176 papers reviewed, 38 contributed data to this analysis.

Mediastinal irradiation for Hodgkin's Disease. Twenty-one studies (1,659 patients), were identified as fitting inclusion criteria for investigation of long-term ventricular function after mediastinal irradiation for Hodgkin's disease. Sixteen were over a decade post-publication and 5 were ≥30 years post-publication. Ten used transthoracic echocardiography (TTE) as the non-invasive imaging testing modality, eight used radionuclide angiography (RA), 2 utilized both TTE and RA, and one utilized cardiac MRI (CMR). The differing modalities, different endpoints and definitions of ventricular dysfunction precluded performance of a meta-analysis.

Table 2-1: Summary of studies that have investigated systolic or diastolic function over 5 years after mediastinal radiotherapy for Hodgkin's Disease

First author, Year, (Ref.#)	Imaging	Patients (n)	Age at RT	Women (%)	Total Radiation Dose	Follow-up	Findings
Groarke et al, 2015 (65)	Rest TTE	263 (153 had TTE)	30±12.4 years (mean±SD)	54%	38 Gy (IQR 36-40)	19 years (median)	Mean diastolic parameters for RT patients within reference range No comparison with control diastolic values.
Chen et al, 2014 (66)	Rest/stress TTE	182	28.5 (median)	60%	39.6 Gy	15 years	26 (14%) had LVEF<55%
Machann et al, 2011 (67)	CMR	31	21 (median) (range 6-41)	42%	40 Gy (median)	24 years median (range 20-28)	Mean LVEF 48±3%; 23% had LVEF<55% 29% had LGE
Tsai et al, 2011 (68)	TTE (LVEF, GLS and GCS)	47	38 ± 9 (mean)	70%	41 ± 2 Gy	22 ± 2 years	Mean LVEF 55.4%; Mean GLS -16.1±1.9% in RT + anthracyclines, vs -17.5±1.7% for RT alone; 20 (42.5%) had GLS<17% GCS -18.3± 3.2% for RT + anthracyclines, vs -17.8±3.6% for RT alone No difference in diastolic measurements (e.g. e' 4.9±1.5 cm/sec vs 5.1±1.2 cm/sec)
Busia et al 2010 (69)	TTE (M-mode, 2D)	147	38.2 (mean)	56%	34.3 Gy	At least 5 years	Mean LVEF 59.9% Mean LVEDD 4.35 cm
Heidenreich et al, 2005 (70)	TTE, stress echo, RNV	282	42 (mean)	50%	43.5 Gy	15 years (mean)	Mild diastolic dysfunction in 9% Moderate diastolic dysfunction in 5%
Salloum et al 1999 (71)	RNV	24	27 (median) (range 27-51)	28%	23.4 Gy	6 years (median)	Mean LVEF decline of 4.7%, but only 1 pt (4.2%) had LVEF<50% Normal diastolic function and LV volumes in all pts
Glanzmann et al, 1998 (72)	TTE (M-mode, 2D)	144	30.2 (range 4 -65	Not stated	30-40 Gy	14 years (mean, range 1.9-31.5 years)	LVEF ≥55% in 95% Normal diastolic function in pts without hypertension/CAD
Constine et al, 1997 (73)	Rest/stress RNV	50	26.0±8.6 (mean±SD)	64%	35.1±7.8 Gy (mean)	9 years (mean)	Mean LVEF 59.6±6.2% PFR 3.46±0.88
Lund et al, 1996 (60)	TTE (2D, M-mode)	116	28±7	42%	40.6 Gy	9 ± 3 years	E/A 1.1 (vs 2.0 for controls). No significant difference in LV-FS or chamber size
Kreuser et al, 1993 (74)	TTE (2D, M-mode and Doppler)	31	35 (median) (range 15-38))	45%	20-30 Gy	5.4 years (range 2-10)	18.4% had reduced LV-FS, 14% had reduced resting LVEF 12% had dilated left atrium, No significant difference in diastolic parameters (E.A, DecT)
Allavena et al, 1992 (75)	TTE (2D, M-mode)	73	29 (median)	35%	36.5 Gy	5 years (range 3-10)	Mean LVEF 60% (range 51-75%), 4 pts (5.5%) had hypokinetic septum or apex 1 pt (1.4%) had mildly dilated RV
Gustavsson et al, 1990 (76)	TTE (2D, M-mode) RNV	26	38 (median) (range 21-45)	35%	40 Gy	15 years (median) (range 4-20)	44% had decreased LV fractional shortening 50% had diastolic dysfunction (E/A<1.0)
Savage et al, 1990 (77)	Radionuclide Angiography	16	24.9 ± 6.2			9 ± 6	Mean resting LVEF 60 ± 7%, No abnormal LVEF measurements. Peak Filling Rate 3.5 EDV/sec, 2 (12.5%) had abnormally low PFRs
Pohjola-Sintonen et al, 1987 (78)	TTE (2D, M-mode)	28	23.3 (mean)	Not stated	4130 rads	9 years (mean) (range 5-14	2 pts (7%) had resting LVEF<50% 34% had RV thickness increased by >2SD
Perrault et al, 1985 (79)	TTE (2D and M-mode)	38 HD 3 seminoma	41 (median)	41%	Not stated	12 years	Resting LV systolic dysfunction in 13% (i.e. LVEF<50%)
Morgan et al, 1985 (80)	RNV	25	20.1 ± 5.6 (mean)	40%	Not stated	20 ±6	5% had resting LVEF<50%, 15% had <5% LVEF increase to exercise 6 (30%) had RV dilatation
Burns et al, 1983 (81)	RNV	21	44 ± 11 (mean±SD)	48%	3,589 ± 1,101 rads	14 ± 5 years	Rest LVEF 68± 9.2, RVEF 43± 9.7 Exercise LVEF 68±11, RVEF 40±12; Significantly reduced exercise RVEF response vs controls
Applefeld et al, 1983 (82)	RNV	41	25 (mean)	Not stated	Total mid-plane dose 4,000 rads	97 months (mean), range 37-172	Mean resting LVEF 59%, 7 (17%) had LVEF<45% at rest, Exercise LVEF 69%; 7 (17%) had abnormal LVEF response to exercise, (increase <8%)) 2 pts (4.2%) developed HF
Gomez et al, 1983 (83)	RNV	55	24 (median)	Not stated	3,500 rads/d over 35 days	(range 30-120 months)	21.8% had LVEEF<43%, 29.1% had LVEF in range 43-50%
Applefeld et al, 1982 (84)	RNV	16 HD	22.9 (mean)	Not stated	3000-4000 radS	8 years (median)	25% abnormal resting LVEF (<45%) 1 pt with HF

CMR – cardiac MRI, IQR – Inter-quartile range, GCS – global circumferential strain, GLS – global longitudinal strain, HD – Hodgkin's Disease, HF – heart failure, LGE – late gadolinium enhancement, LVEDD – LV end-diastolic dimension, LVEF – LV ejection fraction, LVFS – LV fractional shortening, RNV - Radionuclide ventriculography, RT – radiotherapy, RVEF – RV ejection fraction, TTE – transthoracic echocardiography

Systolic dysfunction. Mediastinal irradiation for Hodgkin's disease shows diverse effects on ejection fraction, with studies providing contradictory findings and conclusions (Table 2-1) (60,65-84). In general, LV ejection fraction was found to be significantly reduced in significant proportions in several studies. Publications showing >50% of subjects to have an LVEF<50% (83) and 44% with reduced fractional shortening (76) derive from over 20 years ago, when cumulative mediastinal RT doses were higher than are currently used. Nonetheless, other reports from a similar era report only a 14% prevalence of impaired EF (66), and a similar cumulative total radiation dose 95% of patients had a normal LVEF at 13.7 years post RT (72). More recently, a normal resting LVEF has been reported in 93% patients studied 8.6 years after therapy (78).

Ejection fraction has recognized limitations for identifying mild or subclinical LV dysfunction, which is better measured using 2D speckle tracking strain. In a study of LV systolic dysfunction at an interval of 22 years after mediastinal RT(68), global longitudinal strain (GLS) was significantly impaired compared with age-matched controls (-17.5±1.7% vs 20.4±1.7%, $p<0.05$), and this difference was more pronounced for patients treated with both RT and anthracyclines (-16.1±1.9%, , $p<0.05$). No significant difference was seen in LVEF values between groups.

In addition to the provision of highly accurate and reproducible cardiac chamber volumes, CMR has the benefit of providing tissue characterization, including the quantification of myocardial scar. In a study showing that 23% of asymptomatic screened patients had resting LVEF values <55% (mean LVEF 43±3%), Machann et al reported that 29% had late gadolinium enhancement that was not explainable by other etiologies (67). No specific anatomical pattern of LGE was discerned.

Diastolic function. Of the 21 studies using noninvasive cardiac imaging in long-term HD survivors treated with RT, 10 (47.6%) included measurements of diastolic function. The results reported were inconsistent, with 6 studies demonstrating no significant long-term change in diastolic parameters(65,68,71-74), and 4 studies reporting abnormal diastolic function (60,70,76,77). The 6 studies reporting no change comprised 4 echocardiographic studies and 2 radionuclide ventriculography studies, with a total of 450 patients followed after an average of 13.5 years and underwent an average

of 36.9 Gy (mean of all 5 studies). These studies were relatively recent, with 5 of the studies published from 1997 onwards.

In contrast, the 4 studies reporting significant change in diastolic function included 3 echocardiographic and 1 radionuclide ventriculography studies. Two studies (60,76) used solely an E/A ratio to define diastolic dysfunction, 1 used peak flow rate <2.54 EDV/sec as definition of abnormal (77), with 12.5% termed abnormal, and one study used composite of E/A, deceleration time (DecT) and pulmonary venous flow velocity systolic/diastolic ratio to grade diastolic function (70). These 4 studies (n=440 patients) were generally older than the studies reporting no diastolic change, with 3 published earlier than 1997 (73,76,77) and 1 in 2005 (70). Their follow-up was incrementally shorter (12.2 years) compared with the 6 negative studies (13.5 years) and involved greater doses of mediastinal irradiation (41.4 Gy, averaged over three studies that reported average radiation dose). The largest of these studies, Heidenreich et al, consisted of 64% of the patients in these 4 studies, had the longest follow-up (mean 15.4 years) and the highest average radiation exposure (43.5 Gy). It reported 14% prevalence of diastolic dysfunction (9% mild, 5% moderate, none severe), and compared these findings with Rochester community published data suggesting an expected prevalence of 6.4% in this age group (85). All patients underwent stress echocardiography, with 28% of the diastolic dysfunction patients demonstrating inducible myocardial ischemia, compared with 11% of patients with normal diastolic function. Two studies (76,77) used treadmill exercise testing to exclude ischemic heart disease as a cause of diastolic dysfunction, with neither study demonstrating ischemia in their small patient groups, and the fourth study (60) not using any test for ischemic heart disease.

Right ventricular size and function. Of the 20 identified studies, only 5 (25%) assessed right ventricular (RV) size or function in post-irradiated Hodgkin's survivors (75,78-81). One study (75) included a reference of "slight RV dilatation" in a cohort of 73 patients, inferring but not explicitly stating that RV size was normal in the remaining subjects, and did not provide any tabulated RV data. The remaining four studies (20%) consist of two echocardiographic and two radionuclide ventriculography studies with an average follow-up of 13.7 years. Small numbers of patients were recruited (mean number of subjects per study was 28), and notably all four studies were published approximately 30 years ago

(time period 1983-1987). Two studies (79,80) did not specify the average dose of radiation administered, and for the remaining two the mean dose was 3,860 rads. All four studies found a high prevalence of abnormal RV findings. Two studies examined solely RV structure, with one (78) finding 34% had RV wall thickness increased above 2 standard deviations and another (80) finding that 24% had resting RV dilatation. Neither of these studies had a non-irradiated control cohort. Of the two studies that assessed RV systolic function (79,81), one reported 39% prevalence of RV dilatation or hypokinesis, and the other reported a significant difference in RVEF response to exercise compared with healthy controls (resting RVEF 43±9.7% vs 37±5.1% with p=NS, exercise RVEF 40±12% vs 53±12%, $p<0.005$ for irradiated patients and controls respectively).

Mediastinal irradiation for breast cancer

Systolic function: The majority of noninvasive cardiac imaging studies in long-term breast cancer survivors were focused on investigating ischemic heart disease and described ventricular findings in the context of inducible perfusion defects. Once these were excluded, only 4 studies were found that fitted the inclusion criteria (Table 2-2) (67,86-88). Three used echocardiography (86-88) and 1 utilized radionuclide ventriculography (67), and together, they totaled 253 patients, followed over an average of 10.6 years, with total radiation doses from 20-50Gy. The study that demonstrated systolic dysfunction (87) found that 5% of irradiated patients had resting LVEF<50%. This study involved a small number of patients (37 breast cancer survivors, mean age 65 years) but had the longest follow-up of all four studies (median 18.4 years). Although the mean total radiation dose in this study was not specified, it was the oldest of the four (published in 1994), and hence likely involved a higher radiation dose than the more contemporary studies. This study also found increased LV wall thickness in 30% (defined as end-diastolic wall thickness > 11mm), whereas for the two other studies that reported LV wall thickness and mass (67,88), no significant abnormalities were reported.

Table 2-2: Summary of studies investigating subclinical cardiac dysfunction after radiotherapy for breast cancer.

First author	Method	n	Age at RT	Women (%)	Total Radiation	Follow-up	Findings
Magne et al, 2009 (67)	RNV	64	48 (median) (range 29-65)	100%	Not stated	6 years (median)	No significant change in LVEF for any pt (mean LVEF69%, range 63-74%)
Pistevou-Gompaki et al, 2008 (86)	TTE (2D, M-mode)	62	56 (mean) (range 48-64)	100%	50 Gy	5 years	No significant change in LVEF, EDV or LV wall thickness
Gyenes et al, 1994 (87)	TTE	37 (20 treated with XRT)	65.1 (mean) (range 54-72)	100%	Not stated	18.4 years (median) (range 16.8-21.2)	5% had LV systolic dysfunction (LVEF<50%) 40% had LV diastolic dysfunction used multiple parameters) 30% had LVH (end-diastolic wall thickness >11mm)
Gustavsson et al, 1999 (88)	TTE (2D, M-mode)	90 (34 left-sided XRT, 35 right-sided XRT,23 no XRT)	57.2 (median) (range 45-64)	100%	20 Gy (received by anterior LV wall))	13 (median)	All had normal systolic function (defined as LV-FS>25%) E/A lower in RT pts (1.05 vs 1.2, p=0.04) No difference in LV mass, LVEDD or LA size.

Table 2-3: Summary of studies that have investigated the risk of developing symptomatic heart failure after radiotherapy.

First Author	Method	Number	Age	Female	Radiation exposure	Follow-up	Findings
Van Nimwegen, 2015 (58)	Data-linkage study	2524 HD	27.3 (median)	45.7%	37 Gy (median)	20.3 years (median)	HR for HF 2.7, (95%CI 1.6-4.8) SIR 6.8 (95%CI 5.9-7.6) compared with general population
Boekel et al, 2014 (89)	Data-linkage study	10,444 BC (27.7% treated with XRT)	20% < 49 y.o. 39.3%>60 y.o.	100%	Not stated	8 years	Left-sided XRT HR 1.04 (95%CI .53-2.03) Right-sided XRT HR 0.83 (95%CI 0.34-2.03)
Boerman et al, 2014 (90)	Data-linkage study	561 BC (229 treated with XRT)	56 (median) (range 22-77)	100%	Not stated	9 (median) (range 5-57)	2.2% all XRT patients developed HF HF HR 0.5 (95%CU 0.2 – 1.8) for XRT vs no XRT Left vs right XRT HR 0.98 (95%CU 0.3 – 3.6)
Bouillon et al;, 2011 (91)	Data-linkage study	4456 BC (68.2% treated with XRT, 62.2% treated with XRT alone)	55 (mean) (range 22-90)	100%	Not stared	28 years (median)	In XRT group, HF deaths were 2.9% of all deaths; XRT HF HR 2.39 (95%CI 1.41 – 4.03)
McGale et al, 2011 (55)	Data-linkage study	34,825 BC	56%<50 y.o. 39%>70 y.o.	100%	6.3 Gy applied to heart for left-sided tumors 2.7 Gy for right-sided tumors	5-30 years	1.8 % developed heart failure (compared with 2.9% non-irradiated BC pts)
Park et al, 2011 (92)	Retrospective cohort	129 BC (59 left-sided, 70 right-sided)	55 (mean)	100%	56.6 Gy	8.2 years (median)	2 (1.6%) developed HF
Hardy et al, 2010 (93)	Data-linkage study	34,209 NSCLC (59.5% treated with XRT)	73 (median)	42.6%	Not stated	8-19 years	In XRT group: Cardiac dysfunction HR 1.54 (95%CI 1.29-1.83) Cardiomyopathy 0.46 (95%CI 0.25-0.80) HF 1.06 (95% 0.96 1.18)
Myrehaug et al, 2008 (94)	Data-linkage study	615 HD	29 (median)	52%	30-35 Gy in >90% pts	11.8 years (median)	SIR 0.9 (95%CI 0.1 to 2.5) in RT-alone group for HF hospitalization.
Hooning et al, 2007 (95)	Data-linkage study	4410 BC (86.5% treated with XRT)	49 (median)	Not stated	Not stated	17.7 years (median)	In XRT group: HF HR1.47 (95%CI 1.04 – 2.08) Increased with longer follow-up, e.g. >20 years FU, HR 2.1, p<0.001
Aleman et al, 2007 (96)	Data-linkage study	1,474 HD (84% treated with XRT)	25.7	46.4%	Not stated	18.7 years (median)	SIR 25-year cumulative incidence of HF after XRT and anthracyclines 7.9% HR 7.37 (95%CI 1.81-30)
Van den Belt-Dusebout et al (2006)(97)	Data-linkage study	2,491 testicular cancer patients (51.9% treated with XRT)	33.9 (median)	0%	Not stated	18.4 years (median)	Cumulative incidence HF 66 pts (2.6%), SIR0.93 (95%CI 0.71 to 1.20) HF HR 3.1 (95%CI 1.7 to 4.7)
Patt et al, 2005 (98)	Data-linkage study	16,270 BC (100% treated with XRT)	66 (median)	Not stated	Not stated	9.5 years (median) (range 0-15)	9.7% cumulative incidence for HF hospitalization For left vs right XRT: HF HR 1.05 (995%CU 0.95 – 1.17)
Hancock et al, 1993 (99)	Data-linkage study	2232 HD	28% aged <10 y.o. 42% aged > 40 y.o.	59%	Not stated	9.5 years	10 pts (0.45%) developed heart failure

Diastolic function. Two of the four studies examined left ventricular diastolic dysfunction after RT for breast cancer (87,88). Gyenese et al found diastolic dysfunction in 8 patients (40%), determined by composite of E/A ratio, DecT and IVRT. However, this prevalence was not different from a non-irradiated breast cancer control group, which had a diastolic dysfunction prevalence of 53%. Gustavsson et al found lower resting E/A ratio in irradiated breast cancer survivors after a median 13 years of follow-up (E/A 1.05 vs 1.2, p=0.04), but found no significant difference between irradiated a non-irradiated patient in regards to LV mass, wall thickness or left atrial size. To date, no studies have been identified that have used advanced imaging modalities for assessing LV diastolic function in long-term breast cancer survivors (e.g. tissue Doppler imaging, diastolic speckle strain).

There were no identified studies examining right ventricular size and function after mediastinal irradiation for breast cancer. There were also no identified studies using advanced non-invasive cardiac imaging techniques (e.g. 2D speckle-tracking strain, three-dimensional echocardiography, CMR) for investigating long-term myocardial performance after irradiation for breast cancer.

Mediastinal irradiation for other malignancies

No clinical studies were identified fitting the inclusion criteria for other malignancies, including esophageal, lung cancers and seminomas.

Heart failure after mediastinal irradiation

A total of 12 studies (Table 2-3), (55,58,89-96,98,99) were identified that investigated the incidence of cardiac failure after irradiation in survivors of long-term malignancy, including those with Hodgkin's disease (58,94,96,99), breast cancer (55,89-92,95,98) and non-small-cell lung cancer (93). The majority were based on data-linkage and one was a retrospective cohort study. These studies included a total of

112,149 patients followed up for a total average of 14.3 years. Females accounted for 73% of the patients due to the high proportion of breast cancer trials included. There was a diverse range of age groups represented, with a median age of 25-35 years old in the HD studies, 49 to 66 years old in the breast cancer studies, and 73 years in the NSCLC study. The average radiation dose could not be determined in most studies. Of the 12 studies, most (83%) were published in the past 10 years, thereby reflecting radiotherapy practice mainly over the last 25 years.

In the earliest study of HD (99), the cumulative incidence of HF mortality of 0.45% over a follow-up of 9.5 years. Although no information on nonfatal HF events was included, another study (94) examined the incidence of HF hospitalization, and found that RT alone had a standardized incidence ratio (SIR) of 0.9 (95% 0.1 to 2.5), suggesting no significant association. In contrast, studies with longer follow-up found increased risks of developing HF with mediastinal RT. Aleman et al (96) investigated 1474 HD survivors with a median of 18.7 years post-treatment, and found HF was associated with RT with a SIR of 4.9, resulting in 25.6 excess cases of HF per 10,000 patient-years. In comparison with HD survivors not treated with RT, RT was significantly associated with HF (HR 7.37, 95%CI 1.81 to 30.0). The second study (58) investigated 2524 HD survivors at median 20.3 years post-treatment and found an increased incidence of HF (SIR 6.8, 95% 5.9 to 7.6) resulting in 58 excess HF cases per 10,000 patient-years. The observed incidence was higher in patients treated at younger ages, with 18-24-year age group demonstrating SIR 18.7 (95%CI 14.5 – 23.6) and 40-50 year age group demonstrating SIR 2.7 (95%CI 2.0 to 3.7). Mediastinal RT also conferred increased risk for HF (HR 2.7, 95%CI 1.6 to 4.8).

Seven studies (55,89-92,95,98) examined the association of RT for breast cancer with HF, six using a data-linkage design and one using a retrospective cohort design (92). Together they totaled 71,095 patients followed up for an averaged 13.4 years. It was not possible to estimate the mean radiation dose from information provided. Five studies provided median ages, for which the mean was 56.2 years. All studies had been published in the past 10 years. The retrospective cohort study (92) found a low cumulative incidence of 1.9% of HF in 129 BC patients treated with mean 56.6 Gy RT with median follow-up of 8.2

years. A data-linkage study (90) found no significant association between RT and newly diagnosed HF (HR 0.5, 95%CI 0.2 to 1.8) after following 561 BC patients for median of 9 years. One study (89) followed 10,444 BC patients (28% treated with mediastinal RT) and found no significant association of RT with HF for left-sided disease (HR 0.83, 95%CI 0.34 to 2.03) or right-sided disease (HR 0.87, 95%CI 0.45 to 1.67) when compared with surgery alone. Another (55) investigated 34,825 patients and did not find an increased incidence of hospitalized HF (1.8% in RT arm, vs 2.9% in non-irradiated arm). Amongst irradiated patients who developed HF, there was no association with laterality of disease (left vs right incidence ratio 0.95, 95%CI 0.81 to 1.11). In contrast, three other studies suggested an association between RT and HF. One study(98) investigated 16,270 patients, all treated with RT and followed-up for median 9.5 years, and found 9.7% cumulative incidence of HF hospitalization, with laterality having no effect (left vs right HR1.05, 95%CI 0.95 to 1.97). Two other studies which contained non-irradiated cohort patients that could serve as controls demonstrated significantly increased hazard ratios for CF after RT, with one (95) investigating 4410 BC patients followed up over 17.7 years (HR 1.47, 95%CI 1.04 to 2.08) and another (91) following up 4456 BC patients over 28 years for HF deaths (HR 2.39, 95%CI 1.41 to 4.03).

A single study (93) was identified that examined 34,209 patients treated with RT for NSCLC and found no significant association with HF (HR 1.06, 95%CI 0.96 to 1.18). Another study investigated 2,491 with testicular cancer, 51.8% treated with mediastinal radiotherapy, and found HF was significantly associated (HR 3.1, 95%CI 1.7 to 4.7) (43).

Discussion

The studies selected for this systematic review display a large degree of heterogeneity, both in terms of study characteristics and findings. Notably, a large number of studies (17 of 40) were published over 20 years ago, and many consist of cohorts with small numbers of patients. It is therefore difficult to reach definitive conclusions regarding the etiology and presentation of radiation-induced myocardial disease,

despite RT being used as a therapeutic modality for almost a century. However, it is possible to consider new steps in researching radiation-induced cardiomyopathies.

Ventricular dysfunction. Current contemporary opinion of radiation-induced cardiomyopathy emphasizes diastolic dysfunction (56,59), a highly prevalent finding in the elderly. Evidence for diastolic dysfunction attributable to RT is predominantly based on autopsy findings of increased fibrosis (100) and a cohort study conducted 20 years earlier (70). However, the autopsy studies were conducted decades earlier when RT delivered higher dosages, and likely represent a selection bias with over-representation of patients with severe RT complications. The use of population-derived values as a comparator in the retrospective cohort study might be confounded by a lower rate of hypertension and smoking than in the cancer population. Our review suggests that most studies that examined diastolic function did not find significant long-term changes, although many had methodological limitations. There therefore still remains need to characterize long-term diastolic function in RT patients.

LV systolic dysfunction was prevalent in half of noninvasive imaging studies conducted on HD and BC survivors and was detectable in more contemporaneous studies using advanced imaging techniques (e.g. speckle-tracking strain, CMR). This is relevant as unlike diastolic dysfunction, treatments (e.g. ACE inhibitors, β-blockers) for systolic dysfunction have been shown to alter the condition's natural history even in the pre-symptomatic stage, and therefore potentially support the concept of screening of asymptomatic RT patients. Determining the risk of LV systolic dysfunction after RT, and the benefits of screening and cardioprotection represent interesting research strategies.

In contrast to the previous entities, RV dysfunction was commonly found in studies that specifically investigated the issue. This may not be unexpected as RV is the most anterior cardiac chamber and may have less functional reserve due to lower mass. RV dysfunction is an independent adverse prognostic marker in heart failure (101) and accounts for a large proportion of symptomatic burden. Whether regular screening of RV function in long-term RT survivors may be beneficial is unclear.

Heart failure. Recent advances in data-linkage research has allowed very large groups of patients to be investigated for infrequent complications without the cost or difficulties associated with cohort studies. Excellent studies have reported associations between RT and ischemic heart disease (57), cardiovascular mortality (102) and combined cardiac events (103), but few studies have used congestive cardiac failure as a specific endpoint. Although the associations reported in this systematic review were varied, there was a trend for the larger, more recent studies that included patients not treated with RT (58,91,93,95) to demonstrate significantly increased HF risk, with HR values ranging from 2.7 to 7.4 for Hodgkin's lymphoma, and 1.5 to 2.4 for breast cancer. In total, these findings support the current guidelines for evaluating cardiovascular complications after RT (63), which currently recommend screening echocardiogram 10 years after RT, with further echocardiograms every 5 years onwards if no pathology is detected.

Limitations. The selection criteria for this review sought to focus the data on the population most likely to be suitable for screening. Due to biological differences in tissue response to injury in different age-groups and the much higher prevalence of malignancies in the adult population compared to the pediatric population, we excluded studies that predominantly investigated children or adolescents. A minimum of average 5-year follow-up period was chosen because by convention the initial 5 years represents the period of highest mortality risk from malignancy or acute treatment complications, and also because current guidelines (63) define a five-year period as the onset of increased cardiac risk, and recommend screening in 5-year intervals. Because our aim was to investigate specifically myocardial diseases, which have distinct disease manifestations and treatments, papers either examining non-myocardial diseases alone (e.g. coronary artery disease, pericardial disease, valvular disease) or failing to specify myocardial outcomes were excluded. No statistical meta-analytical techniques could be performed due to the significant heterogeneity in malignancies, imaging modalities and endpoints studied.

A challenge for further researchers is to determine the post-RT cardiovascular risk in malignancies besides HD and BC, including esophageal cancer, lung cancer and seminoma. It is likely that differences in population characteristics (e.g. older age and smoking in esophageal and lung cancers) and treatment differences may make results from HD and BC trials non-generalizable. However, despite using a broad-based search strategy, this systematic review did not identify any long-term cardiovascular imaging studies in these subgroups. Ideally, optimal screening regimens could be individualized based on malignancy, but there is currently insufficient scientific information to adopt such an approach.

Conclusions. With successful advances in contemporary cancer treatment, clinical challenges are slowly pivoting from increasing 5-year survival to managing chronic health conditions in cancer survivors. This vulnerable population requires further research to develop strategies for identifying patients at high-risk for RT-induced myocardial disease and provision of early and effective treatment.

Postscript

This thesis demonstrated that the majority of studies assessing imaging endpoints of long-term cardiac function after chest-directed radiotherapy found that left ventricular function worsens and raises the possibility of significant right ventricular long-term effects. The next thesis chapter will assess the relationship between chest-directed radiotherapy and the clinical endpoint of heart failure.

Chapter 3

Risk of Heart Failure and Radiotherapy

- Published as Nolan MT, Russell DJ, Negishi K and Marwick TH. Meta-Analysis of Association Between Mediastinal Radiotherapy and Long-Term Heart Failure. *Am J Cardiol* 2016; 118(11):1685-91

Chapter 3- Heart Failure and Radiotherapy

Preface

The previous chapter of this thesis demonstrated the differing phenotypes of cardiac dysfunction resulting from chest-directed radiotherapy for cancer. These findings were clinically significant as phenotypes of systolic and diastolic cardiac dysfunction have different treatment paradigms, as does right and left ventricular cardiomyopathy. Therefore, there is a discordance between the traditional definition of anti-cancer treatment cardiac dysfunction, which is defined by an absolute decrement in LVEF with or without the presence of symptoms, and the clinical reality of a derangement of multiple axes of cardiac homeostasis with different CTRCD patients displaying differing degrees of involvement for each axis. This provides a rationale for using more than one cardiac imaging modality for selected patients so to further characterise their dysfunction.

The next thesis chapter changes the focus from cardiac imaging findings to the patient's clinical characteristics and an endpoint that is more significant for the patient, namely that of heart failure. The aim of this chapter is to quantify the risk of heart failure secondary to chest-directed radiotherapy. As over 50% of cancer treatments involve radiotherapy administration, if a significant association is seen then a cogent argument can be made that CTRCD is a predictable complication of anti-cancer therapy and merits societal resources, including sequential cardiac imaging, to reduce the burden of this disease in the cancer survivor community.

Abstract

Background: This investigation sought to identify and quantify any increased risk of long-term heart failure after thoracic radiotherapy for cancer and identify any population covariates that corresponded with increased risk.

Methods: Electronic databases were systematically searched for studies reporting relative risk, odds ratio and hazard ratio for symptomatic heart failure more than 5 years after radiotherapy administration. Clinical characteristics, study design, univariable effect sizes and associated 95% confidence intervals were extracted. Univariable effect size was pooled and computed in a meta-analysis using random-effects models weighted by inverse variance.

Results: Six studies (45,669 patients) with weighted median follow-up duration of 13.9 years were included, each data-linkage study that reported hazard ratios for heart failure. Pooled hazard ratio for long-term heart failure was significant (HR 1.83, [1.09 to 3.08], p = 0.022), with significant between-study heterogeneity (Q 43.38, df 5, p<0.001, I2 88.47%). Statistical significance was lost when excluding studies of malignancies other than breast cancer or haematological malignancies, and excluding studies with Newcastle-Ottawa scores <8, but the direction of effect and magnitude remained approximately the same. Subgroup analyses and meta-regression demonstrated that study differences in age at time of radiotherapy administration and duration of follow-up explained approximately 80% of observed heterogeneity. Earlier publication date was associated with increased heart failure risk. Other variables, including female proportion, proportion of adjuvant chemotherapy use and sample size did not significantly impact the conclusions.

Conclusions: In conclusion, radiotherapy approximately doubled the long-term risk of heart failure. This finding was associated with younger age at time of radiotherapy and longer follow-up duration, which explained approximately 80% of inter-study variability.

Chapter 3- Heart Failure and Radiotherapy

Introduction

Heart failure (HF) affects approximately 1-2% of population in developed countries, with prevalence rising to >10% in persons aged ≥70 years(33). Radiotherapy (RT) treated patients represent a rare group with a clearly identifiable onset of risk for myocardial injury, and as such may represent an attractive target for preventative screening and treatment. However, consensus guidelines by professional medical societies have been inconsistent in their recommendations. According to recent HF guidelines(61), previous chemotherapy represents a HF risk factor and confers a stage A HF status, but no specific guidance is given for patients treated with RT. The European Society of Medical Oncology 2010 guidelines(104) states that "RT-induced risk is lifelong and requires long term follow-up", but also note that "follow-up protocols are based on departmental or personal experience". Expert consensus from the American College of Cardiology and European Association of Cardiovascular Imaging suggest echocardiography at ten years post-RT, with subsequent echocardiograms every 5 years (63), but further guidance regarding high-risk populations, disease manifestations and prevalence are needed to optimally guide cardiac screening. Thus, we performed this systematic review and meta-analysis to quantify the long-term risk of HF after thoracic RT for malignancy.

Methods

We followed the Preferred Reporting Items for Systematic Reviews and Meta-Analyses (PRISMA) guidelines(64) for reporting the systematic review. The search strategy was defined prospectively and listed in the PROSPERO database (registration number CRD42015020508). Citations and details were stored in a database (EndNote X7.4, Thomson Reuters, New York, NY). A liberal search strategy was employed to increase sensitivity. Two reviewers conducted a literature search of Medline/PubMed and EMBASE that investigated cohorts of patients treated with thoracic RT for HF for

all years from inception to July 2015. HF was defined as the clinical syndrome associated with insufficient cardiac function to meet the body's demands.

Publications were limited to those published in English. References of publications and relevant papers were also searched for further reports. The search excluded studies of paediatric populations to prevent confounding of results, as a child's heart appears to be more susceptible to chronic RT adverse effects than an adult's heart(105), as evidenced by recognition of younger age at RT being a risk factor for cardiotoxicity(106) in addition to experimental evidence demonstrating greater biological susceptibility to RT in developing hearts(107). Publications in peer-reviewed, English-language journals evaluating long-term HF were included in this study if they met the following inclusion criteria: 1) average patient age (either median or mean) of ≥18 years at time of RT administration, 2) administration of adjuvant RT therapy (either tangential or mediastinal) for cancer, 3) measure of risk of HF reported as a binary outcome, either as hazard ratio, risk ratio or odds ratio and 4) presence of a time interval of at least 5 years between RT and determination of HF status. Exclusion criteria included 1) studies not meeting all of the inclusion criteria, 2) non-human studies and 3) abstracts or conference proceedings. No restrictions were applied to the types of patients, study's country of origin or institution type where outcome was determined.

Relevant studies were selected from literature searches by 2 review authors (M.N. and D.R.), who also extracted relevant data. Discrepancies between review authors were resolved by consensus or, if necessary, by a third author (T.H.M.). Information on publication year, sample size, follow-up duration, average age (either median or mean), gender ratio, RT dose and use of concurrent chemotherapy were extracted independently from each study.

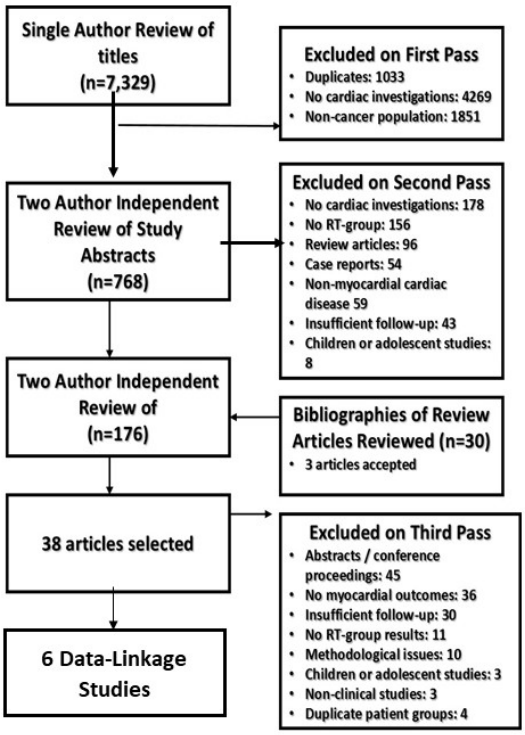

Figure 3-1: Flow diagram for study search and selection

Reported measures of risk, including odds ratio (OR), hazard ratio (HR) or risk ratio (RR), were pooled and analysed using a random-effects model weighted by inverse variance as described by DerSimonian and Laird. Assumption of heterogeneity was tested by using Q, and between-study heterogeneity was quantified using the I^2 value. Sensitivity analyses were performed by removing studies with following characteristics; studies examining cancers other than breast cancer or haematological cancers, studies with Ottawa-Newcastle quality score <8, and studies with low sample size. Subgroup analyses were performed using mixed-effects model with pooled τ^2 estimates. Meta-regression was performed using random effects model. Publication bias was assessed visually by funnel plots of effect estimates and by Begg statistical test. If the number of studies assessed was <10, then further assessment

of possible publication bias would be undertaken with Orwin's fail-safe N and Duval and Tweedie's Trim and Fill test. Statistical analysis was performed by Comprehensive Meta-Analysis® software, version 2.

Results

The study selection process (Figure 1) initially identified 7,329 individual studies, of which 6 satisfied our selection criteria (Table 3-1). All 6 were data-linkage studies, using population-level electronic databases to match very large numbers of patients with desirable baseline characteristics (in this case, treatment with thoracic RT) with hospital-record diagnoses of HF. Two of the studies investigated breast cancer patients, two investigated Hodgkin's disease patients, one investigated lung cancer patients and another metastatic testicular cancer. Of the 6 studies, a total of 45,669 patients were enrolled. Of these, 58.8% also received concomitant chemotherapy. Weighted mean age of the selected studies was 65.1 years with weighted mean follow-up of 13.9 years. 46.8% of subjects were female. Mean Newcastle-Ottawa observational cohort quality score was 8 (Table 3-2). Due to the data-linkage nature of the studies, specific information on RT dose, anthracycline administration and anthropomorphic information or ethnicity data were unavailable in the majority of published studies. Of the studies selected, 5 originated from the Netherlands.

RT was found to increase the long-term risk of HF (HR 1.83, [1.09 to 3.08], $p = 0.022$). Test of heterogeneity was applied using Q, with Q value of 43.38 with 5 degrees of freedom, $p<0.001$ (Figure 2). This indicated significant heterogeneity not explained by random sampling error. I^2 value was 88.47%, suggesting a high degree of inter-study variability. We hypothesised that this inter-study variability could potentially be explained by differences in either study population characteristics or study design. Sensitivity analyses (Table 3-3) revealed that restricting meta-analysis to studies involving breast cancer or haematological malignancies did not meaningfully alter the effect estimate, but it did fail to reach statistical significance. Removing studies with Newcastle-Ottawa scores <8 reduced the effect estimate

and removed statistical significance. Removing studies with sample size <2000 subjects' participants did not meaningfully alter effect estimate, which remained statistically significant.

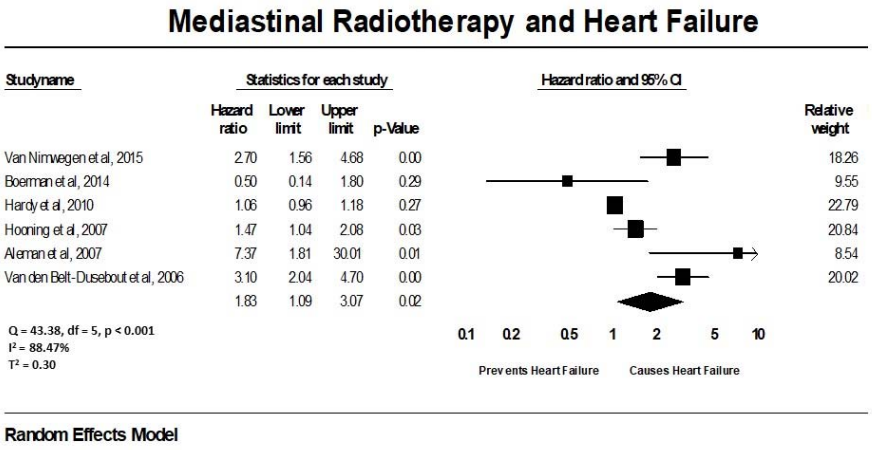

Figure 3-2: Forrest plot for pooled Hazard Ratio for HF after mediastinal radiotherapy

Subgroup analyses were performed on the following study variables; i) median age less than 50, ii) follow-up less than 15 years, iii) female proportion less than 50% and iv) year of RT administration before 1981 (Table 3-4). For studies with median participant age ≤ 50 years old, there was increased RT effect on HF which was statistically significant, whilst no significant effect was seen with studies with median age > 50 years, with test of difference in risk between two subgroups (Q = 5.39, df =1, p=0.02) suggesting that impact of RT likely does vary with median age. For studies with less than or equal to 15 years follow-up, there was no significant association between RT and HF but a significant association was seen if more than 15 years of follow-up occurred, with test of difference (Q = 5.39, df = 1, p = 0.02) suggesting that impact of RT likely does vary with length of follow-up. Trials with median age ≤50 years were an identical subset to that of trials with ≤15 years follow-up, explaining the identical pooled point

estimate and test of difference findings. Subgroup analysis based on female proportion >50% demonstrated no effect of RT on HF. Studies with female proportion ≤ 50% did demonstrate an association, however the test of difference in effects (Q = 1.639, df=1, p=0.20) provided no evidence that impact of RT significantly depends on female proportion. Subgroup analysis of studies with RT administered before median weighted year 1981 showed an increased effect estimate while studies with RT applied after median weighted year 1981 did not have a statistically significant effect, with test of difference (Q=1.099, df=1, p = 0.294) suggesting that impact of RT does not vary with publication year. Therefore, of the four subgroup analyses, excluding studies based on median age and duration of follow-up significantly varied effect estimate between groups, however female proportion and median weighted RT-administration year did not.

Meta-regression analysis was performed to assess impact of study characteristics as continuous rather than binary variables (Figure 3). Study covariates utilised for meta-regression included i) female proportion, ii) length of follow-up, iii) median age at RT administration, iv) proportion of patients receiving adjuvant chemotherapy, v) publication year and vi) sample size. The following two characteristics did not have statistically significant impact on effect estimate slope; female proportion (β -0.387, p = 0.13) or proportion in each trial receiving chemotherapy (β -0.855, p=0.08). Follow-up duration significantly predicted effect estimate outcome (β 0.146, p <0.001). Both median age (β -0.023, p <0.001) and publication year (β -0.076, p = 0.016) demonstrated significant inverse associations. Sample size had a statistically significant inverse association of very small magnitude (β -0.00002, p<0.001).

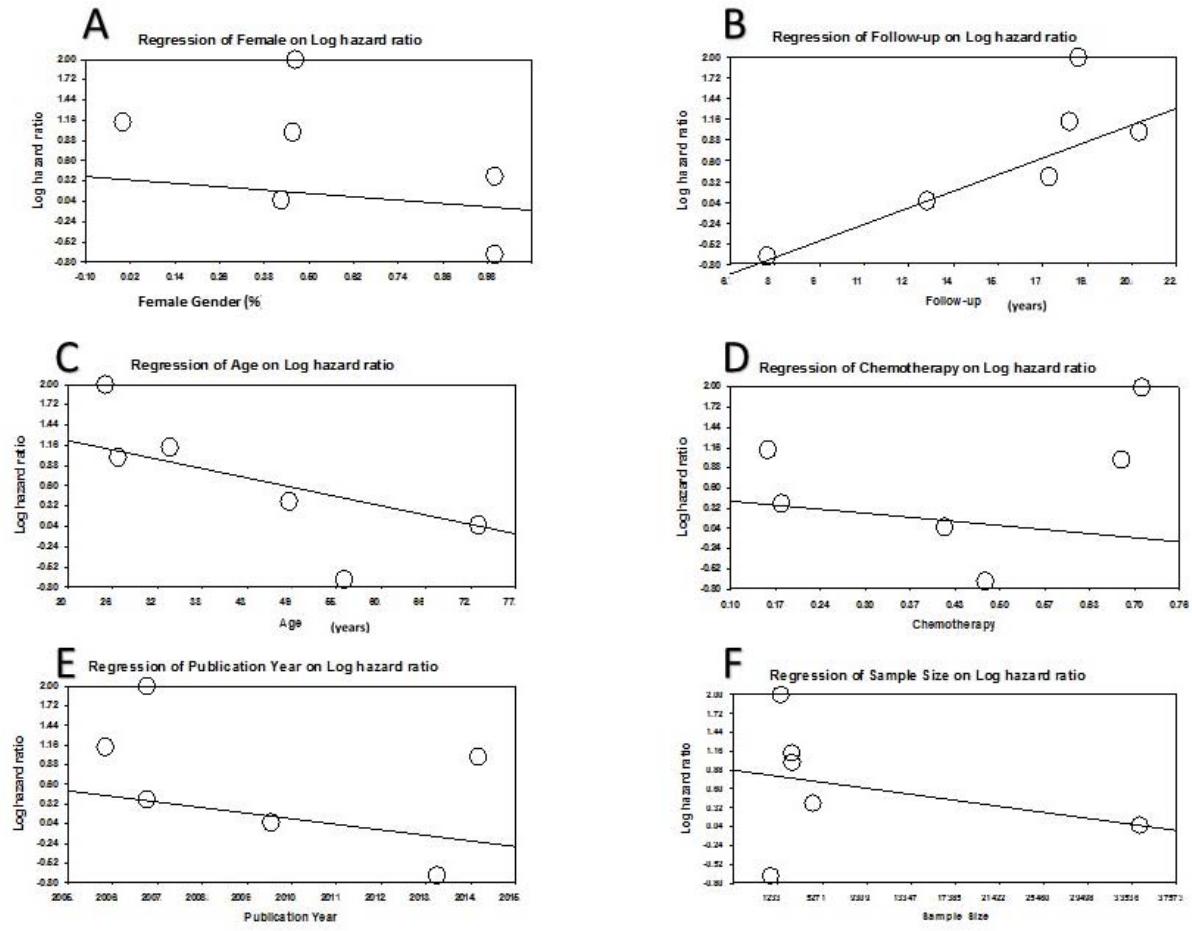

Figure 3-3: Meta-regression models for following covariates plotted against log hazard ratio: a) female gender (%), b) length of follow-up (years), c) median age at RT administration (years), d) proportion of patients receiving chemotherapy (%), e) publication year and f) sample size.

Goodness of fit analysis was applied to meta-regression models for age (unexplained τ^2 0.051, Q_{resid} 4.8 at 4 degrees of freedom, R^2= 83%) and follow-up duration (unexplained τ^2 0.07, Q_{resid} 4.4 at 4 degrees of freedom, R^2 = 77%). Thus, patient age and duration of follow-up each accounted for approximately 80% of observed between-study heterogeneity. The individual R^2 values sum to over 100%, most likely because age and follow-up duration are not independent of one another and the same variance source is captured twice.

The risk of publication bias was assessed by funnel plot, shown in Figure 4, with visual inspection not revealing any obvious asymmetry and Begg's test not demonstrating evidence of bias. However, these tests have low power due to small number of studies. If one assumes that publication bias did exist, Orwin's fail-safe N test revealed an additional 15 studies with mean HR of 1.0 would be needed for cumulative effect estimate to become trivial (defined as HR <1.05). To assess the robustness of study conclusions against publication bias, Duval and Tweedie's Trim and Fill test demonstrated an adjusted HR (HR 1.11, [1.02 to 1.22], p =0.022), which was reduced in magnitude from the observed values (HR 1.83, 95%CI 1.08 to 3.08, p=0.020) but remained statistically significant.

Discussion

The main findings of the present study are the following: firstly, that thoracic RT approximately doubles the risk of long-term HF (as defined by clinical HF), and secondly that covariates associated with increased HF risk included younger median age at time of RT, longer follow-up duration, and earlier publication year. The present meta-analysis is the only study that pools long-term risk of HF after RT in adult cancer survivors. Our results broadly agree with a systematic review of increased HF in children(108), as well as observed increased rates of coronary heart disease(57) and valvular heart disease in adults(109) and is broadly consistent with research findings in the field.

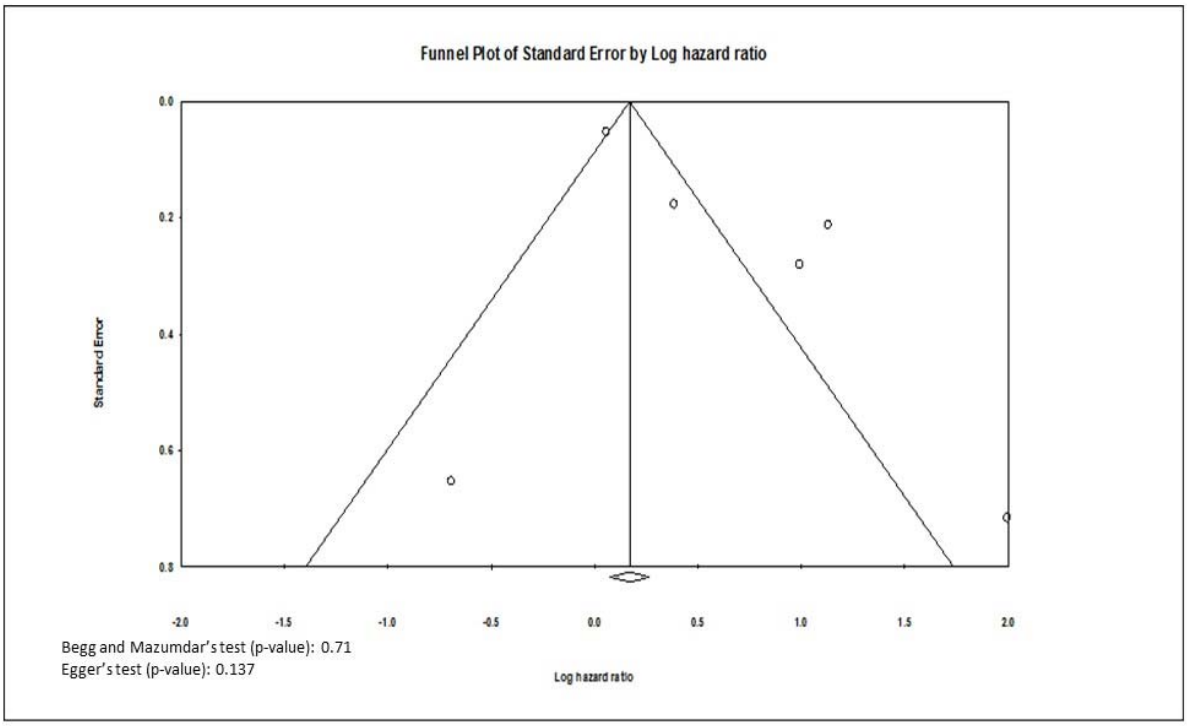

Figure 3-4: Funnel plot for assessing publication bias.

To date, the understanding of radiation-induced myocardial disease has lagged behind improvements in the knowledge base of radiation-induced coronary and valvular dysfunction. Current reviews suggest that RT is associated with increased prevalence of diastolic dysfunction, however this conclusion is based on small studies performed without appropriate comparator groups. A systematic review conducted by the authors suggested that either systolic or diastolic dysfunction may characterise late HF associated with prior mediastinal RT(110). Histological examination of explanted hearts exposed to RT demonstrates widespread inflammation, microvascular obstruction and intimal proliferation of myofibroblasts(111), and agents designed to protect endothelial function have demonstrated utility in small animal studies(112). These findings support a proposed "two-hit" hypothesis(113), where cancer therapy causes subclinical myocardial damage in majority of patients, which reduces myocardial reserve for future cardiovascular risk factors. This hypothesis is in keeping with our finding of increased long-term HF risk in studies that had younger patients and longer durations of follow-up and suggests potential benefit for prolonged cardiovascular surveillance of cancer survivors. Current guidelines suggest screening echocardiogram in high-risk patients 5 years after RT and after 10 years for low-risk patients, with repeat echocardiography every 5 years afterwards(63). The results of our meta-analysis broadly support these recommendations; however we note that in contemporary practice only a minority of patients may actually receive recommended monitoring even in the short-term setting(114).

We also note that cardio-protection against anthracycline and trastuzumab-mediated cardiotoxicity is a rapidly developing field of research, with several randomised controlled trials recently being published(52,115). No comparable research exists for radiation-induced cardiotoxicity, and this study adds to the case that such research is needed to reduce HF prevalence in the community.

There are several important limitations in our present study. Firstly, we acknowledge that we primarily recruited data-linkage publications, which carry specific advantages and disadvantages. The advantages of this approach are that large numbers of patients can be studied over a longer time period

than would be impractical using randomised controlled trials or observational cohorts. However, the observational nature of data-linkage studies means we cannot exclude possibility that RT-treated group differed from comparison group in important aspects. Long-term randomised trials to resolve this point would be very challenging to perform and are not likely to eventuate in the foreseeable future. Secondly, we note that our results yielded a large degree of heterogeneity amongst trials. We used advanced meta-analytical results to account for sources of heterogeneity and note that significant residual heterogeneity may be unavoidable for such a diverse clinical field. Thirdly, the number of studies recruited was small, which reflects the real-world complexity of accessing historical data of infrequent adverse effects over long time periods. Of the 6 studies selected, 5 originated in the Netherlands, which has an administrative register which contains near-complete and high-quality national hospitalization data from 1995 onwards for the entire country, making such studies possible. It is hoped that other health-care systems will follow the Netherlands lead in the future, to enable publication of further relevant studies. We also acknowledge that the small number of studies reduce the statistical power of subgroup analyses and meta-regression techniques, and therefore consider that these findings should be considered hypothesis-generating at current time. Fourth, due to the data-linkage aspect of the studies, aspects of patient demographics and treatment could not be provided, including proportion and cumulative dose of anthracycline use and RT technique and dose. Of the six studies analyzed, only 2 reported hazard ratios for heart failure associated with anthracycline administration; 1 study reported HR 3.0 (95%CI 1.9 – 4.7)(116) and 1 study reported HR 2.81 (95%CI 1.44 – 5.49)(96). Because the second study was confounded by the fact that anthracycline-treated patients had significantly shorter follow-up times than non-anthracycline treated patients, a decision was made not to perform meta-analysis on the 2 studies. Lastly, a fifth limitation was that we could not exclude the possibility of publication bias due to reduced statistical power due to low number of studies, however further testing suggested that it is unlikely that sufficient number of investigations were unpublished to alter this meta-analysis's conclusions.

Disclosures

The authors have no conflicts of interest to disclose.

Acknowledgements

We wish to acknowledge the generous assistance of Ms. Libby Seymour, Research Services Librarian from the University of Tasmania. This study was sponsored by a Health Professional Scholarship from the Heart Foundation, Australia.

Postscript

Despite current attention to the cardiotoxicity associated with chemotherapy and the identification of cardioprotective strategies, there has been little work done on risk protection from the cardiac consequences of radiotherapy. The work in the last two chapters identifies the magnitude of this problem and the features of the patients who are most at risk. Further studies are needed to improve protection against these cardiac sequelae.

The initial chapters of this thesis have focused on the cardiac consequences of cancer therapy. However, the association of cancer with cardiac disease also arises because the two illnesses share aetiologic agents. In the next chapter, I sought to understand the relative magnitude of these joint risk factors, as a potential target for intervention.

Chapter 4

Late Cardiac Effects of Childhood Cancer Treatment

Part of the research in this chapter has been published as(117):

- Nolan MT, Marwick TH, Plana JP, Zhenghong L, Ness KK, Joshi VM, Srivistava D, Green DM, Robison LL, Hudson MM and Armstrong GT. Effect of Traditional Heart Failure Risk Factors Relative to Cardiotoxic Therapy for Impairment of Myocardial Function in Adult Survivors of Childhood Cancer. *J Am Coll Cardiol Img* 2018; 11(8):1202-3

Chapter 4- Childhood Cancer and Cardiac Dysfunction

Preface

The preceding chapters have demonstrated that CTRCD can occur relatively frequently in response to either chemotherapeutic or radiotherapeutic treatment strategies, and that cardiac monitoring in the peri-treatment setting is a reasonable strategy for reducing burden of cardiomyopathy in the cancer survivor population. However, many adverse cardiac events are delayed until up to many years after completion of anti-cancer therapy, and even subclinical cardiac dysfunction may lead to heart failure if left untreated for prolonged periods of time. Two separate strategies for reducing heart failure burden in this population include 1) extending cardiac monitoring to beyond anti-cancer treatment completion with commencement of heart failure medications if cardiac dysfunction is detected and 2) aggressively treating traditional heart failure risk factors on the basis that cancer survivors represent an at-risk population of heart failure.

This chapter aims to quantify the incremental risk of cardiac dysfunction due to traditional heart failure risk factors in the childhood cancer survivor population, and to compare the effect sizes of traditional risk factors with those of cancer-therapy-related risk factors.

Abstract

Background: Treatment of childhood malignancies is associated with risk for late-onset cardiac dysfunction.

Objectives: To determine the relative contribution of traditional heart failure risk factors (HFRFs) and cardiotoxic therapy to impairment of myocardial function and functional capacity in adult survivors of childhood malignancies.

Methods: We recruited 1807 adult survivors of childhood cancer (48% female, median age 31.6 years, range 18 - 62) with a median interval of 22.6 years (range 10.4 – 48.3 years) from treatment with anthracyclines (57.7%), chest-directed radiotherapy (16.8%) or both (25.5%.) Assessment included comprehensive echocardiographic examination (including two- [2D] and three-dimensional [3D] left ventricular ejection fraction (LVEF), global longitudinal strain (GLS) and diastolic grading). HFRFs included hypertension, insulin resistance, obesity and smoking history. Functional capacity was assessed by six-minute walk test (6MWT). Logistic models were used to adjust for the effects of known risk factors (including sex, age and anthracycline and radiotherapy dose).

Results: Among 1807 participants with an evaluable echo, 13% had abnormal 2D-LVEF, 15% had abnormal 3D-LVEFs, 29% had abnormal global longitudinal strain and 46% had diastolic dysfunction. Presence of hypertension (OR 1.81, 95% confidence interval [CI] 1.25–2.62) was associated with an abnormal 3D-LVEF. Insulin resistance (OR 1.72, 95%CI 1.30–2.28) and obesity (OR 1.58, 95%CI 1.19-2.11) were associated with abnormal GLS. Diastolic dysfunction was associated with insulin resistance (OR 1.44, 95%CI 1.08–1.92), obesity (OR 1.92, 95%CI 1.42–2.58) and hypertension (1.41, 95%CI 1.03–1.94). Smoking status was not associated with changes in myocardial functional indices. Effect size (ES) of insulin resistance on GLS (ES $1.09x10^{-2}$, p=0.002) was greater than traditional risk factors of age at assessment (ES $0.20x10^{-2}$, p=0.05) and cumulative anthracycline dose (ES $0.06x10^{-2}$, p=0.17). Obesity was the only HFRF associated with abnormal 6MWT results (OR 2.06, 95%CI 1.45 – 2.94).

Conclusions: The effects of traditional HFRFs on echocardiographic markers of myocardial dysfunction are similar to those of treatment-related variables. HFRFs may be appropriate targets for active clinical intervention in childhood cancer survivors.

Introduction

The five-year survival rates from childhood malignancies have increased to over 80% (105), and as a result the number of adult survivors of childhood cancer is growing. Compared with the general population, this group has a higher lifetime risk of cardiovascular disease, including heart failure (HF), with up to 32% developing subclinical left ventricular dysfunction (LVD) at a median of 23 years from cancer diagnosis (118). Cardiac late-effects of cancer therapy are considered the cause of this increased risk; the majority of these survivors have a history of anthracycline or chest-directed radiotherapy treatment. Indeed, up to 86% of patients treated with anthracyclines will have myocardial histopathological changes (119). While this irreversible myocardial damage predisposes to HF, the delay of decades before HF onset suggests that it is not itself sufficient for HF development.

The risk of non-ischemic HF is linked to a number of HF risk factors (HFRFs). It may be that exposure to cardiotoxic therapy reduces the heart's tolerance for other cardiometabolic risk factors, culminating in the eventual progression to cardiomyopathy. There are no specific recommendations for optimal management of these HFRFs in the cancer survivor population (120), and thresholds for their treatment in the survivor population may be similar to the normal population. It is possible that this approach poorly serves the survivor population due to depleted LV functional reserve. However, there is currently a paucity of research assessing the additional impact of traditional HFRFs on cardiac dysfunction in the survivor population. Therefore, we sought to determine the relative impact of conventional HFRFs and the presence and intensity of potentially cardiotoxic therapy on echocardiographic measures of myocardial function and exercise tolerance in survivors of childhood cancer.

Methods

Participant recruitment. Subjects were participants from the St Jude Lifetime cohort study (SJLIFE). Inclusion criteria included; i) treatment for childhood cancer at St Jude Research Children's Hospital, ii) received anthracycline and /or chest-directed radiotherapy, iii) 18 years of age or older and iii) at least 10

years distant from treatment. Recruitment was completed by April 2013. Further details of SJLIFE recruitment and study design have been published previously (121). The local Institutional Review Board approved the study.

Demographic and Exposure variables. Demographic and treatment data, including cumulative anthracycline dose and chest-directed radiotherapy radiation dose was obtained by abstraction of participants' medical records. Patients completed a questionnaire and attended a clinical assessment for direct assessment of current medical conditions and presence of risk factors. Height and weight were recorded. Seated resting blood pressure was recorded three times, with the lowest reading selected for analysis. Blood samples were collected after an overnight fast.

The following HFRFs were included in the current analysis, based on established association with incident HF in the non-cancer survivor population (122): presence of hypertension (defined as systolic blood pressure (BP) >140 mm Hg or diastolic BP > 90 mm Hg or self-reported history of hypertension or current treatment with anti-hypertensive medications), insulin resistance (defined as homoeostatic model assessment for insulin resistance (HOMA-IR) > 2.86), obesity (defined as body mass index [BMI] > 30 mg/m^2) and smoking status (defined as self-reported current, former or never).

A 6-minute-walk test (6MWT) was performed indoors by experienced technician with a 6MWT distance of <490m considered abnormal (123).

Echocardiographic Assessment. All echocardiographic examinations were performed by experienced sonographers using a standard echocardiographic system (Vivid 7, GE Medical Systems, Milwaukee, WI). LVEF and left ventricular morphology were measured using techniques outlined in American Society of Echocardiography (ASE) 2015 guidelines (124), with LVEF threshold of <53% designated as abnormal for both 2D and 3D-LVEF techniques. Given that formal thresholds for HF treatment are based on LVEF alone, abnormalities of 2D or 3D-LVEF were described as clinical cardiac dysfunction, and abnormalities in GLS or diastolic dysfunction without HF symptoms were described as subclinical cardiac dysfunction.

Diastolic echocardiographic assessment included measurements of peak mitral inflow velocity (E), mitral septal and lateral early diastolic tissue velocities (e'), the ratio of these variables using the medial e' velocity

as the denominator (E/e') and indexed left atrial volumes calculated using biplane orthogonal measurements. Diastolic grade was determined using criteria described in ASE 2016 guidelines (125). Diastolic dysfunction was defined as a binary variable with grade 1 or higher constituting dysfunction.

The apical 2-chamber, 3-chamber and 4-chamber views were obtained for offline global longitudinal strain (GLS) measurement, with temporal resolution of 50-60 fps for image optimization. GLS was assessed using peak systolic strain measured by 2D-speckle tracking by EchoPAC version 10.0 software (GE Medical Systems). 2D-speckle strain measurements were considered abnormal if ≥ 2 standard deviations from age-specific and sex-specific values from normal controls, extrapolated from the JUSTICE cohort of 817 healthy volunteers (126). All measurements were performed in a core laboratory at the Cleveland Clinic.

Statistical analyses. Baseline demographic and treatment characteristics of participants and nonparticipants were described using percentages for categorical variables and means ± standard deviations for continuous variables, with a chi-square test to assess for significant differences between groups. HFRFs were evaluated using Bayesian model averaging to automatically select the final logistic regression model for testing. All variables underwent univariable analysis, and variables with $p \geq 0.1$ were included in multivariable analysis; variables associated with abnormal cardiac function (gender, anthracycline cumulative dose, chest-directed radiotherapy, time since diagnosis, age at diagnosis) were included in all models. Each cardiac outcome variable was modelled independently. Multivariable odds ratios (OR) and 95% confidence intervals (95%CI) were estimated using models adjusted for treatment exposure. The final model with the lowest Akaike Information Criterion was selected for interpretation of findings. Standardised β coefficients were calculated by subtracting the mean from the variable and dividing by the standard deviation. Effect sizes were calculated using the semi-partial omega-square method to measure the adjust effect as proportion of total variation in the dependent variable.

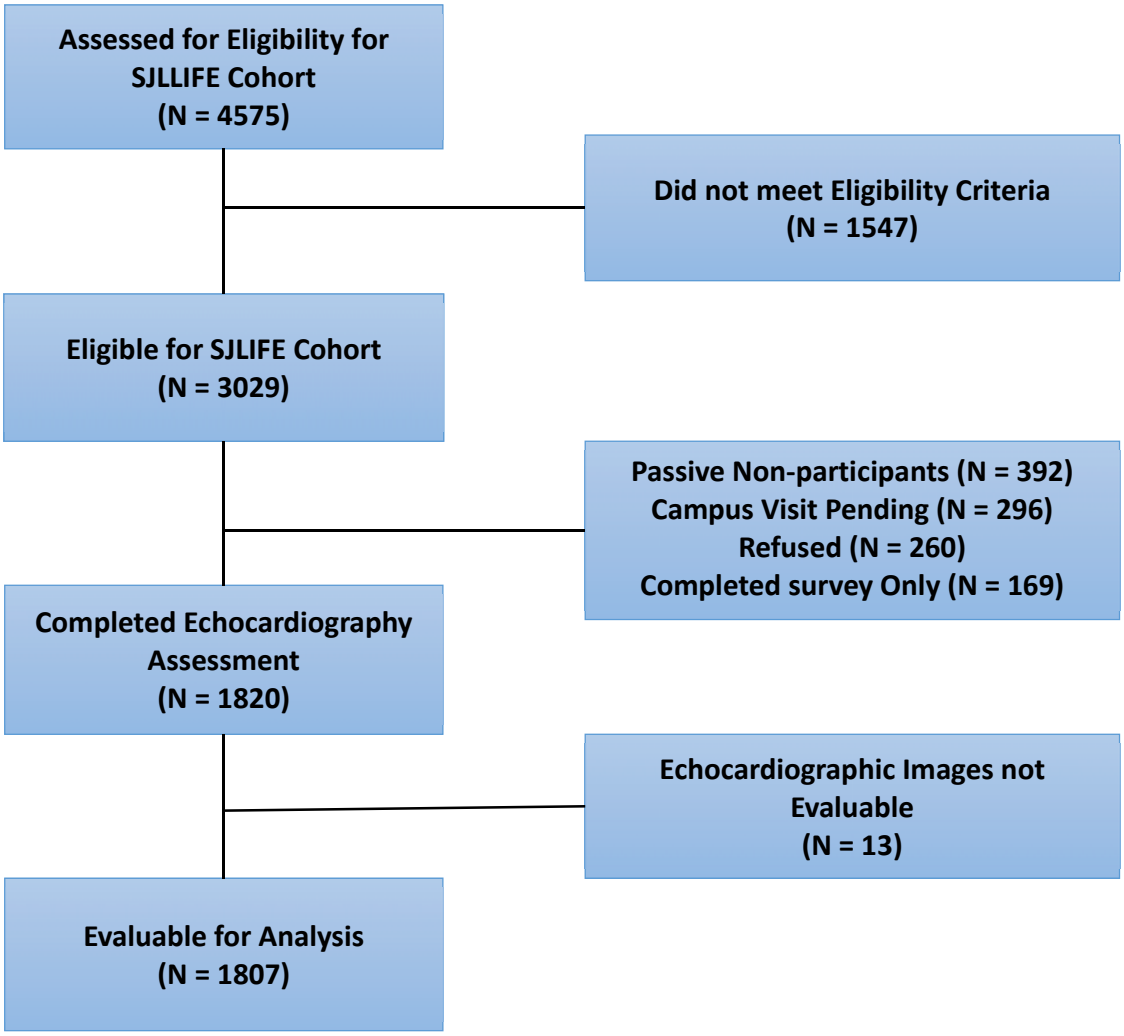

Figure 4-1: CONSORT Diagram of SJLIFE Population Eligible for Echocardiographic Evaluation

CONSORT = Consolidated Standards of Reporting Trials; SJLIFE = St. Jude Lifetime Cohort study

Results

Clinical features. Of 4575 patients assessed for eligibility for inclusion in SJLIFE cohort, 3209 were confirmed to have received anthracyclines and/or chest-directed radiotherapy for childhood malignancy (Figure 1). Echocardiographic assessments were completed in 1820 subjects; after exclusion of 13 due to inadequate echocardiographic images, 1807 participants (48% female, median age 31.6 years, median time

from diagnosis 22.6 years) were included in the final analysis. Compared with 1209 non-participants, participants were more likely to be female (44.4% vs 48.0%, $p < 0.0001$) and more likely to be non-Caucasian (15.8% vs 20.1%, $p = 0.01$), with no other significant differences in baseline characteristics (Table 4-1).

Associations with cardiac dysfunction. On echocardiographic assessment, 13% were found to have abnormal 2D-LVEF, 15% had abnormal 3D-LVEF, 29% had abnormal GLS and 46% had abnormal diastolic function. Of patients with abnormal diastolic function, 98% had grade 1 dysfunction, 1.3% had grade 2 dysfunction and 0.7% had grade 3 dysfunction.

Baseline demographic factors had significant associations with systolic, diastolic and morphological echocardiographic parameters of cardiac dysfunction. Systolic dysfunction was independently associated with male gender, age >15 years at diagnosis and time since diagnosis. Chest-directed RT and anthracycline co-treatment was associated with greater change in LVEF, compared with treatment with anthracyclines alone. Diastolic dysfunction was independently associated with male gender and chest-directed radiotherapy.

The associations of HFRFs with abnormal LV functional parameters are shown in Table 4-2. Insulin resistance (defined as HOMA-IR > 2.86 mmol/L) and obesity were associated with abnormal GLS and abnormal diastolic grade, but not with abnormal cardiac morphology. There was no association between CAD and any abnormal echocardiographic parameters.

Standardized coefficients were calculated in order to compare the effect sizes for HFRFs and other features associated with HF (Figure 4-2) (Table 4-3). The greatest effect on GLS appeared to originate from HOMA-IR, and this (together with age) had the greatest effect on LAVi. In contrast, LVMI was influenced strongly by hypertension. The effect of anthracycline dose had a minor effect on each of these variables and was the most important effect only for 3D-LVEF. HOMA-IR was sole HFRF that affected diastolic function (as measured by LAVi).

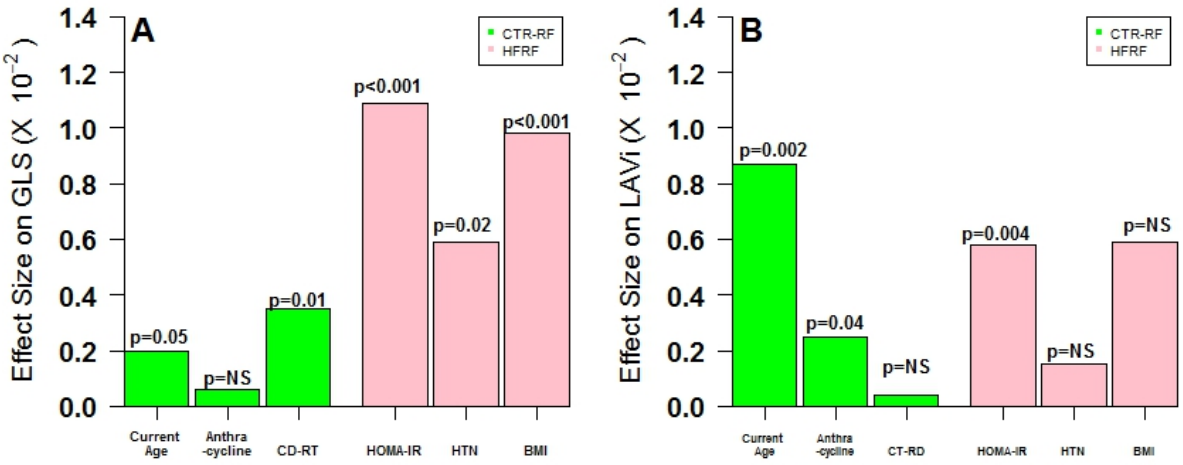

Figure 4-2: Effect sizes of impact of treatment-related risk factors and conventional HFRFs on A) Systolic function (GLS) and B) diastolic function (LAVi). Anthracycline refers to cumulative anthracycline dose.

BMI – Body mass index; CD-RT – Chest Directed Radiotherapy; CTR-RF – Cancer-Therapeutic-Related Risk Factor; GLS – Global Longitudinal Strain; HFRF – Heart Failure Risk Factor; HOMA-IR – Homeostatic Model Assessment Insulin Resistance; HTN – Hypertension.

6MWT was performed in 1635 participants (90.5%), with 326 (18.0%) achieving <490 metres. Obesity was the only HFRF associated with abnormal 6MWT distance (Table 4-4). Chest-directed RT alone was associated with abnormal 6MWT distance, but anthracyclines and chest-directed RT together was not.

Association with functional capacity. Clinical systolic dysfunction (2D-LVEF, 3D-LVEF), subclinical systolic dysfunction (GLS), diastolic dysfunction and changes in cardiac morphology all significantly and negatively impacted 6MWT distance, with the greatest effect size associated with abnormal GLS (Table 4-4).

Discussion

The current study indicates that traditional HFRFs are associated with novel echocardiographic markers of myocardial dysfunction in childhood cancer survivors. Furthermore, effect sizes for HFRFs were frequently on the same order of magnitude as baseline demographics of age and cumulative anthracycline dose.

Effect of HFRFs. It is generally accepted that aggressive treatment of HFRFs in the non-oncological setting may delay or prevent development of symptomatic HF to a degree similar to pharmacological therapy (127). However treatment of HFRFs remains suboptimal; 32% of population attributable risk of incident HF is due to obesity, hypertension and diabetes (128), suggesting a significant opportunity to reduce global HF burden.

Table 4-1: Demographic and Treatment Characteristics of Adult Survivors of Childhood Cancer

	Eligible (n= 3029)		**Nonparticipants (n= 1209)**		**Participants (n= 1820)**	
	n	%	n	%	n	%
Sex						
Male	1684	55.6	946	52.0	738	61.0
Female	1345	44.4	874	48.0	471	39.0
Race						
Non-Hispanic White	2499	82.5	966	79.9	1533	84.2
Non-Hispanic Black	417	13.8	195	16.1	222	12.2
Non-Hispanic Other	37	1.2	18	1.5	19	1.0
Hispanic	76	2.5	30	2.5	46	2.5
Therapeutic Exposure						
Anthracycline alone	1765	58.3	715	59.1	1050	57.7
Chest-directed RT alone	510	16.8	204	16.9	306	16.8
Anthracycline + chest-directed RT	754	24.9	290	24.0	464	25.5
Age at Diagnosis, years						
0 – 4	1023	33.8	404	33.4	619	34.0
5 – 9	718	23.7	296	24.5	422	23.2
10 – 14	731	24.1	286	23.7	445	24.5
15 – 19	530	17.5	210	17.4	320	17.6
>19	27	0.9	13	1.1	14	0.8
Time since diagnosis (years)						
10 – 20	-	-	-	-	664	36.5
21 – 30	-	-	-	-	738	40.6
31 – 40	-	-	-	-	365	20.0
41 – 50	-	-	-	-	53	2.9
Age at Assessment, years						
≤30	-	-	-	-	859	47.2
31 – 40	-	-	-	-	654	35.9
41 – 50	-	-	-	-	268	14.7
51 - 60	-	-	-	-	38	2.1
>60	-	-	-	-	1	0.1
Anthracycline Cumulative Dose, mg/m^2						
0	511	16.9	205	17.1	306	16.9
1 – 100	784	26.0	296	24.6	488	26.9
101 - 200	882	29.2	364	30.3	518	28.6
201 – 300	336	11.1	141	11.7	195	10.8
301 – 400	332	11.0	107	8.9	225	12.4
401 – 500	100	3.3	41	3.4	59	3.3
501 – 600	23	0.8	5	0.4	18	1.0
>600	48	1.6	43	3.6	5	0.3
Missing	13	0.4	7	0.6	6	0.3
Chest-directed RT (Gy)						
0	1765	58.33	715	59.2	1050	57.8

1 – 19.9	362	11.96	144	11.9	218	12.0
20 – 29.9	474	15.66	182	15.1	292	16.1
≥30	425	14.04	167	13.8	258	14.2
Unknown	3	0.1	1	0.1	2	0.1
Diabetes Mellitus						
Yes	-	-	-	-	108	6.8
No	-	-	-	-	1490	93.2
Missing	-	-	-	-	222	-
HOMA-IR						
>2.86	-	-	-	-	821	45.8
< 2.86	-	-	-	-	971	54.2
Missing	-	-	-	-	28	-
Hypertension						
Yes	-	-	-	-	367	21.0
No	-	-	-	-	1379	79.0
Missing	-	-	-	-	74	-
Dyslipidemia (TC/HDL > 3.5 mmol/L)						
Yes	-	-	-	-	143	8.1
No	-	-	-	-	1629	91.9
Missing	-	-	-	-	48	-
Obesity						
Yes	-	-	-	-	602	33.2
No	-	-	-	-	1210	66.8
Missing	-	-	-	-	8	-
Coronary Artery Disease						
Yes	-	-	-	-	107	5.9
No	-	-	-	-	1713	94.1
Smoking status						
Never	-	-	-	-	1162	64.7
Ex-smoker	-	-	-	-	210	11.7
Current smoker	-	-	-	-	424	23.6
Missing	-	-	-	-	24	-

Table 4-2: Multivariable Association Between Cardiovascular Risk Factors and Echocardiographic Abnormalities

	2D-LVEF <53%			3D-LVEF <53%			Abnormal GLS			Diastolic Dysfunction Grade 1-3			LAVI >35 mL/m2		
	OR	**95%CI**	**p**	**OR**	**95%CI**	**p**	**OR**	**95%CI**	**p**	**OR**	**95%CI**	**p**	**OR**	**95%CI**	**p**
Therapeutic Exposure															
Anthracycline alone	1.0	-	-	1.00	-	-	1.00	-	-	1.0	-	-	-	-	-
Chest-directed RT alone	1.32	0.9 – 2.0	0.19	1.09	0.70-1.71	0.69	1.11	0.78-1.59	0.55	2.54	1.78-3.62	<0.0001	-	-	-
Anthracycline + chest-directed RT	1.44	1.01 – 2.06	0.04	1.30	0.91-1.87	0.15	1.37	1.03-1.82	0.03	1.82	1.36-2.44	<0.0001	1.0	-	-
HOMA-IR															
>2.86	-*	-	-	1.09	0.75-1.56	0.63	1.72	1.30-2.28	0.0002	1.44	1.08-1.92	0.01	1.0	-	-
<2.86	-	-	-	1.00	-	-	1.0	-	-	1.0	-	-	-	-	-
Hypertension															
Yes	1.19	0.83-1.71	0.35	1.81	1.25-2.62	0.002	1.34	0.98-1.82	0.06	1.41	1.03-1.94	0.03	1.82	0.47-6.98	0.38
No	1.00			1.00			1.0	-	-	1.0	-	-	1.0	-	-
Dyslidipemia															
Yes	-	-	-	1.27	0.76-2.13	0.37	1.07	0.69 –1.66		1.94	1.19-3.17	0.01	2.52	0.58-10.96	0.22
No	-	-	-	1.00	-	-	1.00		0.76	1.94	-	-	1.0		-
Obesity															
Yes	-	-	-	1.47	1.02-2.12	0.04	1.58	1.19-2.11	0.002	1.92	1.42-2.58	<0.0001	-	-	-
No	-	-	-	1.00	-	-	1.00	-	-	-	-	1.0	1.0		-

CI – Confidence Interval; GLS -Global Longitudinal Strain, HOMA-IR – Homeostatic Model Assessment Insulin Resistance; LAVI – Indexed Left Atrial Volume; LV – Left Ventricular; LVEF – Left Ventricular Ejection Fraction;
OR – Odds Ratio; RT – chest-directed radiotherapy
*Absence of calculated OR indicates that dependent variable did not produce p value ≤0.1 on univariable analysis, and hence were not included in the multivariable analysis.

There are several reasons to think that effects of HFRFs on cardiac function are accentuated in the childhood cancer survivor population. First, survivors have a high risk of undetected cardiac dysfunction, and 39% of childhood cancer survivors have subclinical cardiac dysfunction (118). These findings suggest that a sizable proportion of survivors may meet criteria for stage B HF. Second, asymptomatic cardiac dysfunction is under-treated in the non-oncological population - 50% of newly diagnosed patients in the hospital setting do not receive appropriate pharmacological treatment (129) – and it is likely that initiation of appropriate treatment may be even lower in the relatively younger cancer survivors. Additionally, the younger age of cancer survivors indicates that HFRFs may have a larger time window to exert a cumulative myopathic effect. Hypertension and obesity precede the diagnosis of HF by 10-16 years (128) and cancer survivors may become victims of a confluence of adverse risk factors at a younger age than the general population. The prevalence of cancer survivors is projected to increase by 29% by 2016 (130), which suggests that an active approach to preventing incident HF in the cancer survivor population should be undertaken to prevent a substantial increase in HF burden in the population.

Table 4-3: Standardized Coefficients and Effect Sizes of Cardiovascular Risk factors on Abnormal Echocardiographic Findings.

	3D-LVEF				Abnormal GLS				LVMI				LAVI			
	B	**SE**	**p**	**Effect size**	**B**	**SE**	**p**	**Effect size**	**B**	**SE**	**p**	**Effect size**	**B**	**SE**	**p**	**Effect Size**
Age at Assessment	0.04	0.03	0.09	0.0016	0.02	0.01	0.05	0.002	-0.03	0.08	0.73	-0.0006	0.09	0.03	0.002	0.0070
Anthracycline Cumulative Dose	0.01	0.001	<.0001	0.0151	0.001	0.001	0.17	0.0006	0.001	0.004	0.66	-0.0006	-0.003	0.001	0.04	0.0025
HOMA-IR	0.64	0.38	0.09	0.0015	0.71	0.17	<0.0001	0.0109	-1.02	1.18	0.39	0.0002	-1.23	0.43	0.004	0.0058
Hypertension	1.25	0.45	0.01	0.0055	-0.62	0.20	0.002	0.0059	-6.30	1.33	<0.0001	0.0151	-0.83	0.49	0.09	0.0015
BMI																
<25	1.22	0.72	0.09	0.0017	-1.10	0.31	0.0004	0.098	-0.19	2.09	0.93	0.0051	-0.006	0.76	0.94	0.0059
25-29	1.26	0.71	0.07		-1.00	0.31	0.001		3.63	2.03	0.07		1.32	0.74	0.08	
30-35	0.37	0.71	0.60		-0.84	0.31	0.01		2.40	2.04	0.24		0.60	0.75	0.42	
35-49	0.49	0.79	0.53		-0.24	0.35	0.49		2.19	2.33	0.35		1.10	0.89	0.20	
Smoking																
Ex-smoker	0.43	0.50	0.39	0.0010	0.06	0.22	0.78	0.0009	0.65	1.54	0.67	0.0054	0.75	0.56	0.18	0.0013
Current smoker	0.17	0.37	0.65		0.14	0.17	0.39		3.53	1.13	0.002		0.67	0.41	0.11	

BMI – Body mass Index; GLS – Global Longitudinal strain; HOMA-IR – Homeostatic Model Assessment Insulin Resistance; LAVI – Indexed Left Atrial Volume; LVEF – Left Ventricular Ejection Fraction; LVMI – Indexed Left Ventricular Mass; SE – Standard Error

On an individual HFRF level, our results broadly agree with previously published findings in non-oncological populations. Hypertension is associated with subclinical cardiac dysfunction, and the population attributable risk for HF is 20% (128). Recent large clinical trials such as SPRINT suggest there are patient subgroups who may benefit from aggressive HFRF management (131).

Although there is a clear appreciation of the relationship between diabetes and both clinical and subclinical HF (132), the relationship between insulin resistance and subclinical myocardial dysfunction is less well-known. HOMA-IR has been associated with abnormal GLS and LVH (133). These findings broadly agree with our findings of subclinical cardiac dysfunction associated with elevated HOMA-IR and suggest that insulin resistance should be considered a therapeutic target in childhood cancer survivor population.

Associations between obesity and subclinical cardiac dysfunction are recognized in the non-oncological population; reported OR 1.60 (95%CI 1.06 – 2.41) for diastolic dysfunction, are similar to our observed value (OR 1.92 (95%CI 1.42 – 2.58)) (134). This association is manifest with diastolic dysfunction and LVH rather than 2D or 3D-LVEF, and this was confirmed in our study. Childhood cancer survivors are 14% more likely to be obese than their healthy peers (134,135), again supporting the need for active intervention to prevent and treat obesity in this group.

Smoking is a HF risk factor. Nonetheless, the lack of association of smoking status with systolic or subclinical systolic or diastolic cardiac dysfunction is broadly in agreement with previously published findings in participants free of hypertension and diabetes (136).

Table 4-4: Standardized coefficients and effect sizes of echocardiographic parameters on exercise capacity

	Abnormal 6MWT (< 490 m)			
	β	SE	P	Effect size
3D-LVEF	2.00	0.57	0.0005	0.0076
GLS	-6.95*	1.08	<0.0001	0.0260
LVMI	0.46	0.16	0.004	0.0044
LAVI	1.92	0.45	<0.0001	0.0107

6MWT = 6 minute walk test; 3D-LVEF = 3D Left Ventricular Ejection Fraction; GCS = Global Circumferential Strain; GLS = Global Longitudinal Strain; LAVI = Left Atrial Volume Indexed; LVMI = Left Ventricular Mass Index; Se = Standard Error
*Note that as 2D speckle-tracking strain measurements within reference range are reported as negative values, the standardized coefficients will also be negative

Comparison of echocardiographic techniques for assessing myocardial function. Our results confirm a hierarchy of imaging modalities for detecting effects of myocardial consequences of HFRFs that corresponds to previously published reports of sensitivity for earlier phenotypes with different techniques (137). Three HFRFs were associated with abnormal GLS and diastolic dysfunction, and two HFRFs associated with abnormal 3D-LVEF, but only one factor was associated with 2D-LVEF decline. The lack of association of HFRFs with the traditional method of 2D-LVEF may reflect the late onset of LVEF decline, which may not have had time to develop in our cohort. Current guidelines suggest periodic echocardiographic follow-up for adult survivors of childhood cancers (105,120). However, several of the echocardiographic parameters recommended, such as fractional shortening, wall stress and velocity of fiber shortening corrected for heart rate, are no longer widely measured, and the empiric basis for LVEF monitoring was established 25 years ago (138). Our results suggest that an emphasis should be placed on subclinical LV dysfunction preceding LVEF decline, and recognition of such changes should be followed by search for modifiable HFRFs.

Each of the HFRFs modelled significantly increased the risk of diastolic dysfunction, even after correcting for baseline risk of anthracycline and chest-directed-RT treatment. Because it is a continuous variable, LAVI was used as an outcome rather than diastolic grade for quantifying the effect size of HFRFs on diastolic dysfunction. Only one HFRF, elevated HOMA-IR, was associated with increased LAVI. This may be because the majority of patients with diastolic dysfunction were in grade 1, which is not associated with elevated left atrial pressures.

GLS has been reported to demonstrate a greater association with mortality than 2D-LVEF (139). It is unclear as to whether this difference reflects an inherent problem with EF, or whether it simply reflects the ambiguity of echo measurement of EF. The limitations of single-point LVEF measurements are widely recognized (140), and GLS is recognized to have lower intra- and inter-observer variability (141).

Functional Capacity. Despite the association of HFRFs with echocardiographic findings of subclinical systolic and diastolic dysfunction, there was no association between the majority of HFRFs and abnormal 6MWT, with the sole exception of obesity. However, reduction in 6MWT distance is frequently due to

disturbance of multiple physiological systems so potential contributions to 6MWT distance by improving HFRFs may be masked by the real-world complexity of exercise physiology. Nonetheless, it is of interest to measure the effect of echocardiographic markers of cardiac dysfunction on 6MWTD for several reasons. First, 6MWTD has been demonstrated to an equally strong and independent mortality predictor as LVEF in HF patients, so demonstrating association would provide a prognostic context for the effects of HFRFs on echocardiographic markers. Second, exercise testing has been demonstrated to facilitate earlier diagnosis of cardiac dysfunction in patients without a diagnosis of HF (142), indicating that exercise intolerance may be an early phase in the evolution of HF. Third, although studies have been performed demonstrating that GLS is more closely associated with reduced cardiopulmonary exercise function than is LVEF (143) in patients with symptomatic HF, there is limited evidence of the association of GLS and exercise tolerance in patients with HF risk factors. Our study's findings that echocardiographic markers of cardiac dysfunction were significantly associated with reduced 6MWTD is novel and clinically important and adds further support to the concept that HFRFs should be actively managed if cardiac dysfunction is present. GLS had the strongest association with 6MWTD, which is in keeping with prior studies in HF patients (143). The pathophysiological mechanisms underlying this finding remain uncertain.

Limitations. Several limitations should be taken into account when assessing the implications of our results. First, the cross-sectional study design meant that historical data was not collected contemporaneously, and it is possible that baseline information may contain inaccuracies. Second, of all eligible subjects recruited into the SJLIFE cohort, 43% did not have an echocardiographic assessment, and it is possible that these excluded subjects differed from participants in unmeasured characteristics. Third, given the relatively young age of our cohort, we are unable to assess hard cardiovascular outcomes such as HF incidence, although such analyses may be possible in the future as the cohort ages. Fourth, participants had only a single echocardiogram, and it is possible that sequential echocardiographic studies may have detected decrements in cardiac function over time while remaining within normal reference ranges. Fifth, echocardiography is operator-dependent and it is possible that other centres may not reproduce findings with similar accuracy, although it should be noted that the newer echocardiographic modalities used in our

study, including GLS and 3D-LVEF, have superior intra-observer and inter-observer reproducibility compared to 2D-LVEF measurements. Last, thresholds for abnormal GLS measurements were derived from reported normal reference ranges derived from a large population of Japanese healthy volunteers and it is possible that population differs from ours, although similar strain ranges were seen in a European population (144).

Conclusions.

The results of the current study have added new information on the effects of traditional HFRFs on novel echocardiographic markers of myocardial dysfunction in survivors of childhood cancer. The effect sizes for HFRFs were larger than that of cumulative anthracycline dose. Guideline recommendations for frequency and extent of monitoring, and thresholds of treatment and management of HFRFs are based on expert consensus derived from studies and guidelines from the non-oncological population (120). This approach may not be ideal for the childhood cancer survivor population, in whom HFRFs may be appropriate targets for aggressive clinical interventions.

Postscript

Despite a focus on cancer therapy as a cause for HF, the results of the current study show that traditional HFRFs are at least as important (if not more so) than cumulative anthracycline dose as determinants of myocardial dysfunction in survivors of childhood cancer. In addition to cardioprotection at the time of chemotherapy, ongoing detection and management of classical HFRFs appear to be important and should be considered as part of guidelines.

Chapter 5

Real-World Practice of Cardiac Imaging For Cancer Patients

Preface

The first section of this thesis demonstrated that CTRCD is a significant source of morbidity and mortality in the cancer survivor population and requires sequential monitoring using cardiac imaging due to variable onset of cardiac dysfunction. Effective therapeutics for cardiac dysfunction exist, but targeted use is only possible in the context of cardiac imaging at appropriate time-intervals to successfully identify patients prior to irreversible dysfunction. Presently CTRCD is defined by significant decrement in LVEF from a baseline value. Although many modalities are available for measuring LVEF, values are not interchangeable between them(145). Therefore the choice of imaging modality directly affects the physician's ability to diagnose CTRCD, and the modality with highest accuracy, reproducibility and predictive value should be prioritized.

Currently cardiac tests for cancer patients can be ordered by either the patient's treating oncologist or haematologist, or alternatively by a cardiologist who has been invited to participate in the patient's care. For purposes of simplicity, further reference to oncologists will include physicians with specialist accreditation in either oncology or haematology. In practice, the two most common techniques for assessing cardiac function in cancer patients are MUGAs and echocardiography. Alternative non-invasive techniques, such as CMR and positron-emission tomography are not reasonable first-line choices due to reasons of cost and variable regional availability of services. Since oncologists and cardiologists may have differing training and treatment goals (e.g. cancer remission versus long-term cardiovascular risk), it is possible that one modality maybe considered more appropriate than the other. Whether each modality has recent technological advances that could potentially improve diagnostic performance could also be taken into account.

The next section of this thesis is concerned with comparing the most commonly used techniques for measuring LVEF and exploring potential avenues for optimising their diagnostic and predictive yield in cancer populations, so that the test with the greatest utility can be recommended at a societal level.

Abstract

Background: Previous studies has suggested that sequential cardiac imaging modalities in patients treated with chemotherapy are discordant with recommendations in international guidelines, possibly related to issues of access and cost. It is unknown if this difference affects rates of cardiotoxicity diagnosis or has treatment implications.

Objectives: To perform a prospective cohort study comparing real-world practice predominantly using MUGA scans at an Australian regional tertiary hospital with a strategy utilizing sequential novel echocardiographic techniques.

Methods: Patients were recruited from a single center if they had been identified by their treating oncologist or hematologist as scheduled for treatment with potentially cardiotoxic chemotherapeutics. Patients underwent concurrent MUGA-based cardiac imaging by treating team and echocardiographic-based cardiac imaging by researchers. Conventional strategy was MUGA screening as intervals deemed appropriate by the treating team. The echocardiographic strategy was performed in all patients at timepoints advised by international society guidelines. Outcomes included adherence to society recommendations, agreement between MUGA and echocardiographic LVEF measurements and detection of cardiac dysfunction (defined as >5% LVEF decrement from baseline by 3D-LVEF). A secondary endpoint was accuracy of global longitudinal strain in predicting cardiac dysfunction.

Results: 35 patients were recruited, including 15 breast cancer patients, 19 hematological malignancy patients and 1 gastric cancer patient. MUGA and echocardiographic LVEF measurements correlated poorly with limits of agreement of 30% between 2D-LVEF and MUGA-LVEF and 37% for 3D-LVEF and MUGA-LVEF. Only 1 case (2.9%) of CTRCD was diagnosed by MUGA, compared to 12 (34.2%) cases by echocardiography. Four patients had >10% decrement in 3D-LVEF that was not detected by MUGA. GLS at 2 months displayed significant ability to predict CTRCD (AUC 0.75, 95% 0.55 – 0.94).

Conclusions: MUGA correlates poorly with echocardiographic measurements with substantial disagreement between MUGA and echocardiography in CTRCD diagnosis. MUGA and echocardiographic imaging strategies should not be considered equally appropriate for imaging cancer patients.

Introduction

Cardiac dysfunction after potentially cardiotoxic chemotherapy for cancer can cause cancer-therapy-related cardiac dysfunction (CTRCD) in up to 20% of patients (146). CTRCD is associated with significantly increased adverse cardiac event rates, with higher rates observed in patients treated >2 months from chemotherapy administration(22). Contemporary oncological guidelines recommend LVEF measurement prior to starting cardiotoxic chemotherapy at baseline, every 3 months during treatment and at 12 and 18 months after the initiation of treatment (104). However recent studies have demonstrated that adherence to guideline-directed cardiac monitoring can be as low as 46% (147).

Older cardiological and oncological guidelines have recommended that LVEF measurements may be performed by either echocardiography or multiple-acquisition-gated nuclear (MUGA) scans. Recently concerns have been raised regarding the accuracy of MUGA for detecting baseline cardiac dysfunction(46) and paucity of evidence demonstrating improved cardiac outcomes with MUGA screening(148). However, in many centres around the world, LVEF monitoring by MUGA is the most frequent modality ordered by oncologists(149), often due to accessibility and cost concerns regarding echocardiography.

We performed a head-to-head study comparing traditional oncologist-directed cardiac imaging at our local institution, where MUGA screening is standard practice, and advanced echocardiographic techniques, including 3D-LVEF and global longitudinal strain (GLS). Our goals were the following; 1) to compare agreement between MUGA-LVEF and echocardiographic measures of LVEF, 2) to compare rates of detection of CTRCD and 3) to determine if changes in GLS are predictive for CTRCD in a real-life prospective cohort.

Methods

Patients and Data Collection. The study sample consisted of patients referred prospectively from Royal Hobart Hospital between May 2014 and November 2015. Inclusion criteria included 1) age ≥ 18 years; 2)

planned anthracycline or trastuzumab chemotherapy (as determined by treating oncologist); 3) ability to provide written informed consent; 4) recruitment within three months of commencing anti-cancer therapy. Exclusion criteria included 1) life expectancy <12 weeks, 2) history of myocardial infarction in prior 3 months and 3) unwillingness to comply with study and follow-up procedures. Pre-existing left ventricular dysfunction was not a contraindication to treatment. All patients underwent concurrent cardiac screening for cardiotoxicity with standard institutional practice and advanced echocardiographic imaging.

Ethics approval was granted by the Tasmanian Human Research Ethics Committee (approval number H13115). All patient contact and data collection was conducted in compliance with the second Declaration of Helsinki. Written informed consent was obtained from all patients prior to enrolment.

Conventional Cardiac Imaging. All patients underwent cardiac imaging as decided by their treating oncologist. The most common practice was to order a baseline multiple-gated acquisition scan (MUGA scan) prior to administration of potentially cardiotoxic anticancer treatment, with need for subsequent sequential cardiac imaging at the discretion of the oncologist. The MUGA scan report described the LVEF but diastolic function, as assessed by nuclear peak filling rate, was not routinely assessed.

Echocardiographic Imaging. All patients underwent baseline history physical examination, including blood pressure, heart rate, height and weight measurements. Standard transthoracic 2-dimensional and Doppler echocardiographic studies were performed using standard equipment (GE Vivid E9; Vingved, Norway) in accordance with contemporary echocardiographic practice. LV peak global longitudinal strain was (GLS) measurements were obtained from gray-scale recorded images in the apical 4-chamber, 2-chamber and long-axis views. Strain was analyzed using commercial speckle-tracking software (Echopac, GE Medical Systems). GLS was measured by averaging strain from regions of interest from 3 apical views.

Patients underwent transthoracic echocardiographic imaging at baseline, and at 2 months after treatment (which is usually in the period after anthracycline or other chemotherapy agents are completed, but prior to trastuzumab administration for breast cancer patients).

Echocardiographic studies were performed in accordance with professional society guidelines and included cine imaging of biventricular function from multiple planes, diastolic interrogation and colour Doppler imaging of valvular function. 2D-LVEF was calculated by Simpson biplane technique. Global longitudinal strain used left ventricle-focused images at 50-70 frames/second. Images were discarded if ≥2 segments were uninterpretable.

Outcomes. First outcome was agreement between MUGA and echocardiographic measurements, as described by correlation coefficients and limits of agreement. Second outcome was detection of changes in LVEF per patient that may meet criteria for CTRCD. Because current position statements suggest that a 5% decrement in LVEF from baseline is the smallest change that can justify diagnosis of CTRCD and merits clinical assessment, we used this threshold. Third, we assessed prognostic ability of global longitudinal strain to detect later decrements in LVEF >5% (CTRCD-3D). We chose 3D-LVEF decrements ≥5% because 3D-LVEF has 95% confidence interval limit of temporal variability of 5% with greater decrements unlikely to be due to test imprecision and hence represent true pathological change(150).

Multiple-Gated Acquisition Scanning (MUGA). MUGA scans were performed per standard recommendations to quantify LVEF(151). Erythrocyte labelling using technetium 99-m labelled blood cells was employed with the modified in vitro method with activity of 11 to 13 MBq/kg. Images were acquired using a Siemens e-cam dual-head gamma camera (Siemens, Erlangen, Germany) equipped with a parallel hole, low-energy high-resolution collimator, with energy window of 15% symmetrically placed over a photopeak of 140 keV. Acquisition times were adjusted to achieve a minimum of 200,000 count per frame. LVEF analysis was performed by nuclear physicians with 2-10 years' experience. Clinically reported LVEF analyses were used, and analyses were not remeasured for the study.

Statistical analysis. Continuous data was expressed as mean ± standard deviation, and categorical data was expressed as numbers and percentages. Correlation between continuous variables was expressed using Pearson's correlation coefficient and Bland-Altman analyses. All data was first assessed first for normality by visual inspection and by Kolmogorov-Smirnov test. No transformations were necessary. Comparisons

of means were performed using paired or unpaired t-student's test as appropriate, and one-way ANOVA was used to compare means of >2 groups. If the assumption of normality was not held, then Wilcoxon's paired or unpaired test was used. Longitudinal data analysis was performed using generalized linear mixed models with individual patients used as random-effect models and timepoint used as in fixed-effect models with singular covariance matrix with Cholesky parameterization. Receiver-operating curves were calculated to assess predictive accuracy. Statistical analysis was performed using R statistical software (Vienna, Austria) and the lme4 package(152). P values ≤ 0.05 were considered significant.

Results

Study sample. Patient characteristics of the 35 patients were recruited between May 2014 and November 2015 are described in Table 5-1. Four patients died from their cancers during the study period (2 patients with AML, 1 patient with NHL and I patient with lymphoproliferative disease).

Follow-up. Of the 15 breast cancer patients, 14 received trastuzumab therapy over 12 months, with median 4 MUGA scans per patient (range 1 to 5). A single metastatic breast cancer patient treated with doxorubicin had a single baseline MUGA scan. Amongst the trastuzumab-treated patients 8 (62%) received sequential LVEF monitoring during treatment every 3 months (as recommended by oncology guidelines) but did not undergo post-treatment LVEF monitoring (i.e. 8 had total of 4 MUGA-LVEF measurements). Only 3 trastuzumab-treated patients (21%) had baseline, 3-monthly and post-treatment MUGA-LVEF measurements (i.e. 5 MUGA scans over 14 months).

The 19 patients with haematological malignancy had a median of 1 MUGA-LVEF measurement (range 0 to 3). Only 7 patients (37%) with haematological malignancy had both baseline and post-treatment MUGA-LVEF measurements. One patient did not receive any MUGA test. A single patient with gastric cancer had a baseline MUGA scan only. In total, 37% of patients received both baseline and post-treatment LVEF

assessment by MUGA monitoring. None of the 35 patients were admitted to hospital with diagnosis of heart failure during study duration.

In comparison, of the 14 trastuzumab-treated patients, 11 (78.5%) completed all 5 planned echocardiographic assessments at the planned 3-monthly intervals. One patient missed her baseline TTE study due to medical illness, 1 patient had 4 TTE exams but could not attend her final scan and 1 patient dropped out from the study after her third study. Haematological malignancy patients had a median of 4 TTE assessments (range 1-5). 16 patients (84.2%) had both baseline and post-treatment TTE scans.

Comparison between MUGA and echocardiographic LVEF. Among all 35 patients, there was a total of 73 MUGA-LVEF measurements, 131 2D-LVEF measurements and 117 3D-LVEF measurements. Feasibility of 2D-LVEF measurement was 100%, and feasibility of 3D-LVEF measurement was 89%. There was median of 10 days between echocardiographic and MUGA examinations (range 0 – 85 days). No significant correlation was seen between MUGA-LVEF and 2D-LVEF (r = 0.15, 95%CI -0.09 to 0.37, p = 0.22) (Figure 1). There was little bias between the measurements for MUGA-LVEF and 2D-LVEF but the limits of agreement were wide (Bias = 0.2%, LoA = 37.0%, 95% range -18.4 to 18.7%). A weak albeit significant correlation was seen between MUGA-LVEF and 3D-LVEF (r = 0.33, 95%CI 0.1 to 0.53, p = 0.0053), with small bias towards higher LVEF values with MUGA-LVEF and wide limits of agreement (Bias = +1.8%, LoA = 29.9%, range -13.1% to 16.8%). A stronger association was observed between 2D-LVEF and 3D-LVEF (r = 0.65, 0.48 to 0.77, p < 0.0001), with small bias towards higher LVEF values with 2D-LVEF and limits of agreement were narrower (Bias = +2.1%, LoA = 23.2%, range -9.5% to 13.7%) compared to comparisons with MUGA-LVEF. Overall, MUGA-LVEF did not correlate with 2D-LVEF and only weakly with 3D-LVEF measurements, and limits of agreement between MUGA and either 2D or 3D echocardiographic LVEF measurements were ≥30%.

Detection of Cancer Treatment-Related Cardiac Dysfunction (CTRCD). Ten patients were determined to have new cardiac dysfunction by 2D-LVEF (29%), as were 6 (17%) patients by 3D-LVEF. 5(15%) of patients had cardiac dysfunction diagnosed by both 2D-LVEF and 3D-LVEF. In contrast, only 1 patient demonstrated new cardiac dysfunction by MUGA, which was also detected on 2D-LVEF (3D-LVEF could not be measured in this patient at this timepoint due to image artifact from radiation-induced skin changes). By using a combined echocardiographic approach (i.e. ≥5% LVEF decrement from baseline as measured by either 2D-LVEF or 3D-LVEF or both), 11 additional cases of cardiac dysfunction (31.4%) were detected by regular echocardiography compared to MUGA, which may have prompted cardioprotective treatment. Inter-rater agreement for significant cardiac dysfunction was non-significant between MUGA-LVEF and 2D-LVEF (κ= 0.14, p = 0.11) and MUGA-LVEF and 3D-LVEF (κ = -0.51, p = 0.61). However there was significant inter-rater agreement between 2D-LVEF and 3D-LVEF (κ = 0.46, p = 0.01). Notably 4 patients were found to have >10% decrement in 3D-LVEF by 3D-TTE, none of which were detected by MUGA screening approach.

GLS prediction of CTRCD. Relative changes in GLS at 2 months, 5 months and using the greatest decrement of either timepoint were used to predict CTRCD (Figure 1). Change in GLS at 2 months was modestly predictive of CTRCD (AUC = 0.74, 95%CI 0.55 to 0.94), with threshold of 10.4% decrement from baseline in GLS demonstrating greatest accuracy. There was no significant predictive ability of change in GLS at 5 months (AUC = 0.51, 95%CI 0.28 to 0.74) or using the greatest decrement of either timepoint (AUC = 0.57, 95%CI 0.35 – 0.80).

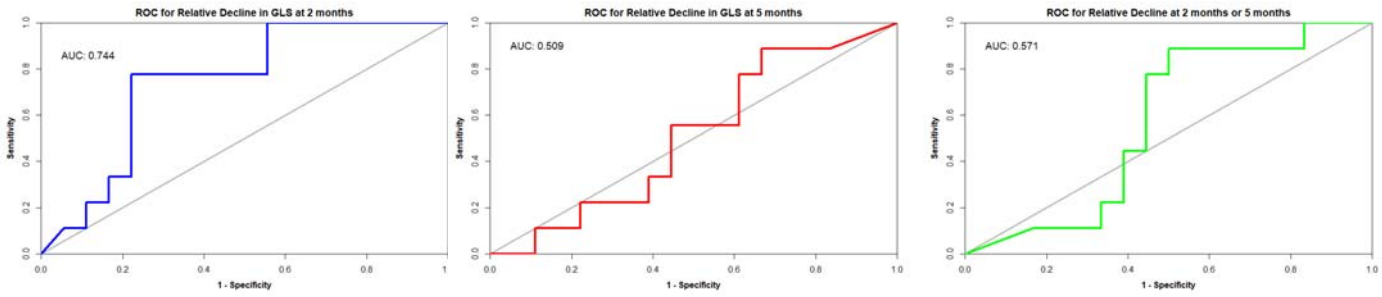

Figure 5-1: Receiver-Operating Curves to assess the predictive accuracy of relative changes in GLS for predicting CTRCD. A) Relative reduction in GLS from baseline at 2 months as predictor variable; B) Relative reduction in GLS from baseline at 5 months as predictor variable; C) using greatest decrement at either 2 or 5 months as predictor variable

Sequential LVEF change over time. There was no significant change in LVEF over time as measured by 2D-LVEF (β = -0.61 p = 0.17) or 3D-LVEF (β = -0.53 p = 0.15) (Figure 5-2). In contrast, a significant decline in MUGA- LVEF was observed (β = -0.76, p = 0.03). However, this finding was confounded by small numbers of MUGA scans (8 scans) performed at 8 month and 14-month timepoints, with no significant change seen between average MUGA-LVEF values at baseline and 2 months (p=0.29) or baseline and 5 months (p=0.36).

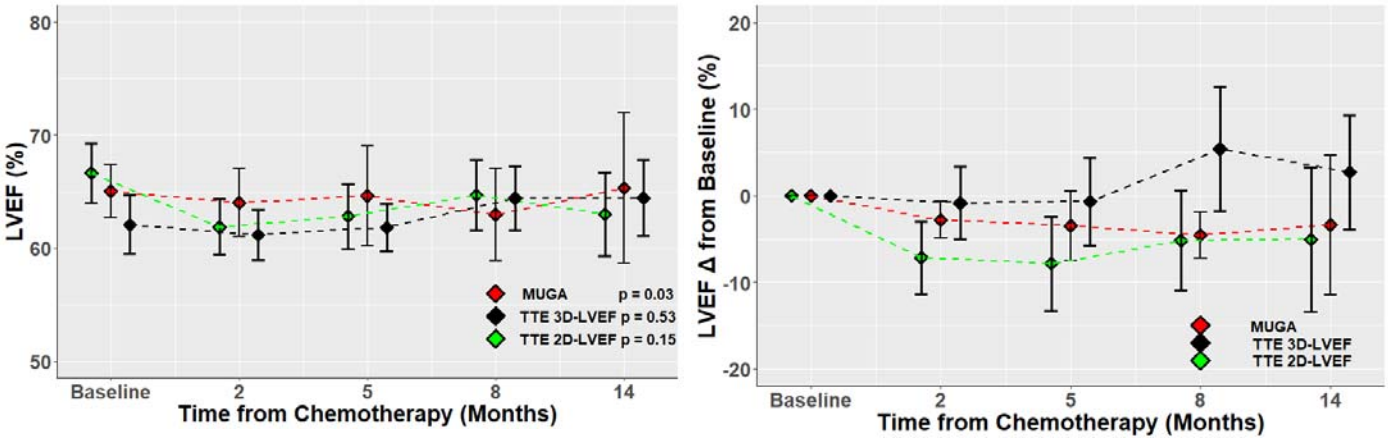

Figure 5-2: Trajectories of LVEF change over time with different modalities. A) Absolute change in LVEF over time for each modality. B) change relative to Baseline LVEF over time.

Table 5-1: **Patient Baseline Demographics**

Age (years)	55.0 ± 13.0
Female	24 (68.6%)
BMI (mg/m2)	29.9 ± 7.2
Cancer	
Breast	16 (45.7%)
NHL	13 (37.1%)
AML	3 (8.6%)
Hodgkin's	1 (2.9%)
Lymphoproliferative	1 (2.9%)
Gastric	1 (2.9%)
Diabetes Mellitus	2 (6.3%)
Obesity	13 (37.1%)
Hypertension	8 (22.9%)
Family History	7 (20%)
Heart disease	8 (22.9%)
SBP (mm Hg)	133.8 ± 21.0
DBP (mm Hg)	79.7 ± 10.2
HR (bpm)	79.7 ± 13.7

Abbreviations: AML – Acute Myeloid Leukemia; BMI – Body Mass Index; DBP – Diastolic Blood Pressure; HR – Heart Rate; NHL – Non-Hodgkin's Lymphoma; SBP – Systolic Blood pressure

Discussion

This study has demonstrated three important findings; 1) that there was poor correlation between LVEF measured by MUGA scans and by echocardiography, 2) that use of MUGA-LVEF measurements would have led to missing up to 28% of patients that could potentially benefit from cardioprotective therapy as assessed by echocardiography and 3) relative change in GLS at 2 months was predictive of later 3D-LVEF decrement as measured by echocardiography.

Nuclear and echocardiographic imaging. Our finding that LVEF measurements by MUGA correlate poorly with echocardiographic measurements and that up to 28% of patients had a ≥5% decrement in their LVEF that was missed by MUGA raises the question of which cardiac imaging modality is optimal for the cancer patient. Scientific studies assessing the use of MUGA in the cancer populations are lacking.

However anecdotally MUGA has been favoured by Australian oncologists due to reported difficulties in accessing quality echocardiographic services within a time-frame that does not risk delaying commencement of potentially life-saving chemotherapy. Additionally, oncologists understandably place greater value on cardiac imaging parameters that directly influence choice of cancer treatments, principally LVEF, and may be less inclined to incorporate other dimensions of cardiac function available from echocardiography, including strain, diastology and valvular function, into their treatment strategies.

However, several concerns have been raised recently regarding the use of MUGA scans for monitoring chemotherapy. Firstly, quoted studies demonstrating utility of MUGA scanning used different modalities of MUGA imaging than used in current day practice. The number of published studies on utility of MUGA in cancer peaked in approximately 1992, when MUGA used single-headed, small field of view cameras that allowed separation of photon counts between the cardiac chambers, so that the left ventricle could be measured without contamination from atria or right ventricle(153). Contemporary single photon emission cameras are two- and sometimes three-headed cameras that allow greater photon collection, but concerns have been voiced over the accuracy of this method for volumetric analysis, given that the spatial resolution of contemporary gamma camera is approximately 7-9 mm, and that LV volume measurements may be confounded by photons from adjacent chambers(148). A second concern is the unavoidable exposure to radiation, for which the typical dose from a MUGA scan is 6-7 mSv. This especially becomes an issue when sequential LV monitoring is required, such as for cardiac monitoring. In our study, 2 patients had a total of 5 MUGA scans each, which approximates a total radiotherapy dose of 30-35 Gy. This dose represents a third of the lifetime total medical radiation dose that is considered reasonable. A third concern is that, as seen in this study and confirmed in other studies(145), LVEF measurements between cardiac modalities are not inter-changeable. This creates the risk that if cardiac dysfunction develops, the MUGA modality would need to be continued to allow for comparison to baseline. This would result in loss of additional relevant clinical data, such as diastolic and valvular function, as well as increased cumulative radiation dose.

Our finding that 31% of patients had significant LVEF declines detected echocardiographically, of which one was detected by contemporary oncologist-directed monitoring, raises the issue of whether MUGA has adequate sensitivity for cardiotoxicity. An alternative consideration is whether echocardiography is nonspecific, resulting in excessive numbers of false-positive results. The difference between modalities likely cannot be attributed to technical differences alone, as it is probable that higher cardiac dysfunction rates would have detected by MUGA is monitoring adherence had been higher. However, as 60% of oncology-directed patients had ≥2 sequential MUGA scans, it is very likely that significant inter-modality differences also contribute to the disparate findings of cardiac dysfunction. One attribute of MUGA scanning that contributes towards uptake is reported superior reproducibility(45) with the underlying principle being that changes in accuracy may not be clinically important so long as the changes between LVEF between time-points is accurately quantified. This has become more debatable in past years, as recent publications have demonstrated that anthracycline-treated patients with LVEF in the "low-normal" range of 50-54% have a 6.7-fold increased risk of cardiac dysfunction(154). A head-to-head comparison of LVEF values derived from MUGA and the gold-standard of CMR found minimal bias, however the limits of agreement were wide at 35%(46). In practice, this means that for an individual with a MUGA-derived LVEF of 55%, we can be 95% confident that their CMR-derived LVEF would be between 37% and 71%. In contrast, the limits of agreement with CMR-LVEF with 3D end-diastolic volume and end-systolic volumes as calculated by echocardiography has been reported as 4.4% and 7.9% respectively(155), suggesting that echocardiographic measurements may indeed be superior to MUGA in terms of accuracy. The evidence for superior reproducibility of MUGA is also less settled in the author's view than described in recent review publications. The claims for superior reproducibility predominantly quote a study of 73 anthracycline-treated patients, which compared an LVEF derived from visual inspection of echocardiographic images to LVEF derived from automated software analysis of MUGA images with minimal operator intervention(156). The comparison of automated software to visual estimation likely reflects differences between machine and human estimation which would mask true inter-technique differences. It is possible that advances in nuclear camera technology may have improved

temporal variability, but the peak number of publications of MUGA-LVEF studies was in 1992, and there has been a precipitous decline in number of studies published since(153). If MUGA scans are to remain a first-line test for cancer-therapy-related cardiac dysfunction, then there is an urgent need for new research to determine the applications and limits of this technology.

Limitations. Several significant limitations of this study need to be addressed. Firstly, the incidence of heart failure was not quantified in a systematic manner, and therefore the predictive ability of either imaging strategy for heart failure cannot be assessed. However, our observed rates of cardiac dysfunction by echocardiography were similar to rates observed in other prospective clinical studies(44,157). Secondly as the echocardiographic reports were made available to the treating oncologist or haematologist, this may have affected their ordering MUGAs at intervals as advised by international guidelines, and this may have on turn affected their sensitivity for CTRCD diagnosis. Appropriate steps were taken during patient recruitment to emphasise that oncologist-guided monitoring should be independent of echocardiographic monitoring, and it would been ethically inadvisable to withhold information from echocardiographic studies from the treating physicians. Thirdly, we did not use a gold standard comparator of CMR-LVEF to determine accuracy. In contemporary clinical practice, CMR is difficult to access due to cost, local availability and frequent contraindications amongst patients. Hence our study reflects what can be reasonably achieved in majority of hospitals. Lastly, we did not measure biomarkers (e.g. troponin) for predicting or diagnosing cardiac dysfunction. Presently the evidence base for use of biomarkers in this setting is not concordant, and this is reflected in their delegation to second tier monitoring strategy behind cardiac imaging in contemporary guidelines(148).

Conclusions.

MUGA correlates poorly with echocardiographic measurement of LVEF with substantial disagreement between MUGA and echocardiography in CTRCD diagnosis. MUGA and echocardiographic imaging strategies should not be considered equally appropriate for imaging cancer patients.

Postscript

This chapter has demonstrated that there are clear differences in real-world clinical performance between MUGA and echocardiography. Differences in choice of cardiac imaging and suboptimal adherence to guidelines may be related to the makeup of physicians caring for the cancer patient and highlight the need for implementing cardio-oncology services in Australian hospitals. Additionally, there does not appear to be any patient-level variables that make one test preferable to the other in different patient populations, save perhaps for the desire to avoid the unavoidable radiation dose in younger patients. Therefore it would be reasonable to uniformly advise one test over another. This chapter has demonstrated increased sensitivity and earlier CTRCD detection properties of echocardiography over MUGA, which may potentially be counteracted by reduced specificity. Given the potential consequences of either false negative or late diagnosis of CTRCD and relatively benign implications of false positive result, keeping in mind that disruption of chemotherapy should be reserved for severe CTRCD cases where diagnosis is unlikely to be incorrect, it seems reasonable to state the echocardiography should be the initial cardiac imaging modality of choice. From this point on, this thesis will focus on echocardiography as the appropriate cardiac imaging modality. Subsequent chapter in this thesis will focus on strategies to improve specificity and reduce the rate of false negatives from echocardiography.

Chapter 6

Strategy for Improving Echocardiographic Measurement Accuracy

Part of the research in this chapter has been accepted for publication as:

- Nolan MT, Thavendiranathan P. Automation in Echocardiography. *J Am Coll Cardiol Img* 2019; 12(6): 1073-92.

Chapter 6- Improving Echocardiographic Accuracy

Preface

The first four chapters of this thesis provided evidence that CTRCD is a significant source of morbidity and mortality amongst cancer survivors. In addition, it was demonstrated that there were significant performance differences between MUGA, the technique most commonly used by oncologists and hematologists at the single centre sampled, and echocardiography. If one also includes the additional health risks from the unavoidable radiation exposure and lack of additional information regarding valvular and pericardial function associated with MUGA, then it may be considered likely that echocardiography is a more appropriate modality and should be by default the first-line cardiac imaging test for chemotherapy-treated patients. It is notable that recently published cardio-oncology clinical guidelines from Spain explicitly advise against the use of MUGA for screening for CTRCD(12). Echocardiography does also have significant limitations that may impair performance in guiding cardioprotective therapy. Notably the temporal variability of 2D-LVEF measures can be as high as 11%, which is a greater absolute change than that required for CTRCD diagnosis. This raises the likelihood that if echocardiography is used solely to diagnose CTRCD, then a large number of CTRCD diagnoses might be false positives attributable to measurement imprecision. There is therefore an unmet clinical need for a strategy to improves accuracy of echocardiographic measurements. One approach is to utilize novel echocardiographic technologies with demonstrated reductions in temporal variability, such as use of three-dimensional datasets. However this approach requires substantial hardware and software changes, incurs additional financial and time costs and therefore may not be available to all providers. An alternative strategy is to use automated measurements, which may potentially provide the advantages of reduced inter-observer variability. The next chapter will examine the evidence base for utilising automation for echocardiographic measurements and will advance a proposed plan for cardio-oncology departments to utilize these recent advances in technology.

Introduction

Echocardiography has become the primary method for non-invasive imaging of the heart. The use of echocardiography has significantly increased from 1990s with echocardiograms comprising 11% of all U.S. Medicare spending on imaging services in 2010, with $1.2 billion in annual spending(158). Approximately 20% of Medicare enrollees receive at least 1 echocardiogram annually, accounting for 7.1 million echocardiograms in the U.S. each year(159).

Due to the progress in echocardiography (Figure 6-1), the echocardiography examination has become longer over time due to routine addition of multiple newer parameters. A good example of this is the patient receiving cancer therapy where a clinical examination has evolved from bi-plane left ventricular ejection fraction (LVEF) only to now including 3D LVEF, diastolic function assessment, and myocardial strain analysis. Overall, this growth in echocardiography has added stress to echocardiography labs, increased time for studies to be performed and reported and potentially results in delays in diagnosis. Time restraints combined with multiple manual analyses also introduces a source of variability between successive tests (150,160).

Automation of echocardiographic measurements has the potential to change the landscape of echocardiography. Potential benefits of automation include time and cost savings associated with streamlining of image acquisition, rapid analysis and reporting, and greater accuracy and reproducibility of measurements. The possible drawbacks of a strategy of widespread automation adoption include increased costs of software upgrading and staff training and erroneous results, which would be more likely if baseline image quality was not assessed or if automation was applied to patient groups lacking a supporting evidence base. In this manuscript we describe some of the promising advances with automated quantification in echocardiography and how these methods could be incorporated into echocardiography laboratories. We have used the term “semi-automated” to describe methods where the user needs to define regions of interest or anatomical landmarks, but the measurement process is automated and “fully-automated” to describe methods where the software automatically identifies the

landmarks and initiates measurements. However, even in the latter scenario manual adjustments can be made by the user if necessary.

Chamber and Doppler Quantification

A complete echocardiography study involves multiple measurements of chamber dimensions and Doppler spectra. In most cases a single measure is obtained, and the lack of routine use of an average of multiple measurements despite current guideline recommendations(124) is due to the limited time in busy echocardiography laboratories. Regardless of underlying rhythm, there is likely an added benefit to using an average of multiple measurements as opposed to a single measurement for determining chamber size or quantification of velocities, gradients, or stroke volumes. Automation makes it possible to rapidly obtain multiple measurements(161,162) and is now a reality for quantification of chamber dimensions and Doppler spectra from multiple heart beats with some vendors. These measurements have been shown to be accurate (R^2 0.90-0.98)(161) when compared to expert annotations, add time savings and may contribute to improved reproducibility of the measurements.

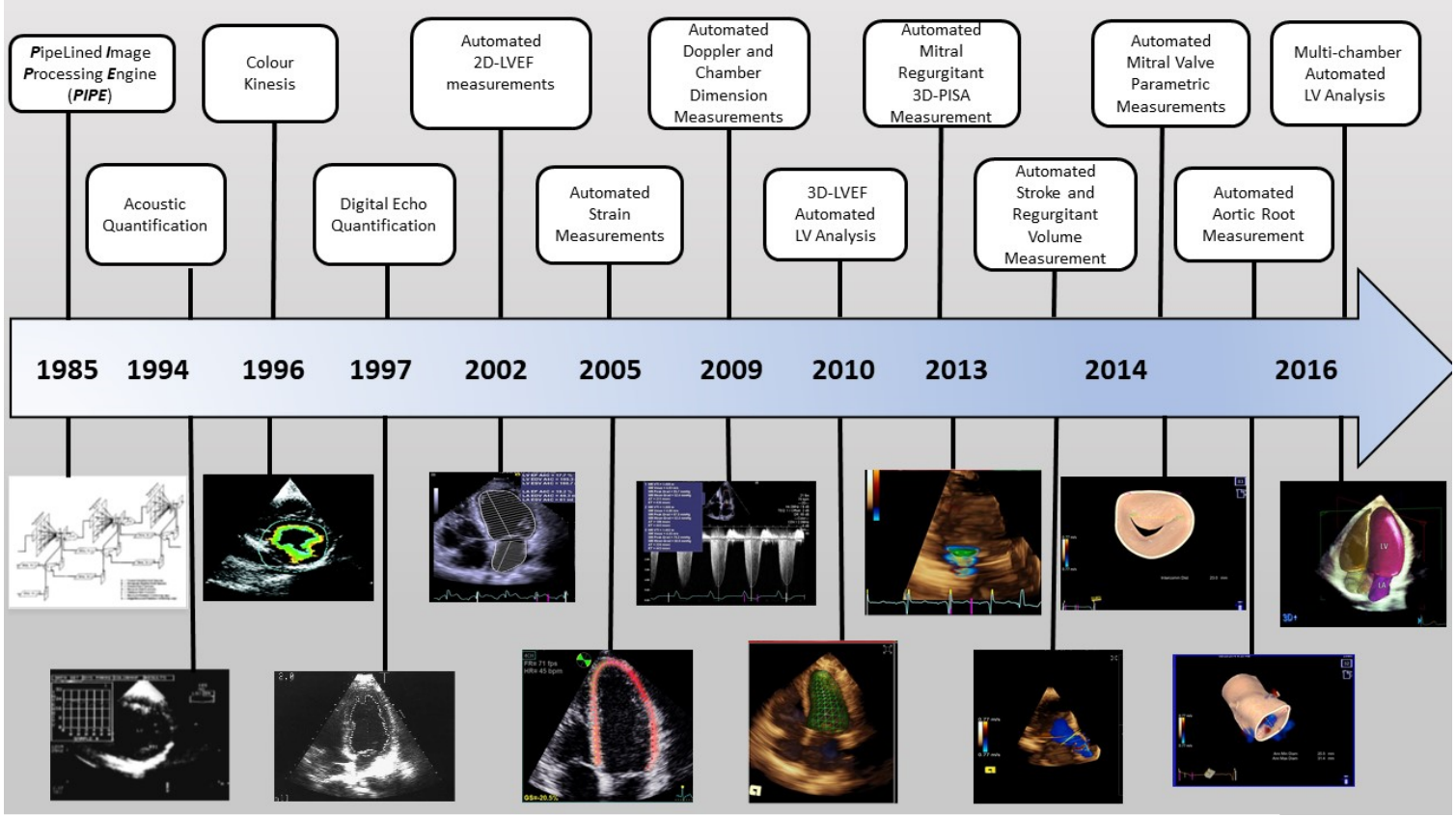

Figure 6-1: Temporal progression in automated quantification in echocardiography. Description of the progression in automated quantification in echocardiography over the past 33 years

Assessment of myocardial function

Automated Measurements of 2D LV Volumes and Function

Non-invasive measurement of LVEF was first performed by one-dimensional (M-mode) measurement in late 1960's, but computer technology of the time was insufficient to automatically analyze images on a frame-by-frame basis. Contemporary automated software use intelligence technology with "knowledge base" gained from large datasets of echocardiographic images to improve detection of endocardial borders. Multiple imaging companies are now marketing automated 2D-LVEF measurement software that is gain-independent and accurate (e.g. eSie Left Heart by Siemens, AutoEF by General Electric, AutoLV by Tomtec, a2DQ^{AI} by Philips). In early studies (Table 6-1) of automated analysis(163,164) correlation with 2D-LVEF and accuracy for grading cardiomyopathy severity was sub-optimal(163). However multiple studies using software from several vendors involving >1300 patients have now shown high feasibility (83-100%) for bi-plane 2D-LVEF measurements and excellent agreement with core-lab measurements or other external reference standards such as CMR (Table 6-1)(165). The fully automated methods have no inter-observer variability (ICC=1.0)(165,166) when repeated on same echocardiographic images, while semi-automated methods have better reproducibility than manual methods (Table 6-1). Furthermore automated methods reduce the gap in reproducibility between expert and novice readers and improve accuracy and reproducibility in multicenter settings for 2D LVEF measurements. (163,165) The analysis time is shortened by >50% with fully automated analysis providing the greatest time savings (as short as 10 seconds analysis time(165)) when compared to semi-automated(163), manual, or even CMR methods(167-171). Therefore, given the existing data, bringing automation of 2D-LVEF measurements into the echocardiographic laboratory is now a reality and may be considered by all centers

Table 6-1: Studies Assessing Automated Echocardiographic Measurements of 2D-LVEF

Studies	Patients	Software (Company)	Feasibility	Comparator	Correlation / Agreement (Bias±LOA)	Time Cost	Inter-observer variability
Cannesson et al 2007(168)	218 -165 with abnormal LV	Auto EF (Siemens)	92%	Manual Simpson Biplane 2D-LVEF and CMR LVEF	Manual 2D-LVEF r=0.98 / 0±2.9%% CMR-LVEF r=0.95 / -0.3±6.0%	Automated 2D-LVEF:48 ± 26 sec; Manual 2D-LVEF: 102 ± 21 sec	Automated 2D-LVEF: 1.3 ± 1.7%, Manual 2D-LVEF 2.9 ± 2.1%
Maret et al 2008(163)	60	Auto EF (Siemens)	100%	Manual Simpson Biplane 2D-LVEF	Uncorrected Auto-EF: r=0.81 / +2.2±12.1% Corrected Auto-EF r=0.89 /+0.8±10.5%	Uncorrected Auto-EF: 79 ± 5 sec; Corrected Auto-EF: 159±46 sec; Manuel 2D-LVEF: 177 ± 66 sec	Uncorrected Auto-EF no variability, Corrected Auto-EF: ICC=0.88, Manual EF: ICC=0.74
Rahmouni et al 2008(164)	92	Auto EF (Siemens)	100%	Manual Simpson Biplane 2D-LVEF and CMR-LVEF	Manual 2D-LVEF; r=0.64/+7.0±13.0% CMR: r=0.64/+3.7±13.8%	NA	NA
Szulik et al 2011(171)	81 (hospitalized)	AutoEF (GE)	90%	Average of 4 visual LVEF measurements and 2CMR reads	Manual 2D-LVEF: r=0.80/-0.66±10.4% AutoEF :r = 0.77 / -1.88±11.6%	Auto LVEF: 54±22 sec; Manual LVEF: 104±22 sec	AutoEF: r=0.80 Manual EF: r=0.52
Aurich et al 2014(167)	47	AutoEF (GE)	100%	Manual Simpson Biplane 2D-LVEF CMR LVEF	2D-LVEF; r=0.85 / +3±12%, CMR r=0.74 / +9±17%	AutoEF: 74±18 secs, Manual 2D-LVEF; 113 ± 30 secs, CMR; 139 ± 18 secs	Auto LVEF: CoV = 12% Manual 2D-LVEF: NA
Knackstedt 2015 (165)	255 pts (multicenter)	AutoLV (TomTec)	98%	Manual Simpson Biplane 2D-LVEF; Visual LVEF	2D-LVEF, Simpson: r=0.83/+0.3±18.7% 2D-LVEF, Visual: r=0.83/+2.2±17.4%	AutoLV: 8 ± 1 sec Manual LVEF – NA	AutoLV:ICC=1.00 2D-LVEF, Simpson ICC=0.78 2D-LVEF, Visual ICC=0.87
Frederickson et al 2015(169)	102 pts	AutoEF (GE)	83%	Manual Simpson Biplane 2D-LVEF, Visual LVEF	2D-LVEF, Simpson: r=0.82 / NA; 2D-LVEF Visual: r = 0.82 / 0±19%	Automated: 41±5 sec; Manual: 98±8 secs	NA
Houvnanians et al 2017(170)	184 pts	A2DQ (Philips)	100%	Manual Simpson Biplane 2D-LVEF	ICC=0.93/ +0.4±15.3	Automated: 116 ± 57 sec; Manual: 217±69 sec	ICC=0.96
Abazid et al 2018(172)	268 pts	AutoEF (GE)	89.5%	Visual LVEF M-mode LVEF	2D-LVEF, Visual) r=0.92/-0.3±4.5% M-mode LVEF r=0.77/-2.4±8.4%	NA	NA

Abbreviations: BA – Bland-Altman; CMR – Cardiovascular Magnetic Resonance; CoV – Coefficient of Variance; GE – General Electric; ICC – Intraclass Correlation Coefficient; LoA – Limits of Agreement (2SD); LV – Left Ventricle; LVEF – Left Ventricular Ejection Fraction; TTE – Transthoracic Echocardiogram ; NA: Not available.

Automated measurements of 3D left ventricular volumes and function

Three dimensional (3D)-LVEF with echocardiography is a more accurate and reproducible method of measuring LV function than 2D-LVEF(173), with test-retest variability approximating half that of 2D-LVEF(150). However, acquisition and manual post-processing takes 3-5 minutes per study (174,175). Despite recommendations for routine use of 3D-LVEF in contemporary guidelines(176,177), time restraints and need for analysis expertise have remained bottlenecks for widespread uptake. Automated analysis removes some of these limitations and can lead to significant potential benefits for busy echocardiography laboratories.

Several vendors have produced fully-automated software (e.g. eSieLVA, Siemens and HeartModel, Philips) that requires minimal user interaction other than initiation of the analysis package. eSieLVA offers single-click analysis of the left ventricle, whereas HeartModel provides single-click analysis of all four cardiac chambers although only the left sided analysis is clinically available. Most studies have demonstrated >90% feasibility for fully- or semi-automated 3D-LVEF measurements (Table 6-2).(174,175,178-181) with single beat fully-automated measurements taking <30 seconds(175,182,183) and 3-5 consecutive beats taking 30-60 seconds depending on volume rates(184). Using HeartModel (Philips®) the time required for 3D LVEF and atrial volumes for a single volume is <30 seconds.(175) Overall fully-automated methods have been shown to reduce analysis times by >75% compared to semi-automated or manual methods.(174,175,181,185) For a busy echocardiographic department that reports 80-100 studies daily, >4-5 hours (assuming 3 minutes per study) may be spent performing manual 3D-LVEF measurements, and in ideal circumstances full-automation could potentially save over 3-4 hours of post-processing.

The agreement of the automated methods for 3D-LVEF measurements have ranged from r=0.75-0.98 compared to manual 3D methods or CMR(186). Interestingly there appears to be small improvements in agreement with reference method with manual adjustment of automated contours made by expert readers, but not novice readers, when compared to fully-automated measurements.(175,180,186-188) However, fully-automated 3D-LVEF measurements offer the advantage

of significantly reducing or eliminating measurement variability, as measurements are deterministic and outcomes are invariable for a given study regardless of the user experience.(186) This results in decreased inter-observer and test-retest variability (174,175,181,185,187), likely leading to more uniform clinical decision making. Therefore unless there are major errors in full-automated contours and adjustments are made by experienced observers, contour adjustments should be minimized.

Another contemporary challenge for accurate 3D-LVEF measurement is in patients with irregular rhythms due to substantial beat-to-beat variation in their LVEF. Current guidelines recommend averaging of sequential LVEF measurements over 5 beats(177). Use of single-beat 3D acquisitions followed by automated 3D-LVEF measurements in 5-10 consecutive beats(189) has the potential to substantially improve workflow. Automated analysis with eSieLVA using multiple 3D datasets from multiple consecutive heart beats demonstrated average 3D-LVEF measurements similar to individual beat 2D measurements.(189) Additionally, automated 3D-LVEF measurements from single index beats correlate with manually-measured averaged beats with absolute reductions of time to analysis of 22 minutes per study(190).This suggests that automated single-beat 3D-LVEF measurement may be a reasonable approach in patients with AF and possibly other arrhythmias

Table 6-2: Studies Assessing Automated Echocardiographic Measurements of 3D Left Ventricular Ejection Fraction

Studies	Patients	Software (Company)	Feasibility	Comparator	Correlation / Agreement (Bias±LOA)	Time Cost	Inter-Observer Variability
Muraru et al 2010(180)	103	4DAutoLVQ (GE)	100%	Manual 3D LVEF / CMR LVEF	Corrected contours: 3D-LVEF (Manual): r=0.95 / -0.1±4.9% CMR:r =0.85/ +2.9±8.4 Uncorrected contours: 3D-LVEF (Manual): r=0.75/ -4.4±11.6% CMR: r = 0.64 / -1.5±12.5%	Automatic: 142 ± 30 sec, Manual: 226 ± 114 sec	4DAutoLVQ r=0.98, 6.5±6.0% 3D-LVEF(Manual): r = 0.98, 4.6±4.3%
Barbosa et al 2013 (179)	24	BEAS algorithm	100%	Manual 3D LVEF	r=0.91 / -1.0±9.8%	Automatic: 30.7 ± 7.5 sec	Semi-automated: 3.6±4.3% 3D-LVEF (Manual): 7.0±5.5%
Thavendiranathan et al 2012(189)	91 (67 SR, 24 AF)	eSie LVA (Siemens)	71.1%	LVEF as measured by CMR for SR, and manual 2D LVEF for AF	SR:r=0.98 / +0.3±2.5% AF:r=0.91/ -2.0±4.0%	Automatic: 30 – 60 secs	eSie LVA: 0.4±4.5%; CMR: 1.0 ± 2.0%; Test-Retest: r=0.98, 0.4±2.8%
Shibiyama et al 2013(174)	44	eSie LVA (Siemens)	93.2%	Manual Simpson Biplane 2D-LVEF; CMR LVEF	2D-LVEF, Simpson r = 0.89 / -5.5±15.4% CMR: r=0.90 / -1.0±15.1%	Fully automated: 37 ± 8 sec; Semi-automated: 371 ± 116 sec	Fully automated: ICC=0.95, 0.6±7.0% Semi-automated: ICC=0.92 +3.6±11.5%
Aurich et al 2014(167)	268	3D AutoLVQ (GE)	100%	Manual Simpson Biplane 2D-LVEF CMR LVEF	2D-LVEF: r=0.79/ +3.0±14% CMR; r = 0.73 / +9.0±17	3D AutoLVQ; 261 ± 93 secs; Manuel EF 113 ± 30 secs; CMR 139 ± 18 secs	3D AutoLVQ: COV = 11%
Tsang et al 2016(175)	159	HeartModel (Philips)	90.5%	Manual 3D-LVEF (94 pts), CMR LVEF (65 pts)	Manual 3D-LVEF No contour adjustment r=0.87/-6±16% Contour adjustment r=0.92/-4±12% CMR: No contour adjustment r=0.85/-2±18% Contour adjustment r=0.91/-2±16%	Fully automated 26±2 sec; Semi-automated: 76 ± 6 sec; Manual 3D-LVEF:144 ±32 sec	Fully automated; 0±0%; Semi-automated; 9±6%; Test-retest: Fully automated; 8 ± 9%; Semi-automated; 8 ± 8%

Otani et al 2016(190)	88 with AF	HeartModel (Philips)	92.4%	LVEF as measured by manual 3D-LVEF	r=0.91/-0.3±10.4%	Automated: 5 min; Manual: 27 min	Test-retest variability: COV = 3.8%; ICC = 0.99
Levy et al 2017(184)	63	HeartModel (Philips)	85.7%	CMR LVEF	r=0.91 /0.7±7.0%	NA	r=0.90; CoV=5% Test-retest: r=0.91, CoV=6%
Medvedofsky et al 2017(187)	180	HeartModel (Philips)	90%	LVEF as measured by manual 3D-LVEF	Fully Automated: r=0.88 . -2.0±15% Semi-automated: r=0.90/ +1±14%	NA	HeartModel: 13 ± 12%, Manual: 17±14% Test-Retest: Fully automated: 9±11% , Semi-automated: 14±9%
Tamborini et al 2017(183)	200	HeartModel™ (Philips)	94.5%	3D-LVEF semi-automatic method; CMR LVEF	3D-LVEF: r=0.88 / +7.3±12.9%; CMR: r=0.79 / +4±20%	HeartModel: 29 ± 10 sec; 3D-LVEF: 160 ± 30 sec	For LVEDV: CoV=5.0%; ICC = 0.98 For LVESV: CoV = 10.7% ICC = 0.97
Spitzer et al 2017(185)	67	HeartModel™ (Philips)	93%	Manual 3D-LVEF	Correlation: r=0.84	Automated: 0.5 min, Automated with manual corrections: 2.5 min Manual: 7.0 min	Automated corrected: CoV=11.9% Test-retest variability: Automated without corrections: CoV = 6.9%
Sun et al 2018(188)	103	HeartModel (Philips)	94.2%	Manual 3D-LVEF	Fully Automated: r=0.96/ -1±4% Semi-Automated: r=0.97/-1±3%	Automated: 1.1 ± 0.3 min; Manual: 4.9 ± 2.4 min	Fully Automated: 7 ± 4% Semi-Automated: 7±4%; 3D-LVEF (Manual):7±3%
Muraru et al 2018(181)	92	AutoLVQ (GE), 3DQ ADV (Philips), eSie LVA (Siemens)	Auto LVQ 90% ; 3DQ ADV NA; eSie LVA 96%	CMR LVEF (35 patients)	AutoLVQ: r = 0.80 / -2.0±12%; 3DQ ADV: r = 0.79 / -1.6±14% eSieLVA r = 0.77 / -0.4±14%	AutoLVQ = 224±29 sec 3DQ ADV = 358±36 sec sSie LVA = 135±24 Automated : 30±10 seconds Semi-automated : 187±46 sec	Semi-automated : AutoLVQ = +1±10%; 3DQ ADV=0±10% eSieLVA= +3±10% Automated : AutoLVQ=+0±4% eSie LVA=0±4%

Abbreviations: AF – Atrial Fibrillation; BEAS – B-Spline Explicit Active Surfaces; CMR – Cardiovascular Magnetic Resonance; CoV -Coefficient of Variation; GE – General Electric; LoA – Limits of Agreement; LVEF – Left Ventricular Ejection Fraction; SR – Sinus Rhythm; AF-Atrial fibrillation; TTE – transthoracic Echocardiogram;

Automated Strain measurements

Assessment of myocardial mechanics, referred to as strain imaging, has many strengths, including detection of subclinical cardiac dysfunction(137,191)and has superior ability to predict mortality compared to traditional 2D-LVEF measurements(137,192). Although strain imaging was introduced 20 years ago(193), clinical uptake was initially delayed by suboptimal reproducibility of manual measurements. With advancements enabling high frame rate images, successful implementation of semi-automated strain measurements using speckle tracking methods achieved similar accuracy to manual measurements, allowing time savings of up to 82% and positioned semi-automated 2D-speckle strain for widespread clinical uptake.(194) Today very few physicians need to undertake manual strain analysis. Given that 2D-speckle tracking based strain measurements were introduced clinically as a semi-automated technique and were validated using sonomicrometry(195), there is limited literature comparing the accuracy and reproducibility of automated versus manual methods (Table 6-3).(194,196-198)

Currently strain measurements are made using vendor specific software - AFI (General Electric®) and QLAB (Philips®) – and vendor neutral software – AutoSTRAIN (TomTec), VVI (Siemens), and EchoInsight (Epsilon Imaging®). These programs require manual identification of certain ventricular landmarks followed by specification of the width of the region of interest, which is then automatically tracked through the cardiac cycle(199). Although some degree of manual input may introduce variability, contemporary analysis packages have demonstrated excellent inter-observer reproducibility for semi-automated GLS measurements compared to manual methods (Table 6-3)(165,197). For example, one study of 546 patients analyzed with AFI reported an inter-observer ICC of 0.92 for GLS compared with ICC of 0.80 for 2D-LVEF.(192) Similarly in a multicenter setting semi-automated measurement of GLS have been shown to be more reproducible that 2D LVEF.(141) As opposed to GLS, regional strain measurements are less reproducible(195) and currently not encouraged for routine clinical practice. More recently, fully-automated GLS strain measurements are now possible with some vendors (165). Whether this will likely further improve the reproducibility of the global and segmental strain measurements and optimize workflow remains to be seen.

Currently clinical strain measurements are limited to systolic GLS and are obtained using multiple 2D left ventricular apical images. Small studies have demonstrated that semi-automated 3D-LVstrain is feasible and reproducible(200), but larger studies are required to quantify clinical benefit. It is likely that further advances in automation and efforts in standardization of strain measurements between vendors may allow GLS to supersede LVEF as the primary measure of left ventricular systolic function and enhance its use in point-of-care imaging.

Table 6-3: Studies Assessing Automated Echocardiographic Measurements of Myocardial Strain

Studies	Patients	Software	Feasibility	Comparator	Correlation / Agreement	Time Cost	Inter-observer Variability
Ingul et al 2005(194)	60 (30 prior MI, 30 healthy controls)	GcMat (GE Vingmed Ultrasound)	81.5% of segments (GLS)	Manual strain analysis	Accuracy speck tracking method = 95.8%, manual method 96.2%	Automated: 2 min; manual: 11 min	CoV Automated 15%, Manual 30%
Delgado et al 2008(197)	222 (CAD)	AFI (GE)	100% (GLS)	2D-LVEF	r=0.83	NA	ICC=0.92; -0.2± 2.6%
Belghiti et al 2008(199)	65 (referred for catheterization)	AFI (GE)	97% (GLS)	LVEF as measured by 2D-LVEF	r=0.87 (experience did not affect correlation), r=0.96 between expert and beginner (LOA 3.4%)	<60 secs	Variability: 7.1% experienced reader, 8.7% inexperienced reader 2D LVEF 14.5%
Brown et al 2009(196)	62 (prior MI)	4D analysis (TomTec)	93% of segments (GLS)	LVEF as measured by CMR	r=-0.69	Strain: 132 ± 30 sec; CMR: 630 ± 60 sec	8.6%
Villanueva-Fernandez et al, 2012(198)	59	QLab (Philips)	91% amongst expert, 89% amongst non-experts (GLS)	NA		NA	-0.09±4.45 (experts) 0.66±7.68 (expert vs non-expert)
Knackstedt et al 2015(165)	255	AutoLV (TomTec)	98% (GLS)	Manual Biplane Longitudinal Strain	ICC = 0.83 / +0.7 (95%CI 0.1-1.3)%	NA	Automated ICC=0, LOA 0 Manual ICC=0.88, LOA 9.6%
Medvedofsky et al 2017(186)	30	EchoInsight (Epsilon)	93% (GLS)	Manual Biplane LVEF	NA	GLS 1 minute, 2D LVEF 2 minutes	GLS r=0.98, 2D EF r=0.91. Minimal impact of reader experiences on GLS, FF ICC 0.89, GLS 0.98

Abbreviations: AFI – Automated Function Imaging; AS – Aortic stenosis; CAD – Coronary Artery Disease; CoV – Coefficient of Variance; DCM – Dilated Cardiomyopathy; MI – Myocardial Infarction; TDI – Tissue Doppler Imaging; TTE – Transthoracic Echocardiography; NA - not reported

Assessment of Valvular Heart Disease

Automated measurement of stroke volume and regurgitant volume

The American Society of Echocardiography's Valvular Regurgitation Guidelines recommend the use of the volumetric techniques to quantify valvular regurgitation severity(201). However this is not routinely performed due to concerns of wide inter-observer measurement variability from squaring of measurements leading to exaggeration of imprecisions and time demands with multiple measurements taking up to 4-6 minutes(202).

Semi-automated measurement of stroke volume using real-time 3D color Doppler datasets allow measurement of velocities over the entire orifice (e.g. mitral or tricuspid annulus) of interest to provide a measure of stroke volume(202-204). The benefits of this approach are avoidance of assumptions of orifice geometry, rapid simultaneous stroke volume measurements at multiple valves and improved accuracy and reproducibility(Table 6-4).(202-204) Stroke volume calculations are determined by fully-automated detection of the relevant landmarks using an expert-annotated database of sample images, followed by placement of hemispheric velocity-sampling planes and automated de-aliasing for Doppler velocity ambiguity. Measurements of stroke volume have been shown to be feasible in >85% of the patients with good agreement with CMR phase-contrast imaging(202) and take <60 seconds without manual adjustments, whereas manual methods may take 4-5 minutes(202). Notably, these studies excluded patients with multi-valvular disease, significant arrhythmia and poor images, and it is possible that accuracy, reproducibility, and time-efficiency may be reduced in these patient subgroups.

A promising application of automated 3D color Doppler stroke volume technique is quantification of valvular regurgitation. Mitral or aortic regurgitant volume can be calculated indirectly as difference in mitral inflow and aortic outflow stroke volumes using the same cardiac cycle(205,206). For functional mitral regurgitation for example, the time required to obtain automated mitral and aortic stroke volume for 3-5 cardiac cycles has been reported to be 30-60 seconds, and the calculated regurgitant volume had excellent correlation and agreement with CMR and was superior to that for 2D manual

methods(205). The value of the automated 3D color Doppler technique for regurgitation quantification has now been consistently illustrated in multiple studies, including for the assessment of aortic regurgitation(206). The strength of this technique is particularly notable in patients with eccentric jets and multiple jets. The clinical applicability of this automated method is currently limited by its vendor specific nature and limited awareness.

Table 6-4: Studies Assessing Automated Echocardiographic Measurements of Stroke Volumes and Regurgitant Volumes using 3D Color Doppler Echocardiography.

Studies	Patients	Software (Company)	Feasibility	Comparator	Correlation / Agreement (Bias±LOA)	Time Cost	Inter-observer Variability
Matthews et al 2010(207)	15 (post cardiac surgery)	Unnamed	100%	CO as measured by PA catheterization	Cardiac Output; R^2 = 0.71/ 0.09±1.3L	NA	Not reported
Son et al 2013(208)	32 patients ≥mod MR	Unnamed (Siemens)	93.8%	PC-CMR for MR severity	RV r = 0.85 / -5.7±33.6ml	NA	ICC = 0.89
Thavendiranathan et al 2012(202)	44 pts -referred for assessment of cardiac function	Unnamed (Siemens)	100%	PC-CMR, 2D Manual Stroke volume method	CMR vs Auto 3D SV: MV: r=0.91/ 1.1±18.9ml ; AV SV: r=0.93 / -0.7±17.8ml CMR vs 2D SV: MV r=0.66 / 10.6±36.0ml; AV 0.6 /10.6 ±40.3ml	Unadjusted: 20-40 sec; Adjustments: 40-60 sec 2D manual = 4-6 minutes	Automated 3D MV r=0.97, AV 0.95, 2D manual MV r=0.79, AV 0.92. 2D manual MV
Thavendiranathan et al 2013(205)	30 (functional MR)	Unnamed (Siemens)	100%	PC-CMR for MR severity	RV r=0.91/ -1.6±17.0ml; RF r=0.92 / -0.3 ±14.6%	30-60 seconds	RV 0.9 ±11.5ml, CCC 0.96; RF 0.2±10.9%; CCC 0.93; Test re-test RVol 1.2±8.8ml, RF 1.6±9.7%
Gruner et al 2014(209)	27 (post mitral clip for MR)	Unnamed (Siemens)	89%	Visual MR classification	3D Automated Color Doppler better agreement with visual MR than 2D manual method	NA	ICC 088 for MV SV 0.86 of AV SV
Choi et al 2015(206)	32 (moderate-to-severe AR)	Unnamed (Siemens)	93.8%	PC-CMR for AR severity	AR RV r=0.93, LOA 9.5ml, AR severity agreement k=0.94	5.6 ±2.0 min	RV ICC=0.96
Heo et al 2017(210)	152 (MR)	Unnamed (Siemens)	97.4%	PC-CMR for MR severity (37 patients)	MR Rvol volume: r=0.94, 2D Volumetric method r=0.56	Automated: 4.3 ± 2.2 min	ICC = 0.87 automated , 2D manual ICC 0.93
Kato et al 2018(211)	34 Children (29 ASD, 3 heart transplant, 1 arterial duct)	Unnamed (Siemens)	92% for AV 97% for MV 80% for PV 92% for TV	Qp : Qs calculated via Fick method	PV/AV ratio r=0.84; TV/MV ratio: r=0.87	Automated: 3 – 5 min per valve	MV: CoV 12.6% TV: CoV 8.9% AV: CoV 13.2% PV: CoV 8.2%

Abbreviations: 3D RT-VCFD – Three -Dimensional Real Time Volume Color Flow Doppler; ASD – Atrial Septal Defect; AR – Aortic Regurgitation; AV – Aortic Valve; CO – Cardiac Output; CoV – Coefficient of Variation; ICC – Intraclass Correlation Coefficient; MR – Mitral Regurgitation; MV - Mitral Valve; PA – Pulmonary Artery; Qp:Qs – Pulmonary-Systemic Flow Ratio; PC-CMR – Phase Contrast Cardiovascular Magnetic Resonance; PV – Pulmonary Valve; RV – Regurgitant volume; RF – Regurgitant Fraction; SV – Stroke Volume; TV – Tricuspid Valve;

Automated Proximal Isovelocity Surface Areas Measurements

Semi-Automated analysis of the 3D proximal isovelocity surface area (PISA) to estimate effective regurgitant orifice area (EROA) and regurgitant volume (RVol) offers a novel approach to directly quantify regurgitation severity. Manual quantification of EROA and RVol using 2D-PISA makes assumptions regarding the shape of the proximal flow convergence region resulting in significant inter-observer disagreement for severity classification(212). The use of manual 3D-PISA avoids the need to make specific shape assumptions offering improved accuracy compared to the 2D-PISA technique(213,214), but is laborious and impractical(213). Semi-automated software can take advantage of large and information-rich 3D color Doppler datasets to quantify the 3D PISA (205) over the entire cardiac cycle ("integrated PISA") accounting for the dynamic nature of the regurgitant orifice.(215)

Semi-automated 3D-PISA measurements have been demonstrated to be accurate and reproducible in both in vitro models(205) and when applied to patients with functional MR using CMR as a reference standard (Table 6-5). Use of integrated 3D-PISA technique provides further incremental benefit in functional mitral regurgitation, as evidenced by superior agreement with CMR for RVol(205). These multiple measurements of the 3D-PISA over the cardiac cycle are only practical with semi-automated methods and not manual methods due to superior time efficiency (~15±4 seconds per cardiac cycle).(205) The reduced variability in effective regurgitant orifice area measurement by 3D-PISA compared with traditional 2D-PISA methods has been replicated in two other larger studies of >300 patients with both organic and functional MR(216,217). Similar results have been observed for quantification of tricuspid regurgitation severity (218).

To date, studies examining semi-automated measurement for stroke volume or regurgitant volume quantification have consistently demonstrated improvements in accuracy, reproducibility and analysis speed. Further improvements in these automated algorithms are likely with growing vendor interest.

Table 6-5: Studies Assessing Automated Echocardiographic Measurements of 3D-Proximal Isovelocity Surface Area

Studies	Patients	Software	Feasibility	Comparator	Correlation / Agreement (Bias±LOA)	Time Cost	Inter-observer Variability
Thavendiranathan et al 2013(205)	30 pts with functional MR	eSie PISA (Siemens)	85.6%	RV measured by CMR RV	RV by CMR: r = 0.92/ -1.4±18	Automated Integrated PISA: 1.7±0.7 min; Automated Peak PISA: 15±4 sec CMR: 6-8 min	RV: 0.9±11.5mL; RF: 0.2±10.9% Test-Retest: RV: 0.0±13.7mL
De Agustin et al 2012(219)	33 pts (25 primary MR; 8 secondary MR)	eSie PISA (Siemens)	100%	3D-TEE planimetry	Automated 3D-PISA: EROA; r=0.99 / 0.0±0.1cm^2 RV: r= 0.99 Manual 2D-PISA: r=0.93/0.2±0.4cm^2 RV: r=0.95	Automated 3D-PISA: 4-5 minutes Manual 2D-PISA: NA	3D PISA ICC 0.92 2D PISA ICC NA
De Agustin et al 2013(218)	90 pts (chronic TR)	eSie PISA (Siemens)	100%	3D VCA	Vs VCA 3D PISA r=0.97 / 0.01±0.12cm^2, 2D PISA r=0.89 / 0.1±0.27cm^2	2-3min for 3D PISA, 3-4 min for 2D PISA	3D PISA ICC 0.88, 2D PISA 0.79
Schmidt et al 2014(216)	93 pts (17 primary; 76 secondary MR)	eSie PISA (Siemens)	100%	Manual 3D-PISA measurement	RV: r=0.91 EROA: r= 0.93	Not reported	Not reported
Choi et al 2014(217)	221 pts (111 primary; 110 secondary MR)	eSie PISA (Siemens)	95.5%	PC-CMR	RV: Semi-automated 3D-PISA; r=0.97/-0.9±13.8mL; Manual 2D-PISA r=0.84/10.4±19.4mL	Automated: 4.6 ± 2.0 min	3D PISAICC 0.97 2D PISA ICC 0.95

Abbreviations: CMR – Cardiac Magnetic Resonance; EROA – Estimated Regurgitant Orifice Area; ICC – Intraclass Correlation Coefficient; MR – Mitral Regurgitation; PC-CMR – Phase Contrast Cardiac Magnetic Resonance; PISA – Proximal Isovelocity Surface Area; RV – Regurgitant Volume; RF – Regurgitant Fraction

Guidance for intervention

Automated measurement of aortic annulus and root

Clinical outcomes of transcatheter therapies for aortic valvular disease depend on accurate measurements of AV landmarks. Measurements of aortic annulus size using 2D-TEE under-estimate aortic annular area due to incorrect geometric assumptions. Although 3D-TEE-based measurements offer incremental improvement, they still underestimate area by ~9% compared with multi-detector CT (MDCT)(220). Currently MDCT is the recommended imaging modality for accurate aortic annulus and root dimensions prior to transcatheter aortic valve implantation (TAVI) but is limited by risk of nephrotoxicity from contrast use, radiation exposure, limited temporal resolution, and susceptibility to calcium blooming artifact obscuring true annular border. Automation of 3D-TEE measurements may avoid these undesirable effects and lead to safer, accurate and reproducible measurements.

Several vendors have now produced automated software specifically designed for measuring aortic annular and root measurements from 3D-TEE datasets with good feasibility, accuracy, and reproducibility (Table 6-6)(221,222). These software allow fully automated analysis, but also allow for manual adjustments(221). For TAVI assessment, the bias of automated 3D-TEE measurements for annular diameter, perimeter, and area appears small (approximately -1.2% to -2.2%) and agreement with MDCT for selection of device size has been excellent ($\kappa = 0.90$)(222). Time required for automated aortic root measurements from 3D-TEE datasets has ranged from 2.3 ± 0.6 minutes(221) to 4.2 ± 1.0 minutes(222), with longer times required if excessive calcium or poor image quality present. Smaller studies have demonstrated similar promising results in terms of accuracy in comparison to MDCT(220,223,224).

Beyond the annulus, automated modeling of aortic root and valve is now feasible using software based on learned-pattern recognition(221), with cross-sectional diameter measurements displaying good agreement with MDCT(221). Additionally, several published studies display similar reproducibility to MDCT measurements with ICC for intra- and inter-observer variability ranging from 0.91-0.98 (Table 6-

6). This reproducibility is particularly important in longitudinal follow-up to determine timing of surgical intervention(221,222,225).

Automated 3D-TEE appears to be a viable strategy for enhancing the precision and reproducibility of future aortic measurements. Larger studies using clinical endpoints are required prior to widespread clinical use.

Table 6-6: Studies Assessing Automated Echocardiographic Measurements of Aortic Annulus and Root

Studies	Patients	Software	Feasibility	Comparator	Correlation / Agreement (Bias±LOA)	Time Cost	Inter-observer Variability
Calleja et al 2013(221)	69 pts (20 healthy volunteers, 14 severe AS, 35 dilated aortic root ± AR)	eSie Valve (Siemens)	100%	MDCT, Automated annular diameter measurement	0.5±5.87 mm	Automated: 1.1–3.4 minutes	ICC=0.90 to 0.93
Garcia-Martin et al 2016(223)	31 pts (referred for TAVI)	eSie Valve (Siemens)	88.6%	Manual 3D-TEE measurements	Aortic Annular diameter: ICC 0.85; Aortic Annular Area: ICC 0.74	NA	Aortic Annular diameter: ICC=0.94; Aortic Annular Area: ICC=0.95
Mediratta al 2017(220)	52 pts -severe AS	Unnamed (Philips)	90%	MDCT	Aortic Annular Area: r=0.92; Aortic Annular perimeter: r=0.91	NA	Aortic Annular Area: ICC 0.70; Aortic Annular Perimeter: ICC 0.72
Prihadi et al 2018(222)	150 pts -severe AS	Aortic Valve Navigator (Philips)	100% for aortic annular dimensions; 89% for aortic root dimensions	MDCT	Aortic Annular area: r=0.91; Aortic annular perimeter: r=0.83	Automated Aortic root measurements: 4.2 ± 1.0 min	ICC 0.93
Queiros et al 2018(226)	101 pts	Specqle 3D (KV Leven)	92.1%	MDCT	Fully Automated: ICC 0.78; Contour correction: ICC 0.83	Automated: 19.0 ± 1.9 sec	ICC 0.94, CoV 5.6%
Podlesnikar et al 2018(227)	83 pts (severe AS Separated into high and low aortic valve calcium (AVC)	4D Auto AVG (GE-Vingmed)	97.6%	MDCT	For selecting prosthesis size Low AVC: K= 0.93; High AVC: K=0.71	NA	Perimeter ICC 0.96; Area: ICC 0.97
Kato et al 2018(228)	43 pts -severe AS	eSieValves(Siemens)	93.5%	MDCT	Automated annular area: r = 0.86; Semi-automated annular area: r= 0.94Manual annular area: r=0.93	Automated 3D-TEE: 30.1 ± 5.8 sec; Semi-automated 3D-TEE; 74.1±15 sec Manual 3D-TEE; 81.8 ± 18.5 sec	Automated; ICC 0.99,LoA -28.6 to 26.7; Semi-automated; ICC 0.96 LOA -22.7 to 66.8 Manual; ICC = 0.95 LOA -47.0 to 81

Abbreviations: AS – Aortic Stenosis; AVC – Aortic Valve Calcium; CoV – Coefficient of Variance; ICC – Intra Class Correlation Coefficient; LOA - Limits of Agreement; MDCT – Multi Detector Computed Tomography; TAVI – Transcatheter Aortic Valve Implantation; TEE – Trans-Esophageal Echocardiography

Automated measurement of mitral valve anatomy

The use of 3D echocardiography has significantly enhanced our understanding of the mitral valve and annular anatomy. Specifically, the ability to generate parametric maps has improved the accuracy of identifying mitral valve pathology, has been validated surgically and has the potential to guide surgical planning(229-233). However they are currently not practical for routine echocardiography.

3D mitral valve parametric maps can now be generated using automated software from several vendors, and can be either fully- or semi-automated(Table 6-7). For example, semi-automated analysis in patients with degenerative mitral valve disease has demonstrated that quantitative annular circumference was associated with implanted annuloplasty band length, while posterior mitral valve leaflet segment 2 length and area was associated with performance of intraoperative leaflet resection(230,234). Similar to automation in other areas of echocardiography, intra-and inter-observer variability for semi-automated measurements have been reported to be good with ICC ranging for 0.83-0.99 depending on the structure being measured(234). Also fully-automated methods result in >75% reduction in the time for analysis compared to manual methods.

Table 6-7: Studies Assessing Automated Echocardiographic Measurements for Assessing Mitral Valve Anatomy

Studies	Patients	Software	Feasibility	Comparator	Correlation / Agreement	Time Cost	Inter-observer Variability
Grewal et al 2010(230)	32 pts (moderate-to-severe primary MR)	Q-Lab MVR (Philips)	100%	Direct surgical measurement	Mean difference in aortic annulus measurement: 0.1 ± mm, 95%CI ±4.4 mm	NA	Antero-posterior diameter CoV 5.7% BA 95%CI ±5.1mnm; Inter-commissural distance CoV 4.3%; BA 95%CI ±2.3 mm
Pouch et al 2014(235)	20 pts pre cardiac surgery (6 normal MV, 6 mild MR, 8 severe ischemic MR	ITK-SNAP (open-source) (automated)	100%	Manual 3D-TEE measurements	Mean distance between manual and automatic segment: Diastole 0.8±0.2 mm; Systole: 0.6±0.2 mm	NA	NA
Kagiyama et al 2015(236)	74 pts (15 functional MR; 32 MVP; 27 normal	Mitral Valve Navigator (MVN) (Philips)	100%	Manual 3D-TEE measurements	Agreement using Cronbach's alpha: 3D annulus circumference: α =0.88; Antero-posterior diameter:α=0.90	Automated: 260 ± 65 sec; Manual: 381 ± 68 sec	Inter-observer agreement using Cronbach's alpha: 3D annulus circumference: α =0.97; Antero-posterior diameter: α=0.96
Calleja et al 2015(234)	94 pts-booked for MV surgery	Pending (semi-automated)		Length of surgically implanted annuloplasty ring	Correlation between predicted and implanted annuloplasty band length: r= 0.74	Automated, no contour correction: <60 sec; Automated, contour correction: 8 min	Annular area: ICC = 0.99
Aquila et al 2016(219)	36 pts -referred for 3D-TEE for any reason	eSie Valves (Siemans)	59%	Manual 3D-TEE measurements	Mitral annular area: r=0.94; Inter-commissural distance: r=0.84	Not reported	Mitral annular area: ICC=0.96; Inter-commissural diameter: ICC=0.96
Jin et al 2015(237)	55 pts -33 MVP -11 functional MR -11 normal	Mitral Valve Navigator (MVN) (Philips)	95%	Manual 3D-TEE measurements	Annulus circumference: r=0.95; Antero-posterior diameter: r=0.96	Automated: 144 ± 24 sec; Manual: 770 ± 89 sec	Annulus circumference: ICC=0.98; Antero-posterior diameter: ICC=0.97

Abbreviations: BA – Bland-Altman; CoV – Coefficient of Variation; ICC – Intra-class Correlation Coefficient; MV – Mitral Valve; MR – Mitral Regurgitation; MVP Mitral Valve Prolapse; TEE – Trans-Oesophageal Echocardiogram;

Adoption of Automated Methods in Routine Echocardiography

We have summarized evidence for the use of automated techniques and provided recommendations for its use in Table 6-8. We believe that there is adequate evidence to support the clinical use of semi- or fully-automated analysis of 2D LVEF, 3D LVEF, and measurements of global longitudinal strain. Prior to use of automated 2D LVEF or strain measurements it is prudent to ensure adequate image quality including adequate endocardial definition, non-foreshortened views, minimal to no drop-out or artifacts. For GLS measurements, acquisition of all 3 apical views sequentially with similar heart rates and frame rates (>40 frames per second) is essential. For automated 3D LVEF, in addition to good image quality, volume rates should exceed 20 volumes per second. Once the automated algorithm is applied for LVEF or strain measurements, it is important to visually assess tracking quality and make contour adjustments if necessary. LVEF techniques should be avoided in scenarios in which they have not been adequately assessed.

An approach for echocardiography laboratories to incorporate automated techniques as part of their workflow has been outlined in Figure 6-2. The types of automated quantification techniques available will depend on the vendor and the version of the echocardiography machines being used. Each lab should establish practice guidelines by identifying patient subsets that should be included and excluded from automated quantification. Analysis of the acquired data should ideally be performed immediately so that additional images could be obtained in case of poor tracking. Physicians and sonographers should be trained on 20-30 echocardiographic datasets with the focus on what constitutes adequate automated analysis. Echo templates may need to be modified to accommodate the automated measurement. It is also important to use the same vendor's automated techniques for longitudinal follow-up of EF or strain measurements as there are limited data on inter-vendor comparisons with 2D LVEF and there are known vendor differences with GLS measurements(228). Interestingly, for 3D LVEF, a recent study comparing 3 vendors using semi-automated algorithms has demonstrated good inter-vendor agreement.(181) Therefore inter-vendor differences may be less of an issue for 3D LVEF measurements. It is also important to ensure that the echocardiography image data is stored in a format (e.g.

uncompressed format) that could be re-analyzed by the reporting physician if there is disagreement with the automated analysis. Finally, labs should incorporate a local quality assurance program to verify robust automated analysis processes and to ensure that any software upgrades are carefully considered especially if they will have an impact on measurement accuracy and reproducibility.

Table 6-8: List of recommendations and assessment of evidence base for use of automated echocardiography

2D-LVEF	Moderate number of studies with moderate number of patients with uniform direction of effect • Use of automated 2D-LVEF measurements is reasonable for assessing left ventricular systolic function for purposes of improved time efficiency and reproducibility. • Use of software that has been validated in peer-reviewed literature is recommended • Tracking quality should be visually assessed, with contour adjustment as necessary • TTE report should specify that automated LVEF measurement was utilized • Caution is advised in cases of significant arrhythmia, LV aneurysm and congenital heart disease, as few published studies recruited these patients
3D-LVEF	Moderate number of studies with moderate number of patients with uniform direction of effect. • Use of automated 3D-LVEF measurements is reasonable for assessing left ventricular systolic function for purposes of improved time efficiency and reproducibility. • If available, preference for automated 3D-LVEF should be given over automated 2D-LVEF • All other recommendations for automated 2D-LVEF apply to automated 3D-LVEF
Strain	Moderate number of studies demonstrating clear clinical utility • It is reasonable that automated strain measurements be used. • Commercial package that has been validated in peer-reviewed study should be used. • Manual strain measurements are not recommended for clinical use.
Stroke Volume & Regurgitant Volume	Small number of single-center studies suggestive of clinical utility • Use of automated stroke/regurgitant volume measurements for quantification of mitral regurgitant volume and trans-mitral stroke volume needs further validation before routine clinical use.
PISA	Small number of single-centre studies which included relatively small number of patients • Use of automated PISA measurements for quantification of mitral regurgitant volume and EROA needs further validation before routine clinical use.
Aortic Annulus and Root	Small number of single-centre studies which included moderate number of patients with uniform direction of effect • It would be reasonable to use automated aortic root and annulus measurements for purposes of improved time efficiency and reproducibility, however, further experience is needed before routine clinical use. • Automated measurements should only be taken using datasets obtained by 3D-TEE at present. • Caution should be exercised in cases of reduced image quality and high-grade annular calcification as manual contour adjustments are more likely to be necessary.
Mitral Valve Anatomy	Small number of single-centre studies with small number of patients that did not include variety of mitral valvular conditions • Use of automated mitral valvular dimensional measurements requires further validation before clinical use. • Automated measurements should only be taken using datasets obtained by 3D-TEE at present.

Abbreviations:3D-TEE – 3-Dimensional Trans-Esophageal Echocardiogram; LVEF – Left Ventricular Ejection Fraction; PISA – Proximal Isovelocity Surface Area; TTE – Transthoracic Echocardiogram

Future Directions

Although the described studies have demonstrated net benefit of automated measurements at the group level, it is likely that at an individual level automated accuracy may be substantially different from reported mean values of large groups. This may be due in part to two reasons; firstly, distinct populations such as those with arrhythmia, congenital heart disease, abnormal cardiac chamber configuration, and multi-valvular disease are poorly represented in studies to date; secondly, there is an inherent conflict between reproducibility and accuracy, as algorithms are restricted to a greater degree in the number of variables and approach to analysis than human beings are. Two strategies for increasing effective and safe widespread implementation of automation are expansion of the evidence-base and mindful incorporation of both subjective and automated variables into a holistic reporting process.

We consider that the seven automative techniques described above can be divided into three strata based on their needs for future research before they replace manual measurements in clinical practices. The first strata includes 2D-LVEF, 3D-LVEF and GLS, and is characterized by several studies demonstrating feasibility and accuracy of specific patient groups with moderate number of patients. In order to facilitate uptake of these automated techniques, further studies are desirable to clearly quantify benefits and liabilities. This includes determination of inter-vendor agreement, assessment of multicenter reproducibility, comparison of the diagnostic and prognostic advantage of the automated techniques, and cost-effectiveness analyses. Distinct populations such as those with arrhythmia, poor-quality images secondary to obesity or post-surgical status, obesity, congenital heart disease, abnormal cardiac chamber configuration, and multi-valvular disease need to be studied. Additionally, the hypothesis of cost and time savings with automation should be confirmed in large observational studies of multiple busy echo labs that incorporate automated software. Ideally, large multi-centre randomized control studies that assess automated versus conventional echo measurements for management of cardiac disease using measurable clinical outcomes would be required for automated echo measurements to receive a Class I

recommendation, but such studies would be challenging to conduct and are unlikely to be implemented in the foreseeable future.

These analysis algorithms are now available with multiple vendors but inter-vendor comparisons do not exist. The clinical utility of these methods will become apparent as percutaneous techniques and minimally invasive procedures for valve disease become more common practice.

The second strata includes automated measurements of aortic annulus and root, for which large, multicenter studies with demonstration of efficacy in patients with greater diversity of aortic pathologies are required before being considered suitable for routine clinical use. The third strata includes the three automated techniques of automated stroke and regurgitant volume measurements, PISA measurements and mitral valve anatomy. Data supporting use of these techniques overall is based on small number of single-center studies with small sample sizes. These techniques are also only currently available with a single vendor with ongoing evolution of the analysis software, and requires large, multicenter studies demonstrating a uniform direction of effect of high levels of feasibility, accuracy and reproducibility before large clinical studies can be recommended.

Significant advances in automated quantification in echocardiography are anticipated over the next decade, including improvement in spatial and temporal resolution, better contrast to noise and signal to noise ratios, and enhancement in 3D image visualization. With these advances, automated quantification will likely extend beyond a single chamber to provide simultaneous assessment of the size and function (ejection fraction and strain) of all cardiac chambers and great arteries simultaneously. However, physicians should be mindful that automation does not remove the need for physician review of all echocardiographic images, and automated measurements should be assessed in the context of a holistic appreciation of all available data. Physicians retain the responsibility to visually assess all echocardiographic images, including automated tracking and border detection. If the automated measurements are discordant with other echocardiographic data, then the clinician should inspect automated tracking and border detection images for errors and consider manual measurement if errors are

detected. If there remains clinical uncertainty, an alternative cardiac imaging modality may be utilized. Ideally there should be a process by which automated measurement errors are reported back to the software developer to allow for iterative algorithmic improvements.

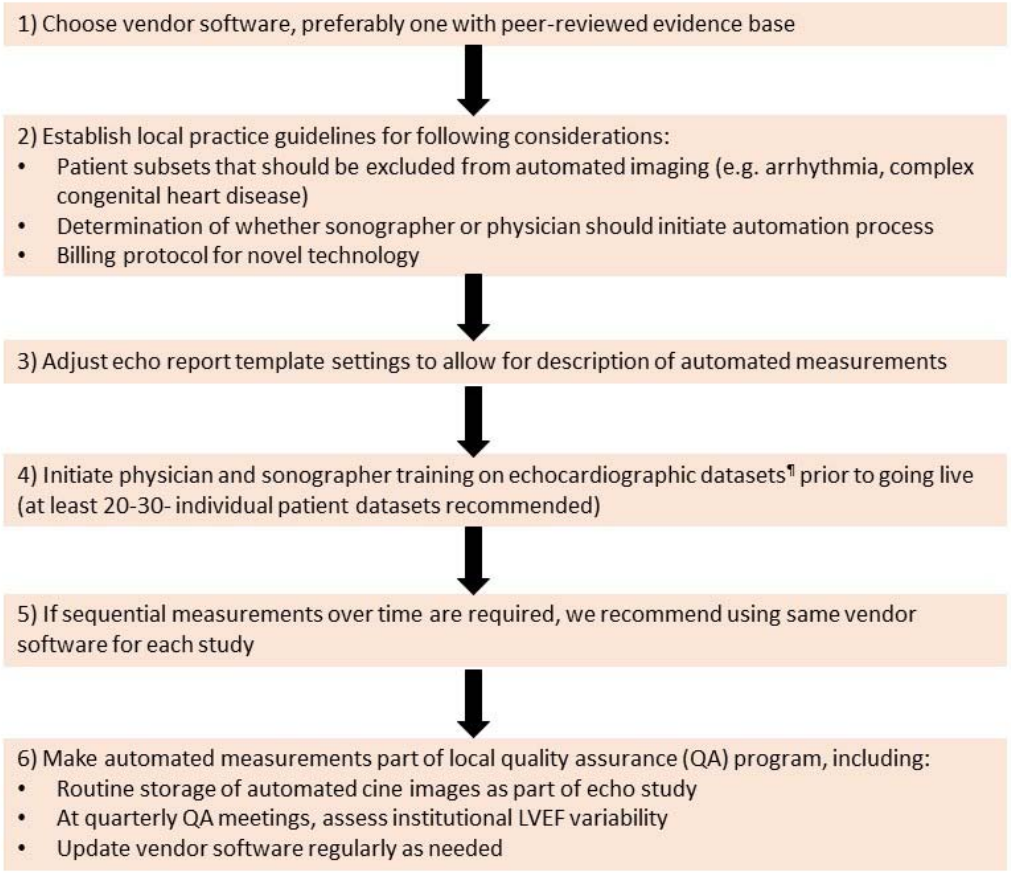

Figure 6-2: Flowchart for steps required for Echo Lab to uptake routine automated measurements

¶Vendor software company may provide de-identified datasets for automated measurement training

Conclusion

Automated quantification in echocardiography has partially fulfilled its early promise and has led to successful and practical uptake of several echocardiographic technologies and affected many aspects of echocardiographic practice. It has consistently and successfully led to significant time savings and improvements in measurement reproducibility, and it is anticipated that further advancements will assist in improving patient outcomes and reining in healthcare costs. Automated quantification will allow clinicians to focus less on the process of measurements and shift their attention to data quality, data synthesis, and diagnosis. To fully reach the potential of automation, innovative partnerships between physicians, technologists, software engineers, and industry need to be encouraged and supported.

Chapter 7

Secondary Cardiac Imaging for Indeterminate Cases of Cardiac Dysfunction

Part of the research in this chapter has been submitted for publication as:

- **Nolan MT**, Altaha MA, Hanson R, Thampinathan B, Amir E, Brezden-Masley C, Satriano A, Connelly K, Mikami Y, Michalowska M, White JA, Wintersperger BJ, Thavendiranathan P. Myocardial Remodeling Early during Cancer Therapy in women With Breast Cancer – A Cardiac MRI and Echocardiography Strain Study. *In process of submission.*

Chapter 7- CMR as Adjunctive Imaging

Preface

The two previous sections of this thesis have established the central importance of sequential cardiac monitoring to prevent and manage CTRCD and have demonstrated echocardiography is the most suitable first-line imaging modality. Improved national uptake of this proactive strategy may potentially decrease both acute and long-term burden of cardiovascular disease in the cancer population, with potential down-stream savings in terms of both survival years and societal resources. It is probable that under-appreciation of the benefits and suboptimal understanding of contemporary cardiac imaging may be a barrier to successful implementation amongst both oncologists and cardiologists.

Up to this point in this thesis, the focus has been on identifying optimal strategies for cardioprotection at the population-based level. However, in practice all medicine is practiced at the individual level, where personal characteristics of patients and cancer treatments may lead to the need for an individualized imaging strategy for successful long-term management. Due to the excellent safety record of echocardiography and the substantial quality clinical information it provides, the number of cancer patients who would be unsuitable for echocardiography as 1st line imaging modality is likely to be vanishingly small. Therefore the next section of this thesis will focus on adjunctive imaging techniques that offer additional information not readily available by echocardiography.

Echocardiography has several notable limitations which should be taken into account. It is dependent on obtaining quality acoustic windows, which may be challenging in patients who have undergone left-sided breast surgery or radiotherapy. Temporal variability of LVEF measurements can be as high as 11% even in the absence of changes in myocardial function(140). Echocardiography cannot reliably detect changes in myocardial tissue composition, such as edema or fibrosis. For these reasons, as well as for excluding significant differential diagnoses and co-existing myocardial diseases, there will be a subgroup of cancer patients who will require a 2nd line imaging test to assess myocardial function. Cardiac MRI is a strong contender for this role, as it is the gold standard technique for measuring left ventricle volumes and can reliably detect acute myocardial tissue changes. The next section of this thesis will assess the utility of

Chapter 7- CMR as Adjunctive Imaging

CMR to firstly assess a cohort of CTRCD patients to determine if there are false positives with preserved contractility, and secondly assess a cohort of early breast cancer patients to determine if cardiac dysfunction can manifest as phenotypes other than that described solely in terms of LVEF decrement. Together, these chapters will expand our understanding of the role of CMR in cancer patients both with and without a formal CTRCD diagnosis.

Abstract

Background: There is concern that intravascular volume depletion (preload) mediated reduction in LVEF and GLS may result in incorrect diagnosis of cancer-therapy related cardiac dysfunction (CTRCD).

Objectives: To explore the mechanisms underlying cancer-therapy-mediated reduction in left ventricular ejection fraction (LVEF) and global longitudinal strain (GLS).

Methods: 112 consecutive women (50.6±9.7 years) with early stage HER2+ breast cancer, receiving sequential anthracycline and trastuzumab, were recruited prospectively. All had CMR pre-anthracycline, within one-month post-anthracycline and at six months. A subgroup of 83 patients had echocardiography with GLS measurements at identical timepoints. Significant change in LV volumes by CMR were defined as LV end-diastolic volume (LVEDV) reduction by >10ml or LV end-systolic volume (LVESV) increase by >5ml. CTRCD was defined either per the Cardiac Review and Evaluation Committee Criteria (CTRCD-LVEF) or a relative reduction in GLS by >15% (CTRCD-GLS). Sensitivity analysis were performed with any reduction in LVEF by >5% or GLS>11%.

Results: Fifteen patients (13.4%) developed CTRCD-LVEF mediated by an increase in LVESV alone in 12(80.0%), combined LVESV increase and LVEDV decrease in two (13.3%) and non-significant volume change in one patient. No patient had CTRCD-LVEF due to isolated reduction in LVEDV (reduced preload). A change in LVEDV was not predictive of CTRCD-LVEF (p=0.74), while a change in LVESV was (p=0.006). CTRCD-GLS occurred in 17 patients (20.5%) of whom one had a primary reduction in LVEDV with a non-significant increase in LVESV. Of the 53 patients (47.3%) with a reduction in LVEF >5% and 29(34.9%) with a reduction in GLS >11%, an isolated reduction in LVEDV was observed in seven (13.2%) and 4 (13.8%) patients respectively.

Conclusions: The dominant mechanism of CTRCD in breast cancer patients receiving anthracycline based therapy relates to an increase in LVESV likely reflecting altered myocardial contractility. Preload reduction may play role in small reductions in LVEF or GLS not meeting criteria for CTRCD.

Chapter 7- CMR as Adjunctive Imaging

Introduction

Cancer therapy related cardiac dysfunction (CTRCD) is primarily defined as a threshold change in left ventricular ejection fraction (LVEF) between baseline and a subsequent follow-up(238,239). Often the recognition of CTRCD results in transient or permanent cessation of cancer therapy, additional cardiac investigations, and the initiation of heart failure medications. Myocardial dysfunction from CTRCD may potentially be detected earlier by the use of myocardial strain measurements.(137) Several studies have demonstrated that a reduction in peak systolic global longitudinal strain (GLS) during cancer treatment is associated with a subsequent reduction in LVEF and heart failure providing an opportunity for earlier intervention.(240)

Since LVEF is calculated as difference between left ventricular end-diastolic (LVEDV) and end-systolic (LVESV) volumes divided by LVEDV, a reduction in LVEF can occur due to either a decrease in LVEDV, an increase in LVESV, or the combination. It is generally assumed that CTRCD is driven by myocardial injury affecting myocardial contractility with resultant increase in LVESV. However, during cancer therapy the potential for nausea, vomiting, and reduced oral intake can result in intravascular volume depletion and an associated reduction in LVEDV (preload) translating to a reduction in LVEF. The treatment for contractile dysfunction would include standard strategies for CTRCD,(238,239) whilst treatment for the latter would include hydration and treatment of nausea and vomiting. Treating patients with reduced preload with heart failure medications (e.g. ACE inhibitors and beta-blockers) could potentially result in adverse hemodynamic alterations and clinical symptoms. Recent cardiovascular MRI (CMR) studies of patients with multiple different cancers and treatment regimens demonstrated that CTRCD occurred due to isolated reduction in LVEDV in 19-26% of the patients.(241,242) Furthermore, a reduction in CMR measured myocardial strain (circumferential and longitudinal) was associated with a reduction in LVEDV. Consequently, additional work is necessary to confirm these findings and to explore the association between preload with GLS measured by echocardiography.

In this study, using a uniform population of women with human epidermal growth factor receptor 2 positive (HER2+) breast cancer receiving anthracycline and trastuzumab-based therapy, our objectives were to (i) quantify proportions of patients with CTRCD secondary to contractile dysfunction versus reduced preload using CMR-measured left ventricular volumes and ejection fraction and (ii) determine whether a reduction in GLS measured by echocardiography is associated with a reduction in preload. We hypothesized that changes in LVEF and GLS meeting CTRCD criteria will be related to myocardial dysfunction and not reduction in preload.

Methods

Study Population

One-hundred and twelve consecutive patients with early stage HER2+ breast cancer were recruited prospectively from outpatient clinics between January 2014 and April 2017 from the Princess Margaret Cancer Centre/University Health Network (UHN) or St. Michael's Hospital in Toronto (N=83) and from February 2015 to February 2017 from the Libin Cardiovascular Institute of Alberta, Calgary, Canada (N=29). We included women ≥18 years of age with stage I-III, HER2+ breast cancer scheduled to undergo treatment with an anthracycline (Epirubicin or Doxorubicin) followed by a combination of trastuzumab and a taxane (paclitaxel or docetaxel). Exclusion criteria were (1) previous anthracycline therapy; (2) current or prior cardiovascular disease; and (3) general contraindications to MRI. Patient characteristics, cardiac risk factors, medications, cancer history, cumulative anthracycline doses, and other cancer treatment exposure were collected. At each visit all patients were weighed, vitals were recorded, and heart failure symptoms were elicited. The study was approved by the respective Research and Ethics Boards and all patients provided written informed consent.

Table 7-1: Clinical and demographic data of cohort.	
Demographics at Baseline:	**(N=112)**
Age (years)	50.6 ± 9.7
Body weight (kg)	66.7 ± 13.9
Body surface area, (m^2)	1.7 ± 0.2
Body Mass Index, (kg/m^2)	25.6 ± 5.4
Heart rate (bpm)	71.3 ± 11.8
Systolic blood pressure (mmHg)	125.5 ± 21.0
Diastolic blood pressure (mmHg)	76.7 ± 14.0
Cardiovascular Risk Factors at Baseline, n (%):	
Hypertension	17 (15.0%)
Diabetes	4 (3.5%)
Hypercholesterolemia	10 (8.8%)
Smoking History, Any	30 (26.5%)
Coronary artery disease	0 (0%)
Chemotherapeutic Regimen:	
Epirubicin dose (mg/m^2), n=110	308.7 ± 40.3
Doxorubicin dose (mg/m^2), n=2	104.3 and 253.1
Cardiac Medications at Baseline:	
Beta-blocker	5 (4.4%)
ACE inhibitor / ARB	13 (11.5%)
Statins	7 (6.2%)

Cardiac Imaging

Cardiovascular MRI (CMR): CMR studies were performed at three time points: prior to initiation of cancer therapy, within 1 month of anthracycline completion (~2-3 months from baseline), and 3 months later (~6 months from baseline and ~3 months after trastuzumab initiation). CMR scans were performed on 1.5T (Toronto) or 3.0T (Calgary) imagers (Magnetom Avanto Fit or Prisma; Siemens Healthcare, Erlangen, Germany), using dedicated array coil systems for optimized signal reception and retrospective electrocardiographic gating. After acquisition of multi-planar localizers (2, 3, and 4 chamber views), a short-axis stack of cine steady-state free precession (SSFP) slices were obtained for ventricular function analysis in consecutive end-expiratory breath-holds. Typical parameters for SSFP sequence were: TR

2.8ms, TE 1.2ms, slice thickness 8mm, in-plain resolution 1.6-1.8 x 1.6-1.8mm, temporal resolution of 35-40ms.

CMR analysis was performed by three experienced readers (MN, MA and RH, 2-5-year experience) on a remote workstation using commercially available software (CVi42; Circle CVI, Calgary, Alberta, Canada). All CMR studies were de-identified and randomized to ensure that the analyst was blinded to all clinical data and imaging time points. Following predefined standard operating procedures for endocardial contouring, LV volumes, function and mass, were quantified, by semi-automatic tracing of endo- and epicardial contours with assignment of trabeculations and papillary muscles to the LV blood pool. Partial basal slice inclusion was based on built-in long axis cross referencing tools and close monitoring of SAX cine movie concurrently. For all patients arterial elastance (EaI) was calculated as end-systolic pressure (0.9 x brachial systolic pressure)/LV stroke volume indexed to BSA (243,244). Systolic blood pressure was measured just prior to the CMR study.

Echocardiography: In the sub-cohort of patients recruited in Toronto (n=83), transthoracic echocardiography (TTE) was performed on average within 2 hours of each CMR exam. TTE studies were performed by experienced sonographers using commercially available GE ultrasound systems (Vivid 7 or E9). In each patient, apical 4, 3, and 2 chamber LV views at high frame rate (>55 frames per second) were acquired for 3 cycles for quantification of LV GLS. Measurement of GLS was performed offline using de-identified images using EchoPAC (GE, version 112) by an experienced dedicated research sonographer (3-year experience with strain) blinded to all clinical data using de-identified and randomized study identifiers. Blood pressure and heart rate (HR) were recorded at the time of each echocardiography study. GLS was measured using automated myocardial contours generated by placing 3 seed points on each of the 3 long axis views.(150) Contour adjustment was performed as necessary; however, after 3 attempts, poorly tracked segments were excluded.

CTRCD Definitions: The primary definition of CTRCD was as a reduction in LVEF by >10% and to <55% without symptoms or a reduction by >5% and to <55% with heart failure symptoms (referred to henceforth as CTRCD-LVEF).(245) If baseline LVEF was <55%, only >10% reduction in LVEF was used to define CTRCD. A secondary definition of CTRCD was based on a reduction in GLS of >15% by echocardiography between pre-cancer treatment at either of the 2 follow-up imaging time points as per the recent American Society of Echocardiography (ASE) recommendations (referred to from hereon as CTRCD-GLS).(239)

A pre-defined sensitivity analyses was performed including a mild reduction in LVEF, defined as any reduction in LVEF of >5% as compared to pre-cancer therapy as a CTRCD event. This threshold was chosen based on data that an LVEF change of 5% is >2 standard deviations (SD) above inter-study variability of CMR measurements of LVEF reported in the literature.(246) A second sensitivity analysis was performed to examine a smaller reduction in GLS (>11%) a CTRCD event based or previous literature.(157)

Definition of significant change in volumes: Significant changes in CMR measured LV volumes were defined to be consistent with published literature as LVEDV reduction >10 mL and LVESV increase >5 mL(241). These thresholds are also higher than the inter-study variability for these measurements reported in the literature.(246)

Intra-observer variability:

In 20 randomly chosen single time point CMR data sets, intra-observer reproducibility was assessed by repeated analysis (>3-month interval) with the same observer blinded to previous results.

Statistical Analysis

Data are summarized as mean (SD) or median (IQR) as appropriate. All data were first assessed for normality based on skewness, kurtosis, and the Kolmogorov-Smirnov test. No transformations were

necessary. Comparison of means was performed using paired or unpaired student's t-test as appropriate. Longitudinal data analysis was performed using linear mixed models with time point as the independent variable and subject as a random effect, which were then fit to examine the impact of time on the outcomes of interest (body weight, HR, systolic (SBP) and diastolic (DBP) blood pressures, EaI, LVEF, LVEDV, LVESV, LV mass, and GLS). The frequency of LVEDV declines or LVESV increases were calculated based on above criteria in those with CTRCD. Association between changes in LVEF and GLS was assessed using Repeated Measures General Linear Model with time as fixed factors, LVEF as a covariate, and patient identifier as a random variable. Univariable logistic regression models were used to examine associations between baseline CMR parameters and their changes (as continuous variables) and CTRCD. Variables with p-values <0.1 were included in multivariate logistic regression models to test independence of association. Presence of collinearality was assessed by measuring variance inflation factors (VIFs), with values >4.0 deemed as demonstrating models with excess collinearality. Intra-observer variability was calculated using co-efficient of variation (COV) and Bland-Altman analysis. A two-sided *p*-value <0.05 was considered significant. Statistical analysis was performed using SPSS version 23 (IBM Corp., Armonk, NY) and R statistical software (Vienna, Austria).

Results

Patients

Patient clinical characteristics are summarized in Table 7-1. Mean ± SD age was 50.6±9.7 years (range 27–70 years). Amongst these patients, 110 received epirubicin (mean cumulative dose 308.7 ± 40.3 mg/m^2) and two patients received doxorubicin. At least one cardiovascular risk factor (Table 7-1) was present in 45 patients (40.2%). Over the six month follow-up period there was no statistically significant change in SBP, DBP, and EaI (Figure 1). There was, however, a statistically significant increase in mean weight and HR (Figure 1) over the follow-up period ($p<0.001$). Mean baseline 71.3±11.8bpm, at 3

months 77.7±10.6 bpm (p<0.001 vs baseline), and at 6 months 75.5±10.4 bpm (p<0.001 vs baseline). There was no change in the mean weight between baseline and 3 months (66.7 ± 13.9kg to 66.9± 14.0kg, p=0.99), but the weight increased significantly at 6 months (68.1 ± 14.3kg, P< 0.001).

Changes in Left Ventricular Volume, Mass and Function

CMR parameters at baseline and follow-up are summarized in Table 7-2. Mean LVEF at baseline was normal at 61.0 ± 4.9%, however, 12 patients had LVEF between 50-55% and one patient had a baseline LVEF of 47%. These patients with a mild reduction in LVEF still received treatment since cardiac screening prior to cancer therapy was based on 2D echocardiography as per standard of care. Over the six month period there was an overall significant increase in LVEDV and LVESV and a significant reduction in LVEF (p<0.001 for all). Changes are summarized in Table 7-2 and Figure 7-2A. There was no change in LV mass over the follow-up period (Figure 1F).

Changes in Global Longitudinal Strain

Mean baseline GLS was 21.9 ± 1.9% in the subgroup of 83 patients who had echocardiography. There was a significant reduction in GLS over the follow-up period (p<0.001) (Table 7-2 and Figure 2B). The changes in GLS were significantly associated with changes in CMR measured LVEF (p<0.001) with a 1.73% absolute change in GLS for every 10% change in LVEF.

Table 7-2: Sequential change in cardiac MRI parameters and echocardiography measured global longitudinal strain (GLS)

Characteristic	Pre-Cancer therapy	3 Months*	P-value (0-3)	6 Months[&]	P-value (0-6)
Cardiac MRI Left Ventricular Parameters (n=112):					
Ejection fraction, (%)	61.0 ± 4.9	59.3 ± 5.0	<0.001	56.3 ± 4.7	<0.001
End-diastolic volume, (ml)	125.7 ± 22.9	128.0 ± 24.9	0.06	137.2 ± 23.2	<0.001
End-diastolic volume indexed ml/m^2	73.6 ± 10.8	75.1 ± 12.9	0.04	80.6 ± 12.5	<0.001
End-systolic volume, (ml)	49.4 ± 12.7	52.1 ± 13.0	<0.001	60.5 ± 13.7	<0.001
End-systolic volume indexed, (ml/m^2)	28.9 ± 6.6	30.6 ± 7.1	<0.001	35.5 ± 7.7	<0.001
Stroke volume, (ml)	76.2 ± 13.0	75.4 ± 14.6	0.37	76.7 ± 12.2	0.59
Stroke volume indexed, (ml/m^2)	44.6 ± 6.0	44.2 ± 7.4	0.40	45.1 ± 6.6	0.40
End-diastolic mass, (gm)	66.1 ± 15.2	65.8 ± 13.9	0.59	67.1 ± 13.8	0.13
End-diastolic mass indexed, (gm/m^2)	38.5 ± 6.6	38.4 ± 6.1	0.73	39.3 ± 6.5	0.06
Echocardiography (n=83):					
Global Longitudinal Strain, **(%)**	21.9 ± 1.9	21.4 ± 2.2	0.02	20.2 ± 1.8	p<0.001

Data presented as frequency mean ± standard deviation,
*Within 1 month of completion of anthracycline,
[&]Within 2-3 months of initiation of trastuzumab

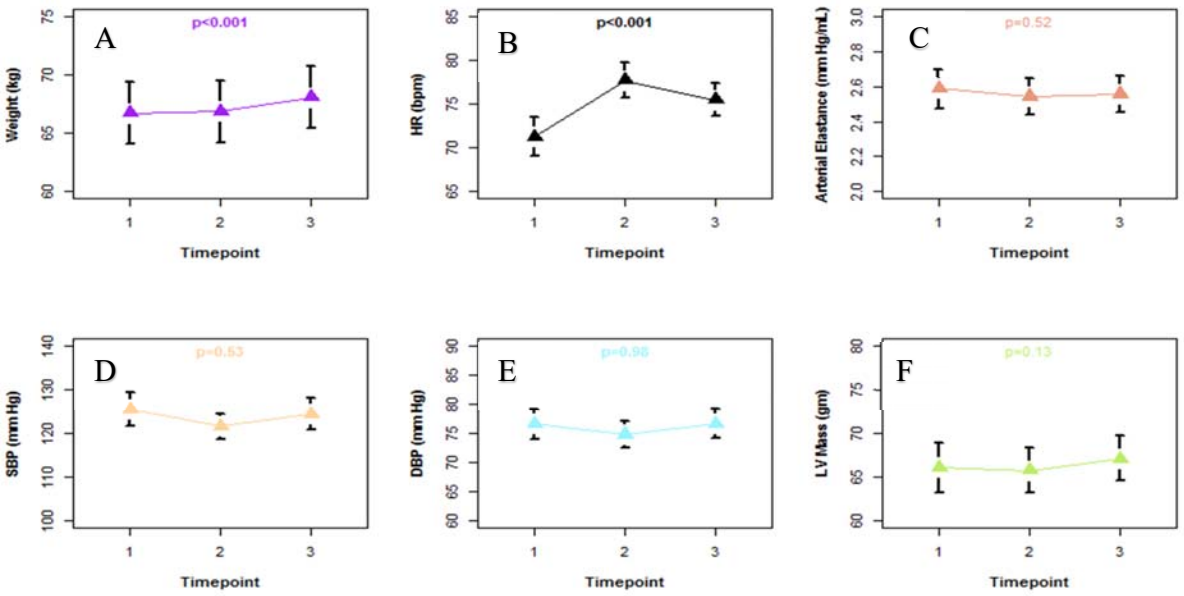

Figure 7-1: Changes in hemodynamic variables and LV mass over time. P-values calculated using linear mixed models. A) weight, B) heart rate, C) arterial elastance, D) systolic blood pressure, E) diastolic blood pressure and F) LV mass

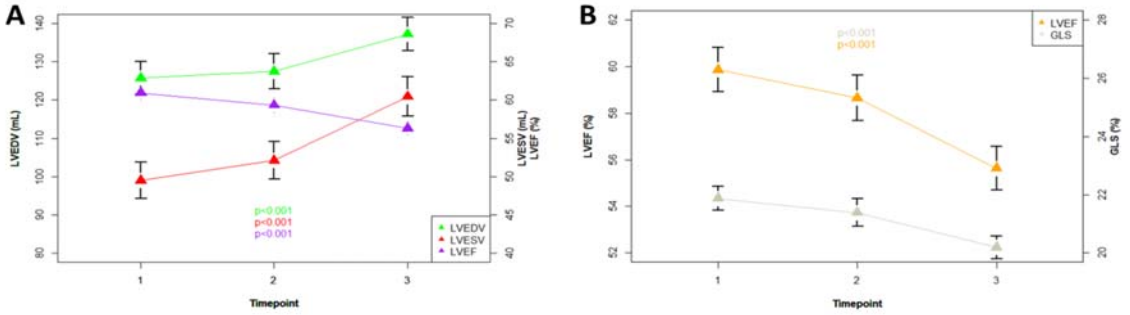

Figure 7-2: Changes in LV volumes, LVEF, and GLS. (A) Changes in LV end-diastolic and systolic volumes and change in LVEF in 112 patients. (B) Change in LV peak systolic global longitudinal strain (GLS) by echocardiography and LVEF by cardiac MRI in 83 patients

Cancer Therapy Related Cardiac Dysfunction

Using our primary definition 15(13.4 %) patients developed CTRCD-LVEF (Table 7-3). This was identified in three patients at three months and 12 patients at six months. The LV volumetric changes that accounted for the development of CTCD are summarized in Figure 3A while its timing is summarized in Table 7-3. The predominant mechanism of CTRCD was an isolated increase in LVESV (80%). None developed CTRCD due to isolated reduction in LVEDV. Using the sensitivity definition for CTRCD, a >5% reduction in LVEF occurred in 53 (47.3%) patients (Table 7-3). Amongst these patients 42 (79.2%) had an isolated increase in LVESV, seven (13.2%) had isolated decrease in LVEDV, two had both, and two had neither (Table 7-3, Figure 3B). As an exploratory analysis we also used the recently published ASE CTRCD criteria(239)(LVEF reduction >10% to <53%) and identified seven (6.3%) patients who developed CTRCD; all seven patients had a significant increase in LVESV.

In the GLS subgroup, 17 patients (20.5%) had a >15% relative reduction in GLS (Table 3); five (6.1%) occurred at between baseline and three months and an additional 12(14.6%) by six months. Amongst these patients 12(70.6%) had an isolated increase in LVESV while one (5.9%) had an isolated reduction in LVEDV (Figure 7-3C). This one patient with significant reduction in LVEDV also had an increase in LVESV of 4.9ml (just below significant threshold). When a lower threshold for strain change was considered (i.e. >11% reduction) 29 (34.9%) patients met criteria (Table 7-3). Amongst these patients, 17 (59%) had an isolated increase in LVESV, 4(13.8%) had an isolated reduction in LVEDV, while the rest had non-significant changes.

To examine the association between changes in LV volumes and GLS, we calculated GLS values at baseline and at the time of any >5% reduction in LVEF (our sensitivity outcome) (Figure 4). A statistically significant reduction in GLS occurred in patients who had an isolated increase in LVESV as the mechanism for reduction in LVEF, but not in those with an isolated change in LVEDV.

Table 7-3: CMR Volumetric determinants of left ventricular ejection fraction decline categorized by

CTRCD*[@]	**3 Month, n**	**6 Month, n**	**Entire Follow Up, n(%)**
Isolated ESV increase	2	10	12 (10.7%)
Isolated EDV decrease	0	0	0
Combined ESV increase and EDV decrease	0	2	2 (1.8%)
No significant Change in ESV or EDV	1	0	1 (0.9%)
Total	3	12	15 (13.4%)
GLS[$@] decline >15%			
Isolated ESV increase	3	9	12 (14.5%)
Isolated EDV decrease	0	1[#]	1 (1.2%)
Combined ESV increase and EDV decrease	0	1	1 (1.2%)
No significant Change in ESV or EDV	2	1	3 (3.6%)
Total	5	12	17 (20.5%)
LVEF decline >5%[@]			
Isolated ESV increase	18	24	42 (37.5%)
Isolated EDV decrease	3	4	7 (6.3%)
Combined ESV increase and EDV decrease	0	2	2 (1.8%)
No significant Change in ESV or EDV	2	0	2 (1.8%)
Total	23	30	53 (47.3%)
GLS[$@] decline >11%			
Isolated ESV increase	5	12	17 (20.5%)
Isolated EDV decrease	1	3	4 (4.8%)
Combined ESV increase and EDV decrease	0	0	0
No significant Change in ESV or EDV	6	2	8 (9.6%)
Total	12	17	29 (34.9%)

different CTRCD definitions and the time of occurrence.

EDV, end-diastolic volume; ESV, end-systolic volume; GLS, global longitudinal strain

*CTRCD is defined by >5% Symptomatic drop in LVEF to <55%, or asymptomatic >10% drop in LVEF to <55%

[$]GLS was measured in a subgroup of 83 patients

[#]LVESV increased by 4.9ml;

[@]LVEDV<-10ml, LVESV>5ml;

Association between changes in volumes and CTRCD

Change in LVESV was associated with CTRCD-LVEF (OR 1.15, 95%CI 1.05 –1.28, p<0.001), with 14.7% increase in odds of CTRCD-LVEF for each 1 mL increase in ESV (Table 7-4). In contrast, change in EDV was not significantly associated with CTRCD-LVEF (OR 1.01, 95%CI 0.96–1.05, p=0.74). Sensitivity analysis demonstrated that both change in ESV (OR 1.31, 95%CI 1.20 – 1.47, p<0.001) and change in EaI (OR 4.7, 95%CI 2.05 – 12.4, p<0.001) were associated with outcome of ≥5% LVEF decrease, however change in EDV was not (OR 1.00, 95%CI 0.98 – 1.03, p=0.87). Baseline ESV (OR 0.95, 95%CI 0.91 – 0.98, p=0.002) was also associated with >5% LVEF decrease, but baseline EDV was not (0.99, 95%CI 0.98 – 1.01, p=0.51). On multivariable logistic modelling, both change in ESV (OR 1.37, 95%CI 1.22 – 1.61, p<0.001) and change in EaI (OR 6.3, 95%CI 2.73 -85.4, p=0.004) demonstrated independent and significant associations, but baseline ESV (OR 1.02, 95%CI 0.94 – 1.08, p=0.20) and baseline LVEF (OR 1.03, 95%CI 0.92 – 1.17, p=0.65) did not.

CTRCD-GLS outcome was significantly associated with change in EDV (OR 0.92, 95CI 0.87 – 0.94, p=0.003), however a stronger association was seen with change in ESV (OR 0.81, 95%CI 0.72 – 0.90, p<0.0001), with lower odds more predictive of pathology due to GLS measurements being in negative units. Multivariate logistic models demonstrated significant and independent association with change in ESV (OR 0.83, 95%CI 0.72 – 0.93, p=0.004), but no independent significant association was seen with change in EDV (OR 0.98, 95%CI 0.92 – 1.04, p = 0.61). Sensitivity analysis using a liberal GLS threshold of 11% decrement demonstrated similar findings as for CTRCD-GLS on both univariable and multivariable logistic modelling. No collinearality was detected in any multivariable logistic models (VIF range 1.33 – 1.41).

Table 7-4: Univariable logistic regression analysis of association between ventricular volume and function measurements and development of CTRCD

	CTRCD-LVEF			**CTRCD-GLS**			**LVEF decrement >5%**			**GLS decrement >11%**		
	OR	95%CI	p	OR	95%CI	p	OR	95%CI	p	OR	95% CI	p
Baseline cardiac measurements												
EDV (mL)	1.00	0.98 – 1.02	0.94	1.02	0.96 – 1.05	0.11	0.99	0.98 – 1.01	0.51	1.00	0.98 – 1.02	0.71
ESV (mL)	0.99	0.94 – 1.03	0.53	1.03	0.98 – 1.08	0.28	0.95	0.91 – 0.98	**0.002**	1.00	0.97 – 1.04	0.80
LVEF (%)	1.07	0.09 – 1.20	0.24	1.01	0.09 – 1.16	0.87	1.41	1.24 – 1.64	**<0.001**	1.00	0.90 – 1.11	0.99
LV mass (gm)	1.01	0.97 – 1.04	0.68	1.04	1.00 – 1.09	0.07	1.02	0.99 – 1.04	0.25	1.00	0.97 – 1.04	0.92
Changes in LV parameters												
ΔEDV (mL)	1.01	0.96 – 1.05	0.74	0.92	0.87 – 0.97	**0.003**	1.00	0.98 – 1.03	0.87	0.91	0.85 – 0.95	**<0.001**
ΔESV (mL)	1.15	1.05 – 1.28	**0.006**	0.81	0.72 – 0.90	**<0.001**	1.31	1.20 – 1.47	**<0.0001**	0.80	0.71 – 0.88	**<0.001**
ΔLVEF (%)	-	-	-	1.21	1.06 – 1.41	**0.008**	-	-	-	1.22	1.08 – 1.39	0.002
ΔEAI (mmHg/mL)	1.53	0.61 – 4.93	0.45	0.95	0.35 – 2.45	0.91	4.7	2.05 – 12.4	**<.0001**	0.89	0.39 – 1.98	0.78
ΔGLS (%),	0.97	0.89 – 1.05	0.42	-	-	-	1.02	0.97 – 1.07	0.51	-	-	-

⁋All GLS measurements performed at single site

CTRCD- Cancer Therapeutic Related Cardiac dysfunction; CTRCD-GLS - Cancer Therapeutic Related Cardiac dysfunction, GLS definition; EAI – Arterial Elastance; EDV – End-Diastolic volume; ESV- End-Systolic Volume; GLS – Global Longitudinal Strain; LV – Left Ventricular; LVEF – Left Ventricular Ejection fraction.

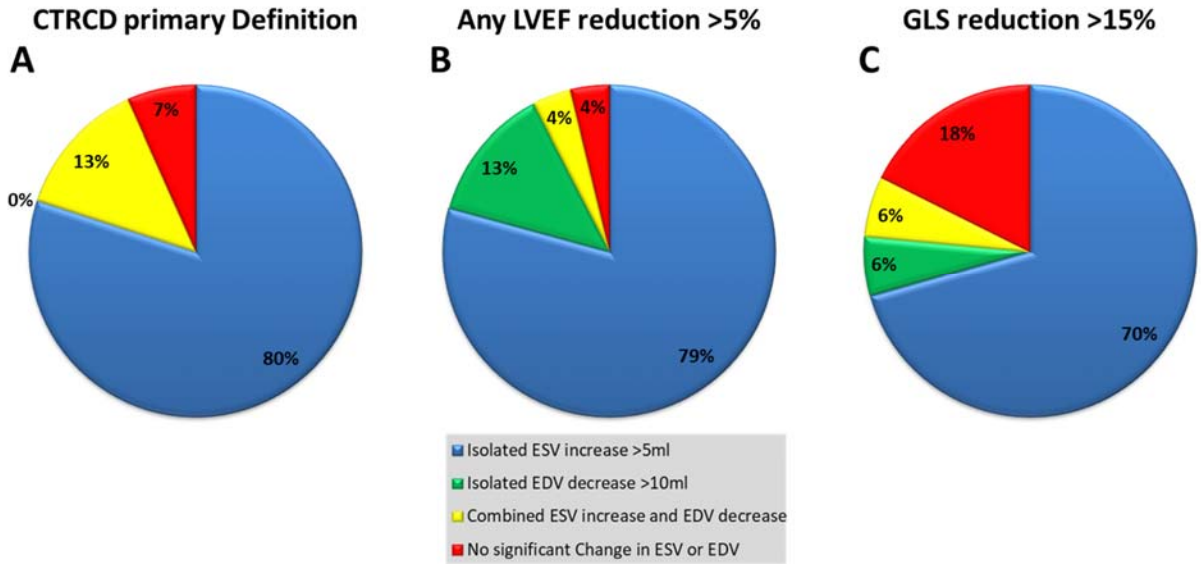

Figure 7-3: Causes for reduction in LVEF and GLS. (A) CTRCD was defined as per CREC recommendations. (B) Any >5% reduction in LVEF at 3 or 6 months compared to baseline. (C) CTRCD defined as a reduction in GLS by >15%.

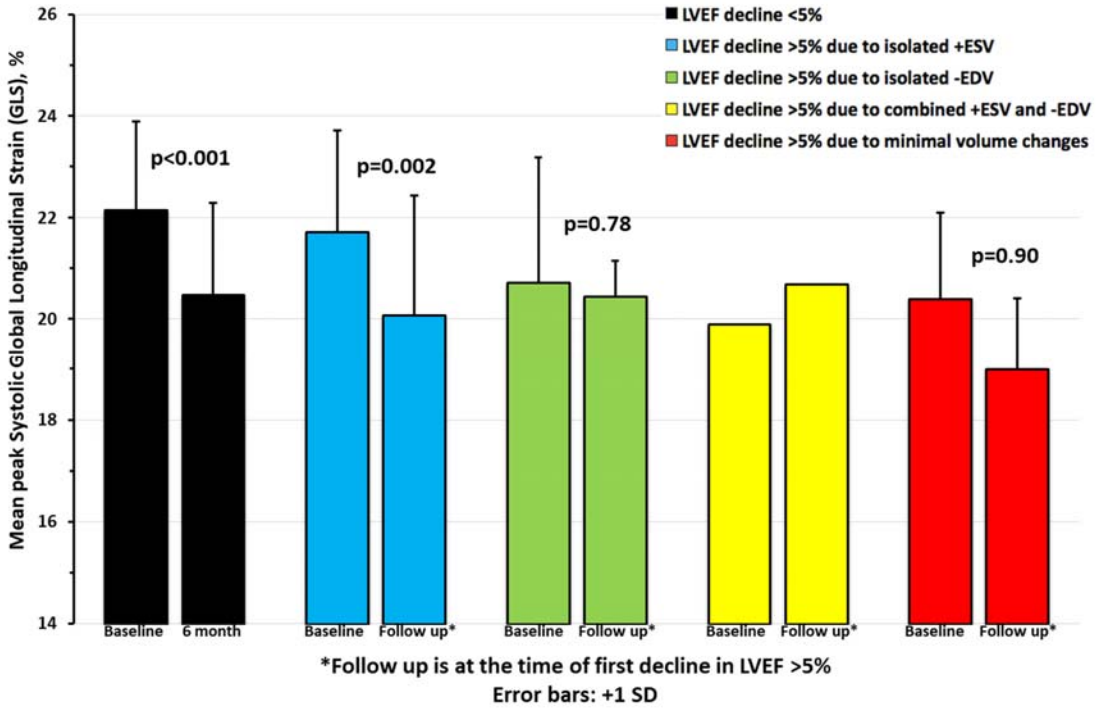

Figure 7-4: Comparison of mean global longitudinal strain between baseline and at time of a reduction in LVEF by >5% or at 6 months in those without a reduction

.

Intra-observer Variability

Intra-observer variability measured as mean difference ± 2SD and COV was as follows: 0.2±3.5ml and 1.5% (95% CI 0.9-2.0%) for LVEDV; 1.7±2.4ml and 3.4% (95% CI 2.4-4.4%) for LVESV; -1.3±1.6% and 2.0% (95% CI 1.4-2.6%) for LVEF; and 4.1 ±1.9g and 4.8% (95% CI 3.3-6.6%) for LV mass.

Discussion

In this cohort of consecutively-recruited HER2-positive breast cancer patients receiving uniform cancer treatment, CTRCD-LVEF at six months was seen in 13.4% of the patients. The reduction in LVEF was associated with a significant increase in LVESV in 93% of the patients. None of these patients had an isolated reduction in LVEDV, as would be seen with reduced preload. These findings are strongly suggestive of a reduction in myocardial contractility from cancer therapy as the primary mechanism of reduction in LVEF rather than isolated reduction in preload. Results were similar with CTRCD defined by echocardiography measured GLS reduction >15%. There was a significant association between CTRCD-LVEF and changes in LVESV over time but not LVEDV. In contrast, when a lower threshold was used to define significant change in LVEF (>5%) or GLS (>11%), a minority of patients attained these changes solely due to a reduction in preload (13.2% and 13.8% respectively). However these changes would not usually trigger interventions for CTRCD.(239) When a definition of CTRCD derived from GLS measurements was used, change in ESV demonstrated a significant and independent association, but change in EDV was not significantly associated if effect of change in ESV was included in model.

Relationship between ventricular volumes and CTRCD

Using a well-established criterion for cardiotoxicity(245), 14 out of 15 (93%) patients in our study developed CTRCD association with an increase in LVESV. None had an isolated reduction in LVEDV. Even using the ASE criteria(239) all patients who developed CTRCD had an increase in LVESV. Our findings were further confirmed by the logistic regression models where a change in LVESV as a continuous parameter showed predictive value for development of CTRCD but this association was not seen with LVEDV. Our work therefore suggests that currently used definitions for CTRCD based on LVEF appear to identify patients who have associated reduction in myocardial contractility. However, some of these patients may also have co-existing reduction in preload as demonstrated by the fact that two (13%) of our patients who met criteria for CTRCD also had a >10ml reduction in LVEDV along with a > 5ml increase in LVESV. A sensitivity analysis using LVEF decrements >5% to define CTRCD identified a larger proportion of patients (13.2%) with a reduction in LVEF due to reduced preload. Association of EaI with smaller decreases in LVEF is likely mediated by increased peripheral resistance causing earlier equalization of ventricular-arterial pressures with consequent reduction in ejection time.

Ventricular Volumes and Global Longitudinal Strain

When CTRCD was defined by a GLS reduction of >15%, our findings were similar. The reduction in GLS was primarily associated with an isolated increase in ESV. Only one patient had an isolated reduction in LVEDV. However this patient had an increase in LVESV of 4.9ml, thereby almost but not quite meeting pre-defined threshold of 5ml for significant ESV increase. Physiologically, an isolated reduction in pre-load results in reduced stroke volume which is partially offset by an increase in HR (in this patient HR increased from 62 to 71 bpm), a decrease in afterload and, as a consequence a reduction in end-systolic volume.(247) Therefore the absence of a reduction in LVESV in this patient suggests possible concomitant reduction in myocardial contractility. Furthermore, when we examined GLS changes in patients with any reduction in LVEF >5% (sensitivity analysis), that fact that only patients with increase in LVESV had a statistically significant reduction in GLS also supports its association with

a reduction in myocardial contractility. However, our work also suggests that if lower threshold changes in GLS (>11%) is used to define CTRCD approximately 1 in 8 patients may meet this threshold due to a reduction in preload. This finding of association with pre-load and small changes in GLS is consistent with a recent study of healthy patients with dehydration.(247)

Comparison to prior work

Our findings are different from two recent studies where CTRCD was driven by an isolated reduction in LVEDV in 19-26% of patients(241,242). In addition, a reduction in CMR-measured circumferential strain and GLS were associated with a reduction in LVEDV.(241) In light of this, it has been proposed that the diagnosis of CTRCD should be considered in the context of changes in LV volumes. These data raised the possibility that a subset of patients diagnosed with CTRCD have normal myocardial contractility and hence should not be subject to the usual management of cancer therapy adjustment and/or addition of cardiac medications. These findings have important clinical consequences as one would need a robust method to measure concomitant changes in LVEF and LVEDV during cancer therapy. The most commonly clinically available 2D and 3D echocardiography techniques have a test-re-test variability for LVEDV measurement between 21-38ml (150) making it challenging to identify a 10ml reduction in LVEDV. The use of CMR in routine clinical practice would be challenging due to availability and cost.

Our findings differ from previous work(241,242) and may be due to the following reasons. There were differences in the types of cancers included (100% breast cancer in our study versus <50% in prior studies) which are associated with different treatment regimens. The inclusion of hematological malignancies in the prior studies would have resulted in a subcohort of patients receiving higher anthracycline than in our study. Also the use of trastuzumab and taxanes was universal in our study and the latter has been associated with fluid retention.(248) Our study included 3 and 6 month follow-up while the prior study only included 3 month follow-up. Although the presence of emesis, nausea, diarrhea

and poor oral intake may have been present at the 3-month follow-up, it is less likely to be present during trastuzumab therapy; majority of our patients developed CTRCD at 6-month follow-up. The definition of CTRCD in the prior studies (>10% decrement in LVEF or any absolute LVEF value <50% between baseline to 3-month) differs from our definition.(245) The definition of LVEF reduction to less to <50% may include patients with a small change in LVEF (e.g. from 54% to 49%). Our data shows that such small changes in LVEF can in fact occur due to isolated reduction in pre-load as shown in the prior studies. Finally Jordan et al(241) primarily demonstrated an association between CMR-measured circumferential strain using tagging and decreased preload whilst we used echocardiography measured GLS, as this is the most readily available and validated modality to assess strain in patients receiving cancer therapy(137).

Strengths and Limitations

Strengths of our study include the use of CMR to measure cardiac volumes, the focus on a uniform population of patients with uniform treatment, consecutive recruitment, prospective follow-up, and the use of contemporary definitions of CTRCD. Limitations include a relatively small number of outcomes. However, our sample size and event rate is consistent with contemporary studies in cardio-oncology.(241,242) Furthermore, each patient had repeated cardiac imaging at three separate time points with the acquisition of echocardiography imaging and CMR within 2 hours in large subset of our patients. We also utilized cardiac imaging findings as surrogate markers for potential future heart failure events, however, this is commonly done in the cardio-oncology literature. Since our cohort was limited to a specific group of HER2+ breast cancer patients, the results may not be extrapolated to non-breast cancer populations treated with other regimens. We made the assumption that a reduction in LVEDV represents reduced preload, however other causes (e.g. diastolic dysfunction secondary to cardiotoxicity) have not been excluded. Unfortunately, a reference standard for assessment of preload does not exist. Similarly, we assumed that an increase in LVESV is a reflection of reduction in contractility. However, there are no non-invasive ways to measure contractility in a reliable manner. A small subset of our patients had

LVEF<55% at baseline, which may have impacted CTRCD incidence. However, only one of these patients developed CTRCD-LVEF. Inclusion of these patients was based on the fact that baseline screening was performed by echocardiography as per clinical practice.(249)

Conclusion

In a cohort of women with HER2+ breast cancer receiving anthracyclines, taxanes, and trastuzumab, our results support the fact that with current CTRCD definitions(239,245), changes in LVEF or GLS are associated with an increase in LVESV (reflective of reduction in myocardial contractility) and not due to a reduction in pre-load. However, if lower threshold changes in LVEF or GLS are used to define CTRCD, approximately 1 in 8 patients will meet this threshold due to isolated reduction in preload. Therefore using current definitions of CTRCD does allow identification of patients who would benefit from interventions to prevent subsequent heart failure.

Postscript

This chapter confirms that when LV volume measurements are made using techniques with greatest degree of accuracy, that CTRCD remains relatively common with an incidence of approximately 13%, a result which has been also seen in many other observational studies. This finding accurately represents cases of reduced myocardial contractility in the context of myocardial dysfunction, and therefore supports continuing use of current CTRCD criteria, which is defined by significant LVEF decrement either with or without accompanying symptoms as measured by contemporary cardiac imaging.

This chapter however only limits itself to identification of myocardial contractility abnormalities secondary to chemotherapy and is based upon a CTRCD definition that was laid down 16 years ago. Since that time our understanding of cardiac function as evolved, and healthy function is now understood

as successful integration in terms of both timing and function of simultaneous processes including cellular, conduction, valvular, mechanical, perfusion, systolic and diastolic dimensions that result in adequate and regular stroke volume ejection without requiring excessive venous pressures to achieve. The next chapter of this thesis will examine whether cardiac functional abnormalities other than LVEF changes are common in CTRCD, and the role of CMR in distinguishing between the predominant abnormality affecting cardiac function.

Chapter 8

Phenotypes of Cardiac Injury After Cancer Treatment

Part of the research presented in this chapter has been submitted as:

- **Nolan MT,** Altaha MA, Amir E, Koch A, Yip P, Michalowska M, Wintersperger B, Thavendiranathan P. Cardiotoxicity Phenotypes in Women with Early Stage Breast Cancer Receiving Cancer Therapy. *In process of submission*

Chapter 8- Cardiac Phenotypes of Chemotherapy Injury

Preface

The previous seven thesis chapters have uncritically adopted the LVEF-based definition of CTRCD, by which patients are separated in a binary fashion depending on their volumetric change from baseline. The rationale for this approach is based on a solid evidence-base describing a direct association between LVEF and mortality, but also risks missing significant and potentially treatable cardiac sources of morbidity and mortality.

Readers might consider the trajectory of heart failure diagnostic criteria as an educational example. It was in 1955(250) that heart failure was recognised as a pathological state of reduced myocardial contractility, and it was over 50 years later until the syndrome of heart failure with preserved fraction (HFpEF) was comprehensively described. Currently the pharmacological and cardiac-device treatment armamentarium for heart failure with reduced ejection fraction with much larger and of greater demonstrated efficacy than that for HFpEF. It could be argued that the delay of several decades before rigorous diagnostic criteria for HFpEF were developed may have delayed research and have indirectly led to potentially avoidable morbidity and mortality. It is also possible that the current focus on reduction in LVEF in CTRCD may cause under-appreciation of other dimensions of cardiac dysfunction.

The next thesis chapter will prospectively investigate the incidence of systolic diastolic dysfunction in a cancer cohort. The aim of this chapter will be to determine the prevalence of both overt and subclinical manifestations of cardiac dysfunction with comparison of frequency of CTRCD as defined by traditional LVEF criteria. The identification of various cardiotoxic phenotypes may allow cardiac imaging findings of cancer patients to be individualized rather than fitted into a binary disease-or-healthy approach and hence permit a more individualized approach to treatment and risk factor modification.

Abstract

Background: There is currently limited data on the effects of early breast cancer (EBC) treatment on different dimensions of cardiac function.

Objectives: To use CMR to identify different phenotypes of cardiac dysfunction in the EBC population.

Methods: 66 consecutive women (50.3 ± 9.4 years) with early stage HER2+ breast cancer, receiving sequential anthracycline and trastuzumab, were recruited prospectively. All had CMR, including both systolic and diastolic assessment at 5 time-points over 14 months. Diastolic dysfunction (DD) phenotype was diagnosed using society guidelines, with abnormal values defined as >2SD from reference ranges calculated from 29 healthy volunteers. SD was diagnosed using CREC criteria. No-diastolic-No-systolic dysfunction (NDNS) phenotype comprised the remainder.

Results: 13 (19.7%) patients developed SD, with median onset at 5 months with 84.6% demonstrating recovery by 14 months. SD patients were older with no other significant baseline differences from NDNS group, had -9.7% decline in LVEF and subclinical diastolic dysfunction (PDSR reduction $p<0.001$). DD phenotype was diagnosed in 13 patients (19.7%), 4 of which also had SD, with median onset 8 months with 38.5% demonstrating recovery by 14 months. DD patients were older, received higher chest-directed radiotherapy doses and more likely to have hypertension and diabetes. There was no significant LVEF change, but clinical systolic dysfunction was present (GLS reduction $p=0.001$). NDNS patients had significant small reductions in LVEF($p<0.0001$) and GLS($p<0.0001$), with no significant change in diastolic parameters

Conclusions: Cardiac dysfunction is common after EBC therapy and can be described by three phenotypes which are characterized by different baseline characteristics, non-invasive imaging findings and different degrees of recovery of cardiac function. Long-term studies are indicated to determine the prognostic significance of each phenotype.

Chapter 8- Cardiac Phenotypes of Chemotherapy Injury

Introduction

Women treated for early stage breast cancer (EBC) are at a 2 to 3 fold higher risk of clinical heart failure (HF) compared to age matched controls(251,252). Despite HF with preserved ejection fraction (HFpEF) being common in the community, much of the focus in cancer survivors has however been on heart failure with reduced ejection fraction (HFrEF). Recent data in older women with breast cancer receiving radiation therapy demonstrated that HFpEF was more common than HFrEF(253). Furthermore dyspnea is a common complaint in breast cancer survivors(254) with prevalence at three year following being two-fold greater than in the general population with rates exceeding that of systolic dysfunction(255). Although changes in diastolic parameters have been demonstrated in anthracycline-treated patients, these were generally short-term studies with small patient numbers(256,257). Also given the challenges in measurement of LVEF with echocardiography, determining whether diastolic functional abnormalities occur independently of systolic function changes has not been reliably assessed. Therefore, there is a paucity of data describing the different cardiotoxicity phenotypes in women with EBC receiving cancer therapy and their temporal relationships during treatment. This knowledge is essential for providing recommendations on strategies to evaluate patients during cancer therapy and to help better appreciate the relationship between cardiac dysfunction and symptoms.

We hypothesized that women with EBC may develop diastolic dysfunction (DD) together or independently from systolic dysfunction, and that DD may contribute to the symptomatic burden in the short-to-intermediate term. To address this hypothesis, we used cardiac magnetic resonance (CMR) to identify the different phenotypes of cardiotoxicity (e.g. systolic versus diastolic) in a cohort of women with Human Epidermal Growth Factor Receptor Positive (HER+) EBC, and examined the association with demographic, imaging and biochemical variables.

Methods

Study population

We prospectively recruited women with HER 2+ EBC (Stages I-III) from the Princess Margaret Cancer Center and St. Michael's Hospital in Toronto, Canada between January 2014 and April 2017. We included women aged ≥18 years of age scheduled to undergo treatment with an anthracycline (Epirubicin or Doxorubicin) followed by trastuzumab and taxanes (Paclitaxel or Docetaxel). Exclusion criteria were (1) previous anthracycline therapy; (2) current or prior cardiovascular disease; and (3) general contraindications to MRI. Patient characteristics, cardiac risk factors, and cancer and treatment history were collected. In addition we recruited 29 healthy volunteers with the same age range as the EBC population to define 95% confidence interval thresholds for normal values, to assist in identifying diastolic dysfunction in our EBC cohort. Healthy volunteers had no cardiovascular disease, symptoms, or risk factors, were not on any medications, and had no systemic diseases. The study was approved by the local Research and Ethics Board, and all patients provided written informed consent.

Cardiac Magnetic Resonance Imaging

Cardiac MRI (CMR) studies were performed at 5 time-points (Figure 1); prior to initiation of cancer therapy, after completion of anthracycline but before initiation of trastuzumab / taxane (~2 months), at 3 and 6 months after trastuzumab initiation, and within 1 month of trastuzumab completion (~12 months after trastuzumab initiation). CMR scans were performed on 1.5T imager (Magnetom Avanto Fit; Siemens Healthcare, Erlangen, Germany), using dedicated array coil systems for optimized signal reception and retrospective electrocardiographic gating. After acquisition of multi-planar localizers (2,3 and 4 chamber views), a short-axis stack of cine steady free-state free precession (SSFP) slices were obtained for ventricular function analysis in consecutive end-expiratory breath-holds. Typical parameters for SSFP sequence were: TR 2.8 msec, TE 1.2 msec, slice thickness 8 mm, in-plane resolution 1.6-1.8 x 1.6-1.8 mm, temporal resolution of 35-40 msec.

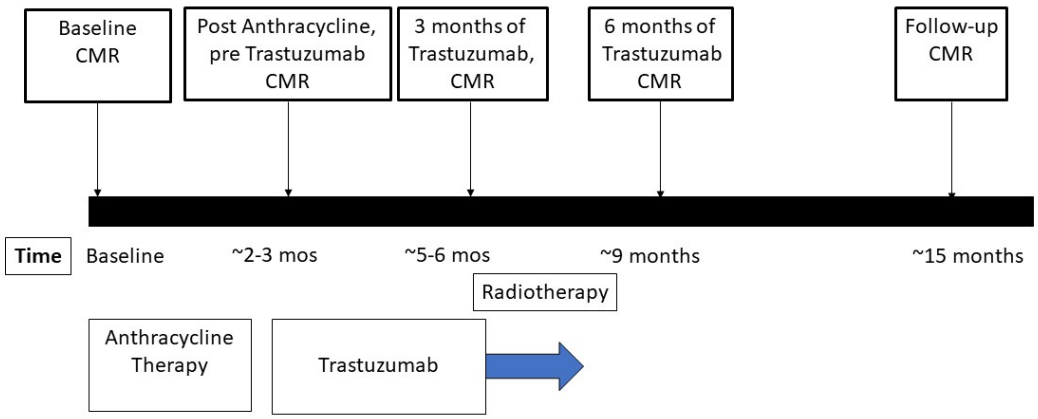

Figure 8-1: Timeline of course of treatment for EBC and associated CMR examinations.

Trans-mitral and myocardial velocity imaging were performed using retrospectively-gated electrocardiographically triggered phase-contrast MR technique, with velocity sensitivity of 150 cm/sec for trans-mitral velocities and 30 cm/sec for myocardial velocities(258). Both imaging techniques used a short-axis view at the level of mitral leaflet tips in diastole with slice thickness 10 mm, in-plane resolution 1.5 x 0.8 mm and temporal resolution 35-40 msec. The following parameters were used for trans-mitral phase-contrast imaging; TR 37.0 msec, TE 3.7 msec, slice thickness 10 mm, in-plane resolution 1.5 x 0.8 mm, temporal resolution 35-40 msec. Parameters for myocardial velocity imaging were: TR 39.5 msec, TE 4.2 msec, slice thickness 10 mm, in-plane resolution 1.5 x 0.8 mm, temporal resolution 35-40 msec. Myocardial T1 mapping was performed in 3 short-axis slices (basal, mid, and apex) using a modified-look-locker inversion recovery (MOLLI) sequence before and 12-15 minutes after IV contrast administration (0.2mmol/kg, Gadovist; Bayer Healthcare, Berlin, Germany). The following recommended MOLLI inversion groups were used for optimal precision pre-contrast (5(3)3) and post-contrast (4(1)3(1)2).(259)

Image post-processing

CMR analysis was performed by two experienced readers (M.N. and M.A, 2-5 years' experience) using commercially available software (CVi42, Circle CVI, Calgary, Alberta, Canada). All CMR studies were de-identified and randomized to ensure that the analyst was blinded to all clinical data, patient identification, and imaging time points. Following predefined standard operating procedures, LV function was quantified by semi-automatic tracing of endo- and epicardial contours with assignment of trabeculations and papillary muscles to the LV blood pool. In addition, using 4 and 2 chamber SSFP cine images, left atrial volume was calculated using biplane area-length method and indexed to body surface area.

Transmitral and myocardial velocities were measured using phase contrast images. For mitral inflow velocities a region of interest (ROI) was generated by tracing around the mitral leaflet borders in diastole on the magnitude images and automatically transferred to the phase images. 10% color scale threshold

was used on all magnitude images to assist in identifying anatomical region of flow and exclude pixels that did not represent transmitral or myocardial tissue velocities of interest. The ROI was propagated and examined in each frame with adjustments made to ensure that the appropriate location of the contours.

For myocardial velocity measurements, a circular ROI 20-40mm2 was placed within the inferior septal and anterior lateral segments on the magnitude image and automatically transferred to the phase image (Figure 8-2). Cine SSFP and color-overlay images were assessed to ensure that the region-of-interest did not capture blood pool or epicardial adipose tissue. Minor adjustments to the region-of-interest were made to ensure that the velocities were being measured from the myocardium and that the highest velocities were recorded(258). Velocity-versus-time curves were assessed to ensure robustness of the measurements and to exclude erroneous measurements. Background velocity correction was performed with contour applied to latissimus dorsi muscle. Measurements recorded include: early (E) and late (A) mitral inflow flow velocities, and medial and lateral annular (myocardial) velocities (e').

Myocardial systolic and diastolic strain analysis was performed offline using tissue tracking module of cvi42 (Circle Cardiovascular Imaging, Calgary, Canada). On SSFP cine images end-diastolic endocardial and epicardial contours were manually traced on 4-chamber, 3-chamber and 2-chamber views. The contours were then automatically propagated through all phases with subsequent generation of a 3D deformable myocardial strain model. Strain values were automatically calculated by software using feature tracking, and peak systolic global longitudinal strain peak diastolic strain rate (PDSR) was recorded.

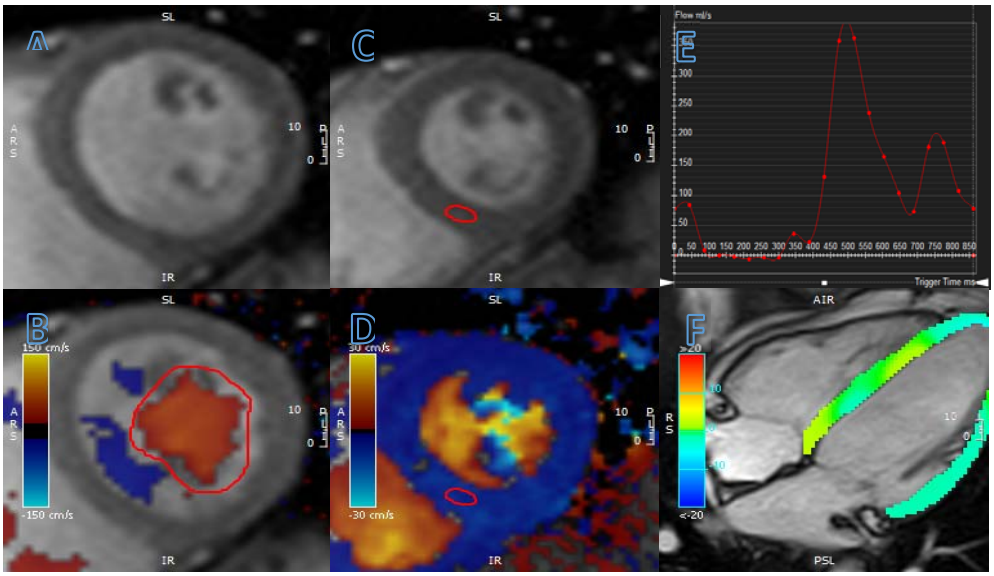

Figure 8-2: Example of measurement of diastolic function by CMR. (A) Phase-contrast through-plane cine images, including both magnitude and phase series, were used to measure mitral flow and tissue velocities. (B) An ROI was traced around trans-mitral flow in all images, with background correction applied. (C) For tissue velocity measurements, a smaller ROI was placed within myocardium in all images. (D) Flow overlay was applied to ensure that ROI corresponded to region of greatest myocardial velocity. (E) Velocities were displayed over time, with greatest velocity selected. (F) Feature-tracking PDSR measurements were obtained by creating end-diastolic contours in 4-chamber, 3-chamber and 2-chamber planes, and semi-automated measurements were extrapolated from all images.

After inline, non-rigid motion correction of individual pre and post contrast MOLLI images, a T1 map was generated using standard three-parameter fitting. T1 measurements were performed using CVI 42 using regions of interest carefully drawn along the endocardial and epicardial borders to avoid blood pool and epicardial fat. A second region of interest was drawn in the LV blood pool carefully avoiding the myocardium and papillary muscles. Myocardial ECV was calculated using pre- and post-contrast T1 values and hematocrit values measured immediately prior to the CMR study as proposed by societal recommendations(260).

For all patients, as a marker of afterload, arterial elastance (EaI) was calculated as end-systolic pressure (0.9xbrachial systolic pressure)/LV stroke volume indexed to BSA. Systolic blood pressure (SBP) was measured just prior to each the CMR study.

Diastolic and Systolic Cardiac Dysfunction Definitions

Normal reference ranges for diastolic parameters were calculated based on 29 healthy volunteers recruited from the community with age range identical to the patients. Values greater than 2 standard deviations beyond mean values of volunteers (Table 7-2) were considered abnormal. Presence or absence of diastolic dysfunction was determined by presence of ≥ 2 of 3 diagnostic criteria; 1) abnormal annular velocity (defined as medial e' or lateral e' < 2 standard deviations (SD) below normal), 2) abnormal E/e' (defined as E/e' > 2 SD above normal), or 3) abnormal left atrial volume index (LAVI) (defined as > 2 SD above normal). If diastolic dysfunction was diagnosed, then the diastolic grade was determined as following; 1) grade 1 diastolic dysfunction if E/A < 2 SD below normal and E velocity < 2 SD below normal, 2) grade 3 if E/A ratio was >2.0 SD above normal, and 3) remaining cases was diagnosed as grade 1 if 1 of abnormal E/e', abnormal annular e' velocity or abnormal LAVI was present, and grade 2 if ≥2 were present. Systolic dysfunction secondary to chemotherapy (SD) was defined using the CREC criteria as a reduction in LVEF by >10% and to <55% without HF symptoms or a reduction by >5% and to <55% with HF symptoms determined by a cardiologist within the Cardio-oncology clinic(245).

Statistical Analysis

Continuous data are summarized as mean ± SD, and categorical data as percentages. All data were first assessed for normality by Kolmogorov-Smirnov test and no transformations were necessary. Comparisons of means was performed using paired or unpaired t-student's test as appropriate, and one-way ANOVA was used to compare means of >2 groups. If assumption of normality was not held, then Wilcoxon's paired or unpaired test was used for 2 groups and Kruskal-Wallis if >2 groups were present. Longitudinal data analysis was performed using generalized linear mixed models with individual patients used as random-effect and timepoint used as fixed-effect and singular covariance matrix with Cholesky parameterization. For mixed linear models, p value was calculated using F test with Satterthwaite approximation. Statistical analysis was performed using R statistical software (Vienna, Austria) and the lme4 package(152). P values ≤ 0.05 were considered significant.

Table 8-1: 95% confidence intervals for diastolic parameters calculated with 29 age-matched volunteers

	LL	UL
E velocity (cm/sec)	**41.1**	**90.2**
A velocity (cm/sec)	**13.8**	**70.1**
Inferoseptal e' (cm/sec)	**4.2**	**15.2**
Anterolateral e' (cm/sec)	**5.02**	**14.7**
Mean e'	**5.0**	**14.7**
E/A ratio	**0.31**	**3.2**
E/e' ratio	**3.5**	**10.3**
LAVI (mL/m^2)	**45.6**	**57.5**

Results

Study Population

Twenty-nine healthy volunteers were recruited to define thresholds for normal abnormal diastolic function (Table 8-1). A total of 66 women with HER2+ EBC were recruited with mean age 50.3±9.4 years. Patients were treated with doxorubicin-equivalent doses of 202.6±8.2 mg/m^2 (Table 8-2). Twenty-four patients (36.4%) had ≥1 cardiovascular risk factor. Sixty women (90.9%) received chest-directed radiotherapy. Heart rate significantly increased to peak values immediately post anthracyclines and returned to baseline by study end($p<0.001$). There were no significant changes in systolic or diastolic blood pressure over the study period. There was an increase in BNP immediately post anthracyclines which then returned to baseline by end of study ($p=0.002$), there was also a nonsignificant trend towards increase in NYHA class during the study ($p=0.08$).

Temporal Changes in Systolic and Diastolic Parameters

Over the treatment period (mean 14.6±1.1 months), systolic function for the entire cohort was characterised by significant declines in both LVEF and GLS (Supplementary Figure 2). LVEF significantly declined from baseline to a nadir (fall of -3.9%) at 4 months (i.e. 2 months into trastuzumab therapy), then displayed incomplete recovery after trastuzumab completion. GLS gradually declined throughout treatment with the largest fall at 4 months, with no recovery after trastuzumab completion ($p<0.0001$). There was no significant change in EaI over time suggesting reduction in systolic function was not secondary to changes in afterload.

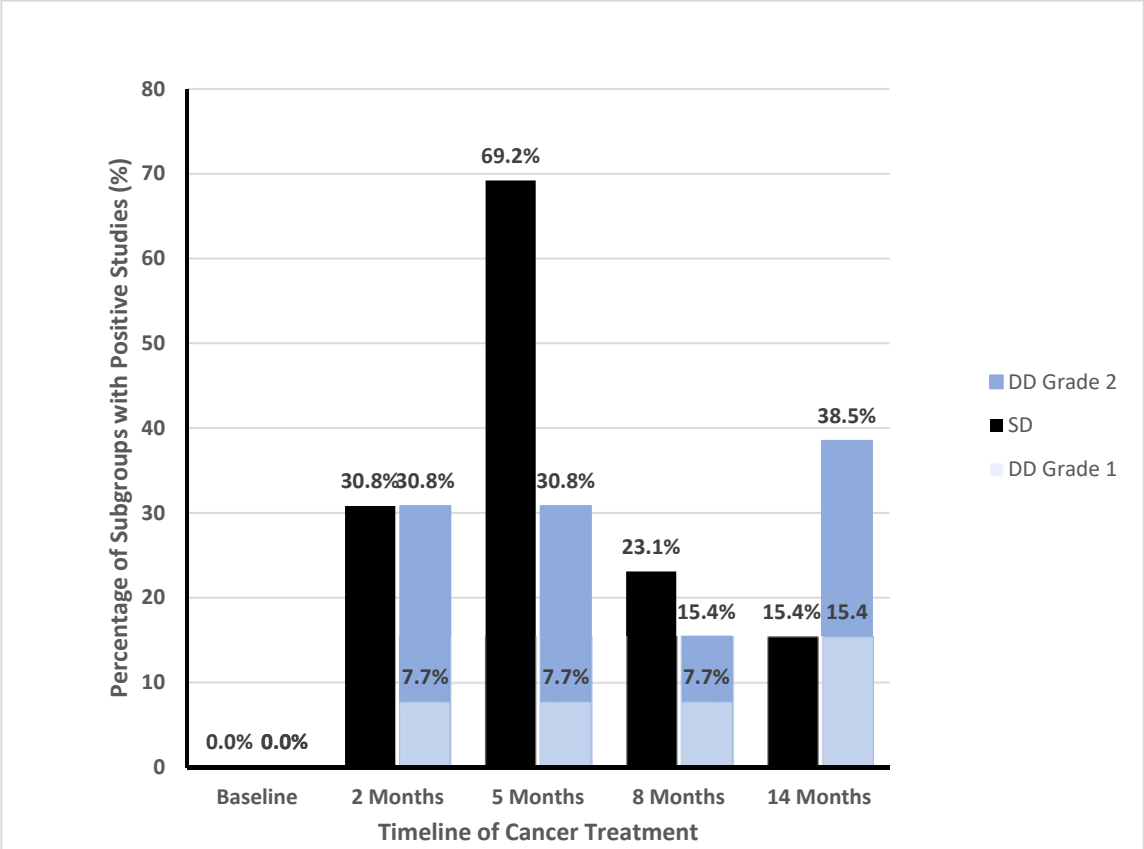

Figure 8-3: Timeline of development of SD and DD per timepoint. A) Proportion of patients with either SD (brown) or DD (blue) that have a study meets criteria for dysfunction at that timepoint. For example, at 5 months, 69.2% of cohort of 13 SD patients have a study that meets SD criteria, and 30.8% of DD patients have a CMR study that meets DD criteria. By 8 months, the proportion of SD patients with CMR study meeting SD criteria has reduced to 23.1%, demonstrating that some patients have normalized their systolic function

Note that the total for SD and DD sums to greater than 100% because patients may have more than 1 study demonstrating cardiac dysfunction. DD studies are broken into diastolic Grade 1 (light blue) or Grade 2 (dark blue), with no cases of Diastolic grade 3 dysfunction occurring during study

Table 8-2: Baseline Demographics of Early Breast Cancer Cohort

	Total (N = 66)	DD (N=13)	SYSD (N = 13)	NDNS (N = 43)	p-value for difference	
					DD vs. NDNS	SYSD vs. NDNS
Demographics						
Age (years)	50.3 ± 9.4	56.7 ± 9.1	54.4 ± 8.0	48.2 ± 9.2	**0.005**	**0.033**
BMI (kg/m^2)	26.5 ± 5.0	25.1 ± 3.7	25.9 ± 4.2	26.3 ± 5.4	0.45	0.83
Weight (kg)	66.7 ± 13.1	62.4 ± 9.9	67.7 ± 11.2	67.7 ± 14.0	0.21	0.99
HR (bpm)	70.0 ± 11.1	69.2 ± 10.5	70.6 ± .6.9	70.2 ± 12.1	0.78	0.90
SBP (mm Hg)	131.7 ± 20.3	141.2 ± 18.7	133.5 ± 21.3	128.0 ± 19.0	**0.03**	0.38
DBP (mm Hg)	77.6 ± 17.0	83.2 ± 19.0	75.7 ± 19.0	75.2 ± 15.5	0.13	0.92
LVEF (%)	55.5 ± 4.3%	59.8 ± 4.5	62.3 ± 3.5	58.9 ± 4.4	0.52	**0.008**
LVEDVi (mL/m^2)	75.7 ± 10.4	69.7 ± 12.8	78.9 ± 14.6	76.6 ± 8.4	0.09	0.61
LVESVi (mL/m^2)	30.8 ± 5.7	28.2 ± 6.7	29.9 ± 7.4	31.7 ± 5.2	0.11	0.42
Co-morbidities						
Diabetes	2 (3.0%)	2 (15.4%)	1 (7.7%)	0	0.07	0.51
Hypertension	12 (18.2%)	6 (46.2%)	3 (23.1%)	4 (9.1%)	**0.008**	0.38
Hyperlipidemia	7 (10.6%)	4 (30.8%)	3 (23.1%)	2 (4.5%)	**0.028**	0.13
Smoking (current or prior)	14 (21.3%)	4 (30.8%)	2 (15.4%)	16 (20.4%)		0.69
Medications						
ACEI/ARB	10 (15.2%)	5 (38.4%)	3 (23.1%)	3 (6.8%)	**0.015**	0.24
BB	4 (6.1%)	2 (15.4%)	1 (7.7%)	1 (2.3%)	0.25	0.94
Statin	6 (9.1%)	3 (23.1%)	3 (23.1%)	2 (4.5%)	0.13	1.0

Abbreviations; BB - Beta-blocker; ACEI – Angiotensin Converting Enzyme Inhibitor; ARB – Angiotensin Receptor Blocker; BMI – Body Mass Index; DD – Diastolic Dysfunction; DBP – Diastolic Blood Pressure; HR – Heart Rate; NDNS – No-Diastolic-No-Systolic Dysfunction; SBP - Systolic Blood Pressure; SYSD – Systolic Dysfunction.

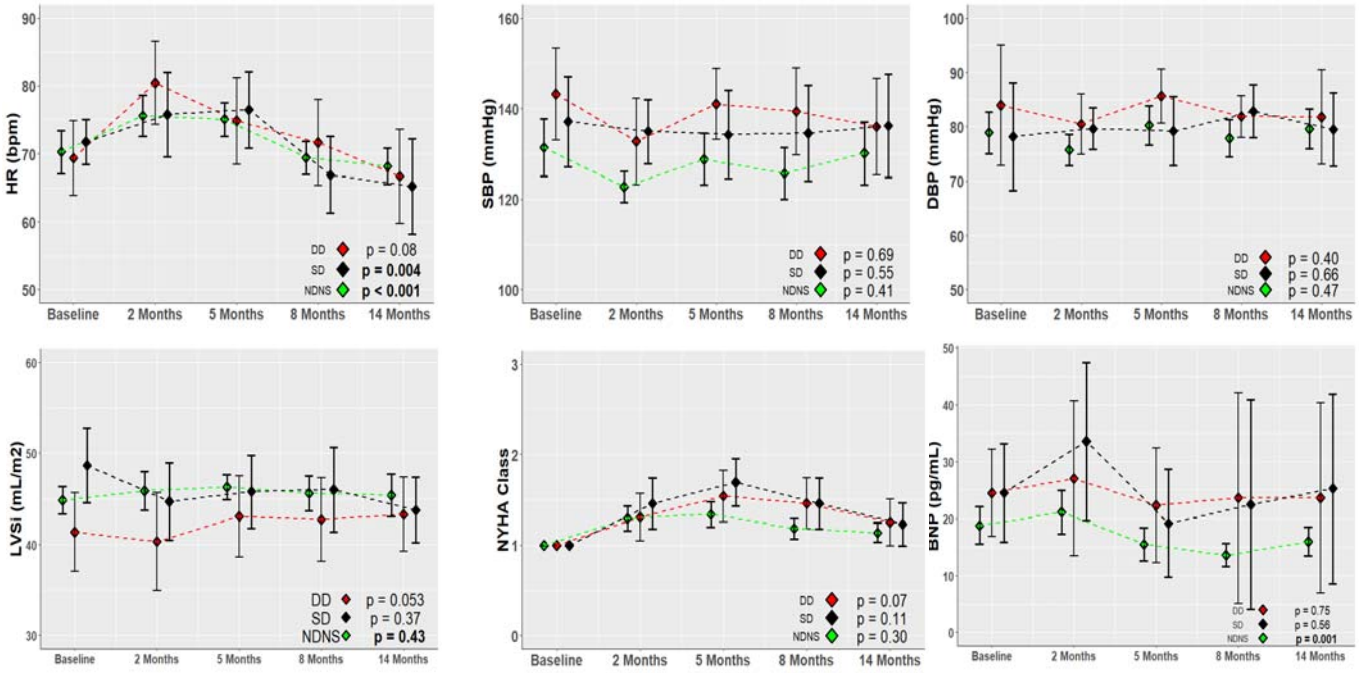

Figure 8-4: Change over time (mean ± SD) for hemodynamic parameters. A) Heart Rate (HR), B) Systolic Blood Pressure (SBP), C) Diastolic Blood Pressure (DBP), D) indexed Left Ventricular Stroke volume (LVSi), E) New York Heart Association (NYHA) dyspnoea class and F) Brain Natriuretic Peptide (BNP). Colour coding: Red for Diastolic dysfunction (DD); Black for systolic Dysfunction (SD); Green for No-diastolic-No-Systolic Dysfunction (NDNS).

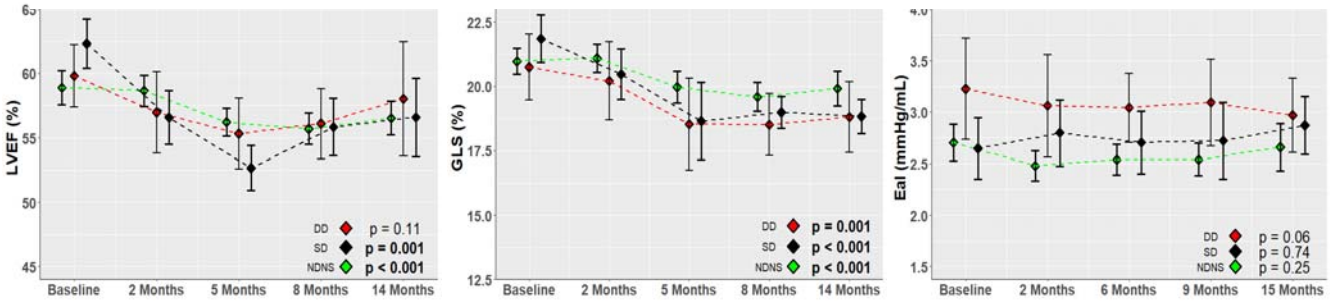

Figure 8-5: Change over time (mean ± SD) for systolic parameters. A) Left Ventricular Ejection Fraction (LVEF), B) Global Longitudinal Strain (GLS) and C) arterial impedance (EaI), an indirect measure if cardiac afterload. Note that GLS has been converted to absolute numbers to facilitate interpretation. Colour coding: Red for Diastolic dysfunction DD; Black for SD; Green for NDNS.

For the entire cohort there was progressive increase in E/A ratio from a baseline value of 1.45±0.48 to 1.62±0.58 at end of treatment (p=0.03) driven primarily by a reduction in A velocity (p=0.01) with no significant change in E velocity(p=0.85)(Figure 8-6). There was also an increase in mean E/e' ratio over study course, from lowest value at baseline of 7.1 ± 1.4 cm/sec to highest value of 7.8 ± 2.4 cm/sec at study end (p=0.003) driven by a progressive decline in both septal and lateral e' velocities. There was no significant change in LAVI. There was however a progressive decline in PDSR (p=0.01) during treatment.

Timeline and Phenotypes of Cardiac Dysfunction

During the study course we identified 3 different cardiac phenotypes in our patient cohort: (1) patients with systolic dysfunction (SD), (2) diastolic dysfunction (DD), and (3) those with no systolic or diastolic dysfunction (NSND). Baseline characteristics and intra-group comparisons are provided in Table 8-2.

Systolic Dysfunction Phenotype

Thirteen patients (19.7%) met criteria for SD; 6 had symptomatic >5% reduction in LVEF to <55% with CHF symptoms and 7 had >10% asymptomatic LVEF reduction to <55%. Median time to diagnosis was 5months (range 2-14 months)(Figure 8-3). By 14 months, 11 patients (84.6%) had incomplete recovery of LVEF values and remaining 2 patients had newly diagnosed SD. At the diagnosis of SD, five patients (38.5%) received heart failure therapy or up-titration of their pre-existing anti-hypertensive therapy, and 2 patients had their trastuzumab held. In the other patients since LVEF was still >50%, Herceptin therapy was continued at the discretion of the oncologist.

At baseline, patients with SD were older and had higher baseline LVEF, but no other significant differences were seen compared to the NDNS subgroup (Table 8-2). There was a significant rise and recovery of HR, but no significant change in SBP, DBP, NYHA class or BNP over time (Figure 8-4). A significant fall in LVEF occurred (p=0.001) with the nadir at 5 months (fall by -9.7 ± 4.7%) followed by

partial recovery by 14 months (Figure 8-5). There was also significant worsening of GLS (change of +3.2 ± 3.0%) with nadir at 5 months with no recovery at 14 months (Figure 8-5).

The SD phenotype displayed a late increase in E/A ratio(p=0.047), primarily driven by a reduction in A velocity, and a gradual, progressive increase in mean E/e' over time(p=0.023) due to reduction in both septal and lateral e' velocities (Figure 8-6). PDSR significantly declined during study duration, with no recovery with completion of trastuzumab (Figure 8-7). There was no significant difference in the change in ECV between baseline and end of treatment between the SD and NDNS phenotype. Comparison of ECV between baseline and 14 months showed a non-significant reduction compared to NDNS and (ΔECV for SD: -1.3±2.9% vs. NDNS: -0.3±2.8%. p = 0.32).

Diastolic Dysfunction Phenotype

Thirteen patients met criteria for DD during treatment, of whom 4 had grade 1 DD and 9 had grade 2 DD with no patients having grade 3 DD (Figure 3). Median time to DD diagnosis was 8 months (range 2-14 months). By 14 months, only 5 patients (38.5%) had incomplete recovery of diastolic function. Eight patients (61.5%) were treated with heart failure or up-titration of anti-hypertensive medications during cancer therapy, at median 9.3 months (range 6.1-21.7 months). Four patients developed concurrent SD, of which 1 patient developed SD 9 months prior to DD, 1 patient developed DD 7 months prior to SD and 2 patients developed SD and DD at same time-point.

Patients with DD phenotype were older than NDNS and SD groups and had higher baseline SBP, were more likely to have a history of hypertension, diabetes or be on ACEI/ARB therapy at baseline (Table 8-2). They also received higher cardiac radiation dose compared to NDNS group. There was no statistically significant change in SBP, but a trend towards increase in HR (p=0.08) and NYHA class over time(p=0.07). Unlike the NDNS phenotype, there was no significant reduction in BNP over time for DD phenotype(p=0.57).

Patients with the DD phenotype had no statistically significant change in LVEF over time (p=0.11) (Figure 8-5). There was, however, a significant worsening of GLS (p=0.001), with nadir at 5 months (change of 2.2±1.7%) with no recovery by 14 months. There was a trend towards reduced EaI (p=0.06)(Figure 4). Patients with DD phenotype demonstrated gradual increase in E/A ratio over time (p=0.035) with peak at 6 months, and gradual rise in E/e' ratio over time (p=0.007) (Figure 8-6). PDSR significantly and progressively declined during study duration, with no recovery at 15 months (p=0.0001). There was no significant change in LAVI over time (p=0.27) (Figure 7). Although the DD group was the only one with an increase in ECV between baseline and 14 months this was not significant compared to NDNS phenotype (ΔECV for DD +1.0±1.7% vs. NDNS, p = 0.29).

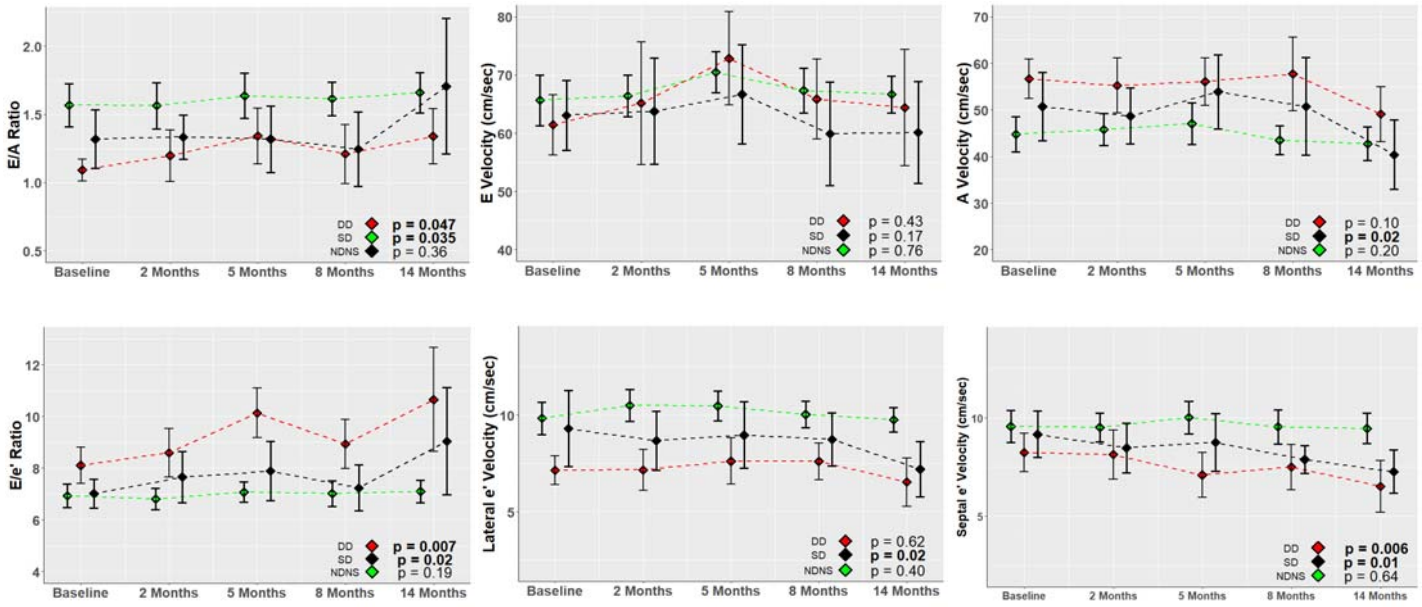

Figure 8-6: Change over time (mean ± SD) for diastolic parameter as measured by phase-contrast CMR. A) E/A ratio, B) E wave peak velocity, C) A wave peak velocity, D) E/e' ratio, E) septal e' velocity and F) lateral e' velocity. Colour coding: Red for Diastolic dysfunction (DD); Black for Systolic Dysfunction (SD); Green for No-Diastolic-No-Systolic dysfunction (NDNS).

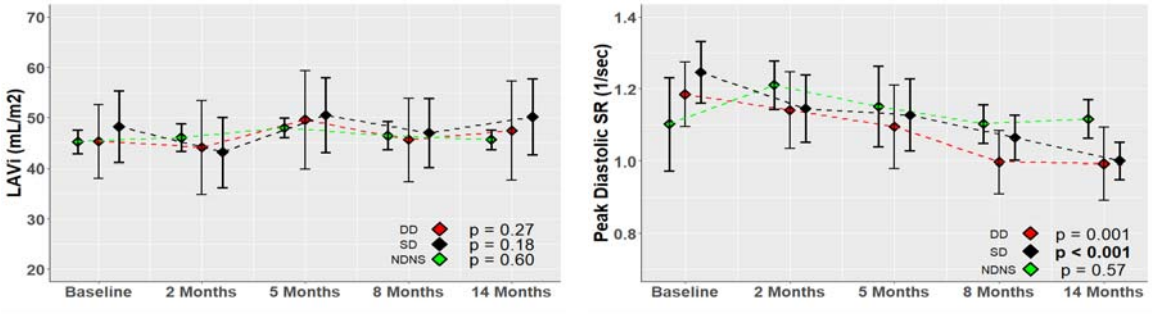

Figure 8-7: Change over time (mean ± SD) for diastolic anatomical parameters. A) Indexed Left Atrial volume (LAVi) and B) Peak Diastolic Strain rate (PDSR). Colour coding: Red for DD; Black for SD; Green for NDNS.

No Systolic or Diastolic Dysfunction Phenotype

There were 44 patients (66.7%) classified into the NSND phenotype. There was a significant rise in HR at 8 months with recovery by the end of treatment (p=0.001), but no significant change in SBP or EaI (Figure 8-4). There was no significant change in NYHA class. There was a significant reduction in BNP from baseline during study duration(p=0.001) (Figure 6).

Even in this group, there was a small but statistically significant fall in LVEF (p<0.0001) with nadir at 8 months ((-3.0 ± 3.6%) with partial recovery at 14 months (Figure 5). There was also a small but statistically significant fall in GLS (p<0.0001), with nadir at 8 months (change of +1.4 ± 1.9%) and no recovery by end of treatment. There was no significant change in E/A ratio, E/e' ratio, septal and lateral e' velocities (Figure 3), LAVI (Figure 6), PDSR (Figure 6), over time.

Discussion

Our results demonstrate that cardiac dysfunction secondary to cancer treatment is a complex phenomenon affecting multiple dimensions of cardiac function, and that using LVEF as the sole measure may cause underestimation of incidence and degree of cardiac injury. Our main findings are that: 1) cardiac dysfunction may be classified as predominantly systolic or diastolic; 2) different baseline characteristics and co-morbidities as well as radiotherapy to the chest has an impact on the phenotype experienced by the patient; 3) the phenotypes exhibit different trajectories, with SD exhibiting earlier onset and greater degree of recovery; ; 4) finally patients who do not meet criteria for SD or DD also have small but statistically significant reduction in LVEF and GLS that remains reduced even at the completion of trastuzumab therapy.

We identified 3 different cardiac function phenotypes can occur with contemporary therapy for breast cancer. Although there are currently no guidelines for monitoring or treating diastolic dysfunction in context of cancer treatment, our results suggest that DD phenotype may have comparable clinical significance to SD, as DD had equal incidence to SD, displayed non-significant trend to increased symptom burden and had cardiac biomarker elevation in comparison to the NDNS phenotype. Both SD

and DD exhibited subclinical systolic and diastolic dysfunction (as evidenced by changes in both systolic and diastolic GLS and PDSR in both phenotypes) that did not show evidence of recovery, suggesting both phenotypes may result in reduced cardiac reserve to future cardiovascular risk factors. However, there were also indications that SD and DD have differences in pathophysiology, as SD exhibited dysfunction primarily secondary to ventricular and atrial cardiomyopathy and DD exhibited milder cardiomyopathy (evidenced by preserved LVEF and lateral e' velocity) with higher baseline left atrial pressures. Given that DD was persistent in a significant proportion of patients at the end of trastuzumab therapy, it is possible that DD phenotype contributes to the long-term heart failure burden in cancer survivors. Additionally, progression of markers of systolic and diastolic dysfunction (e.g. GLS, E/'e) without recovery at study end imply that using LVEF as sole cardiac dysfunction marker may give a false impression of cardiac recovery, and under-appreciation of reduced cardiac reserve. Even the NDNS phenotype had significant reduction in systolic function (evidenced by change in LVEF and GLS) with incomplete recovery at 14 months. This finding suggests that cardiac dysfunction may be a more uniform outcome of EBC therapy than previously appreciated, and current guidelines that diagnose dysfunction in a binary fashion from echo-derived LVEF may inaccurately identify patients at risk of incident HF and lead to missed opportunities for risk factor modification. Long-term studies are warranted to determine the long-term clinical implications of our findings.

Chemotherapeutics can cause cardiomyocyte damage through multiple different pathways and it is plausible that the predominance of certain pathways in susceptible individuals could lead to different clinical phenotypes. Anthracyclines may plausibly cause systolic dysfunction via topoisomerase-2β inhibition and adversely affecting the mitochondrial electron transport chain(261), which may both increase reactive oxygen radical complex (ROC) concentrations. Anthracyclines have also been demonstrated to decouple endothelial nitric oxide synthase from nitric oxide production(262) and inhibit sarcolemmal sodium-calcium exchanger(263), both processes associated with diastolic dysfunction. Additionally, cancer treatment may increase myocardial interstitial fibrosis. Studies of animals treated with anthracyclines have demonstrated 64% increase in extracellular fibrosis by 20 weeks(264), and

increase in ECV has been documented in patients treated for cancer(265). Increased fibrosis may explain the numerically higher ECV values observed in the DD cohort compared to NDNC and SD subgroups, with lack of statistical significance possibly related to the smaller sample size. Prior studies have demonstrated increased incidence of diastolic dysfunction associated with cancer treatment, although these studies are generally published several decades ago, with small groups of subjects and using echocardiography or nuclear imaging. Diastolic dysfunction occurred more commonly by 12 months in older breast cancer patients with more cardiovascular risk factors(266). One study of 125 children treated with anthracyclines found that 20% developed diastolic dysfunction by echocardiography at treatment end,(267) which is an incidence rate similar to our results. Additionally, a cross-sectional study of 1,820 adult survivors of childhood anthracycline or radiotherapy treatment found 8.7% prevalence of diastolic dysfunction at 23 years from diagnosis, which was greater than the prevalence of abnormal LVEF measurements(118), and a population-based case control study of 229 EBC patients demonstrated OR 9.1 (95%CI 3.4-24.4) for incident HF per log mean cardiac radiotherapy dose(253).These findings collectively demonstrate that diastolic dysfunction is a frequent complication of cancer treatment, and support the concept that it may occur in isolation from systolic dysfunction. .

Strengths of our study include prospective recruitment, assessment over multiple timepoints and use of advanced cardiac imaging and biomarkers, however it does also have several limitations. Firstly, current diastolic grading criteria were formulated using data from large echocardiographic registries(125), and the utility of CMR for assessing diastolic function is not as well validated. There are several potential benefits for using CMR to address our primary goal which was to define the cardiac phenotypes in patients receiving cancer therapy. CMR is the gold standard for measuring LVEF(268) which is necessary to differentiate systolic from diastolic dysfunction as well as to understand subtle myocardial abnormalities that may occur in a larger subgroup of patients. Indeed the predominant method of cardiac analysis, 2D-echocardiography, has a 10% temporal variability(150), which means that LVEF decrements of sufficient magnitude for SD diagnosis by 2D-echocardiography may simply reflect measurement error. Although it is possible to perform concomitant CMR and echocardiography, this would be an expensive and labor-

intensive approach. With experienced operators, use of phase-contrast imaging to measure flow and tissue velocity is comparable to that of echocardiography for conventional parameters(258,269,270), and may offer benefits of measuring additional diastolic parameters (e.g. ECV)(271). Additionally, echocardiographic windows can be particularly challenging in breast cancer patients due to surgery and radiotherapy causing soft-tissue fibrosis, and the frequent use of implants(239). For these reasons, the choice of CMR to address our primary question was felt to be ideal. Secondly, published literature on validated normal CMR reference ranges for diastolic dysfunction is lacking, which may reduce confidence in our findings. We agree that further population-based data is needed. However even for echocardiography, reference ranges for diastolic function of cancer patients is lacking, and there are physiological reasons to believe that cut-offs based predominantly on data from populations of older hypertensive patients may not be transferable to our cohort. We therefore felt that creating reference ranges using a cohort of healthy volunteers was reasonable. Thirdly we acknowledge that the assessment of dyspnea aetiology in cancer patients is challenging(272), and cannot exclude the possibility of noncardiac dyspnea being incorrectly attributed to cardiac causes. However, all patients were reviewed at each timepoint by an experienced clinician within a dedicated cardio-oncology program, and our practice for diagnosing cancer-related cardiac dysfunction reflects current guidelines.

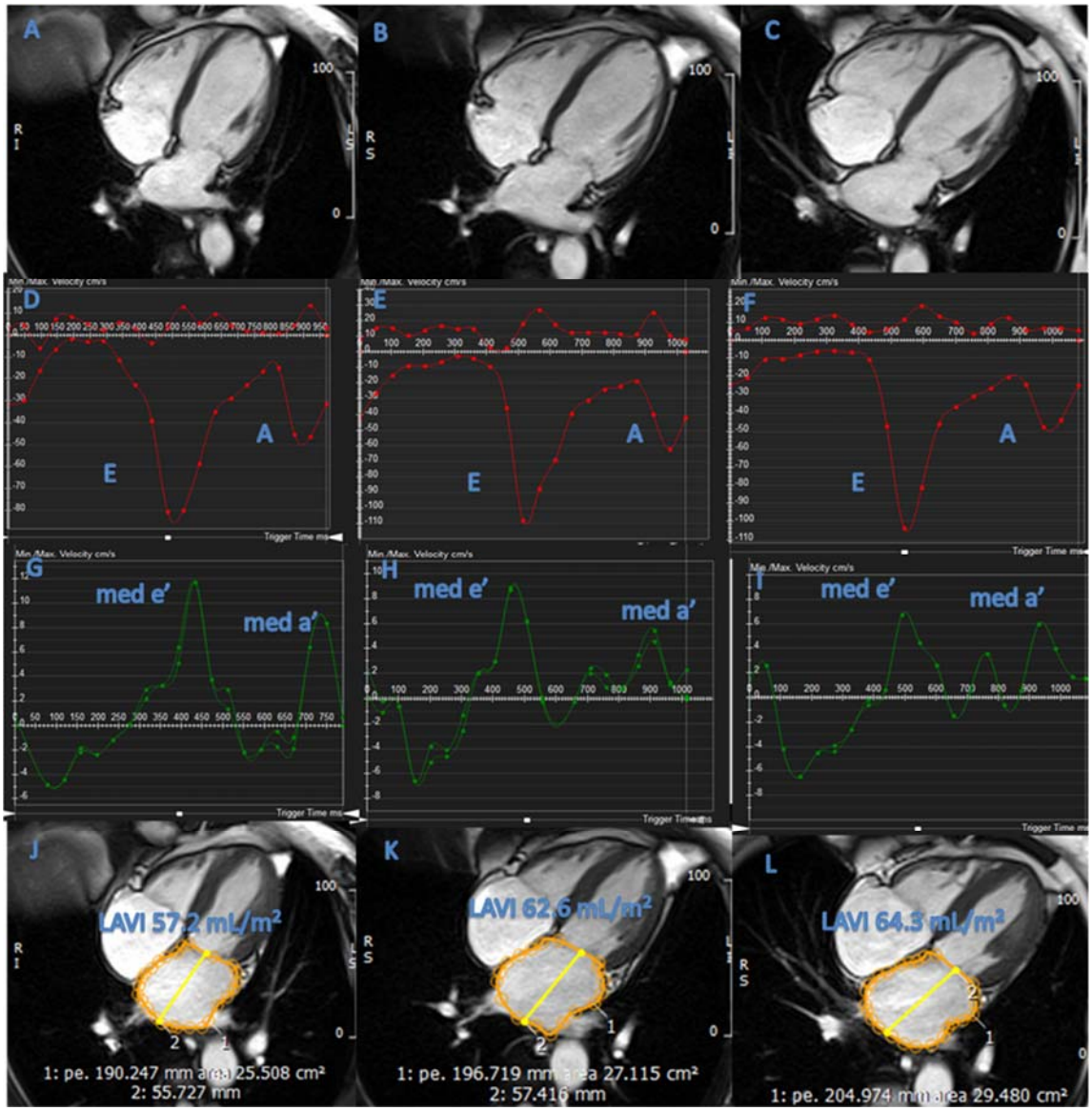

Figure 8-8: Case example of a patient experiencing isolated, progressive diastolic dysfunction during course of breast cancer treatment. Patient was a 57 year-old woman with no cardiovascular risk factors. She received 226 cGy of cardiac radiation. She developed NYHA II dyspnea between 3 and 6 months from baseline. **A)** At baseline her LV volumes were normal, which did not significantly change at end of anthracycline treatment (**B**) or end of trastuzumab therapy (**C**). Her E/A ratio increased from 1.24 at baseline (**D**) to 1.75 (**E**) and finally to 2.2 at final measurement (**F**). This was associated with decline in her medial e' velocity (**G-I**), with E/'e increasing from 7.4 at baseline, to 10.9 at 3 months and to 13.9 at 14 months. Her LAVI increased from upper range of normal (**J**) to mildly dilated **(K-L**). These changes correspond to clinical progression from normal diastolic function to grade 2 diastolic dysfunction, and finally grade

We believe that our study is the first to use CMR to prospectively identify different phenotypes of cancer-therapy-induced cardiac dysfunction. The long-term significance of these findings is undetermined, and further studies to determine the clinical course of this subgroup are warranted.

Conclusion

Cardiac dysfunction is common after EBC therapy and can be described by three phenotypes which are characterized by different baseline characteristics, non-invasive imaging findings and different degrees of recovery of cardiac function. Long-term studies are indicated to determine the prognostic significance of each phenotype.

Postscript

This chapter thesis has demonstrated that cardiac damage from cancer treatments does not fit neatly into a binary categorization based on a single cardiac imaging metric, but rather manifests as disturbance along multiple axes of heart function with individual variations in degree of derangement across each axis. This finding is likely to have future clinical relevance, as clinical trials for potential HFpEF treatments near completion. It also demonstrated that even patients who did not meet current guideline criteria for either systolic or diastolic dysfunction had subclinical dysfunction and lends to support to recommendations for long-term monitoring in this at-risk population.

The end of this thesis section concludes the clinical studies that are designed to provide guidance for practicing healthcare professionals. To date, this thesis has 1) identified potential harms of anti-cancer treatments and confirmed the clinical importance of these conditions, 2) confirmed that these harms can be either short-term or long-term and can occur in survivors of either adult or childhood cancer, 3) demonstrated that contemporary practice for monitoring for these harms are likely suboptimal in Australian hospitals, 4) shown that echocardiography-guided approach is likely superior to MUGA-guided approach for monitoring cancer patients, 5) provided evidence that automation is a viable strategy

for improving utility of echocardiography in the cancer population, 6) demonstrated that in the majority of cases reduced LVEF measurements in cancer patients are truly secondary to decreased contractility in the context of cardiomyocyte damage and 7) demonstrated that cardiac dysfunction manifests as variable phenotypes which are under-appreciated in current guidelines.

The rationale for this thesis was to provide a guide for use of cardiac imaging in Australia to reduce the burden of CTRCD. Current guidelines(104) have been equivocal regarding the optimal imaging modality, do not make specific suggestions to improve accuracy of the most commonly used modalities and do not make recommendations for cardiac measurements beyond LVEF. Partially as a result, the potential of collaboration between cardiologists and oncologists has not to date been made a reality. Therefore we hope this thesis makes a significant contribution that may translate to improved cardiovascular outcomes for cancer survivors.

The challenge of utilizing beneficial cardiac imaging strategies is not solely due to physician preference. Widespread changes in the practice of imaging cancer patients would require significant diversion of resources. These changes would not occur in a vacuum, as there is competition for finite resources within the Australian healthcare system, and the gatekeepers for funding are usually elected public officials. The final chapter of this thesis will examine the issue of whether resource investment for cardiac imaging of cancer patients is likely to provide benefits on a societal level

Chapter 9

Cost-Effectiveness of Strain-Guided Echocardiographic Strategy

Part of the research in this chapter has been published(273) as:

- Nolan MT, Plana JC, Thavendiranathan P, Shaw L, Si L, Marwick TH. Cost-Effectiveness of Strain-Guided Cardioprotection For Prevention of Chemotherapy-Induced Cardiotoxicity. *Int J Cardiol* 2016; 212: 336-45

Preface

It has been the aim of this thesis to provide a vision for and proposed template for utilizing the most effective cardiac imaging strategy to decrease the burden of heart failure in the Australian cancer survivor population. To achieve this, each of the sections to date has focused on one dimension of the heart damage secondary to cancer treatment; the first section demonstrated the scope of the issue and the brought attention to the unmet clinical need for improved services to reduce cardiotoxicity; the second section assessed first-line imaging modalities to determine the most appropriate technique and the third section assessed advanced second line techniques to provide greater understanding of pathophysiology underlying cardiotoxicity and to guide treatment in complex cases. Together these sections provide guidance at the physician level for preventing cardiotoxicity. But imaging decisions are not made by physicians in a vacuum, as there are issues of access, cost subsidization and insurance coverage that require policy changes at the higher levels of political and corporate leadership. The healthcare professionals in these fields have a duty of care to a population as a whole rather than to individual patients and a responsibility to manage finite societal resources, and therefore they require an evidence base that simultaneously measures the potential improvement in quality and quantity of life and resource cost of their decisions. The final section of this thesis will examine whether there is evidence that using the imaging strategy described will lead to significant cost and health savings at a societal level.

Abstract

Background: Cancer chemotherapy increases the risk of heart failure. This cost-effectiveness model compared strain-guided cardioprotection with other protective strategies using a health care payer perspective and five-year time horizon.

Methods: Three cardioprotection strategies were assessed: 1) Usual care (EF-guided cardioprotection, EFGCP) with cardioprotection initiated on diagnosis of LVEF-defined cardiotoxicity (EF-CTX), 2) Universal cardioprotection (UCP) for all such patients, 3) strain-guided cardioprotection (SGCP - treatment of patients with subclinical cardiotoxicity [S-CTX]). A Markov model, informed by the published literature on transitional probabilities, costs and quality-adjusted life years (QALYs) was developed to assess the incremental cost-effectiveness ratio (ICER). Costs, effects and ICER of each specified cardioprotective strategy were assessed over a 5-year range, with sensitivity analyses for significant variables.

Results: In the reference case of a 49 year-old woman with stage IIb breast cancer treated with sequential anthracyclines and trastuzumab, strain-guided cardioprotection (3.79 QALYS and $4159 cost over 5 years) dominated both UCP (3.64 QALYs and $5967 cost over 5 years) and EFGCP (3.53 QALYs and $7033 cost over five year). Model results were dependent on the probabilities of patients developing subclinical LV dysfunction, with UCP dominating alternative strategies at probabilities ≥51%. Variations in the cost of cardioprotective medications and probabilities of cardioprotection side-effects had no effect on model conclusions.

Conclusions: In patients at risk of chemotherapy-related cardiotoxicity, strain-guided cardioprotection provides more QALYs at lower cost than standard care or uniform cardioprotection.

Introduction

Advances in cancer management over recent decades have led to an increasing proportion of cancer survivors. Chemotherapy and radiotherapy (especially in combination) are associated with cardiac dysfunction in up to 26% of treated patients by six months(50) and symptomatic heart failure in up to 20% at 5 years(146) depending on the dose and type of chemotherapy. Heart failure in this setting has a two-year mortality of up to 50%(7). The current standard of care involves regular monitoring of left ventricular ejection fraction (LVEF), with initiation of heart failure medications once LVEF drops to the point when cardiotoxicity (conventionally defined as an asymptomatic drop of LVEF by ≥10% to final value of <55% or a symptomatic drop of LVEF by ≥5% to final value of <55%) is diagnosed(245). This LVEF-guided definition of cardiotoxicity (EF-CTX) is a late stage of progressive myocardial functional impairment initiated at the time of cardiac insult(137). An alternative strategy, based on a small randomised controlled trial of pre-emptive treatment of all patients with maximum tolerated doses of enalapril and carvedilol at the time of chemotherapy, has been demonstrated to reduce the incidence of cardiotoxicity and symptomatic heart failure compared with a control group(52). The disadvantage of this approach is that most treated patients do not develop EF-CTX or symptomatic heart failure and would have unnecessarily been exposed to the potential side-effects and cost of medications.

A third strategy would be to use a highly sensitive test to identify high-risk subgroups within the chemotherapy-treated population, and initiate cardioprotection only in these patients. This could provide the health benefits of cardioprotection while minimizing unnecessary medication costs and side-effects. Global longitudinal strain (GLS) derived from speckle-tracking echocardiography is a novel non-invasive imaging technique that quantitatively measures regional myocardial deformation, a sensitive marker of myocardial function. Strain has been demonstrated to accurately predict development of cardiotoxicity(137,274) and can identify early pathological changes in myocardial systolic function before any appreciable decline in LVEF becomes apparent. This stage of subclinical cardiotoxicity (S-CTX) identifies a population at high risk of EF-CTX and symptomatic heart failure and may represent an attractive

opportunity for targeted cardioprotection (CP). No randomized trial has compared these options, so we developed a Markov model to incorporate probabilities and risks of three cardioprotection strategies to determine the costs and quality-adjusted life-years (QALYs) obtained by each strategy in patients treated with potentially cardiotoxic chemotherapy.

Methods

Model design. This decision-analytic model evaluated the morbidity, mortality, and costs inherent in three clinically-relevant strategies; 1) the current standard strategy of initiating cardioprotection medications after diagnosis of EF-CTX (diagnosed as an asymptomatic decline in LVEF by >10% to value of <55%) or symptomatic heart failure, 2) a strategy of uniform cardioprotection (UCP) for all patients at the time of chemotherapy, and a 3) a strategy of using S-CTX (defined as a decline in global longitudinal strain (GLS) of ≥11% from baseline by 3 months post chemotherapy-initiation) to commence cardioprotection treatment. Cardioprotection was defined as concurrent enalapril and carvedilol up-titrated to their maximum dose, as used in the active treatment arm of a large recent randomised controlled trial(52), and used throughout the 5-years of modelling. Correction factors for time lapsing were used if cardioprotection was commenced after echocardiographic or clinical findings. This Markov model used Monte Carlo simulations (TreeAge Software Inc. Williamtown, MA), to assess the clinical and economic consequences of alternative strategies of using cardioprotective strategies in a hypothetical cohort of 10,000 patients in a micro-simulation model without tracker variables. Beta distributions were assigned to probabilities and utilities, and gamma distributions for costs based on standard errors derived from the associated literature. Means and 95% credible intervals (95% CI) were computed on the basis of 10,000 micro-simulations. Cost-effectiveness acceptability curves (CEACs, a method to quantify and graphically represent uncertainty in economic evaluation studies of health-care technologies) were used to report the probability that the ICER for an intervention was below the predefined willingness to pay threshold. This study was performed in

accordance with the Consolidated Health Economic Evaluation Reporting Standards (CHEERS) guidelines, as detailed by the International Society for Pharmacoeconomics and Outcomes Research (ISPOR).

We estimated costs and benefits of the interventions (deaths averted and quality-adjusted life-years [QALYs] gained) over a 5-year period of the cohort, because transition probabilities beyond this period are not currently well-described. We assumed that all interventions took place at the start of the time horizon, and discounted all future costs and benefits by 3% per annum. Cycle length is the time-frame of transition from one state to the next, during which period all information is held constant. For the purposes of this analysis, cycle length was assumed to be 1 year.

Decision tree. The Markov model (Figure 1) accounted for the dynamics of cardiac screening and utilization of cardioprotective medications in a cohort of 10,000 patients scheduled to receive chemotherapy for cancer. The base case (a 49 year-old woman with stage II breast cancer receiving sequential anthracycline and trastuzumab therapy) was applied to all cohort patients. At commencement of the time horizon, this hypothetical individual was assigned to one of the three screening strategies. These patients progressed through the Markov model on the basis of transition probabilities.

The model was intended to capture the high-level costs and effectiveness of screening and treating a large cohort. In sensitivity analysis, we considered a range of values reported in scientific literature for transition probabilities, costs and utilities. Where data were available, low and high values were chosen to reflect ranges in the literature. The model structure was based in part on other models in the literature and was reviewed by clinicians involved in the care of cancer patients and chemotherapy-related cardiotoxicity.

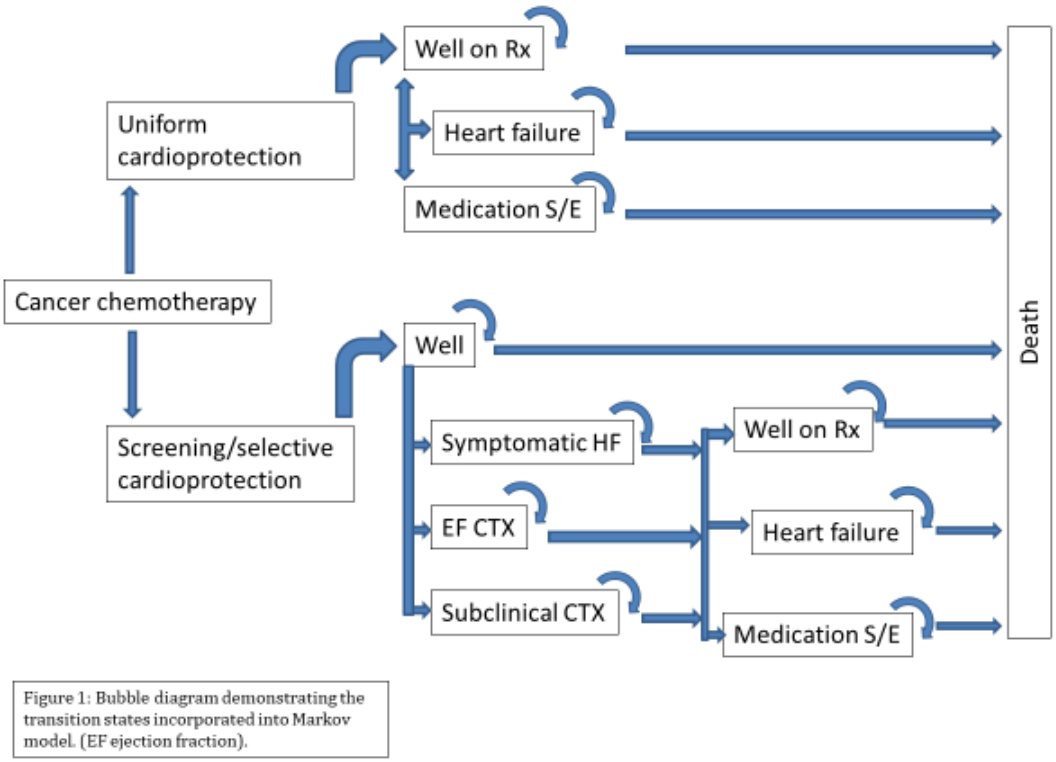

Figure 1: Bubble diagram demonstrating the transition states incorporated into Markov model. (EF ejection fraction).

Figure 9-1: Bubble diagram demonstrating the transition states incorporated into Markov model.

Health states and transitions. Data on transitions between health states were obtained from the literature and expert sources (Table 9-1);

The *asymptomatic post-chemotherapy* state described patients without any cardiac symptoms or apparent structural changes on cardiac imaging.

Asymptomatic cardiotoxicity (referred to in this study as EF-CTX) was identified in patients with a ≥10% asymptomatic drop of LVEF.

Subclinical LV dysfunction (referred to in this study as S-CTX) was diagnosed in patients without EF changes but with a ≥11% reduction of GLS.

Other health states were *heart failure* and *death.* The background mortality rate was calculated from USA life tables specific to the base case of breast cancer or scenario analyses of other cancers (www.cdc.gov/nchs/products).

Transition probabilities were separated into the categories of initial year of treatment, and for subsequent years. Further details regarding mortality in each health state is provided in the next section.

Costs. We conducted our economic analysis from the perspective of the healthcare payer and therefore used the amount reimbursed to the provider as the cost of care. Information regarding costs was obtained primarily from the literature, including diagnostic related groups (DRGs), Medicare payments for current procedural terminology (CPT) codes and discounted drug prices (Table 3). LVEF-guided echocardiographic screening costs were calculated by taking the CPT reimbursement cost and assuming a regimen of five echocardiographic studies (baseline and 3-monthly in the first year only). Strain-guided echocardiographic screening costs were calculated using the same CPT cost(275), but assuming the performance of monthly echocardiographic studies in the first year – which is the maximum that might be anticipated with trastuzumab therapy after anthracyclines. Medication costs were obtained from the Walmart Retail Prescription program drug list(276). Costs of routine biochemical or haematological screening for medication side-9-effects were not included as it was considered likely that patients receiving

chemotherapy would receive regular investigations regardless of whether they received cardioprotective medications. Costs were expressed to 2015 US$ and a willingness to pay threshold of $53,000 per QALY was applied, as this represents the 2015 average annual gross domestic product (GDP) of the US and a national GDP value per capita has been suggested by the World Health Organization to represent how much a nation can reasonably be spend to save each QALY(277). The costs published in the literature more than two years earlier were corrected for intervening currency fluctuations using a commercial past currency converter (www.fxtop.com/en/currency-converter-past.php).

Health outcomes. Information regarding health outcomes was obtained from searches linking health states with the words "utility" and "quality of life" (QOL). Table 9-1 lists the findings for utilities (values obtained from preferences associated with health-related quality of life where full health = 1.0 and dead = 0.0).

Sensitivity analysis. Critical sources of variation in the input data were gathered by one-way sensitivity analyses, varying each input factor by its standard error. A threshold analysis was performed on the most influential factors to identify the point where the additional cost per QALY was <$53,000. The Net Monetary Benefit (NMB) was defined as the difference between the gain in QALYs and the ratio between the willingness to pay threshold and the difference in cost. Because of concerns regarding model sensitivity to synergistic influences of cardioprotective side-effects on costs and health-state utilities (as these represent the only trade-offs for uniform use), these transition probabilities were subject to two-way sensitivity analyses.

Scenario analysis. To determine the applicability of cost-effectiveness of cardioprotective strategies for high-risk cancer patient subgroups other than breast cancer, two additional scenario analyses were run using the same Markov model. The first scenario utilized a reference case of a 50 year-old man with stage III non-Hodgkin's lymphoma and a low-to-intermediate International Prognostic Index score. The second scenario utilized a reference case of a 48 year-old man with acute myeloid leukaemia. Both cases involved treatment with anthracyclines. Transition probabilities and mortality rates were utilized from published

literature and transition probabilities of significant GLS drop were utilized from subgroups of trials (see Online Appendix 1).

Internal model validation: Markov model validation was performed as advised by ISPOR guidelines(278). In the base case analysis, distributions were sampled 100 times, and after each sample, 1000 trials were run using values drawn from each sample in order to calculate the mean costs and effectiveness. For internal validity, we compared the life-expectancy generated by our Markov model with life-expectancy of non-metastatic breast cancer patients with clinical characteristics as our base case reported in the US Surveillance, Epidemiology and End Results (SEER) database of the National Cancer Institute. Goodness of fit was predicted by plotting model predictions versus SEER database observed data and fitting a linear curve through points with an intercept of zero. The squared linear correlation coefficient (R^2), obtained using linear regression, was used as an index of association. External validation was not performed, due to insufficient studies which were not included in the Markov model construction.

Results

Health outcomes and costs. In the reference case (49 year old woman taking anthracycline and trastuzumab for breast cancer, annual cost of cardioprotective medication of $81 with 56% probability of medication side-effects, leading to 38% overall abandoning cardioprotection), the outcomes of SGCP (3.73±0.87 QALYs, $4161±$3997 over 5 years) were superior to those of UCP (3.64±0.75 QALYs, $5,753±$5840) and EFGCP (3.53±0.86 QALYs, $6820±$6450). Both UCP and EFGCP were dominated by SGCP strategy.

Sensitivity analyses. One-way sensitivity analyses were performed over a clinically plausible range for all variables. The impact of these variations on health outcomes is depicted in a tornado diagram (Figure 2). This sensitivity analysis revealed that the variables that had the largest impact on model outcomes were probability and utility of S-CTX, medication side-effects and cost of managing those side-effects.

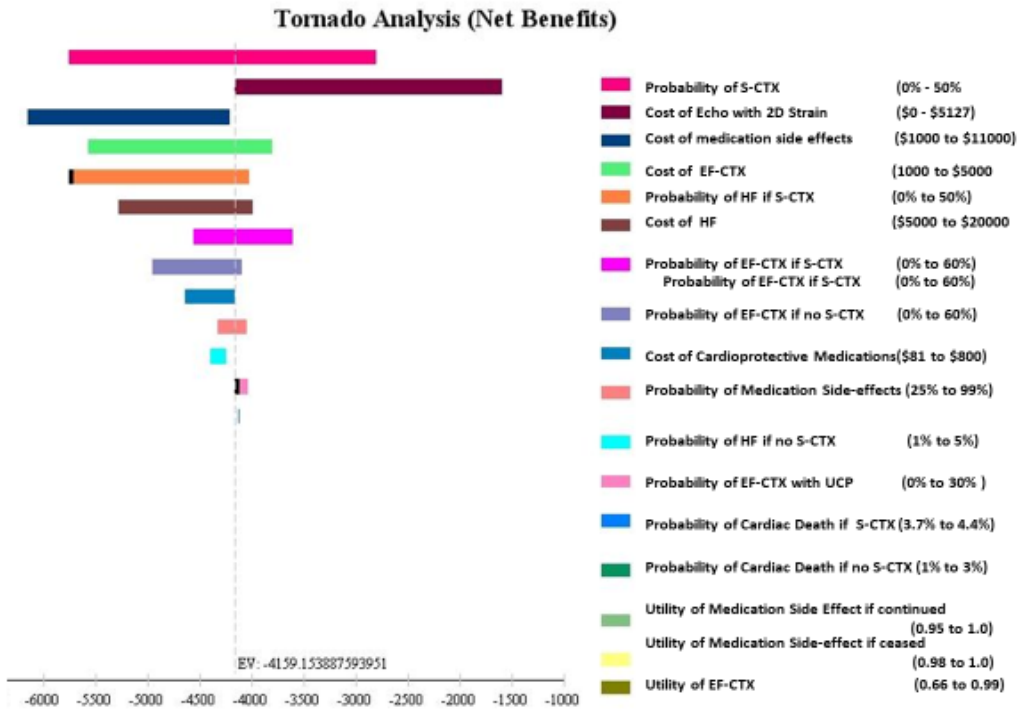

Figure 9-2: Tornado diagram demonstrating influence of cost, utilities and transition probabilities on expected value, assuming a willingness-to-pay value of US$53,000. EF-CTX –cardiotoxicity with reduced ejection-fraction, HF – symptomatic heart failure, S-CTX – subclinical cardiotoxicity, UCP – uniform cardioprotection

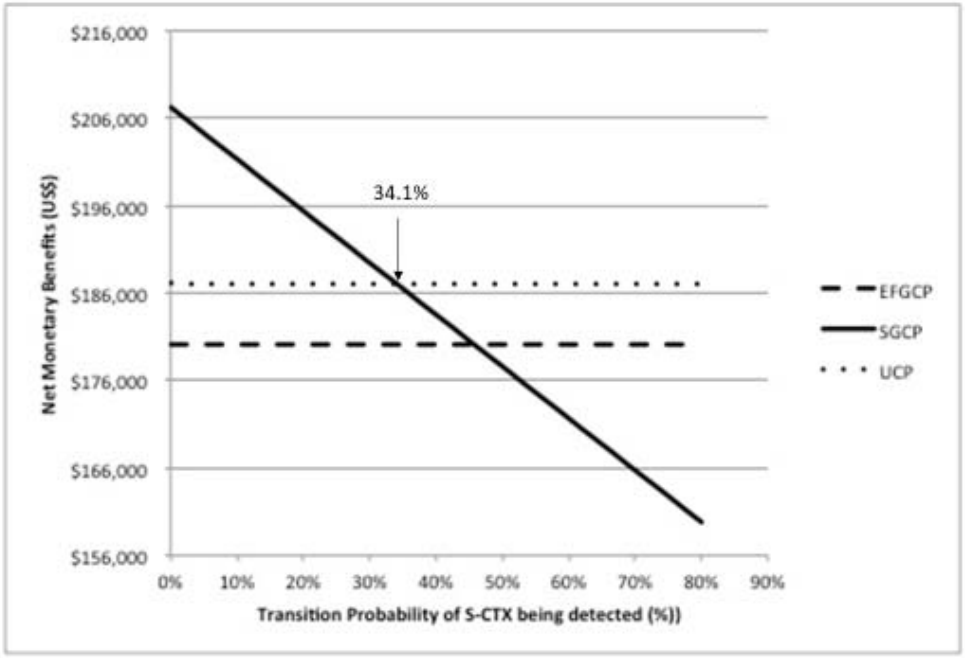

Figure 9-3: One-way sensitivity analysis evaluating net monetary benefits (NMB) across a range of transition probabilities of patients having detectable subclinical cardiotoxicity when utilizing a strain-guided strategy (SGCP). A willingness-to-pay threshold of $53,000 was assumed. At probability values higher than 34.1%, uniform cardioprotection (UCP) yielded higher NMB than SGCP.

One-way sensitivity analysis of probability of a decrease in GLS revealed a strong impact on model's conclusions (Figure 3). At S-CTX transition probabilities of ≤34%, SGCP dominated alternative strategies. Above these transition probabilities, UCP delivered higher net monetary benefits. EFGCP did not provide superior benefits at any level of transition probability.

The impact of parameter uncertainty in the frequency of side-effects and the cost of side-effects was explored further in an additional sensitivity analysis across the plausible range of the frequency and cost of side-effect and showed that SGCP dominated both UCP and EFGCP throughout the plausible ranges of medication side-effects transition probabilities and costs. An additional sensitivity analysis revealed SGCP strategy remained below the willingness-to-pay threshold throughout a range of plausible EF-CTX transition probabilities.

Monte Carlo simulation. The impact of parameter uncertainty in the frequency of transition probabilities, utilities and costs were examined using a Monte Carlo analysis with 10,000 simulations. This demonstrated that SGCP was the optimal strategy, with a mean survival of 4.66 years with SGCP, 4.56 years with UCP and 4.48 years with LVGCP.

A cost-effectiveness acceptability curve (Figure 5) demonstrated that strain-guided strategy was consistently the most cost-effective strategy across a broad plausible range of willingness-to-pay thresholds (from $0 to $100,000 per annum). An incremental cost-effectiveness scatterplot of results of 1000 pairs of differences in costs and QALYs shows that both SGCP (Figure 6a) and UCP (Figure 6b) are more cost-effective than the current standard of care (EFGCP). The comparison between SGCP and UCP (Figure 6c) does not show clear benefit for either approach, with SGCP being more cost-effective in 56% of instances.

Scenario analysis: In a scenario analysis examining the cost-effectiveness of imaging-guided CP strategies in haematological malignancies, the index case consisted of a 50 year-old man with stage III non-Hodgkin's lymphoma. Transition probabilities were altered to reflect the higher incidences of cardiovascular complications (Online Appendix 1) due to more aggressive chemotherapeutic regimens. The most

significant change consisted of increase of cardiotoxicity in absence of CP from 20% to 36%. An incremental increase in costs and QALYs gained with SGCP (ICER $18,264 per QALY gained) with overall higher costs and lower QALY per strategy was seen than with breast cancer reference case (over a five-year period, SGCP 3.49±0.72 QALYs, $23,012±31,611; UCP 3.24±1.45 QALYs, $18,400±27,538; EFGCP 3.15±0.89 QALYs, $27,537±25,528). These findings are broadly similar to those of the base case of the main study with the ICER for SGCP falling below WTP threshold. The second index case, a 45 year-old man with acute myeloid leukaemia, demonstrated extended dominance by UCP over both alternative strategies (over a five-year period, UCP 2.97±1.07 QALYs, $26,458±22,941; SGCP 2.87±1.29, $48,997±30,992; EFGCP 2.86±1.10 QALYs, $31,114±31,092). There was no clinically significant difference in QALYs gained between SGCP and EFGCP in this scenario.

Model validation: The results generated by the model closely match the input data from which the input probabilities were derived: the linear regression slope was close to 1 (1.04, $p<0.001$), and the adjusted R^2 was 0.9993 ($p<0.001$), demonstrating that the model faithfully reproduced the published data. For the first scenario analysis, the linear regression slope was 2.71, and adjusted R^2 was 0.9559 ($p<0.001$). For the second scenario analysis, linear regression slope was 1.41, and adjusted R^2 was 0.9376. This suggests good model approximation to observed life expectancy in studies utilised for the model.

Discussion

In this analysis of the cost-effectiveness of three strategies for targeting cardioprotective medications for the prevention of chemotherapy-related cardiomyopathy, global longitudinal strain provided additional QALYs at lesser cost compared with UCP and LVGCP. SGCP also produced the highest value of 5-year survival and was the optimal strategy in the majority of Monte Carlo simulations. The increased 5-year survival reflects the high mortality burden of heart failure, even small reductions in incidence of heart failure complicating chemotherapy can affect population survival rates. Sensitivity analyses demonstrated

that cost-effectiveness was highly dependent on probability of reduced GLS. Scenario analyses revealed similar findings for an index case of non-Hodgkin's lymphoma, but UCP was found to dominate both alternative strategies in the case of acute myeloid leukaemia. This is likely due to the higher incidence of reported cardiotoxicity and heart failure due to more aggressive chemotherapeutic regimens, which would lead to greater clinical benefit from a UCP approach. The conclusions of the model were robust when tested with sensitivity analyses, with a change in conclusions only if the cardiotoxicity incidence and cost of cardioprotective side-effects increased.

Cardiotoxicity from cancer chemotherapy Both European and US cardiovascular society guidelines recognize the need to monitor and manage this patient subgroup(176) although they do not make specific recommendations regarding strategies for targeting therapy. The large population at risk of chemotherapy-related cardiomyopathy, the time difference between chemotherapy and onset of cardiomyopathy symptoms and the high morbidity and mortality associated with the condition suggest that the financial and health burden that it places on society is likely underestimated, and a cost-effective method of decreasing its incidence could translate into tangible and wide-reaching benefits for healthcare systems as a whole. Specialized cardio-oncology clinics have been created in many countries in recognition of the special cardiovascular challenges of cancer survivors, and this analysis adds to the growing published literature, showing that promoting optimal cardio-oncology practice can provide both health and cost benefits.

Strain-guided management. The adoption of strain guided therapy places little financial burden on the healthcare system, as it requires only an update in echocardiography software and a modest time investment in training for sonographers and cardiologists. This training would likely have additional benefits in a cardiology practice, as 2D strain echocardiography has shown clinical benefit in diagnosis and prognosis of many cardiac diseases.

As the majority of costs in the models relate to managing chemotherapy-related cardiovascular complications arising either from HF, or alternatively managing predictable side-effects of medications, a method of minimizing HF by treating the smallest possible at-risk group could be expected to be optimal.

Strain identifies a population with subclinical dysfunction who are at-risk of overt CTX, thereby targeting patients most likely to benefit from cardioprotection. The current strategy of EFGCP does not represent an effective use of healthcare resources, as therapy is targeted towards an advanced disease subgroup in which up to 58% of patients may not respond(22). In contrast, sensitivity analysis showed that the cost-effectiveness of SGCP remained below the conservative willingness-to-pay threshold of $53,000 even if the transition probability of cardiotoxicity was equal or higher than 45%.

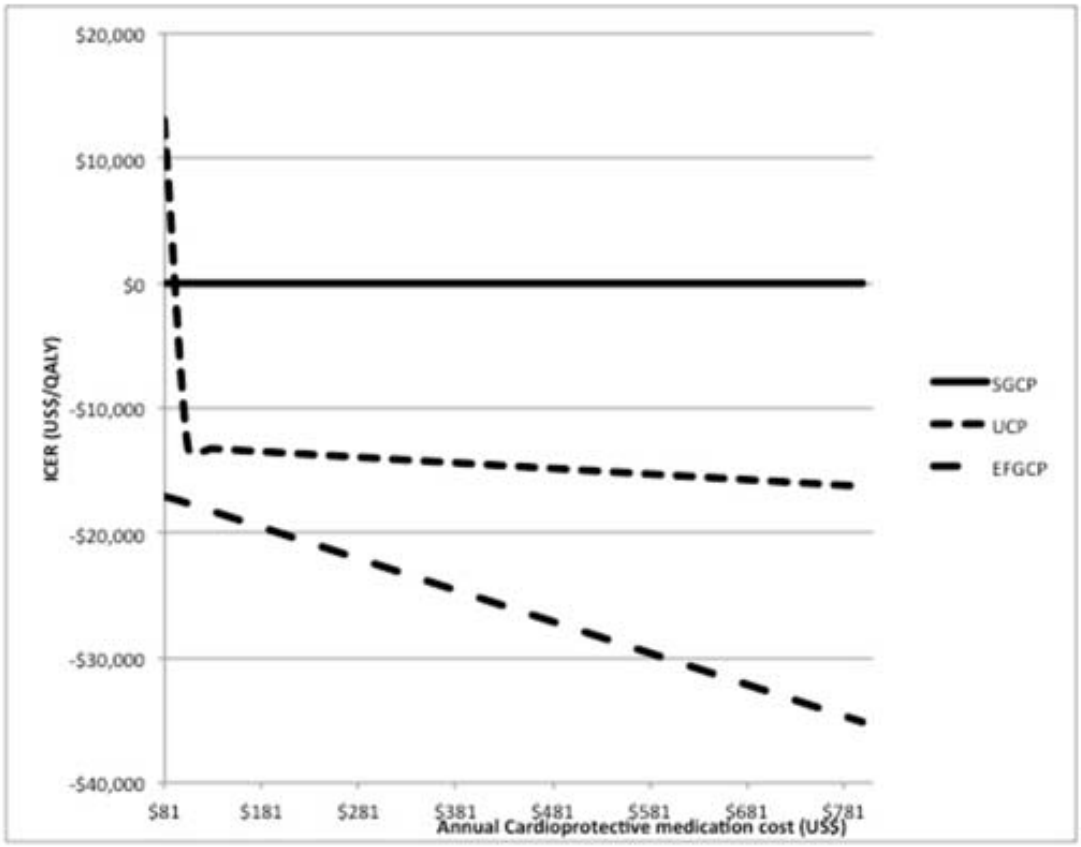

Figure 4: One-way sensitivity analysis evaluating incremental cost-effectiveness across a broad range of plausible annual medication costs.

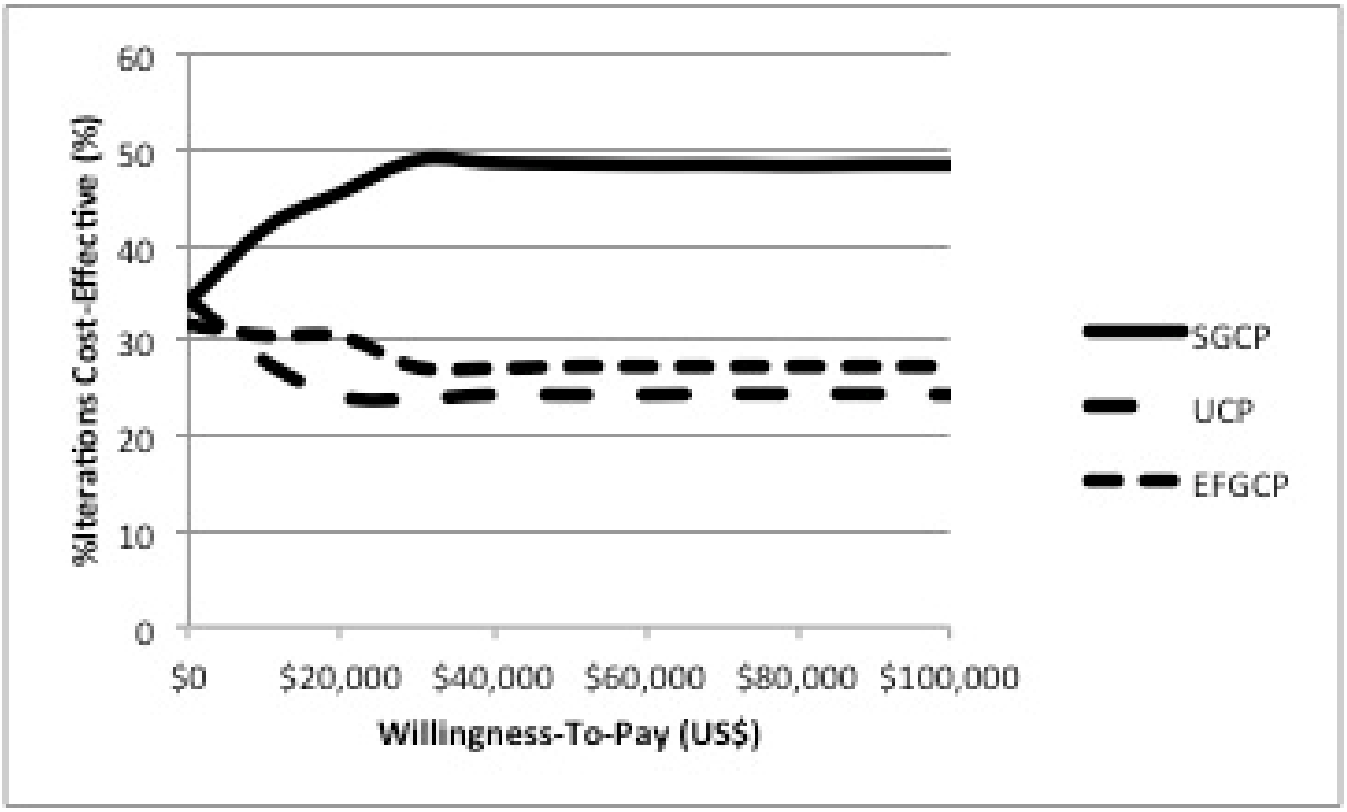

Figure 9-5: Cost-effectiveness acceptability curve representing the probability that each treatment strategy is cost-effective for a given maximum willingness-to-pay threshold per QALY gained. The graph is based on 10,000 Monte Carlo simulations, drawing parameters for each input from probability distributions

Figure 6: Incremental cost-effectiveness boot strap scatterplot. The y-axis represents the difference in mean costs (2015 US$) between strain-guided therapy and uniform therapy strategies, and the y-axis represents the difference in mean QALYs. Quadrant 1 represents iterations for which new strategy is more expensive and less efficacious (i.e. inferior) than its comparator. Quadrant 2 represents iterations for which the new strategy provides additional QALYs at additional cost (cases below the willingness-to-pay (WTP) line represent iterations where this additional cost is deemed desirable. Quadrant 3 represents iterations where the new strategy is less expensive and less efficacious than the comparator. Quadrant 4 represents iterations where new strategy was less expensive and more efficacious (i.e. superior). The ellipse represents the region containing 95% of iterations.

A) Strain-guided cardioprotection strategy **(**SGCP) vs ejection-fraction guided cardioprotection strategy (EFGCP). 94.9% of iterations were either superior (15.1% of iterations) or provided additional QALYs at additional cost that was less than WTP (79.8%).

B) Uniform cardioprotection (UCP) vs. ejection-fraction guided cardioprotection (EFGCP). In 88.4% of iterations, UCP provided additional QALYs at additional cost but remained below the WTP threshold.

C) SGCP vs UCP. In 55.9% of iterations, the SGCP strategy yielded either higher QALYs at lower cost (39%) or at additional cost that was below WTP (21.2%).

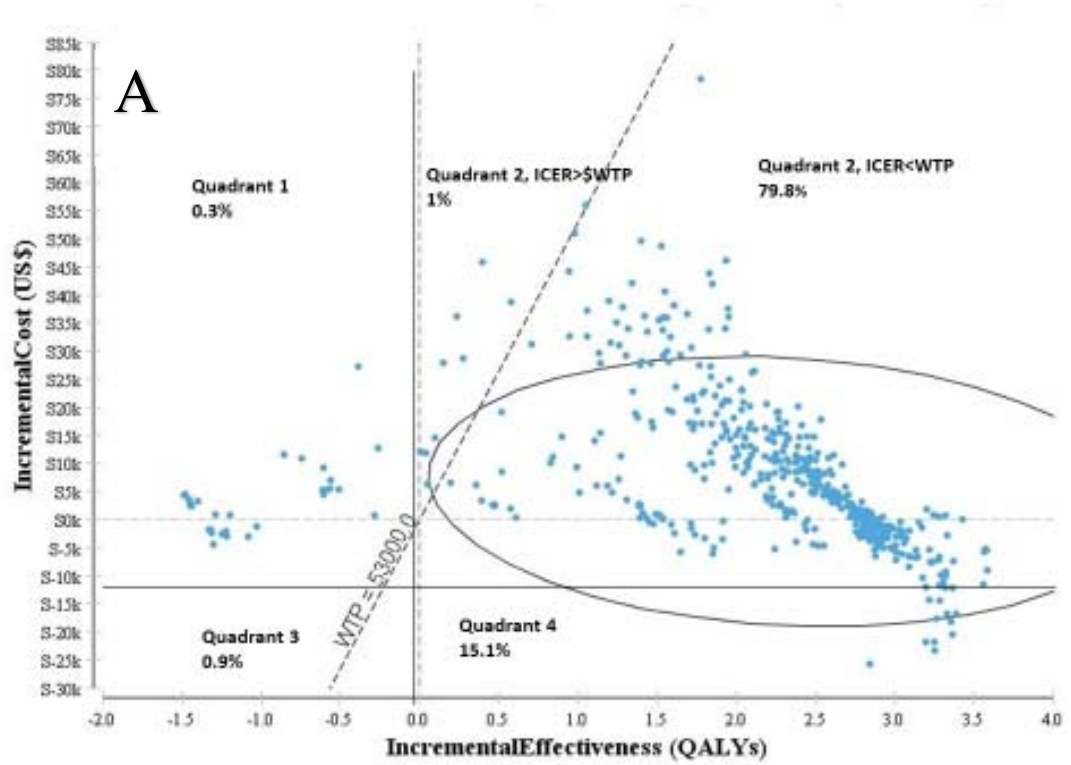

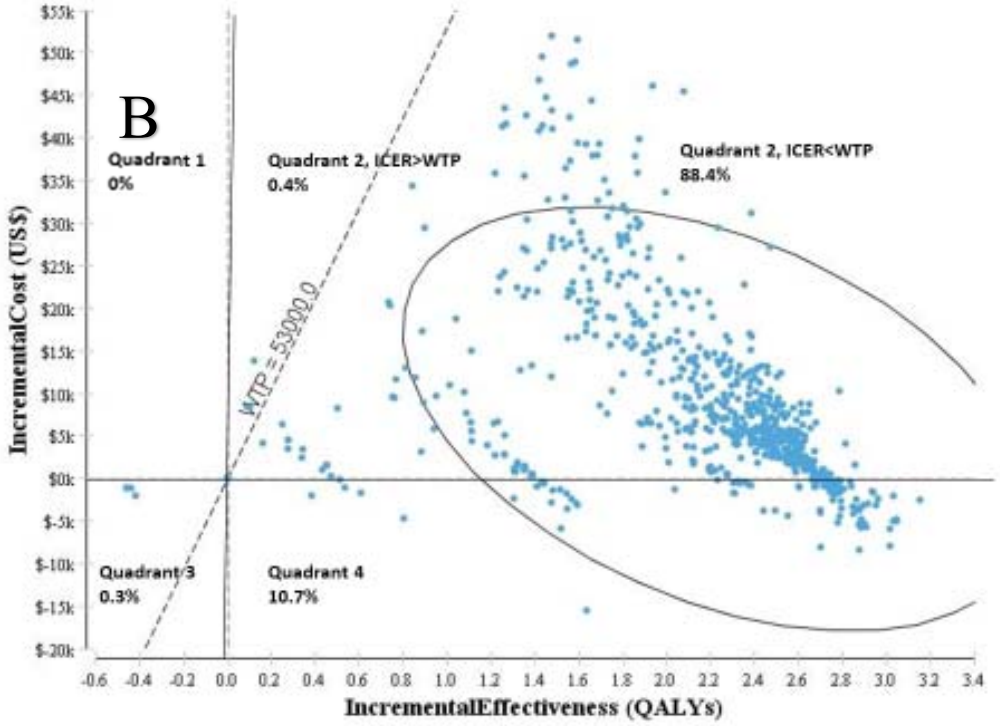
B
Quadrant 1
0%
Quadrant 2, ICER>WTP
0.4%
Quadrant 2, ICER<WTP
88.4%
Quadrant 3
0.3%
Quadrant 4
10.7%
WTP = 53000.0
IncrementalCost (US$)
IncrementalEffectiveness (QALYs)

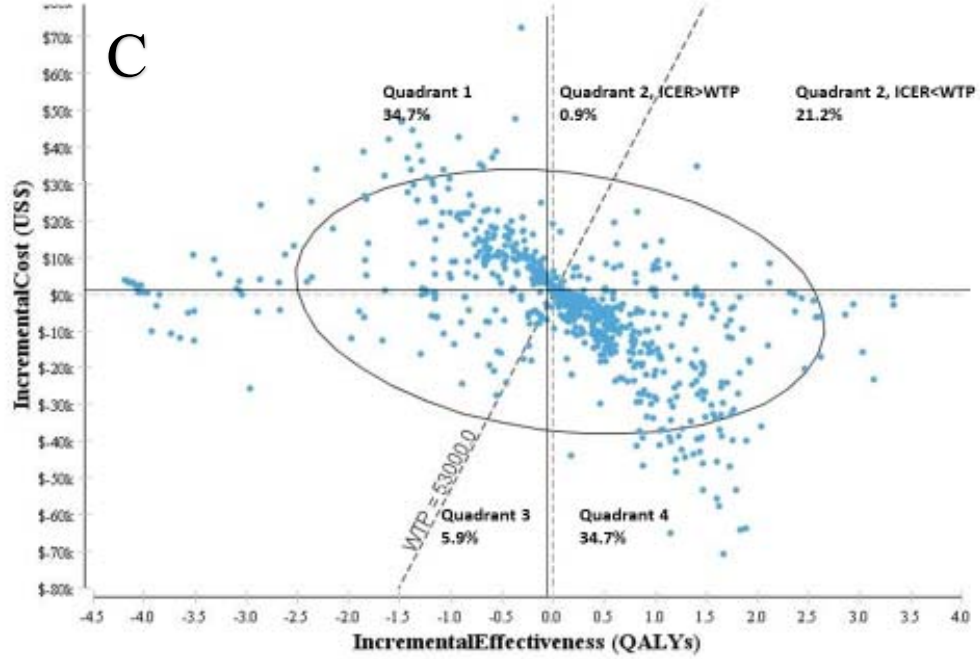
C
Quadrant 1
34.7%
Quadrant 2, ICER>WTP
0.9%
Quadrant 2, ICER<WTP
21.2%
Quadrant 3
5.9%
Quadrant 4
34.7%
WTP = 53000.0
IncrementalCost (US$)
IncrementalEffectiveness (QALYs)

Scenario analysis: Scenario analyses were also conducted to investigate the cost-effectiveness of these cardioprotective strategies in haematological malignancies. These malignancies differ from breast cancer in having higher annual mortality rates, and also higher incidences of cardiotoxicity and cardiac failure due to more aggressive chemotherapeutic regimens. For non-Hodgkin's lymphoma (NHL), the results were broadly similar to those of breast cancer, with SGCP offering incremental clinical benefit over UCP at higher costs. The ICER was higher for NHL ($15,251/QALY vs. $3,906/QALY), which was driven by a higher background mortality rate. For the scenario analysis of a man with AML, the high five-year mortality mitigated any clinical benefit from a cardiac imaging strategy, and UCP dominated both alternative strategies. These results suggest that significant differences may exist in cost-effectiveness of strategies depending on malignancy involved. However only strain echocardiography findings in haematological malignancies are limited to small subgroups of trials that predominantly recruited breast cancer patients, so at present the findings of these scenario analyses should be considered hypothesis-generating.

Assumptions. Strengths of this analysis include accounting for a spectrum of cardiotoxicity after chemotherapy, explicitly accounting for changes in costs and quality-of-life due to cardioprotective treatment and accounting for changes in incidence of conditions in first and then subsequent years. Nonetheless, the value ranges were drawn from retrospective data from different studies involving different populations and time-periods. Generally, when a range of transition probabilities and outcomes was considered, we used the most conservative assumptions. For example, we assumed cost for an annual cardiac screening regimen utilizing 2D-strain echocardiography to be five times higher than for a regimen using LVEF echocardiography, although the two techniques are approximately similar in terms of infrastructure and training. It is also entirely possible that 2D-strain echocardiography could reduce the need for further cardiac screening after three months due to its inherently higher sensitivity, which would significantly reduce costs and improve net monetary benefits associated with SGCP. However large clinical-outcome driven trials assessing shorter cardiac imaging protocols are yet to be conducted. Because some of these strategies are novel (e.g. strain echocardiography), clinical trials have been mostly small-

scale and single centre. However these trials have consistently reported similar findings, and sensitivity analyses of these variables did not substantially change the study's conclusions.

Publications detailing costs of adverse drug reactions are scarce in scientific literature, and most studies examined emergency or hospitalized patients. We recognise that this could potentially be a source of discrepancy between our model and current clinical practice. However, side-effects of ACE inhibitors and β-blockers encompass a spectrum that include life-threatening side-effects, and even milder side-effects may necessitate emergency room visits and expensive further investigations.

Rare outcomes (e.g. death) were frequently not reported in these single-centre trials, and we needed to extrapolate from larger observational trials in which patient population characteristics differed in several regards. Additionally, costs of medical care and conditions differ in different countries and in different medical contexts (outpatient care, hospital inpatient care), which could affect modelling results.

A health-payer perspective was taken, in order to make this study highly applicable for health-care managers and decision-makers. We recognise that a societal perspective may confer some advantages, such as detecting cost-shifting between sectors, but we think this is unlikely in this particular clinical setting. Changes in utility values for health states in sensitivity analyses had little effect on cost-effectiveness ratios and, in all cases the current strategy of LVEF-guided therapy was dominated with strain-guided therapy providing additional QALYs at modest additional cost. We also did not alter the baseline patient utilities to include reduced utilities of non-metastatic breast cancer diagnosis. The reason is that because the aim of the study was to assess three different strategies and applying breast cancer utilities would have added an unnecessary extraneous variable which would not alter the conclusion, as it would apply equally to all three strategies. Additionally utility values quoted in the literature for adjuvant chemotherapy for breast cancer are in the range of 0.94 – 0.99(279), so would not be expected to significantly change final derived utilities.

Limitations. The specific clinical characteristics of the chosen index case and scenario analyses may limit the applicability of this study to a selection of cardio-oncology cases. This is unavoidable, as the wide

spectrum of cancers treated with anthracyclines, the variability of chemotherapy regimens, the different cardiac screening modalities and regimens available, and different cardioprotection strategies available (including dexrazoxane) and the decision whether to continue chemotherapy would introduce so many variables that the model's conclusions would lose applicability to specific patient subgroups. Nevertheless, we feel that our model encompasses the most common clinical scenarios.

The use of troponin measurements for predicting cardiotoxicity represents an alternative strategy. However, studies of the utility of troponin for targeting cardioprotective medications have usually tested a population treated with relatively high doses of anthracyclines(280), with mean cumulative anthracycline doses of approximately 350 mg/m^2. A subsequent study that investigated a strategy of concurrent strain echocardiography and ultrasensitive troponin I measurements for predicting cardiotoxicity in a population treated with low-to-moderate anthracycline doses found that in multivariate analysis, strain was an independent predictor of later cardiotoxicity, but troponin was not(44). For these reasons, we did not include troponin measurements into our model.

Clinical relevance. The strategy of a screening process with strain imaging may be applicable to other situations where there is a risk of developing HF. Heart failure management costs the US economy $53 billion/year(281), and treatments that reduce its incidence have the potential to be substantially cost-saving. Use of 2D strain echocardiography would represent an investment in potentially improving outcomes and reducing future healthcare costs of HF.

Conclusions. A strain-guided strategy for targeting cardioprotective medications for patients at risk of chemotherapy-related cardiotoxicity provides more QALYs at lower cost than standard care and provides more QALYs at a reasonable additional cost compared with uniform CP strategy.

i

Table 9-1. Values for model variables.

Variable	**Base value**	**Range**		**Source**
		Minimum	**Maximum**	
Annual Transition Probabilities				
Initial Year				
Probability of global longitudinal strain (GLS) drop after chemotherapy	0.23	0.23	0.51	(157,274,282)
Patients with GLS drop (S-CTX); -Cardiotoxicity (EF-CTX) -Cardiac Failure -Cardiac Death	 0.25 0.02 0.01	 0.2 0 0	 0.5 0.14 0.02	(44,282,283)
Patients without GSL drop; -Cardiotoxicity (EF-CTX) -Cardiac Failure -Cardiac Death	 0.01 0.005 0.005	 0.005 0.001 0.001	 0.0015 0.0015 0.0015	(44,282,283)
Patients on uniform therapy; -Cardiotoxicity -Cardiac Failure -Death	 0.1 0.03 0.01	 0 0 0	 0.35 0.05 0.05	(19,280,284)
EF-guided strategy; -Cardiotoxicity	 0.2	 0.05	 0.3	

-Cardiac Failure -Death	0.05 0.03	0.01 0	0.2 0.1	(52,280,285)
Cardioprotective Medication Side-Effects	0.33	0.25	0.64	
Cardioprotective Medication discontinuation	0.1	0.05	0.13	
Years 2-5				
Patients without GLS drop				
-Cardiotoxicity	0.005	0.001	0.009	*
-Cardiac Failure	0.001	0.0005	0.0015	*
-Cardiac Death	0.001	0.0005	0.0015	*
Patients with GLS Drop (S-CTX)				
-Cardiotoxicity	0.008	0.005	0.015	*
-Cardiac Failure	0.002	0.001	0.003	*
-Cardiac Death	0.001	0.005	0.0015	*
Clinically Well Patients				
-Cardiotoxicity	0.03	0.01	0.05	(19,52,280)
-Cardiac Failure	0.01	0.005	0.015	(52,280,285)
-Cardiac Death	0.005	0.001	0.009	(52,280,285)
Cardioprotective Medication Side-Effects	0.2	0.1	0.3	*
Cardioprotective Medication Discontinuation	0.05	0.02	0.08	*
Cardiotoxicity Patients (EF-CTX)				

Congestive Cardiac failure	0.026	0.0	0.052	*
Death	0.04	0.0	0.08	*
Costs (annual, 2015 US$)				
Strain-Guided Echocardiographic Screening	5127	2000	8000	[8]
LVEF-Guided Echocardiographic Screening	2564	1000	3000	[8]
Cardiotoxicity	1800	1000	5000	[24, 25, 26]
Cardiac Failure	7000	5000	20000	[27, 28]
Cardioprotective Medications	81	81	800	[9]
Cardioprotective medication side-effects	750	50	5000	[29, 30]
Utilities				
Cardiotoxicity	0.94	0.68	0.99	[31, 32, 33]
Cardiac Failure	0.6	0.52	0.74	[32, 34, 35]
Death	0	0	0	*
Medication side-effects (medication continued)	0.96	0.92	1.0	[36]
Medication side-effects (medications ceased)	0.99	0.95	1.0	[37]

- * represents expert opinion in the context of insufficient information in published literature due to low incidence (typically <1%) in small trials
- EF-CTX refers to cardiotoxicity, as diagnosed by Seidman et al[4], as either an asymptomatic decline in left ventricular ejection fraction of ≥10% or a symptomatic decline of ≥5%.
- S-CTX refers to patients who develop as a decline in global longitudinal strain (GLS) of ≥11% from baseline by 3 months post chemotherapy-initiation

Table 9-2: Scenario analysis of index case of a 50 year-old man with stage III Non-Hodgkin's Lymphoma and low-to-intermediate IPI risk.

Variable	Base value	Range		Source
		Minimum	Maximum	
Annual transition probabilities				
Patients with S-CTX: -Cardiotoxicity - Cardiac Failure	 0.40 0.05	 0.20 0.01	 0.60 0.10	(286) (166)
Patients on uniform therapy -Cardiotoxicity - Cardiac Failure	 0.15 0.05	 0.10 0.01	 0.20 0.10	(286)
Patients on LV-guided cardioprotection: -Cardiotoxicity - Cardiac Failure	 0.36 0.05	 0.20 0.01	 0.52 0.10	(287)
Mortality rates: First year Second year Third year Fourth year Fifth year Cumulative five-year mortality	 4.6% 6.2% 0.7% 4.1% 5.2% 20.8%			(288)

Table 9-3: Scenario analysis of an index case of a 45 year old man with acute myeloid leukemia.

Variable	Base value	Range		Source
		Minimum	Maximum	
Annual transition probabilities				
Patients with S-CTX: -EF-CTX -Cardiac Failure	 0.40 0.05	 0.20 0.01	 0.60 0.10	(286) (166)
Patients on uniform therapy: -EF-CTX -Cardiac Failure	 0.15 0.05	 0.10 0.01	 0.20 0.10	(286) (166)
Patients on LV-guided strategy: -EF-CTX -Cardiac Failure	 0.18 0.05	 0.20 0.01	 0.52 0.10	(287)
Mortality rates: First year Second year Third year Fourth year Fifth year Cumulative 5 year mortality	 33% 5% 5% 5% 5% 52%			(288)

Chapter 10

Summary and Conclusion

The research in this thesis has endeavoured to illustrate the gap between the contemporary and projected burden of CTRCD and the current suboptimal clinical practices for preventing it and identifying strategies for reducing the morbidity and mortality associated with this condition. Earlier chapters confirmed that CTRCD affects 20% of cancer patients treated with potentially cardiotoxic regimens (35% if diastolic dysfunction is included as an adverse outcome), yet only 37% of such patients undergo sequential cardiac imaging as advised by contemporary guidelines. Subsequent chapters identified echocardiography as the optimal imaging technique with myocardial deformation imaging and automated measurements as feasible strategies for further improving the diagnostic and prognostic accuracy. Such imaging and management strategies were shown to be cost-effective with significant financial and quality-of-life savings on a societal scale. Cardiac MRI was demonstrated to provide yet further clinical information that may guide management on a per-patient basis, when echocardiography findings in isolation are ambiguous. Together, these findings constitute a strong argument for improving Australian's access to cardio-oncology services.

There remain several further research pathways that this thesis could potentially have explored if further time and resources were available, and it can be hoped that future higher-degree candidates may use this thesis as a starting point to those pathways. One translational outlook is to explore the complementary role that cardiac biomarkers may play in identifying CTRCD. Blood-based biomarkers (e.g. NT-pro-BNP and troponin T) have the benefits of being inexpensive, not burdensome for the cancer patient and can be easily integrated into routine oncological care without delaying anti-cancer treatments(289). Future prospective studies assessing both cardiac imaging and biomarker approaches for diagnosing CTRCD could assist physicians and are highly desirable. Additionally, the optimal cardiac protection strategy remains to be determined. There remain ongoing debates regarding whether cardioprotection should be administered prospectively or after diagnosis of cardiac dysfunction (indeed one of the chapters of this thesis contains work published as a viewpoint arguing for prospective cardioprotection(290)).

These conclusions of this thesis are broadly in agreement with a recent report by the European Cardio-Oncology Council(291), that recommended that even district-level hospitals should have access to cardio-oncology services, with larger hospitals having an in-house cardio-oncology team. The cardio-oncology team should ideally utilize a multidisciplinary approach in a specialized setting with access to advanced cardiac imaging, including CMR. However, the current status of cardio-oncology in Australia is in its infancy. To the best of my knowledge, the author of this thesis is the only cardiologist in Australia who has completed a dedicated cardio-oncology Fellowship. It is the author's hope that this thesis may provide a road-map for creation of cardio-oncology units within Australia.

This PhD thesis assists in identifying future paths for improving cardio-oncology care. Firstly, it is likely that part of the reason for poor utilization of cardiac imaging and referral rates to cardiologists for detected abnormalities relate to under-appreciation to the degree of cardiovascular burden shouldered by cancer survivors. It is a simple fact that medical specialities are to some degree fenced off from each other, with little opportunity for inter-disciplinary communication and team-building. It is therefore imperative that attempts are made to reach across this artificial rift and establish a model for collaboration. Because cardiologists are traditionally the gatekeepers to cardiac imaging and treatments and have primary responsibility for managing cardiac complications of cancer treatment, they should take the initiative of advocating for improved cardio-oncology services in Australia. One initial step would be to present research similar to that contained in this thesis at oncological meetings and conferences. Standardization of LVEF measurements in the cancer population would be ideal, as currently two competing modalities are used, and results are not interchangeable between modalities. This could be addressed by cardiologists altering the current "first-come-first-served" model for booking echocardiograms to a model triaged based on clinical characteristics, where the time-sensitive nature of cancer patient screening is appreciated. Efforts should be made to improve collaboration between

cardiologists and radiologists to improve CMR accessibility to cardio-oncology patients. Lastly further cost-effectiveness analyses should be performed regarding cardio-oncology intervention to assist in guiding policy makers.

CTRCD has historically been an invisible burden shouldered largely by cancer survivors in Australia. This is now starting to slowly change as increased collaboration, both in the research and clinical domains, are leading to improved patient care. Hopefully this PhD thesis, which was created with the assistance of oncologists, hematologists, cardiologists, sonographers, statisticians and health economics experts, will constitute another step down this path.

References

1. Fonseca R, Marwick TH. Appropriateness and outcomes: is it time to adopt appropriate use criteria outside of North America? Heart 2014;100:357-358.
2. Fonseca R, Marwick TH. How I do it: judging appropriateness for TTE and TEE. Cardiovasc Ultrasoun 2014;12:22.
3. American Cancer Society A, Georgia. Cancer Facts & Figures. 2013.
4. La Rovere MT, Bigger JT, Jr., Marcus FI, Mortara A, Schwartz PJ. Baroreflex sensitivity and heart-rate variability in prediction of total cardiac mortality after myocardial infarction. ATRAMI (Autonomic Tone and Reflexes After Myocardial Infarction) Investigators. Lancet 1998;351:478-84.
5. Oeffinger KC, Mertens AC, Sklar CA et al. Chronic health conditions in adult survivors of childhood cancer. N Engl J Med 2006;355:1572-82.
6. Patnaik JL, Byers T, DiGuiseppi C, Dabelea D, Denberg TD. Cardiovascular disease competes with breast cancer as the leading cause of death for older females diagnosed with breast cancer: a retrospective cohort study. Breast Cancer Res 2011;13:R64.
7. Felker GM, Thompson RE, Hare JM et al. Underlying causes and long-term survival in patients with initially unexplained cardiomyopathy. N Engl J Med 2000;342:1077-84.
8. Ainger LE, Bushore J, Johnson WW, Ito J. Daunomycin: a cardiotoxic agent. J Natl Med Assoc 1971;63:261-7.
9. Slamon DJ, Leyland-Jones B, Shak S et al. Use of chemotherapy plus a monoclonal antibody against HER2 for metastatic breast cancer that overexpresses HER2. N Engl J Med 2001;344:783-92.
10. Ewer MS, Lippman SM. Type II chemotherapy-related cardiac dysfunction: time to recognize a new entity. J Clin Oncol 2005;23:2900-2.
11. Chu TF, Rupnick MA, Kerkela R et al. Cardiotoxicity associated with tyrosine kinase inhibitor sunitinib. Lancet 2007;370:2011-9.
12. Lopez-Fernandez T, Martin Garcia A, Santaballa Beltran A et al. Cardio-Onco-Hematology in Clinical Practice. Position Paper and Recommendations. Rev Esp Cardiol (Engl Ed) 2017;70:474-486.
13. Telli ML, Hunt SA, Carlson RW, Guardino AE. Trastuzumab-related cardiotoxicity: calling into question the concept of reversibility. J Clin Oncol 2007;25:3525-33.
14. Narayan HK, Finkelman B, French B et al. Detailed Echocardiographic Phenotyping in Breast Cancer Patients: Associations With Ejection Fraction Decline, Recovery, and Heart Failure Symptoms Over 3 Years of Follow-Up. Circulation 2017;135:1397-1412.
15. Giordano SH, Lin YL, Kuo YF, Hortobagyi GN, Goodwin JS. Decline in the use of anthracyclines for breast cancer. J Clin Oncol 2012;30:2232-9.
16. Slamon DJ EW, Robert N, Pienkowski T, Martin M, Pawlicki M. . Phase III randomized trial comparing doxorubicin with cyclophosphamide followed by docetaxel with doxorubicin and cyclophosphamide followed by docetaxel and trastuzumab with docetaxel, carboplatin and trastuzumab in HER2 positive early breast cancer patients: BCIRG006 study. Breast Cancer Research Treatment 2005;94 (suppl):s5.
17. Jones SE, Savin MA, Holmes FA et al. Phase III trial comparing doxorubicin plus cyclophosphamide with docetaxel plus cyclophosphamide as adjuvant therapy for operable breast cancer. J Clin Oncol 2006;24:5381-7.

18. Chairs J. Biophysical chemistry of the daunomycin-DNA interaction. Biophysical Chemistry 1990;35:191-202.
19. Kalam K, Marwick TH. Role of cardioprotective therapy for prevention of cardiotoxicity with chemotherapy: a systematic review and meta-analysis. Eur J Cancer 2013;49:2900-9.
20. Zhang S, Liu X, Bawa-Khalfe T et al. Identification of the molecular basis of doxorubicin-induced cardiotoxicity. Nat Med 2012;18:1639-42.
21. Von Hoff DD, Layard MW, Basa P et al. Risk factors for doxorubicin-induced congestive heart failure. Ann Intern Med 1979;91:710-7.
22. Cardinale D, Colombo A, Lamantia G et al. Anthracycline-induced cardiomyopathy: clinical relevance and response to pharmacologic therapy. J Am Coll Cardiol 2010;55:213-20.
23. Ewer MS, Ali MK, Mackay B et al. A comparison of cardiac biopsy grades and ejection fraction estimations in patients receiving Adriamycin. J Clin Oncol 1984;2:112-7.
24. Jensen BV, Skovsgaard T, Nielsen SL. Functional monitoring of anthracycline cardiotoxicity: a prospective, blinded, long-term observational study of outcome in 120 patients. Ann Oncol 2002;13:699-709.
25. Lenihan DJ, Cardinale DM. Late cardiac effects of cancer treatment. J Clin Oncol 2012;30:3657-64.
26. Jones LW, Haykowsky MJ, Swartz JJ, Douglas PS, Mackey JR. Early breast cancer therapy and cardiovascular injury. J Am Coll Cardiol 2007;50:1435-41.
27. Yarden Y. The EGFR family and its ligands in human cancer. signalling mechanisms and therapeutic opportunities. Eur J Cancer 2001;37 Suppl 4:S3-8.
28. Force T, Krause DS, Van Etten RA. Molecular mechanisms of cardiotoxicity of tyrosine kinase inhibition. Nat Rev Cancer 2007;7:332-44.
29. Zhao YY, Sawyer DR, Baliga RR et al. Neuregulins promote survival and growth of cardiac myocytes. Persistence of ErbB2 and ErbB4 expression in neonatal and adult ventricular myocytes. J Biol Chem 1998;273:10261-9.
30. Slamon D, Eiermann W, Robert N et al. Adjuvant trastuzumab in HER2-positive breast cancer. N Engl J Med 2011;365:1273-83.
31. Ewer MS, Ewer SM. Cardiotoxicity of anticancer treatments: what the cardiologist needs to know. Nat Rev Cardiol 2010;7:564-75.
32. de Korte MA, de Vries EG, Lub-de Hooge MN et al. 111Indium-trastuzumab visualises myocardial human epidermal growth factor receptor 2 expression shortly after anthracycline treatment but not during heart failure: a clue to uncover the mechanisms of trastuzumab-related cardiotoxicity. Eur J Cancer 2007;43:2046-51.
33. McMurray JJ, Adamopoulos S, Anker SD et al. ESC Guidelines for the diagnosis and treatment of acute and chronic heart failure 2012: The Task Force for the Diagnosis and Treatment of Acute and Chronic Heart Failure 2012 of the European Society of Cardiology. Developed in collaboration with the Heart Failure Association (HFA) of the ESC. Eur Heart J 2012;33:1787-847.
34. Hunt SA, Abraham WT, Chin MH et al. ACC/AHA 2005 Guideline Update for the Diagnosis and Management of Chronic Heart Failure in the Adult: a report of the American College of Cardiology/American Heart Association Task Force on Practice Guidelines (Writing Committee to Update the 2001 Guidelines for the Evaluation and Management of Heart Failure): developed in collaboration with the American College of Chest Physicians and the International Society for Heart and Lung Transplantation: endorsed by the Heart Rhythm Society. Circulation 2005;112:e154-235.
35. Wang TJ, Evans JC, Benjamin EJ, Levy D, LeRoy EC, Vasan RS. Natural history of asymptomatic left ventricular systolic dysfunction in the community. Circulation 2003;108:977-82.

36. Wojnowski L, Kulle B, Schirmer M et al. NAD(P)H oxidase and multidrug resistance protein genetic polymorphisms are associated with doxorubicin-induced cardiotoxicity. Circulation 2005;112:3754-62.
37. Katayama M, Imai Y, Hashimoto H et al. Fulminant fatal cardiotoxicity following cyclophosphamide therapy. J Cardiol 2009;54:330-4.
38. Perez EA, Koehler M, Byrne J, Preston AJ, Rappold E, Ewer MS. Cardiac safety of lapatinib: pooled analysis of 3689 patients enrolled in clinical trials. Mayo Clin Proc 2008;83:679-86.
39. Atallah E, Durand JB, Kantarjian H, Cortes J. Congestive heart failure is a rare event in patients receiving imatinib therapy. Blood 2007;110:1233-7.
40. Cortes JE, Kim DW, Pinilla-Ibarz J et al. A phase 2 trial of ponatinib in Philadelphia chromosome-positive leukemias. N Engl J Med 2013;369:1783-96.
41. Ali MK, Buzdar AU, Ewer MS, Cheng RS, Haynie TP. Noninvasive cardiac evaluation of patients receiving adriamycin-containing adjuvant chemotherapy (FAC) for stage II or III breast cancer. J Surg Oncol 1983;23:212-6.
42. Sandri MT, Cardinale D, Zorzino L et al. Minor increases in plasma troponin I predict decreased left ventricular ejection fraction after high-dose chemotherapy. Clin Chem 2003;49:248-52.
43. Cardinale D, Sandri MT, Colombo A et al. Prognostic value of troponin I in cardiac risk stratification of cancer patients undergoing high-dose chemotherapy. Circulation 2004;109:2749-54.
44. Sawaya H, Sebag IA, Plana JC et al. Assessment of echocardiography and biomarkers for the extended prediction of cardiotoxicity in patients treated with anthracyclines, taxanes, and trastuzumab. Circ Cardiovasc Imaging 2012;5:596-603.
45. Altena R, Perik PJ, van Veldhuisen DJ, de Vries EG, Gietema JA. Cardiovascular toxicity caused by cancer treatment: strategies for early detection. Lancet Oncol 2009;10:391-9.
46. Huang H, Nijjar PS, Misialek JR et al. Accuracy of left ventricular ejection fraction by contemporary multiple gated acquisition scanning in patients with cancer: comparison with cardiovascular magnetic resonance. Journal of cardiovascular magnetic resonance : official journal of the Society for Cardiovascular Magnetic Resonance 2017;19:34.
47. Otterstadt JE FG, Sutton MS, Holme I. Accuracy and reproducibility of biplane two-dimensional echocardiographic measurements of left ventricular dimensions and function. European Heart Journal 1997;18:507-13.
48. Walker J, Bhullar N, Fallah-Rad N et al. Role of three-dimensional echocardiography in breast cancer: comparison with two-dimensional echocardiography, multiple-gated acquisition scans, and cardiac magnetic resonance imaging. J Clin Oncol 2010;28:3429-36.
49. Yang H, Negishi K, Wang Y, Nolan M, Marwick TH. Imaging-Guided Cardioprotective Treatment in a Community Elderly Population of Stage B Heart Failure. JACC Cardiovasc Imaging 2017;10:217-226.
50. Drafts BC, Twomley KM, D'Agostino R, Jr. et al. Low to moderate dose anthracycline-based chemotherapy is associated with early noninvasive imaging evidence of subclinical cardiovascular disease. JACC Cardiovasc Imaging 2013;6:877-85.
51. Tebbi CK, London WB, Friedman D et al. Dexrazoxane-associated risk for acute myeloid leukemia/myelodysplastic syndrome and other secondary malignancies in pediatric Hodgkin's disease. J Clin Oncol 2007;25:493-500.
52. Bosch X, Rovira M, Sitges M et al. Enalapril and carvedilol for preventing chemotherapy-induced left ventricular systolic dysfunction in patients with malignant hemopathies: the OVERCOME trial (preventiOn of left Ventricular dysfunction with Enalapril and caRvedilol in patients submitted to intensive ChemOtherapy for the treatment of Malignant hEmopathies). J Am Coll Cardiol 2013;61:2355-62.

53. Seicean S, Seicean A, Plana JC, Budd GT, Marwick TH. Effect of statin therapy on the risk for incident heart failure in patients with breast cancer receiving anthracycline chemotherapy: an observational clinical cohort study. J Am Coll Cardiol 2012;60:2384-90.
54. Gillan C, Briggs K, Goytisolo Pazos A et al. Barriers to accessing radiation therapy in Canada: a systematic review. Radiat Oncol 2012;7:167.
55. Early Breast Cancer Trialists' Collaborative G, Darby S, McGale P et al. Effect of radiotherapy after breast-conserving surgery on 10-year recurrence and 15-year breast cancer death: meta-analysis of individual patient data for 10,801 women in 17 randomised trials. Lancet 2011;378:1707-16.
56. Groarke JD, Nguyen PL, Nohria A, Ferrari R, Cheng S, Moslehi J. Cardiovascular complications of radiation therapy for thoracic malignancies: the role for non-invasive imaging for detection of cardiovascular disease. Eur Heart J 2014;35:612-23.
57. Darby SC, Ewertz M, McGale P et al. Risk of ischemic heart disease in women after radiotherapy for breast cancer. N Engl J Med 2013;368:987-98.
58. Cutter DJ, Schaapveld M, Darby SC et al. Risk of valvular heart disease after treatment for Hodgkin lymphoma. J Natl Cancer Inst 2015;107.
59. Jaworski C, Mariani JA, Wheeler G, Kaye DM. Cardiac complications of thoracic irradiation. J Am Coll Cardiol 2013;61:2319-28.
60. Lund MB, Ihlen H, Voss BM et al. Increased risk of heart valve regurgitation after mediastinal radiation for Hodgkin's disease: an echocardiographic study. Heart 1996;75:591-5.
61. Yancy CW, Jessup M, Bozkurt B et al. 2013 ACCF/AHA guideline for the management of heart failure: a report of the American College of Cardiology Foundation/American Heart Association Task Force on Practice Guidelines. J Am Coll Cardiol 2013;62:e147-239.
62. Bovelli D, Plataniotis G, Roila F, Group EGW. Cardiotoxicity of chemotherapeutic agents and radiotherapy-related heart disease: ESMO Clinical Practice Guidelines. Ann Oncol 2010;21 Suppl 5:v277-82.
63. Lancellotti P, Nkomo VT, Badano LP et al. Expert consensus for multi-modality imaging evaluation of cardiovascular complications of radiotherapy in adults: a report from the European Association of Cardiovascular Imaging and the American Society of Echocardiography. Eur Heart J Cardiovasc Imaging 2013;14:721-40.
64. Liberati A, Altman DG, Tetzlaff J et al. The PRISMA statement for reporting systematic reviews and meta-analyses of studies that evaluate healthcare interventions: explanation and elaboration. BMJ 2009;339:b2700.
65. Groarke JD, Tanguturi VK, Hainer J et al. Abnormal exercise response in long-term survivors of hodgkin lymphoma treated with thoracic irradiation: evidence of cardiac autonomic dysfunction and impact on outcomes. J Am Coll Cardiol 2015;65:573-83.
66. Chen MH, Blackington LH, Zhou J et al. Blood pressure is associated with occult cardiovascular disease in prospectively studied Hodgkin lymphoma survivors after chest radiation. Leukemia and Lymphoma 2014;55:2477-2483.
67. Machann W, Beer M, Breunig M et al. Cardiac magnetic resonance imaging findings in 20-year survivors of mediastinal radiotherapy for Hodgkin's disease. Int J Radiat Oncol Biol Phys 2011;79:1117-23.
68. Tsai HR, Gjesdal O, Wethal T et al. Left ventricular function assessed by two-dimensional speckle tracking echocardiography in long-term survivors of Hodgkin's lymphoma treated by mediastinal radiotherapy with or without anthracycline therapy. Am J Cardiol 2011;107:472-7.
69. Busia A, Laffranchi A, Viviani S, Bonfante V, Villani F. Cardiopulmonary toxicity of different chemoradiotherapy combined regimens for Hodgkin's disease. Anticancer Res 2010;30:4381-7.

70. Heidenreich PA, Hancock SL, Vagelos RH, Lee BK, Schnittger I. Diastolic dysfunction after mediastinal irradiation. Am Heart J 2005;150:977-82.
71. Salloum E, Tanoue LT, Wackers FJT, Zelterman D, Hu GL, Cooper DL. Assessment of cardiac and pulmonary function in adult patients with Hodgkin's disease treated with ABVD or MOPP/ABVD plus adjuvant low-dose mediastinal irradiation. Cancer Investigation 1999;17:171-180.
72. Glanzmann C, Kaufmann P, Jenni R, Hess OM, Huguenin P. Cardiac risk after mediastinal irradiation for Hodgkin's disease. Radiother Oncol 1998;46:51-62.
73. Constine LS, Schwartz RG, Savage DE, King V, Muhs A. Cardiac function, perfusion, and morbidity in irradiated long-term survivors of Hodgkin's disease. Int J Radiat Oncol Biol Phys 1997;39:897-906.
74. Kreuser ED, Voller H, Behles C et al. Evaluation of late cardiotoxicity with pulsed Doppler echocardiography in patients treated for Hodgkin's disease. Br J Haematol 1993;84:615-22.
75. Allavena C, Conroy T, Aletti P, Bey P, Lederlin P. Late cardiopulmonary toxicity after treatment for Hodgkin's disease. Br J Cancer 1992;65:908-12.
76. Gustavsson A, Eskilsson J, Landberg T et al. Late cardiac effects after mantle radiotherapy in patients with Hodgkin's disease. Ann Oncol 1990;1:355-63.
77. Savage DE, Constine LS, Schwartz RG, Rubin P. Radiation effects on left ventricular function and myocardial perfusion in long term survivors of Hodgkin's disease. Int J Radiat Oncol Biol Phys 1990;19:721-7.
78. Pohjola-Sintonen S, Totterman KJ, Salmo M, Siltanen P. Late cardiac effects of mediastinal radiotherapy in patients with Hodgkin's disease. Cancer 1987;60:31-7.
79. Perrault DJ, Levy M, Herman JD et al. Echocardiographic abnormalities following cardiac radiation. J Clin Oncol 1985;3:546-51.
80. Morgan GW, Freeman AP, McLean RG, Jarvie BH, Giles RW. Late cardiac, thyroid, and pulmonary sequelae of mantle radiotherapy for Hodgkin's disease. Int J Radiat Oncol Biol Phys 1985;11:1925-31.
81. Burns RJ, Bar-Shlomo BZ, Druck MN et al. Detection of radiation cardiomyopathy by gated radionuclide angiography. Am J Med 1983;74:297-302.
82. Applefeld MM, Wiernik PH. Cardiac disease after radiation therapy for Hodgkin's disease: analysis of 48 patients. Am J Cardiol 1983;51:1679-81.
83. Gomez GA, Park JJ, Panahon AM et al. Heart size and function after radiation therapy to the mediastinum in patients with Hodgkin's disease. Cancer Treat Rep 1983;67:1099-103.
84. Applefeld MM, Slawson RG, Spicer KM, Singleton RT, Wesley MN, Wiernik PH. Long-term cardiovascular evaluation of patients with Hodgkin's disease treated by thoracic mantle radiation therapy. Cancer Treat Rep 1982;66:1003-13.
85. Kane GC, Karon BL, Mahoney DW et al. Progression of left ventricular diastolic dysfunction and risk of heart failure. JAMA 2011;306:856-63.
86. Pistevou-Gompaki K, Hatzitolios A, Eleftheriadis N et al. Evaluation of cardiotoxicity five years after 2D planned, non-simulated, radiation therapy for left breast cancer. Therapeutics and Clinical Risk Management 2008;4:1359-1362.
87. Gyenes G, Fornander T, Carlens P, Rutqvist LE. Morbidity of ischemic heart disease in early breast cancer 15-20 years after adjuvant radiotherapy. Int J Radiat Oncol Biol Phys 1994;28:1235-41.
88. Gustavsson A, Bendahl PO, Cwikiel M, Eskilsson J, Thapper KL, Pahlm O. No serious late cardiac effects after adjuvant radiotherapy following mastectomy in premenopausal women with early breast cancer. Int J Radiat Oncol Biol Phys 1999;43:745-54.
89. Boekel NB, Schaapveld M, Gietema JA et al. Cardiovascular morbidity and mortality in patients treated for ductal carcinoma in situ of the breast. Journal of Clinical Oncology 2013;31.

90. Boerman LM, Berendsen AJ, van der Meer P, Maduro JH, Berger MY, de Bock GH. Long-term follow-up for cardiovascular disease after chemotherapy and/or radiotherapy for breast cancer in an unselected population. Support Care Cancer 2014;22:1949-58.
91. Bouillon K, Haddy N, Delaloge S et al. Long-term cardiovascular mortality after radiotherapy for breast cancer. J Am Coll Cardiol 2011;57:445-52.
92. Park CK, Li X, Starr J, Harris EE. Cardiac morbidity and mortality in women with ductal carcinoma in situ of the breast treated with breast conservation therapy. Breast J 2011;17:470-6.
93. Hardy D, Liu CC, Cormier JN, Xia R, Du XL. Cardiac toxicity in association with chemotherapy and radiation therapy in a large cohort of older patients with non-small-cell lung cancer. Ann Oncol 2010;21:1825-33.
94. Myrehaug S, Pintilie M, Tsang R et al. Cardiac morbidity following modern treatment for Hodgkin lymphoma: supra-additive cardiotoxicity of doxorubicin and radiation therapy. Leuk Lymphoma 2008;49:1486-93.
95. Hooning MJ, Botma A, Aleman BM et al. Long-term risk of cardiovascular disease in 10-year survivors of breast cancer. J Natl Cancer Inst 2007;99:365-75.
96. Aleman BM, van den Belt-Dusebout AW, De Bruin ML et al. Late cardiotoxicity after treatment for Hodgkin lymphoma. Blood 2007;109:1878-86.
97. van den Belt-Dusebout AW, Nuver J, de Wit R et al. Long-term risk of cardiovascular disease in 5-year survivors of testicular cancer. J Clin Oncol 2006;24:467-75.
98. Patt DA, Goodwin JS, Kuo YF et al. Cardiac morbidity of adjuvant radiotherapy for breast cancer. J Clin Oncol 2005;23:7475-82.
99. Hancock SL, Tucker MA, Hoppe RT. Factors affecting late mortality from heart disease after treatment of Hodgkin's disease. JAMA 1993;270:1949-55.
100. Veinot JP, Edwards WD. Pathology of radiation-induced heart disease: a surgical and autopsy study of 27 cases. Hum Pathol 1996;27:766-73.
101. Ghio S, Gavazzi A, Campana C et al. Independent and additive prognostic value of right ventricular systolic function and pulmonary artery pressure in patients with chronic heart failure. J Am Coll Cardiol 2001;37:183-8.
102. Darby SC, McGale P, Taylor CW, Peto R. Long-term mortality from heart disease and lung cancer after radiotherapy for early breast cancer: prospective cohort study of about 300,000 women in US SEER cancer registries. Lancet Oncol 2005;6:557-65.
103. Galper SL, Yu JB, Mauch PM et al. Clinically significant cardiac disease in patients with Hodgkin lymphoma treated with mediastinal irradiation. Blood 2011;117:412-8.
104. Curigliano G, Cardinale D, Suter T et al. Cardiovascular toxicity induced by chemotherapy, targeted agents and radiotherapy: ESMO Clinical Practice Guidelines. Ann Oncol 2012;23 Suppl 7:vii155-66.
105. Lipshultz SE, Adams MJ, Colan SD et al. Long-term cardiovascular toxicity in children, adolescents, and young adults who receive cancer therapy: pathophysiology, course, monitoring, management, prevention, and research directions: a scientific statement from the American Heart Association. Circulation 2013;128:1927-95.
106. Hull MC, Morris CG, Pepine CJ, Mendenhall NP. Valvular dysfunction and carotid, subclavian, and coronary artery disease in survivors of hodgkin lymphoma treated with radiation therapy. JAMA 2003;290:2831-7.
107. Huang C, Zhang X, Ramil JM et al. Juvenile exposure to anthracyclines impairs cardiac progenitor cell function and vascularization resulting in greater susceptibility to stress-induced myocardial injury in adult mice. Circulation 2010;121:675-83.

108. van der Pal HJ, van Dalen EC, Kremer LC, Bakker PJ, van Leeuwen FE. Risk of morbidity and mortality from cardiovascular disease following radiotherapy for childhood cancer: a systematic review. Cancer Treat Rev 2005;31:173-85.
109. Cutter DJ, Schaapveld M, Darby SC et al. Risk of valvular heart disease after treatment for Hodgkin lymphoma. J Natl Cancer Inst 2015;107:djv008.
110. Nolan MT RDaMT. Long-Term Risk of Heart Failure and Myocardial Dysfunction after Thoracic Radiotherapy: A Systematic Review. Canadian Journal of Cardiology 2015;In-press.
111. Nellessen U, Zingel M, Hecker H, Bahnsen J, Borschke D. Effects of radiation therapy on myocardial cell integrity and pump function: which role for cardiac biomarkers? Chemotherapy 2010;56:147-52.
112. Paris F, Fuks Z, Kang A et al. Endothelial apoptosis as the primary lesion initiating intestinal radiation damage in mice. Science 2001;293:293-7.
113. Groarke JD, Nohria A. Anthracycline cardiotoxicity: a new paradigm for an old classic. Circulation 2015;131:1946-9.
114. Chavez-MacGregor M, Niu J, Zhang N et al. Cardiac Monitoring During Adjuvant Trastuzumab-Based Chemotherapy Among Older Patients With Breast Cancer. J Clin Oncol 2015;33:2176-83.
115. Gulati G, Heck SL, Ree AH et al. Prevention of cardiac dysfunction during adjuvant breast cancer therapy (PRADA): a 2 x 2 factorial, randomized, placebo-controlled, double-blind clinical trial of candesartan and metoprolol. Eur Heart J 2016;37:1671-80.
116. van Nimwegen FA, Schaapveld M, Janus CP et al. Cardiovascular disease after Hodgkin lymphoma treatment: 40-year disease risk. JAMA Intern Med 2015;175:1007-17.
117. Nolan MT, Marwick TH, Plana JC et al. Effect of Traditional Heart Failure Risk Factors on Myocardial Dysfunction in Adult Survivors of Childhood Cancer. JACC Cardiovasc Imaging 2018;11:1202-1203.
118. Armstrong GT, Joshi VM, Ness KK et al. Comprehensive Echocardiographic Detection of Treatment-Related Cardiac Dysfunction in Adult Survivors of Childhood Cancer: Results From the St. Jude Lifetime Cohort Study. J Am Coll Cardiol 2015;65:2511-22.
119. Torti FM, Bristow MM, Lum BL et al. Cardiotoxicity of epirubicin and doxorubicin: assessment by endomyocardial biopsy. Cancer Res 1986;46:3722-7.
120. Armenian SH, Hudson MM, Mulder RL et al. Recommendations for cardiomyopathy surveillance for survivors of childhood cancer: a report from the International Late Effects of Childhood Cancer Guideline Harmonization Group. Lancet Oncol 2015;16:e123-36.
121. Hudson MM, Ness KK, Nolan VG et al. Prospective medical assessment of adults surviving childhood cancer: study design, cohort characteristics, and feasibility of the St. Jude Lifetime Cohort study. Pediatr Blood Cancer 2011;56:825-36.
122. Agarwal SK, Chambless LE, Ballantyne CM et al. Prediction of incident heart failure in general practice: the Atherosclerosis Risk in Communities (ARIC) Study. Circ Heart Fail 2012;5:422-9.
123. Pollentier B, Irons SL, Benedetto CM et al. Examination of the six minute walk test to determine functional capacity in people with chronic heart failure: a systematic review. Cardiopulm Phys Ther J 2010;21:13-21.
124. Lang RM, Badano LP, Mor-Avi V et al. Recommendations for cardiac chamber quantification by echocardiography in adults: an update from the American Society of Echocardiography and the European Association of Cardiovascular Imaging. J Am Soc Echocardiogr 2015;28:1-39 e14.
125. Nagueh SF, Smiseth OA, Appleton CP et al. Recommendations for the Evaluation of Left Ventricular Diastolic Function by Echocardiography: An Update from the American Society of Echocardiography and the European Association of Cardiovascular Imaging. J Am Soc Echocardiogr 2016;29:277-314.

126. Takigiku K, Takeuchi M, Izumi C et al. Normal range of left ventricular 2-dimensional strain: Japanese Ultrasound Speckle Tracking of the Left Ventricle (JUSTICE) study. Circ J 2012;76:2623-32.
127. Suskin N, Sheth T, Negassa A, Yusuf S. Relationship of current and past smoking to mortality and morbidity in patients with left ventricular dysfunction. J Am Coll Cardiol 2001;37:1677-82.
128. Dunlay SM, Weston SA, Jacobsen SJ, Roger VL. Risk factors for heart failure: a population-based case-control study. Am J Med 2009;122:1023-8.
129. Kermani M, Dua A, Gradman AH. Underutilization and clinical benefits of angiotensin-converting enzyme inhibitors in patients with asymptomatic left ventricular dysfunction. Am J Cardiol 2000;86:644-8.
130. Miller KD, Siegel RL, Lin CC et al. Cancer treatment and survivorship statistics, 2016. CA Cancer J Clin 2016;66:271-89.
131. Group SR, Wright JT, Jr., Williamson JD et al. A Randomized Trial of Intensive versus Standard Blood-Pressure Control. N Engl J Med 2015;373:2103-16.
132. Wang Y, Negishi T, Negishi K, Marwick TH. Prediction of heart failure in patients with type 2 diabetes mellitus- a systematic review and meta-analysis. Diabetes Res Clin Pract 2015;108:55-66.
133. Sundstrom J, Arnlov J, Stolare K, Lind L. Blood pressure-independent relations of left ventricular geometry to the metabolic syndrome and insulin resistance: a population-based study. Heart 2008;94:874-8.
134. Russo C, Jin Z, Homma S et al. Effect of obesity and overweight on left ventricular diastolic function: a community-based study in an elderly cohort. J Am Coll Cardiol 2011;57:1368-74.
135. Wilson CL, Liu W, Yang JJ et al. Genetic and clinical factors associated with obesity among adult survivors of childhood cancer: A report from the St. Jude Lifetime Cohort. Cancer 2015;121:2262-70.
136. Dalen H, Thorstensen A, Romundstad PR, Aase SA, Stoylen A, Vatten LJ. Cardiovascular risk factors and systolic and diastolic cardiac function: a tissue Doppler and speckle tracking echocardiographic study. J Am Soc Echocardiogr 2011;24:322-32 e6.
137. Thavendiranathan P, Poulin F, Lim KD, Plana JC, Woo A, Marwick TH. Use of myocardial strain imaging by echocardiography for the early detection of cardiotoxicity in patients during and after cancer chemotherapy: a systematic review. J Am Coll Cardiol 2014;63:2751-68.
138. Steinherz LJ, Graham T, Hurwitz R et al. Guidelines for cardiac monitoring of children during and after anthracycline therapy: report of the Cardiology Committee of the Childrens Cancer Study Group. Pediatrics 1992;89:942-9.
139. Kalam K, Otahal P, Marwick TH. Prognostic implications of global LV dysfunction: a systematic review and meta-analysis of global longitudinal strain and ejection fraction. Heart 2014;100:1673-80.
140. Otterstad JE. Measuring left ventricular volume and ejection fraction with the biplane Simpson's method. Heart 2002;88:559-60.
141. Negishi T, Negishi K, Thavendiranathan P et al. Effect of Experience and Training on the Concordance and Precision of Strain Measurements. JACC Cardiovasc Imaging 2017;10:518-522.
142. Borlaug BA, Nishimura RA, Sorajja P, Lam CS, Redfield MM. Exercise hemodynamics enhance diagnosis of early heart failure with preserved ejection fraction. Circ Heart Fail 2010;3:588-95.
143. Hasselberg NE, Haugaa KH, Sarvari SI et al. Left ventricular global longitudinal strain is associated with exercise capacity in failing hearts with preserved and reduced ejection fraction. Eur Heart J Cardiovasc Imaging 2015;16:217-24.

144. Kocabay G, Muraru D, Peluso D et al. Normal left ventricular mechanics by two-dimensional speckle-tracking echocardiography. Reference values in healthy adults. Rev Esp Cardiol (Engl Ed) 2014;67:651-8.
145. Bellenger NG, Burgess MI, Ray SG et al. Comparison of left ventricular ejection fraction and volumes in heart failure by echocardiography, radionuclide ventriculography and cardiovascular magnetic resonance; are they interchangeable? Eur Heart J 2000;21:1387-96.
146. Swain SM, Whaley FS, Ewer MS. Congestive heart failure in patients treated with doxorubicin: a retrospective analysis of three trials. Cancer 2003;97:2869-79.
147. Henry ML, Niu J, Zhang N, Giordano SH, Chavez-MacGregor M. Cardiotoxicity and Cardiac Monitoring Among Chemotherapy-Treated Breast Cancer Patients. JACC Cardiovasc Imaging 2018;11:1084-1093.
148. Plana JC, Thavendiranathan P, Bucciarelli-Ducci C, Lancellotti P. Multi-Modality Imaging in the Assessment of Cardiovascular Toxicity in the Cancer Patient. JACC Cardiovasc Imaging 2018;11:1173-1186.
149. Sabel MS, Levine EG, Hurd T et al. Is MUGA scan necessary in patients with low-risk breast cancer before doxorubicin-based adjuvant therapy? Multiple gated acquisition. Am J Clin Oncol 2001;24:425-8.
150. Thavendiranathan P, Grant AD, Negishi T, Plana JC, Popovic ZB, Marwick TH. Reproducibility of echocardiographic techniques for sequential assessment of left ventricular ejection fraction and volumes: application to patients undergoing cancer chemotherapy. J Am Coll Cardiol 2013;61:77-84.
151. Corbett JR, Akinboboye OO, Bacharach SL et al. Equilibrium radionuclide angiocardiography. J Nucl Cardiol 2006;13:e56-79.
152. Bates D. Fitting Linear Mixed-Effects Models Using lme4. . Journal of Statistical Software 2015;67:doi:10.18637/jssv067.i01.
153. Giubbini R, Milan E. The time for radionuclide ventriculography resurrection is coming. J Nucl Cardiol 2016;23:1139-1141.
154. Romond EH, Jeong JH, Rastogi P et al. Seven-year follow-up assessment of cardiac function in NSABP B-31, a randomized trial comparing doxorubicin and cyclophosphamide followed by paclitaxel (ACP) with ACP plus trastuzumab as adjuvant therapy for patients with node-positive, human epidermal growth factor receptor 2-positive breast cancer. J Clin Oncol 2012;30:3792-9.
155. Jenkins C, Moir S, Chan J, Rakhit D, Haluska B, Marwick TH. Left ventricular volume measurement with echocardiography: a comparison of left ventricular opacification, three-dimensional echocardiography, or both with magnetic resonance imaging. Eur Heart J 2009;30:98-106.
156. van Royen N, Jaffe CC, Krumholz HM et al. Comparison and reproducibility of visual echocardiographic and quantitative radionuclide left ventricular ejection fractions. Am J Cardiol 1996;77:843-50.
157. Negishi K, Negishi T, Hare JL, Haluska BA, Plana JC, Marwick TH. Independent and incremental value of deformation indices for prediction of trastuzumab-induced cardiotoxicity. J Am Soc Echocardiogr 2013;26:493-8.
158. Andrus BW, Welch HG. Medicare services provided by cardiologists in the United States: 1999-2008. Circ Cardiovasc Qual Outcomes 2012;5:31-6.
159. Virnig BA, Shippee ND, O'Donnell B, Zeglin J, Parashuram S. Trends in the use of echocardiography, 2007 to 2011: Data Points #20. Data Points Publication Series. Rockville (MD), 2011.

160. Kaufmann BA, Min SY, Goetschalckx K et al. How reliable are left ventricular ejection fraction cut offs assessed by echocardiography for clinical decision making in patients with heart failure? Int J Cardiovasc Imaging 2013;29:581-8.
161. Zolgharni M, Dhutia NM, Cole GD et al. Automated aortic Doppler flow tracing for reproducible research and clinical measurements. IEEE Trans Med Imaging 2014;33:1071-82.
162. Dhutia NM, Zolgharni M, Mielewczik M et al. Open-source, vendor-independent, automated multi-beat tissue Doppler echocardiography analysis. Int J Cardiovasc Imaging 2017;33:1135-1148.
163. Maret E, Brudin L, Lindstrom L, Nylander E, Ohlsson JL, Engvall JE. Computer-assisted determination of left ventricular endocardial borders reduces variability in the echocardiographic assessment of ejection fraction. Cardiovasc Ultrasoun 2008;6:55.
164. Rahmouni HW, Ky B, Plappert T et al. Clinical utility of automated assessment of left ventricular ejection fraction using artificial intelligence-assisted border detection. Am Heart J 2008;155:562-70.
165. Knackstedt C, Bekkers SC, Schummers G et al. Fully Automated Versus Standard Tracking of Left Ventricular Ejection Fraction and Longitudinal Strain: The FAST-EFs Multicenter Study. J Am Coll Cardiol 2015;66:1456-66.
166. Mantovani G, Madeddu C, Cadeddu C et al. Persistence, up to 18 months of follow-up, of epirubicin-induced myocardial dysfunction detected early by serial tissue Doppler echocardiography: correlation with inflammatory and oxidative stress markers. Oncologist 2008;13:1296-305.
167. Aurich M, Andre F, Keller M et al. Assessment of left ventricular volumes with echocardiography and cardiac magnetic resonance imaging: real-life evaluation of standard versus new semiautomatic methods. J Am Soc Echocardiogr 2014;27:1017-24.
168. Cannesson M, Tanabe M, Suffoletto MS et al. A novel two-dimensional echocardiographic image analysis system using artificial intelligence-learned pattern recognition for rapid automated ejection fraction. J Am Coll Cardiol 2007;49:217-26.
169. Frederiksen CA, Juhl-Olsen P, Hermansen JF, Andersen NH, Sloth E. Clinical utility of semi-automated estimation of ejection fraction at the point-of-care. Heart, lung and vessels 2015;7:208-16.
170. Hovnanians N, Win T, Makkiya M, Zheng Q, Taub C. Validity of automated measurement of left ventricular ejection fraction and volume using the Philips EPIQ system. Echocardiography 2017;34:1575-1583.
171. Szulik M, Pappas CJ, Jurcut R et al. Clinical validation of a novel speckle-tracking-based ejection fraction assessment method. J Am Soc Echocardiogr 2011;24:1092-100.
172. Abazid RM, Abohamr SI, Smettei OA et al. Visual versus fully automated assessment of left ventricular ejection fraction. Avicenna J Med 2018;8:41-45.
173. Dorosz JL, Lezotte DC, Weitzenkamp DA, Allen LA, Salcedo EE. Performance of 3-dimensional echocardiography in measuring left ventricular volumes and ejection fraction: a systematic review and meta-analysis. J Am Coll Cardiol 2012;59:1799-808.
174. Shibayama K, Watanabe H, Iguchi N et al. Evaluation of automated measurement of left ventricular volume by novel real-time 3-dimensional echocardiographic system: Validation with cardiac magnetic resonance imaging and 2-dimensional echocardiography. J Cardiol 2013;61:281-8.
175. Tsang W, Salgo IS, Medvedofsky D et al. Transthoracic 3D Echocardiographic Left Heart Chamber Quantification Using an Automated Adaptive Analytics Algorithm. JACC Cardiovasc Imaging 2016;9:769-782.

176. Plana JC, Galderisi M, Barac A et al. Expert consensus for multimodality imaging evaluation of adult patients during and after cancer therapy: a report from the American Society of Echocardiography and the European Association of Cardiovascular Imaging. Eur Heart J Cardiovasc Imaging 2014;15:1063-93.
177. Lang RM, Badano LP, Mor-Avi V et al. Recommendations for cardiac chamber quantification by echocardiography in adults: an update from the American Society of Echocardiography and the European Association of Cardiovascular Imaging. Eur Heart J Cardiovasc Imaging 2015;16:233-70.
178. Aurich M, Keller M, Greiner S et al. Left ventricular mechanics assessed by two-dimensional echocardiography and cardiac magnetic resonance imaging: comparison of high-resolution speckle tracking and feature tracking. Eur Heart J Cardiovasc Imaging 2016;17:1370-1378.
179. Barbosa D, Dietenbeck T, Heyde B et al. Fast and fully automatic 3-d echocardiographic segmentation using B-spline explicit active surfaces: feasibility study and validation in a clinical setting. Ultrasound Med Biol 2013;39:89-101.
180. Muraru D, Badano LP, Piccoli G et al. Validation of a novel automated border-detection algorithm for rapid and accurate quantitation of left ventricular volumes based on three-dimensional echocardiography. Eur J Echocardiogr 2010;11:359-68.
181. Muraru D, Cecchetto A, Cucchini U et al. Intervendor Consistency and Accuracy of Left Ventricular Volume Measurements Using Three-Dimensional Echocardiography. J Am Soc Echocardiogr 2018;31:158-168 e1.
182. Spitzer E, Ren B, Zijlstra F, Mieghem NMV, Geleijnse ML. The Role of Automated 3D Echocardiography for Left Ventricular Ejection Fraction Assessment. Card Fail Rev 2017;3:97-101.
183. Tamborini G, Piazzese C, Lang RM et al. Feasibility and Accuracy of Automated Software for Transthoracic Three-Dimensional Left Ventricular Volume and Function Analysis: Comparisons with Two-Dimensional Echocardiography, Three-Dimensional Transthoracic Manual Method, and Cardiac Magnetic Resonance Imaging. J Am Soc Echocardiogr 2017;30:1049-1058.
184. Levy F, Dan Schouver E, Iacuzio L et al. Performance of new automated transthoracic three-dimensional echocardiographic software for left ventricular volumes and function assessment in routine clinical practice: Comparison with 3 Tesla cardiac magnetic resonance. Arch Cardiovasc Dis 2017;110:580-589.
185. Spitzer E, Ren B, Soliman OI, Zijlstra F, Van Mieghem NM, Geleijnse ML. Accuracy of an automated transthoracic echocardiographic tool for 3D assessment of left heart chamber volumes. Echocardiography 2017;34:199-209.
186. Medvedofsky D, Kebed K, Laffin L et al. Reproducibility and experience dependence of echocardiographic indices of left ventricular function: Side-by-side comparison of global longitudinal strain and ejection fraction. Echocardiography 2017;34:365-370.
187. Medvedofsky D, Mor-Avi V, Amzulescu M et al. Three-dimensional echocardiographic quantification of the left-heart chambers using an automated adaptive analytics algorithm: multicentre validation study. Eur Heart J Cardiovasc Imaging 2018;19:47-58.
188. Sun L, Feng H, Ni L, Wang H, Gao D. Realization of fully automated quantification of left ventricular volumes and systolic function using transthoracic 3D echocardiography. Cardiovasc Ultrasoun 2018;16:2.
189. Thavendiranathan P, Liu S, Verhaert D et al. Feasibility, accuracy, and reproducibility of real-time full-volume 3D transthoracic echocardiography to measure LV volumes and systolic function: a fully automated endocardial contouring algorithm in sinus rhythm and atrial fibrillation. JACC Cardiovasc Imaging 2012;5:239-51.

190. Otani K, Nakazono A, Salgo IS, Lang RM, Takeuchi M. Three-Dimensional Echocardiographic Assessment of Left Heart Chamber Size and Function with Fully Automated Quantification Software in Patients with Atrial Fibrillation. J Am Soc Echocardiogr 2016;29:955-965.
191. Dahl JS, Videbaek L, Poulsen MK, Rudbaek TR, Pellikka PA, Moller JE. Global strain in severe aortic valve stenosis: relation to clinical outcome after aortic valve replacement. Circ Cardiovasc Imaging 2012;5:613-20.
192. Stanton T, Leano R, Marwick TH. Prediction of all-cause mortality from global longitudinal speckle strain: comparison with ejection fraction and wall motion scoring. Circ Cardiovasc Imaging 2009;2:356-64.
193. Heimdal A, Stoylen A, Torp H, Skjaerpe T. Real-time strain rate imaging of the left ventricle by ultrasound. J Am Soc Echocardiogr 1998;11:1013-9.
194. Ingul CB, Torp H, Aase SA, Berg S, Stoylen A, Slordahl SA. Automated analysis of strain rate and strain: feasibility and clinical implications. J Am Soc Echocardiogr 2005;18:411-8.
195. Amzulescu MS, Langet H, Saloux E et al. Head-to-Head Comparison of Global and Regional Two-Dimensional Speckle Tracking Strain Versus Cardiac Magnetic Resonance Tagging in a Multicenter Validation Study. Circ Cardiovasc Imaging 2017;10.
196. Brown J, Jenkins C, Marwick TH. Use of myocardial strain to assess global left ventricular function: a comparison with cardiac magnetic resonance and 3-dimensional echocardiography. Am Heart J 2009;157:102 e1-5.
197. Delgado V, Mollema SA, Ypenburg C et al. Relation between global left ventricular longitudinal strain assessed with novel automated function imaging and biplane left ventricular ejection fraction in patients with coronary artery disease. J Am Soc Echocardiogr 2008;21:1244-50.
198. Villanueva-Fernandez E, Ruiz-Ortiz M, Mesa-Rubio D et al. Feasibility of bidimensional speckle-tracking echocardiography for strain analysis in consecutive patients in daily clinical practice. Echocardiography 2012;29:923-6.
199. Belghitia H, Brette S, Lafitte S et al. Automated function imaging: a new operator-independent strain method for assessing left ventricular function. Arch Cardiovasc Dis 2008;101:163-9.
200. Kleijn SA, Aly MF, Terwee CB, van Rossum AC, Kamp O. Three-dimensional speckle tracking echocardiography for automatic assessment of global and regional left ventricular function based on area strain. J Am Soc Echocardiogr 2011;24:314-21.
201. Zoghbi WA, Adams D, Bonow RO et al. Recommendations for Noninvasive Evaluation of Native Valvular Regurgitation: A Report from the American Society of Echocardiography Developed in Collaboration with the Society for Cardiovascular Magnetic Resonance. J Am Soc Echocardiogr 2017;30:303-371.
202. Thavendiranathan P, Liu S, Datta S et al. Automated quantification of mitral inflow and aortic outflow stroke volumes by three-dimensional real-time volume color-flow Doppler transthoracic echocardiography: comparison with pulsed-wave Doppler and cardiac magnetic resonance imaging. J Am Soc Echocardiogr 2012;25:56-65.
203. Shimada E, Zhu M, Kimura S et al. Quantitative assessment of mitral inflow and aortic outflow stroke volumes by 3-dimensional real-time full-volume color flow doppler transthoracic echocardiography: an in vivo study. J Ultrasound Med 2015;34:95-103.
204. Kimura BJ, Shaw DJ, Amundson SA, Phan JN, Blanchard DG, DeMaria AN. Cardiac Limited Ultrasound Examination Techniques to Augment the Bedside Cardiac Physical Examination. J Ultrasound Med 2015;34:1683-90.
205. Thavendiranathan P, Liu S, Datta S et al. Quantification of chronic functional mitral regurgitation by automated 3-dimensional peak and integrated proximal isovelocity surface area and stroke volume techniques using real-time 3-dimensional volume color Doppler echocardiography: in vitro and clinical validation. Circ Cardiovasc Imaging 2013;6:125-33.

206. Choi J, Hong GR, Kim M et al. Automatic quantification of aortic regurgitation using 3D full volume color doppler echocardiography: a validation study with cardiac magnetic resonance imaging. Int J Cardiovasc Imaging 2015;31:1379-89.
207. Matthews F, Largiader T, Rhomberg P, van der Loo B, Schmid ER, Jenni R. A novel operator-independent algorithm for cardiac output measurements based on three-dimensional transoesophageal colour Doppler echocardiography. Eur J Echocardiogr 2010;11:432-7.
208. Son JW, Chang HJ, Lee JK et al. Automated quantification of mitral regurgitation by three dimensional real time full volume color Doppler transthoracic echocardiography: a validation with cardiac magnetic resonance imaging and comparison with two dimensional quantitative methods. J Cardiovasc Ultrasound 2013;21:81-9.
209. Gruner C, Herzog B, Bettex D et al. Quantification of mitral regurgitation by real time three-dimensional color Doppler flow echocardiography pre- and post-percutaneous mitral valve repair. Echocardiography 2015;32:1140-6.
210. Heo R, Son JW, B OH et al. Clinical Implications of Three-Dimensional Real-Time Color Doppler Transthoracic Echocardiography in Quantifying Mitral Regurgitation: A Comparison with Conventional Two-Dimensional Methods. J Am Soc Echocardiogr 2017;30:393-403 e7.
211. Kato A SJ, Mroczek D, Chaturvedi R, Houle H, Georgescu B, Yoo SJ, Benson LN, Lee KJ. Automated 3-dimensional single beat real-time volume color-flow Doppler echocardiography in children: a validation study of right and left heart flows. Canadian journal of Cardiology 2018;In Press. Accepted manuscript.
212. Biner S, Rafique A, Rafii F et al. Reproducibility of proximal isovelocity surface area, vena contracta, and regurgitant jet area for assessment of mitral regurgitation severity. JACC Cardiovasc Imaging 2010;3:235-43.
213. Plicht B, Kahlert P, Goldwasser R et al. Direct quantification of mitral regurgitant flow volume by real-time three-dimensional echocardiography using dealiasing of color Doppler flow at the vena contracta. J Am Soc Echocardiogr 2008;21:1337-46.
214. Brugger N, Wustmann K, Hurzeler M et al. Comparison of three-dimensional proximal isovelocity surface area to cardiac magnetic resonance imaging for quantifying mitral regurgitation. Am J Cardiol 2015;115:1130-6.
215. Sitges M, Jones M, Shiota T et al. Real-time three-dimensional color doppler evaluation of the flow convergence zone for quantification of mitral regurgitation: Validation experimental animal study and initial clinical experience. J Am Soc Echocardiogr 2003;16:38-45.
216. Schmidt FP, Gniewosz T, Jabs A et al. Usefulness of 3D-PISA as compared to guideline endorsed parameters for mitral regurgitation quantification. Int J Cardiovasc Imaging 2014;30:1501-8.
217. Choi J, Heo R, Hong GR et al. Differential effect of 3-dimensional color Doppler echocardiography for the quantification of mitral regurgitation according to the severity and characteristics. Circ Cardiovasc Imaging 2014;7:535-44.
218. de Agustin JA, Viliani D, Vieira C et al. Proximal isovelocity surface area by single-beat three-dimensional color Doppler echocardiography applied for tricuspid regurgitation quantification. J Am Soc Echocardiogr 2013;26:1063-72.
219. de Agustin JA, Marcos-Alberca P, Fernandez-Golfin C et al. Direct measurement of proximal isovelocity surface area by single-beat three-dimensional color Doppler echocardiography in mitral regurgitation: a validation study. J Am Soc Echocardiogr 2012;25:815-23.
220. Mediratta A, Addetia K, Medvedofsky D et al. 3D echocardiographic analysis of aortic annulus for transcatheter aortic valve replacement using novel aortic valve quantification software: Comparison with computed tomography. Echocardiography 2017;34:690-699.
221. Calleja A, Thavendiranathan P, Ionasec RI et al. Automated quantitative 3-dimensional modeling of the aortic valve and root by 3-dimensional transesophageal echocardiography in normals,

aortic regurgitation, and aortic stenosis: comparison to computed tomography in normals and clinical implications. Circ Cardiovasc Imaging 2013;6:99-108.
222. Prihadi EA, van Rosendael PJ, Vollema EM, Bax JJ, Delgado V, Ajmone Marsan N. Feasibility, Accuracy, and Reproducibility of Aortic Annular and Root Sizing for Transcatheter Aortic Valve Replacement Using Novel Automated Three-Dimensional Echocardiographic Software: Comparison with Multi-Detector Row Computed Tomography. J Am Soc Echocardiogr 2017.
223. Garcia-Martin A, Lazaro-Rivera C, Fernandez-Golfin C et al. Accuracy and reproducibility of novel echocardiographic three-dimensional automated software for the assessment of the aortic root in candidates for thanscatheter aortic valve replacement. Eur Heart J Cardiovasc Imaging 2016;17:772-8.
224. Bersvendsen J, Beitnes JO, Urheim S, Aakhus S, Samset E. Automatic measurement of aortic annulus diameter in 3-dimensional transoesophageal echocardiography. BMC Med Imaging 2014;14:31.
225. Khalique OK, Kodali SK, Paradis JM et al. Aortic annular sizing using a novel 3-dimensional echocardiographic method: use and comparison with cardiac computed tomography. Circ Cardiovasc Imaging 2014;7:155-63.
226. Queiros S, Papachristidis A, Morais P et al. Fully Automatic 3-D-TEE Segmentation for the Planning of Transcatheter Aortic Valve Implantation. IEEE Trans Biomed Eng 2017;64:1711-1720.
227. Podlesnikar T, Prihadi EA, van Rosendael PJ et al. Influence of the Quantity of Aortic Valve Calcium on the Agreement Between Automated 3-Dimensional Transesophageal Echocardiography and Multidetector Row Computed Tomography for Aortic Annulus Sizing. Am J Cardiol 2018;121:86-93.
228. Farsalinos KE, Daraban AM, Unlu S, Thomas JD, Badano LP, Voigt JU. Head-to-Head Comparison of Global Longitudinal Strain Measurements among Nine Different Vendors: The EACVI/ASE Inter-Vendor Comparison Study. J Am Soc Echocardiogr 2015;28:1171-1181, e2.
229. Tsang W, Weinert L, Sugeng L et al. The value of three-dimensional echocardiography derived mitral valve parametric maps and the role of experience in the diagnosis of pathology. J Am Soc Echocardiogr 2011;24:860-7.
230. Grewal J, Suri R, Mankad S et al. Mitral annular dynamics in myxomatous valve disease: new insights with real-time 3-dimensional echocardiography. Circulation 2010;121:1423-31.
231. Biaggi P, Jedrzkiewicz S, Gruner C et al. Quantification of mitral valve anatomy by three-dimensional transesophageal echocardiography in mitral valve prolapse predicts surgical anatomy and the complexity of mitral valve repair. J Am Soc Echocardiogr 2012;25:758-65.
232. Chandra S, Salgo IS, Sugeng L et al. Characterization of degenerative mitral valve disease using morphologic analysis of real-time three-dimensional echocardiographic images: objective insight into complexity and planning of mitral valve repair. Circ Cardiovasc Imaging 2011;4:24-32.
233. Ender J, Eibel S, Mukherjee C et al. Prediction of the annuloplasty ring size in patients undergoing mitral valve repair using real-time three-dimensional transoesophageal echocardiography. Eur J Echocardiogr 2011;12:445-53.
234. Calleja A, Poulin F, Woo A et al. Quantitative Modeling of the Mitral Valve by Three-Dimensional Transesophageal Echocardiography in Patients Undergoing Mitral Valve Repair: Correlation with Intraoperative Surgical Technique. J Am Soc Echocardiogr 2015;28:1083-92.
235. Pouch AM, Wang H, Takabe M et al. Fully automatic segmentation of the mitral leaflets in 3D transesophageal echocardiographic images using multi-atlas joint label fusion and deformable medial modeling. Med Image Anal 2014;18:118-29.
236. Kagiyama N, Toki M, Hara M et al. Efficacy and Accuracy of Novel Automated Mitral Valve Quantification: Three-Dimensional Transesophageal Echocardiographic Study. Echocardiography 2016;33:756-63.

237. Jin CN, Salgo IS, Schneider RJ et al. Automated quantification of mitral valve anatomy using anatomical intelligence in three-dimensional echocardiography. International journal of cardiology 2015;199:232-8.
238. Armenian SH, Lacchetti C, Barac A et al. Prevention and Monitoring of Cardiac Dysfunction in Survivors of Adult Cancers: American Society of Clinical Oncology Clinical Practice Guideline. J Clin Oncol 2017;35:893-911.
239. Plana JC, Galderisi M, Barac A et al. Expert consensus for multimodality imaging evaluation of adult patients during and after cancer therapy: a report from the American Society of Echocardiography and the European Association of Cardiovascular Imaging. J Am Soc Echocardiogr 2014;27:911-39.
240. Negishi K, Negishi T, Haluska BA, Hare JL, Plana JC, Marwick TH. Use of speckle strain to assess left ventricular responses to cardiotoxic chemotherapy and cardioprotection. Eur Heart J Cardiovasc Imaging 2013.
241. Jordan JH, Sukpraphrute B, Melendez GC, Jolly MP, D'Agostino RB, Jr., Hundley WG. Early Myocardial Strain Changes During Potentially Cardiotoxic Chemotherapy May Occur as a Result of Reductions in Left Ventricular End-Diastolic Volume: The Need to Interpret Left Ventricular Strain With Volumes. Circulation 2017;135:2575-2577.
242. Melendez GC, Sukpraphrute B, D'Agostino RB, Jr. et al. Frequency of Left Ventricular End-Diastolic Volume-Mediated Declines in Ejection Fraction in Patients Receiving Potentially Cardiotoxic Cancer Treatment. Am J Cardiol 2017;119:1637-1642.
243. Bombardini T, Costantino MF, Sicari R, Ciampi Q, Pratali L, Picano E. End-systolic elastance and ventricular-arterial coupling reserve predict cardiac events in patients with negative stress echocardiography. BioMed research international 2013;2013:235194.
244. Chen CH, Fetics B, Nevo E et al. Noninvasive single-beat determination of left ventricular end-systolic elastance in humans. J Am Coll Cardiol 2001;38:2028-34.
245. Seidman A, Hudis C, Pierri MK et al. Cardiac dysfunction in the trastuzumab clinical trials experience. J Clin Oncol 2002;20:1215-21.
246. Grothues F, Smith GC, Moon JC et al. Comparison of interstudy reproducibility of cardiovascular magnetic resonance with two-dimensional echocardiography in normal subjects and in patients with heart failure or left ventricular hypertrophy. Am J Cardiol 2002;90:29-34.
247. Stohr EJ, Gonzalez-Alonso J, Pearson J et al. Dehydration reduces left ventricular filling at rest and during exercise independent of twist mechanics. Journal of applied physiology 2011;111:891-7.
248. Semb KA, Aamdal S, Oian P. Capillary protein leak syndrome appears to explain fluid retention in cancer patients who receive docetaxel treatment. J Clin Oncol 1998;16:3426-32.
249. Armstrong GT, Plana JC, Zhang N et al. Screening adult survivors of childhood cancer for cardiomyopathy: comparison of echocardiography and cardiac magnetic resonance imaging. Journal of clinical oncology : official journal of the American Society of Clinical Oncology 2012;30:2876-84.
250. Sarnoff SJ. Myocardial contractility as described by ventricular function curves; observations on Starling's law of the heart. Physiol Rev 1955;35:107-22.
251. Cardinale D, Colombo A, Bacchiani G et al. Early detection of anthracycline cardiotoxicity and improvement with heart failure therapy. Circulation 2015;131:1981-8.
252. Thavendiranathan P, Abdel-Qadir H, Fischer HD et al. Breast Cancer Therapy-Related Cardiac Dysfunction in Adult Women Treated in Routine Clinical Practice: A Population-Based Cohort Study. J Clin Oncol 2016;34:2239-46.

253. Saiki H, Petersen IA, Scott CG et al. Risk of Heart Failure With Preserved Ejection Fraction in Older Women After Contemporary Radiotherapy for Breast Cancer. Circulation 2017;135:1388-1396.
254. Montazeri A, Vahdaninia M, Harirchi I, Ebrahimi M, Khaleghi F, Jarvandi S. Quality of life in patients with breast cancer before and after diagnosis: an eighteen months follow-up study. BMC Cancer 2008;8:330.
255. Arndt V, Merx H, Stegmaier C, Ziegler H, Brenner H. Persistence of restrictions in quality of life from the first to the third year after diagnosis in women with breast cancer. J Clin Oncol 2005;23:4945-53.
256. Stoddard MF, Seeger J, Liddell NE, Hadley TJ, Sullivan DM, Kupersmith J. Prolongation of isovolumetric relaxation time as assessed by Doppler echocardiography predicts doxorubicin-induced systolic dysfunction in humans. J Am Coll Cardiol 1992;20:62-9.
257. Tassan-Mangina S, Codorean D, Metivier M et al. Tissue Doppler imaging and conventional echocardiography after anthracycline treatment in adults: early and late alterations of left ventricular function during a prospective study. Eur J Echocardiogr 2006;7:141-6.
258. Paelinck BP, de Roos A, Bax JJ et al. Feasibility of tissue magnetic resonance imaging: a pilot study in comparison with tissue Doppler imaging and invasive measurement. J Am Coll Cardiol 2005;45:1109-16.
259. Kellman P, Arai AE, Xue H. T1 and extracellular volume mapping in the heart: estimation of error maps and the influence of noise on precision. Journal of cardiovascular magnetic resonance : official journal of the Society for Cardiovascular Magnetic Resonance 2013;15:56.
260. Messroghli DR, Moon JC, Ferreira VM et al. Clinical recommendations for cardiovascular magnetic resonance mapping of T1, T2, T2* and extracellular volume: A consensus statement by the Society for Cardiovascular Magnetic Resonance (SCMR) endorsed by the European Association for Cardiovascular Imaging (EACVI). Journal of cardiovascular magnetic resonance : official journal of the Society for Cardiovascular Magnetic Resonance 2017;19:75.
261. Renu K AV, Pichiah PBT, Arunachalam S. Molecular Mechanism of Doxorubicin-Induced Cardiomypathy - An Update. *Eur J Pharmacol* 2018;818:241-253.
262. Silberman GA, Fan TH, Liu H et al. Uncoupled cardiac nitric oxide synthase mediates diastolic dysfunction. Circulation 2010;121:519-28.
263. Asp ML, Martindale JJ, Heinis FI, Wang W, Metzger JM. Calcium mishandling in diastolic dysfunction: mechanisms and potential therapies. Biochim Biophys Acta 2013;1833:895-900.
264. Farhad H, Staziaki PV, Addison D et al. Characterization of the Changes in Cardiac Structure and Function in Mice Treated With Anthracyclines Using Serial Cardiac Magnetic Resonance Imaging. Circ Cardiovasc Imaging 2016;9.
265. Melendez GC, Jordan JH, D'Agostino RB, Jr., Vasu S, Hamilton CA, Hundley WG. Progressive 3-Month Increase in LV Myocardial ECV After Anthracycline-Based Chemotherapy. JACC Cardiovasc Imaging 2017;10:708-709.
266. Serrano JM, Gonzalez I, Del Castillo S et al. Diastolic Dysfunction Following Anthracycline-Based Chemotherapy in Breast Cancer Patients: Incidence and Predictors. Oncologist 2015;20:864-72.
267. Bu'Lock FA, Mott MG, Oakhill A, Martin RP. Left ventricular diastolic filling patterns associated with progressive anthracycline-induced myocardial damage: A prospective study. Pediatr Cardiol 1999;20:252-63.
268. Pennell DJ. Cardiovascular magnetic resonance: twenty-first century solutions in cardiology. Clin Med (Lond) 2003;3:273-8.
269. Rathi VK, Doyle M, Yamrozik J et al. Routine evaluation of left ventricular diastolic function by cardiovascular magnetic resonance: a practical approach. Journal of cardiovascular magnetic resonance : official journal of the Society for Cardiovascular Magnetic Resonance 2008;10:36.

270. Rubinshtein R, Glockner JF, Feng D et al. Comparison of magnetic resonance imaging versus Doppler echocardiography for the evaluation of left ventricular diastolic function in patients with cardiac amyloidosis. Am J Cardiol 2009;103:718-23.
271. Flett AS, Hayward MP, Ashworth MT et al. Equilibrium contrast cardiovascular magnetic resonance for the measurement of diffuse myocardial fibrosis: preliminary validation in humans. Circulation 2010;122:138-44.
272. Escalante CP, Martin CG, Elting LS et al. Dyspnea in cancer patients. Etiology, resource utilization, and survival-implications in a managed care world. Cancer 1996;78:1314-9.
273. Nolan MT, Plana JC, Thavendiranathan P, Shaw L, Si L, Marwick TH. Cost-effectiveness of strain-targeted cardioprotection for prevention of chemotherapy-induced cardiotoxicity. International journal of cardiology 2016;212:336-45.
274. Hare JL, Brown JK, Leano R, Jenkins C, Woodward N, Marwick TH. Use of myocardial deformation imaging to detect preclinical myocardial dysfunction before conventional measures in patients undergoing breast cancer treatment with trastuzumab. Am Heart J 2009;158:294-301.
275. Current Procedural Terminology. 4th Edition 2014.
276. Walmart Retail Prescription Program Drug List. Updated May 2014.
277. World Health Organization. CHOosing Interventions that are Cost Effective (WHO-CHOICE): cost-effectiveness thresholds.
278. Eddy DM, Hollingworth W, Caro JJ et al. Model transparency and validation: a report of the ISPOR-SMDM Modeling Good Research Practices Task Force--7. Value Health 2012;15:843-50.
279. Earle CC, Chapman RH, Baker CS et al. Systematic overview of cost-utility assessments in oncology. J Clin Oncol 2000;18:3302-17.
280. Cardinale D, Colombo A, Sandri MT et al. Prevention of high-dose chemotherapy-induced cardiotoxicity in high-risk patients by angiotensin-converting enzyme inhibition. Circulation 2006;114:2474-81.
281. Heidenreich PA, Albert NM, Allen LA et al. Forecasting the impact of heart failure in the United States: a policy statement from the American Heart Association. Circ Heart Fail 2013;6:606-19.
282. Sawaya H, Sebag IA, Plana JC et al. Early detection and prediction of cardiotoxicity in chemotherapy-treated patients. Am J Cardiol 2011;107:1375-80.
283. Fallah-Rad N, Walker JR, Wassef A et al. The utility of cardiac biomarkers, tissue velocity and strain imaging, and cardiac magnetic resonance imaging in predicting early left ventricular dysfunction in patients with human epidermal growth factor receptor II-positive breast cancer treated with adjuvant trastuzumab therapy. J Am Coll Cardiol 2011;57:2263-70.
284. Kalay N, Basar E, Ozdogru I et al. Protective effects of carvedilol against anthracycline-induced cardiomyopathy. J Am Coll Cardiol 2006;48:2258-62.
285. Seicean S, Seicean A, Alan N, Plana JC, Budd GT, Marwick TH. Cardioprotective effect of beta-adrenoceptor blockade in patients with breast cancer undergoing chemotherapy: follow-up study of heart failure. Circ Heart Fail 2013;6:420-6.
286. Mornos C, Petrescu L. Early detection of anthracycline-mediated cardiotoxicity: the value of considering both global longitudinal left ventricular strain and twist. Can J Physiol Pharmacol 2013;91:601-7.
287. Nousiainen T, Jantunen E, Vanninen E, Remes J, Vuolteenaho O, Hartikainen J. Natriuretic peptides as markers of cardiotoxicity during doxorubicin treatment for non-Hodgkin's lymphoma. Eur J Haematol 1999;62:135-41.
288. Howlader N NA, Krapcho M, Neyman N, Aminou R, Waldron W and Edwards BK. SEER Cancer Statistics Review, 1975-2011, National Cancer Institute. Bethesda, MD,

http://seer.cancer.gov/csr/1975_2011/, based on November 2013 SEER data submission, posted to the SEER web site, April 2014.

289. Tan LL, Lyon AR. Role of Biomarkers in Prediction of Cardiotoxicity During Cancer Treatment. Curr Treat Options Cardiovasc Med 2018;20:55.
290. Abdel-Qadir H, Nolan MT, Thavendiranathan P. Routine Prophylactic Cardioprotective Therapy Should Be Given to All Recipients at Risk of Cardiotoxicity From Cancer Chemotherapy. Can J Cardiol 2016;32:921-5.
291. Lancellotti P, Suter TM, Lopez-Fernandez T et al. Cardio-Oncology Services: rationale, organization, and implementation. Eur Heart J 2019;40:1756-1763.